DEPOSITIONAL MODELS OF TEMPERATE CARBONATES:

Insights into in situ and redeposited sediments from Southern Spain, South Australia and North New Zealand

Ángel Puga Bernabéu

Departamento
de
Estratigrafía y Paleontología

UNIVERSIDAD DE GRANADA

2007

Departamento
de
Estratigrafía y Paleontología

UNIVERSIDAD DE GRANADA

DEPOSITIONAL MODELS OF TEMPERATE CARBONATES: INSIGHTS INTO *IN SITU* AND REDEPOSITED SEDIMENTS FROM SOUTHERN SPAIN, SOUTH AUSTRALIA AND NORTH NEW ZEALAND

TESIS DOCTORAL

Memoria de Tesis Doctoral presentada por el Licenciado en Geología
D. Ángel Puga Bernabéu para optar al Grado de Doctor por la Universidad de Granada

Granada, 15 de Octubre de 2007

Fdo. Ángel Puga Bernabéu

VºBº del Director

Fdo. Dr. José Manuel Martín Martín

VºBº del Director

Fdo. Dr. Juan Carlos Braga Alarcón

UNIVERSIDAD DE GRANADA
2007

Editor: Editorial de la Universidad de Granada
Autor: Ángel Puga Bernabéu
D.L.: Gr. 2415 - 2007
ISBN: 978-84-338-4515-3

Departamento
de
Estratigrafía y Paleontología

UNIVERSIDAD DE GRANADA

DEPOSITIONAL MODELS OF TEMPERATE CARBONATES: INSIGHTS INTO *IN SITU* AND REDEPOSITED SEDIMENTS FROM SOUTHERN SPAIN, SOUTH AUSTRALIA AND NORTH NEW ZEALAND

PhD THESIS

MODELOS DE SEDIMENTACIÓN DE CARBONATOS TEMPLADOS: NUEVAS PERCEPCIONES SOBRE SEDIMENTOS *IN SITU* Y REDEPOSITADOS DEL SUR DE ESPAÑA, SUR DE AUSTRALIA Y NORTE DE NUEVA ZELANDA

TESIS DOCTORAL

Ángel Puga Bernabéu

UNIVERSIDAD DE GRANADA
2007

Para orgullo de mi padre,
con el cariño de mi madre
y el amor de mi nena

Todos somos ignorantes, lo que ocurre es que no todos ignoramos las mismas cosas
(Albert Einstein)

ABSTRACT

In the last two decades, research on the temperate-carbonate depositional realm has significantly increased knowledge on these, up to then, poorly known carbonates, achieving a degree of comprehension comparable to that of tropical carbonates. However, some aspects need further research, especially those concerning depositional models due to the high variability and number of controlling factors. In particular, sediment transport, deposition mechanisms, resultant deposits, and cyclicity in outer-ramp and ramp-to-slope transitional settings need better characterisation.

The Mediterranean Sea, New Zealand, and southern Australia are the most important temperate-carbonate sedimentary provinces in the world. The main depositional models on temperate carbonates have been established in these areas, either in recent or fossil sediments. The "shaved shelf" model characterises the deposition style on recent and ancient vast carbonate platforms in southern Australia. Research on temperate carbonates on present New Zealand shelves has resulted in detailed studies on sediment composition. In ancient examples, studies have brought to light important results, especially on the diagenesis and tectonic-sedimentation relationship. Within the Mediterranean region, southern Spain is where depositional models on temperate carbonates are best established and characterised. These models display a great variety of sediment types and composition in inner- and middle-ramp settings.

This thesis deals with the study of temperate-carbonate deposits in the above-mentioned regions. It attempts to expand upon the spectrum of the temperate-carbonate depositional models, clarifying sediment transport mechanisms, describing their resulting deposits, and identifying and analysing some aspects related to cyclicity and sequence stratigraphy in temperate carbonates. The areas selected for study were the Sorbas and Granada basins in southern Spain; Taranaki Basin in the North Island of New Zealand; and the Great Australian Bight in southern Australia.

In the Sorbas Basin, depositional models for Upper Miocene temperate carbonates have been described. Characterisation of high-frequency cycles in the temperate-ramp sediments and identification and description of tsunami-related deposits are the main novel contributions. Studies carried out in the Granada Basin have provided details about the morphology, infill patterns, sediment composition, bed geometries, and origin of a submarine canyon excavated into an Upper Miocene temperate-carbonate ramp. A Middle Miocene mixed carbonate-siliciclastic deep-water submarine channel-fan system (Mangarara Formation) was studied in the eastern margin of the Taranaki Basin. Facies characterisation of channel infills, channel geometries, sediment transport and deposition mechanisms as well as palaeoenvironmental and palaeogeographical issues have been typified in this thesis. Finally, the integrated use of wireline logs, geochemical data, FMS images, and sedimentological analysis performed in the offshore Pleistocene sediments on the Great Australian Bight resulted in the characterisation of sedimentary cycles in upper-slope settings and their relation to sea-level and palaeoceanographic changes.

Interpreted depositional models in the study areas share certain characteristics in common or with comparable classic sedimentary models of temperate carbonates. These features mainly concern the ramp geometry, biogenic composition of the sediment, facies belt distribution, sediment transport and deposition mechanisms, and cyclicity.

New aspects concerning temperate-carbonate deposition were found in platform and offshore environments. In platform settings, the main innovations involve event deposits (tsunamites), sedimentary cyclicity, and submarine canyon occurrence and development. Sea-level driven cyclicity, deep-water submarine channel-fan systems and submarine gullies are the main features found in offshore settings.

Although the most important controlling factors on temperate-carbonate ramp deposition (apart from water temperature and nutrient contents) have been repeatedly shown to be local hydrodynamic conditions and type and geometry of the underlying substrate, there are additional factors to be taken into account. This thesis work has demonstrated that high-energy events (tsunamis), large-scale geomorphic elements (submarine canyons and submarine channel-fan system), and sea-level driven modulations condition the type of temperate-carbonate depositional model that develops, whether in the platform or in offshore settings.

RESUMEN

La investigación llevada a cabo en las últimas dos décadas en el campo de la sedimentación de carbonatos templados ha aumentado significativamente el grado conocimiento de este tipo de carbonatos poco conocido hasta entonces. Los estudios realizados han permitido alcanzar un grado de comprensión sobre los carbonatos templados comparable al que se tiene de los carbonatos tropicales. Sin embargo, existen ciertos aspectos que necesitan ser investigados con más detalle, especialmente aquellos aspectos relacionados con los modelos sedimentarios, debido al gran número y variabilidad de factores que controlan los diferentes modelos deposicionales. Los mecanismos de transporte y depósito y la ciclicidad en los ambientes de rampa externa y de transición rampa-talud necesitan una mejor caracterización.

El Mar Mediterráneo, Nueva Zelanda y el sur de Australia son las regiones más importantes del mundo con sedimentación de carbonatos templados. Los principales y más importantes modelos sedimentarios de carbonatos templados se han establecido en estas zonas, tanto en sedimentos recientes como fósiles. El modelo de "plataforma arrasada" caracteriza el estilo de sedimentación en las extensas plataformas carbonatadas, recientes y fósiles, del sur de Australia. La investigación de los carbonatos templados de las plataformas actuales de Nueva Zelanda ha dado como resultado estudios detallados de la composición del sedimento. En ejemplos fósiles, los estudios realizados han arrojado importantes resultados especialmente sobre la diagénesis de estos carbonatos y la relación entre tectónica y sedimentación. Dentro de la región Mediterránea, el sur de España es la zona donde los modelos de sedimentación de carbonatos templados están mejor establecidos y descritos. Estos modelos se caracterizan especialmente por una gran variedad en la composición y el tipo de sedimento en los ambientes de rampa interna y media.

Esta tesis trata el estudio de depósitos de carbonatos templados en las regiones arriba mencionadas, con el objetivo de ampliar el espectro de los modelos de sedimentación de carbonatos templados, clarificar los mecanismos de transporte y depósito y describir los depósitos resultantes, e identificar y analizar algunos aspectos relacionados con la ciclicidad y estratigrafía secuencial en los carbonatos templados. Las áreas de estudio seleccionadas son las Cuencas de Sorbas y Granada en el sur de España; la Cuenca de Taranaki en la Isla Norte de Nueva Zelanda; y la *Great Australian Bight* en el sur de Australia.

En la cuenca de Sorbas se han detallado modelos deposicionales de carbonatos templados del Mioceno Superior. Las principales novedades del estudio llevado a cabo en esta cuenca han sido la caracterización de ciclos de alta frecuencia en sedimentos de rampa carbonatada y la identificación y descripción de tsunamitas. El estudio desarrollado en la Cuenca de Granada ha proporcionado detalles sobre la morfología, patrones de relleno, composición del sedimento, geometrías de las capas y origen de un cañón submarino excavado en una rampa de carbonatos templados del Mioceno Superior. La Formación Mangarara (Mioceno Medio), interpretada como un sistema de canal-abanico submarino carbonatado-siliciclástico de aguas profundas, fue estudiada en el margen oriental de la Cuenca de Taranaki (Nueva Zelanda). La caracterización de las facies que forman el relleno de los canales, la geometría de los canales, los mecanismos de transporte y depósito, y consideraciones de índole paleoambiental y paleogeográfica han sido plasmadas en esta tesis. Finalmente, el uso intergrado de *wireline logs*, datos geoquímicos, imágenes FMS y análisis sedimentológico llevado a cabo en sedimentos Pleistocenos de la *Great Australian Bight* ha dado como resultado la caracterización de los ciclos sedimentarios y ambientes de talud superior y han permitido relacionar estos ciclos con cambios paleoceanográficos y de nivel de mar.

Los modelos deposicionales interpretados para las áreas de estudio comparten algunas características entre ellos y comparables modelos sedimentarios clásicos de carbonatos templados. Estás características se refieren principalmente a la geometría de la rampa, los tipo de componentes bioclásticos del sedimento, distribución de los cinturones de facies, mecanismos de transporte y depósito de sedimento y ciclicidad.

En relación con la sedimentación de carbonatos templados, se han encontrado algunos aspectos novedosos tanto en ambientes de plataforma como de mar abierto profundo. En la zona de plataforma, las principales innovaciones se refieren a depósitos de evento (tsunamitas), ciclicidad, presencia y modelo de desarrollo de un cañón submarino. Aspectos relacionados con la ciclicidad controlada por el nivel de mar, sistemas de canales-abanicos submarinos profundos y barrancos submarinos son las principales novedades encontradas en ambientes de mar abierto profundo.

Aunque los factores más importantes que controlan la sedimentación en rampas de carbonatos templados (además de la temperatura del agua y el contenido en nutrientes) han sido recurrentemente las condiciones hidrodinámicas locales y el tipo y geometría de sustrato, hay otros factores adicionales a tener en cuenta. El trabajo realizado en esta tesis muestra que los eventos de alta energía (tsunamis), elementos geomorfológicos de grandes dimensiones (cañones submarinos y sistemas de canal-abanico submarino) y modulaciones controladas por el nivel de mar condicionan el tipo de modelo deposicional que se desarrolla, tanto en la plataforma como en áreas profundas.

TABLE OF CONTENTS

PART FOUR

PART ONE

1

INTRODUCTION TO TEMPERATE CARBONATES

Carbonate sedimentation is essentially marine. Carbonate sediments cover approximately 50% of the seafloor in modern-day oceans (Tucker and Wright, 1992, based on Jenkins, 1986). Carbonate sediments are also important in the fossil record as can be deduced from subaerial outcrops, well-log data, and samples collected in petroleum-prospecting campaigns and Ocean Drilling Program/Integrated Ocean Drilling Program (ODP/IODP) expeditions. Carbonate rocks are good potential hydrocarbon reservoirs. This fact promoted research on present-day carbonate systems in order to properly interpret ancient carbonate deposits during the 1960s and 1970s. At first, these studies focused mainly on tropical zones such as the Florida Gulf, the Great Bahamas Bank, the Persian Gulf, the Great Barrier Reef, and Western Australia (e.g. Ginsburg, 1956; Purdy, 1963; Shinn *et al.*, 1969; Davies, 1970; Kamen-Kaye, 1970; Maiklem, 1970; Stoffers and Ross, 1979). This situation led many researchers to believe that shallow-water carbonate sedimentation was restricted to tropical (equatorial) regions (e.g. Rodgers, 1957; Taft, 1967; Bathurst, 1975; Wilson, 1975). However, Chave (1967) questioned those ideas and suggested that shallow-water carbonates could also be deposited in shallow-water settings, in areas where terrigenous supply is very low, regardless of water temperature. Subsequently, Lees and Buller (1972) made an extensive collection of published data and demonstrated that carbonate sedimentation can take place in shallow-water settings from the equator to the poles. Lees and Buller (1972) also found that sediment composition was not the same in all regions where carbonates are deposited. In order to differentiate between carbonates formed in warm and temperate-cool waters, Lees and Buller (1972) introduced the terms chlorozoan (Chlorophyta + Zoantharia) for the former and foramol (benthic foraminifers + molluscs) for the latter. Water temperature appears to be the main factor controlling the distribution of the chlorozoan association, although Lees and Buller (1972) also pointed out that there must be other controlling factors to be taken into account for explaining the distribution of the two associations. Later, Lees (1975) added water-salinity as a complementary factor controlling the composition (grain association) of carbonate sediment in different settings. The term chloralgal was thus introduced to name a chlorozoan-type skeletal-grain association that is dominated by green algae and lacks hermatypic corals, probably due to the low or high water salinity where this association occurs.

In the following years, many geologists began to interpret some carbonate deposits as non-tropical carbonates (term proposed by Nelson, 1988a) (e.g. Nelson, 1978; Scoffin *et al.*, 1980; Rao, 1981; Burne and Colwell, 1982; Nelson *et al.*, 1982; Nelson and Bornhold, 1983; Farrow *et al.*, 1984). The first modern treatise dealing with the non-tropical carbonate realm ("Non-tropical shelf carbonates-modern and ancient") was published in 1988 (Nelson, 1988b). Results of the research papers in this special issue established: a) the importance of shallow-water carbonate sedimentation in zones outside tropical regions, either in present-day sedimentary environments or their ancient counterparts; b) the considerations that must be taken into account in the study and interpretation of carbonate environments to distinguish between tropical/subtropical and non-tropical carbonate sedimentation; and c) the importance of the transition zones between these two types of carbonate sedimentation (Carannante *et al.*, 1988). Since then, temperate- and cool-water carbonate depositional realm data have been extensively expanded (James and Bone, 1991; 1994; Boreen and James, 1993; James *et al.*, 1994, 2004; Martin *et al.*, 1996, 2004; Anastas *et al.*, 1997; Fornos and Ahr, 1997; Henrich *et al.*, 1997; Freiwald, A, 1998; Betzler *et al.*, 1997a, 2000; Lukasik *et al.*, 2000; Braga *et al.*, 2001, 2003a; Pedley and Grasso, 2002; Nelson *et al.*, 2003; Smith and Nelson, 2003; Betzler *et al.*, 2005; Caron *et al.*, 2004a, 2005; Pufahl *et al.*, 2004;

Titschack *et al.*, 2005; Dix and Nelson, 2006; Hetzinger *et al.*, 2006; Mitchell *et al.*, 2007a; Rogala *et al.*, 2007 among others). The principal results on this topic over the last 20 years are summarized in two special publications, *Cool-water carbonates* edited by James and Clarke (1997) and *Cool-water carbonates: depositional systems and palaeoenvironmental controls* edited by Pedley and Carannante (2006). All these studies have provided new data on aspects such as carbonate sequence stratigraphy applied to non-tropical carbonates, early diagenesis in temperate carbonates, differences between cool-water carbonate depositional models in oceanic open ramps and microtidal sea ramps, changes in the composition of carbonate factory areas from inner- to outer-ramp settings and controlling factors on non-tropical carbonate deposition.

Features that define non-tropical carbonates, commonly called "temperate carbonates" (Lees and Buller, 1972) or "cool-water carbonates" (Brookfield, 1988) should be clearly stated before entering more deeply into the state of knowledge and interpretation of temperate- to cool-water carbonate depositional models. The salient characteristics are: bioclast associations, mineralogy, diagenesis and cementation, sedimentation rate, and controlling factors (temperature, salinity, nutrients, light, terrigenous input, hydrodynamic regime and substrate topography).

1.1. Temperate versus tropical shelf carbonate sedimentation. Main characteristics of temperate carbonates

1.1.1. Bioclast associations

Shallow-water tropical and non-tropical carbonates exhibit different skeletal and non-skeletal grain associations. The traditional classification of Lees and Buller (1972) distinguishes two major skeletal grain associations: foramol for temperate- and cool-waters carbonates and chlorozoan for warm-water carbonates (tropical carbonates) (Fig. 1). The temperate association is composed of molluscs, benthic foraminifers, bryozoans, coralline algae, echinoderms, barnacles, sponges (calcareous spicules), ostracods, and ahermatypic corals. The presence, abundance and proportion of these constituents vary from one location to another depending on local conditions. The only non-skeletal grains that may be present in this association are pellets, although they are usually absent. The chlorozoan association may contain the same skeletal-grain components as the foramol association, but it also incorporates significant amounts of calcareous green algae (codiacean algae) and hermatypic corals. Non-skeletal grains (ooliths, aggregates and pellets) may be present in the chlorozoan association (Fig. 1). The chloralgal association is a chlorozoan association that develops in high- or low-salinity waters where hermatypic corals are absent and green algae are the dominant skeletal components (Lees, 1975).

The foramol and chlorozoan carbonate-particle assemblages have global significance. The foramol association can be considered as representative (in global terms) of temperate and cool-water carbonates. However, the term itself emphasizes the presence of benthic foraminifers (fora-) and molluscs (-mol) as the basic and most abundant bioclastic constituents in the non-tropical carbonates even though these bioclasts are not necessarily dominant in all temperate-carbonate sediments. Various other names, which, without any doubt, can be included within the foramol concept in global terms, have arisen in order to qualify the group of organisms that are dominant in the carbonate sediment, such as bryomol (bryozoans + molluscs) (Nelson *et al.*, 1988a), rhodalgal (red algae) (Carannante *et al.*, 1988), molechfor (molluscs + echinoderms + foraminifers) (Carannante *et al.*, 1988), or those collected in the assorted terminology proposed by Hayton *et al.* (1995) (Fig. 1). Nonetheless, although these terms can be useful as descriptive tools to indicate the main components of the carbonate association, their palaeonvironmental significance is limited as they depend on local factors. Hayton *et al.* (1995) defined seven skeletal classes for New Zealand Cenozoic non-tropical limestones and gave them palaeoenvironmental significance. This could be applied to some other New Zealand temperate shelves that share common features, but its application to other basins (for instance, small and/or ocean-restricted basins) may lead to confusion; local factors such as palaeotopography and hydrodynamic conditions might be completely different and, consequently, the skeletal association that characterises the different subenvironments within the ramp as well (e.g. Betzler *et al.*, 2000).

The most recent terminology is that proposed by James (1997). His classification follows Lees and Buller's (1972) trend and groups the tropical and non-tropical carbonate associations according to their general characteristics. James' (1997) classification emphasizes the light-dependent nature of the major biotic constituents and gives less importance to water temperature as a factor controlling skeletal composition. This author proposed the terms heterozoan and photozoan (Fig. 2). The heterozoan association is an association of carbonate particles produced by light-independent organisms, which can also include coralline algae (Fig. 2). The photozoan association is an association of carbonate particles composed of light-dependent organisms and/or non-skeletal carbonate particles (ooliths, aggregates and pelloids), that can also have light-

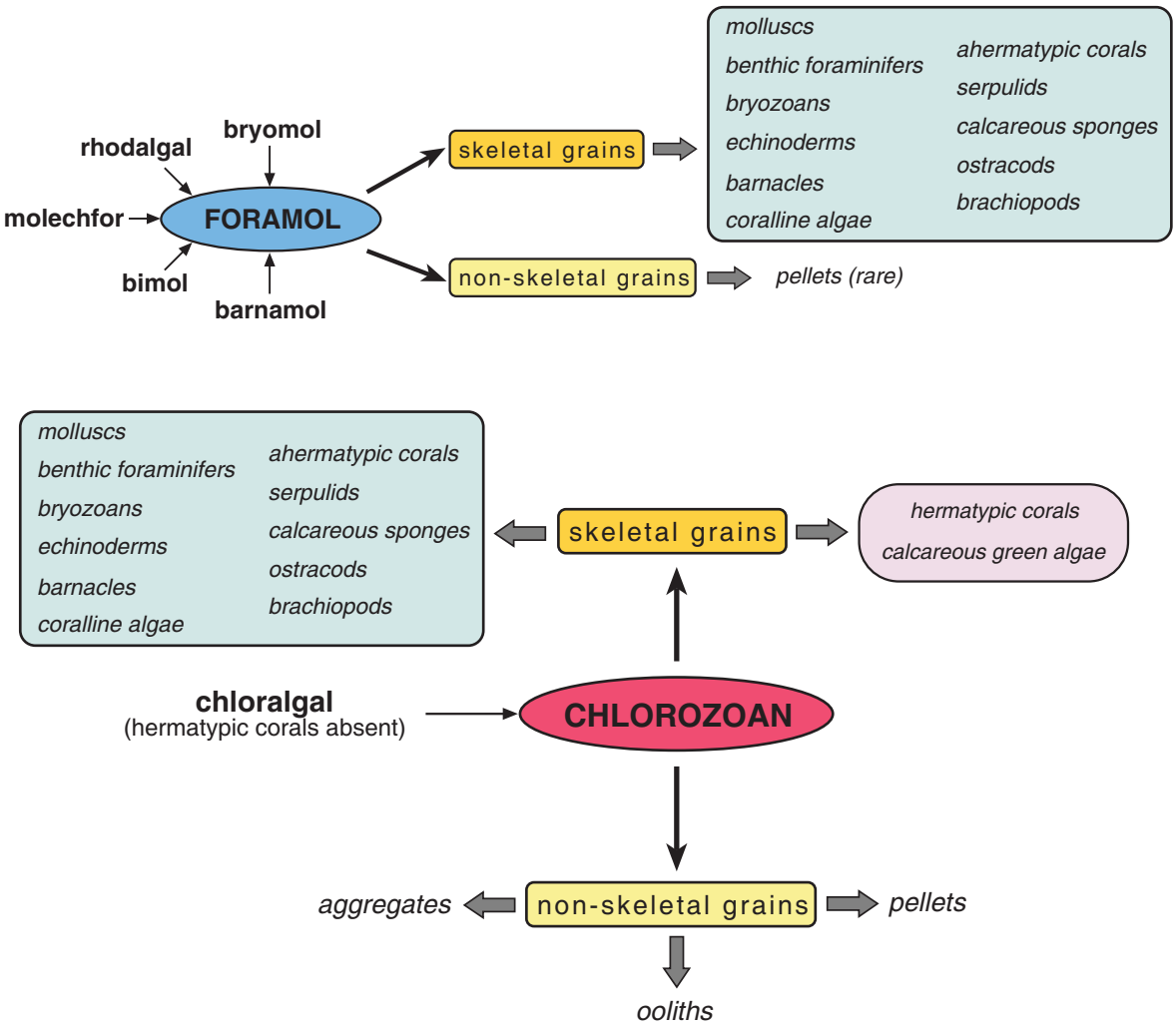

Fig. 1. The main components of the two major grain associations that characterise carbonate sediments formed in shallow waters (*sensu* Lees and Buller, 1972) are: foramol for temperate- and cool-water carbonates and chlorozoan for warm-water carbonates.

independent organisms from the heterozoan association (Fig. 2). The heterozoan association includes organisms not listed initially in the foramol association such as trilobites and crinoids. The heterozoan association is characteristic of cool-water carbonates but not all heterozoan carbonates are necessarily cool water (James, 1997). In warm waters, the heterozoan association may lie below the photic zone in transition with the photozoan association. Otherwise, if environmental conditions (light, nutrients, terrigenous supply, etc.) limit the development of the organisms of the photozoan association, the heterozoan association may dominate in shallower waters.

1.1.2. Mineralogy

In contrast to tropical carbonate sediments, whose mineralogy is dominated by aragonite, modern temperate counterparts are generally dominated by low-magnesium calcite and/or high-magnesium calcite, and minor aragonite (Nelson, 1978; Nelson *et al.*, 1988a). However, aragonite may be more abundant in some platform settings such as the South Australia shelf (James *et al.*, 2005). In ancient non-tropical carbonates, calcite is also the dominant mineralogy of the skeletal components and aragonite is absent or subordinate (Reeckmann, 1988; Hood and Nelson, 1996; Brachert *et al.*, 1998). Due to the special diagenetic scenario in cool-water settings (see Section 1.1.3), aragonite skeletons, if present, are commonly dissolved, and only under special conditions (e.g. high sedimentation rate) is aragonite preserved in the fossil record (e.g. Gillespie and Nelson, 1997; Caron *et al.*, 2005).

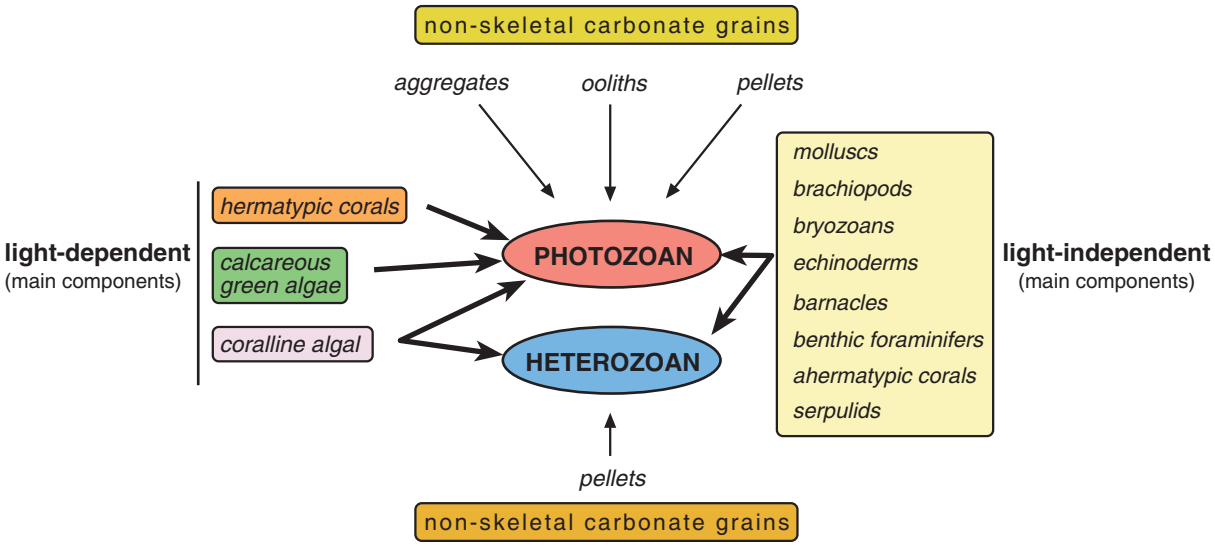

Fig. 2. James' (1997) classification (grain association) for carbonate sediments. This classification highlights the light-dependence of biotic components. The heterozoan association characterises cool-water carbonates (but not exclusively) and the photozoan association typifies warm-water (tropical) carbonates.

1.1.3. Diagenesis

The constructive character of seafloor diagenesis that characterises shelf-carbonates in tropical-water settings cannot be directly applied to those carbonates formed in cooler (non-tropical) waters (Alexandersson, 1979; Nelson *et al.*, 1988b). Early marine diagenesis is dominantly destructive in temperate (cool) shallow-water carbonates (Alexandersson, 1978; Nelson *et al.*, 1988b; Reeckmann, 1988; Smith, 1988). The main reason for these different diagenetic scenarios arises from the water saturation stage with respect to calcium carbonate ($CaCO_3$). Seafloor cementation is produced in response to several environmental factors (Nelson and James, 2000), but it commonly occurs when seawater contains a high concentration of $CaCO_3$ in solution. Tropical sea waters are supersaturated with respect to $CaCO_3$, whereas temperate-carbonate environments with cooler waters are less saturated or even undersaturated with respect to $CaCO_3$. Because of the lack of early seafloor cementation in temperate-water settings, the common low sedimentation rates of non-tropical carbonates (see Section 1.1.4), and the higher solution-resistance of the calcitic mineralogy that generally dominates this type of carbonates (see Section 1.1.2), temperate carbonate sediments remain loose on the seafloor and are affected by destructive processes such as dissolution, transport, abrasion, and bioerosion (Fig. 3). Cementation of non-tropical carbonates is generally delayed to later stages, during shallow- to deep-burial diagenesis.

The effects of the mainly destructive early seafloor processes in temperate carbonate deposits take on an important role in the taphonomy of the skeletal components (Smith and Nelson, 2003). The water chemistry in non-tropical settings leads to the dissolution of metastable $CaCO_3$ phases such as aragonite and high-magnesium calcite and/or the neomorphism of the latter (Hood and Nelson, 1996; Kyser *et al.*, 1998). The degradation of organic matter by microbial activity in the surficial sediment may enhance aragonite dissolution (Smith and Nelson, 2003; James *et al.*, 2005). This dissolution results in a significant loss of aragonitic skeletal components in the remaining carbonate sediment (Nelson, 1978, Nelson *et al.*, 1988a; Brachert *et al.*, 1998; James *et al.*, 2005) and, subsequently, a bias in the sedimentary record of non-tropical carbonates. However, this bias varies from one non-tropical setting to another, probably depending on local factors, as it may be important in some places (James *et al.*, 2005), but be of minor importance in others (Nelson *et al.*, 1988a). In fact, it may not even occur since aragonite can be preserved under special conditions (Nelson *et al.*, 2003). Probably due to the long residence time of carbonate particles (calcium carbonate as a whole) on the seafloor, dissolution processes usually prevail on temperate ramps (see references in Smith and Nelson, 2003). Dissolution depends mainly on the mineralogy of the skeletons (aragonite vs. calcite) and the reactive surface area (Smith and Nelson, 2003). Other destructive processes are related to physical breakdown. Disarticulation and breakage of the carbonate skeletons are produced during transport of the bioclasts along the shelf

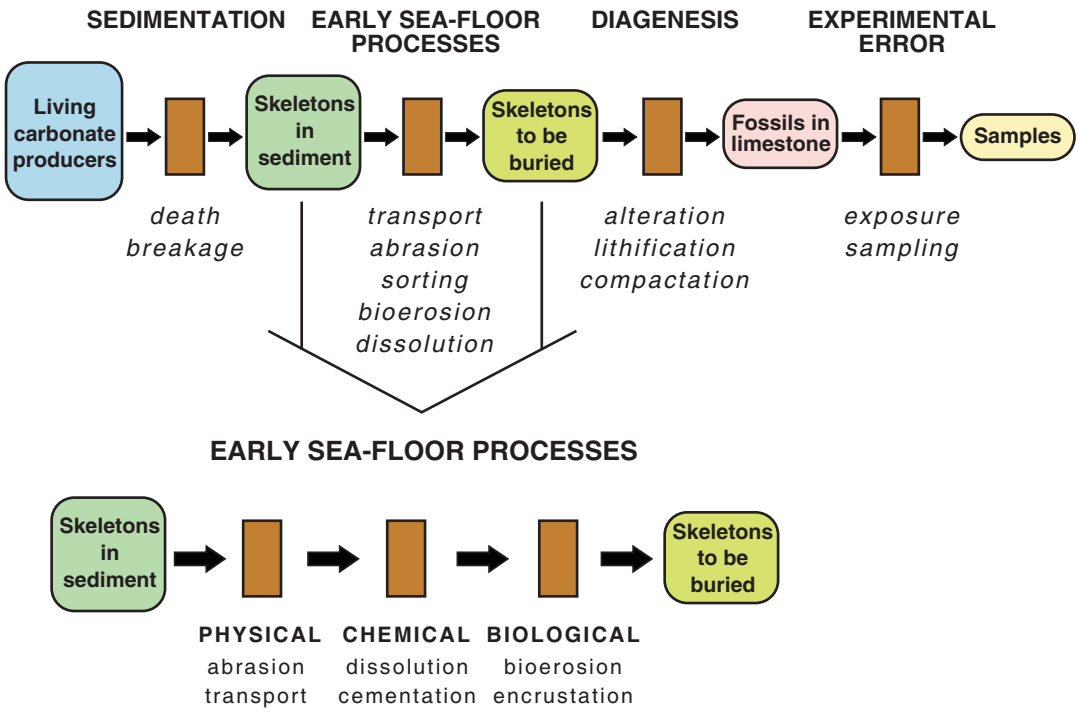

Fig. 3. Taphonomic filters that limit preservation of carbonate sediments, with particular reference to early seafloor that act as destructive processes (from Smith and Nelson, 2003).

(and shelf to basin) due to waves, ocean currents, turbidity flows, seismic shocks, and biological activity. During transport, broken components are increasingly abraded, and thus skeleton size is diminished and bioclast shape can be obliterated. Physical breakdown of non-tropical carbonate particles depends on factors both intrinsic (mineral composition, size and shape of skeletal grains) and extrinsic (hydraulic regime, terrigenous sediment mixing and exposure time) (Smith and Nelson, 2003). Finally, biological processes can also be destructive although they may be constructive as well (either encrustating or redistributing the sediment as bioturbation) during the early seafloor exposure of non-tropical carbonate skeletons. Bioerosion of bioclasts by sponges, echinoderms, gastropods, bivalves, algae, microbacteria, fungi, fish, and other organisms leads to the destruction of the carbonate skeletons. Apart from the loss of sedimentary information, the main sedimentary implication of bioerosion processes (together with abrasion processes) is the production of carbonate mud (Nelson, 1978; Leonard *et al.*, 1981; Farrow and Fyfe, 1988; Young and Nelson, 1988).

Carbonate mud is generally rare or absent in shallow-water non-tropical shelf sediments (Nelson, 1988a) although it can be abundant locally (Blom and Alsop, 1988; Farrow and Fyfe, 1988). In tropical carbonates, carbonate mud is generated by the disaggregation of aragonitic green algae and/or from inorganic precipitation. In contrast to warm-water carbonates, carbonate mud in temperate settings derives from bioerosion and maceration of skeletal components and from calcareous nannoplankton (Blom and Alsop, 1988; Farrow and Fyfe, 1988). This fine-grained carbonate sediment is usually swept from shallow- to deep-water settings or dissolved (Farrow and Fyfe, 1988). Once it accumulates in the deep-sea realm it may have lithification rates similar to tropical deep-water periplatform sediments (Dix and Nelson, 2006).

Although the lack of carbonate precipitation and cementation is overwhelming in shallow cool-water seas, lithification of the seafloor may occur locally (Reeckmann, 1988; Nelson and James, 2000; Mutti and Bernoulli, 2003; Caron *et al.*, 2005). Nelson and James (2000) distinguished four types of cemented horizons in non-tropical limestones from New Zealand and southern Australia: below and/or immediately above major unconformities; at the top of metre-scale subtidal carbonate cycles; within rare *in-situ* biomounds and within some stacked, cross-bedded sandbodies. Marine seafloor cementation in non-tropical ramps occurs preferentially (but not exclusively) under high-energy conditions during lowered sea level (Nelson and James, 2000) and/or during initial stages of a transgression and first stages of falling sea level (Caron *et al.*, 2005). Some authors (Mutti and Bernoulli, 2003) have suggested that lithified horizons in temperate ramps could be used as indicators of palaeoenvironmental changes in the oceans, but much more work is needed in this area.

1.1.4. Sedimentation rates

Overall, sedimentation rates in non-tropical carbonates are one order of magnitude lower than accumulation rates corresponding to tropical carbonates (James, 1997). This slower accumulation may be related to water temperature and carbonate saturation (colder water is less saturated in calcium carbonate and therefore the carbonate precipitation is slower) or to the slow growth rate of the organisms that comprise temperate carbonates.

Carbonate accumulation rates in ancient non-tropical carbonate settings are commonly on the order of 1.0–2.5 cm/ky (Nelson, 1978; James and Bone, 1991), although sedimentation rates up to 10–50 cm/ky are estimated locally (Martín *et al.*, 1996; Holdgate and Gallager, 1997; Nelson *et al.*, 2003) (Fig. 4). In modern (sub-recent) cool-water shelves, carbonate sedimentation rates vary among the different subenvironments across the shelf (Boreen and James, 1993): up to 100 cm/ky in embayments, beach and

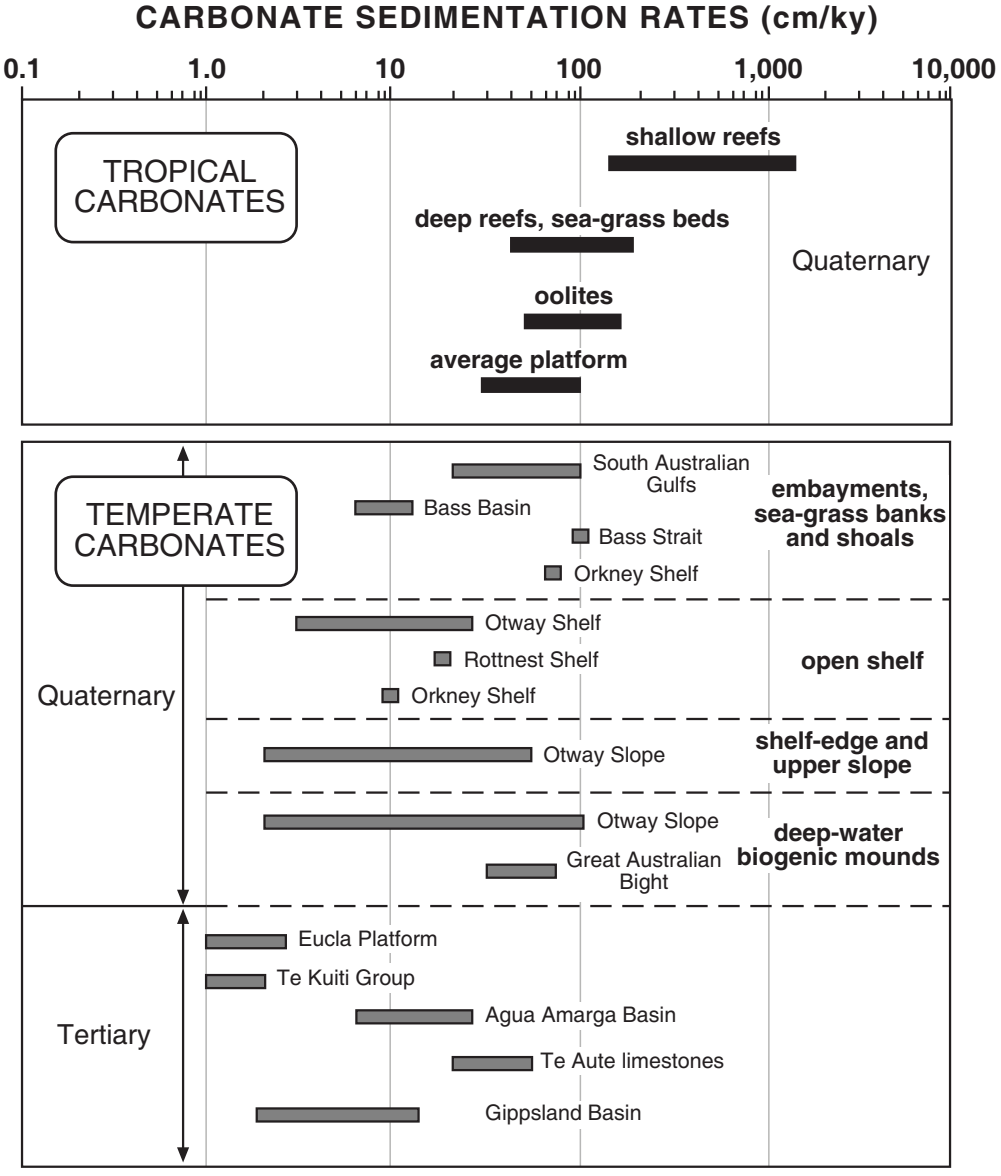

Fig. 4. Accumulation rates for modern and ancient temperate- and cool-water carbonates (adapted from James, 1997 and compiled from Nelson, 1978; James and Bone, 1991; Boreen and James, 1993; Martín *et al.*, 1996; Holdgate and Gallager, 1997; Nelson *et al.*, 2003; James *et al.*, 2004).

shoal systems; 3–23 cm/ky in the open shelf; 2–50 cm/ky in the shelf-edge and upper slope; and 30–105 cm/ky in biogenic (bryozoan and/or sponge) mounds (Boreen and James, 1993; James *et al.*, 2004) (Fig. 4).

Another significant issue is that sedimentation rates calculated for modern non-tropical carbonates are similar to those estimated for their ancient counterparts. High accumulation rates in temperate carbonate ramps are commonly due to hydrodynamic sediment concentration (Freiwald, 1998; Nelson *et al.*, 2003). In contrast, accumulation rates estimated for ancient tropical carbonates are different (much lower) than calculations for present-day tropical environments (James, 1997).

Finally, the carbonate budget is an important key to understanding the different accumulation rates in tropical and cool-water carbonates. Production rates of up to 2000 g m^{-2} y^{-1} are estimated for some temperate shelves, which are locally similar to those in some tropical environments (Smith and Nelson, 2003). However, the long-term sediment accumulation in temperate ramps is smaller, in part due to the destructive nature of the early seafloor processes in these carbonate settings (Smith, 1988). According to Smith and Nelson (2003), carbonate preservation rates are 50–75% of the gross carbonate production in tropical reef environments. These values are in stark contrast to the estimated rates of 0–25% in temperate carbonate shelves. This difference clearly reflects the destructive character of the diagenetic processes in temperate ramps and contributes to explaining the generally low sedimentation rates in non-tropical carbonate settings.

1.1.5. Controlling factors

The major factors that control the type of carbonate deposition (foramol/chlorozoan or heterozoan/photozoan) that develops on a shallow-water carbonate platform are temperature, salinity, nutrients, luminosity, and terrigenous input. Some of these factors are commonly interrelated (e.g. temperature-nutrients, nutrients-luminosity, salinity-temperature, nutrients-terrigenous input) (Fig. 5), which sometimes makes it difficult to discern their relative importance, especially in the sedimentary record. Other global and regional factors such as oceanography and hydrodynamic regime, or local factors such as topographic profile or wind regime, may also contribute.

1.1.5.1. Temperature

Water temperature is the most important factor controlling the worldwide distribution of the different carbonate types (Lees and Buller, 1972; Nelson, 1988a; James, 1997). The temperature threshold between the foramol and chlorozoan associations is located approximately in waters with a minimum near-surface temperature of 14–15º C and a mean annual temperature of at least 23º C (Lees and Buller, 1972). Nelson (1988a) later defined non-tropical carbonates as those deposited in waters with a mean annual surface-water temperature of <20º C, which is the threshold commonly accepted nowadays. This temperature boundary corresponds geographically to approximately 30º latitude, but it should be borne in mind that water-temperature is not exclusively latitude-dependent as global oceanic circulation modifies the normal latitude patterns. Moreover, the influence of other factors that inhibit the chlorozoan/photozoan association development (see below) may result in foramol/heterozoan association spreading towards the equatorial belt.

This water-temperature control also seems to have played a role in the past, not surprinsingly in the Neogene basins of the Betic Cordillera, for example, heterozoan and photozoan associations alternated in the sedimentary record from the late Miocene to early Pliocene. In these basins, stable isotope analysis of planktonic foraminifers and fossil assemblages indicate that the alternation of tropical and temperate carbonates was mainly controlled by sea-surface water temperature (Sánchez-Almazo *et al.*, 2001; Martín *et al.*, *in press*).

As the temperature threshold between chlorozoan/photozoan and foramol/heterozoan associations is not a physical barrier, there may be a certain amount of overlap, permitting carbonate producers from both associations to develop in the same setting. This transition zone (subtropical province *sensu* James, 1997) is commonly characterised by dominant heterozoan components and minor photozoan elements. This transition is well represented along latitudinal transects in modern Brazilian (Carannante *et al.*, 1988), Gulf of California (Halfar *et al.*, 2006), and Australian shelves (James *et al.*, 1999). Carbonate shelves with mixed tropical and temperate features have also been described in the fossil record (Brandley and Krause, 1997; Martindale and Boreen, 1997).

The global oceanic circulation (global conveyor belt) and surface ocean currents play an important role in the distribution of surface-water temperatures along the shallow-water shelves and consequently in determining the distribution of carbonate associations. For instance, warm-water currents such as the Gulf Current in the Caribbean region, the Kuroshio Current in south Japan, and the East Australian Current flowing along the eastern coast of Australia allow coral-reef (chlorozoan carbonates) development outside the tropic belt. Similarly, cool-water currents (upwelling currents) such as the Humbolt Current flowing along the north coast of Peru and Chile

and the Benguela Current in western South Africa favour the presence of foramol carbonates in tropical shelves.

Water temperature is usually related to and/or controls other factors such as nutrients, salinity, and luminosity, making it difficult to discern the true importance of the latter factors in determining carbonate type. One example are upwelling currents, which are cold, deep, nutrient-riched and oxygen-poor waters that flow up the continental shelves as a consequence of the Coriolis Effect and Ekman transport. So, do these currents inhibit chlorozoan carbonate production on the shelves because of the cool water? Or are the nutrient contents the key?

1.1.5.2. Salinity

Salinity appears to be a complementary controlling factor of temperature to explain the overall worldwide distribution of different carbonate-producer organisms (Lees, 1975). Foramol/heterozoan associations develop in normal (or slightly brackish) marine waters (Lees, 1975; Nelson, 1988a). In tropical carbonates, although some corals (hermatypic), which are important components of the chlorozoan association, can tolerate highly saline water (up to 46 ‰; Kinsman, 1968), corals are extremely sensitive to changes in salinity and consequently usually grow in water of normal salinity (27–40 ‰). Green algae are more tolerant to salinity changes and therefore dominate tropical settings with slightly hypersaline or hyposaline waters in the absence of hermatypic corals (chloralgal association). As temperature and salinity are commonly compensated, the foramol association may develop as well in warmer waters than normal but too brackish for the growth of the chlorozoan association (Lees, 1975). Non-skeletal particles (ooids, pellets and aggregates) also show distribution dependence on the temperature/salinity relationship (Lees, 1975).

1.1.5.3. Nutrients

Nutrient availability (basically nitrogen and phosphorous ions needed for the protein synthesis and cellular material) is another factor that controls the biogenic composition in modern and ancient settings. Nutrient input to the carbonate shelves is associated to terrigenous input (see below) and/or to upwelling currents that supply additional nutrients to shallow platforms.

Nutrient content is especially important as a limiting factor of hermatypic coral growth and, in this respect, it partially conditions the distribution of the tropical chlorozoan/photozoan association. Although hermatypic corals are essentially zooxanthellate, they need a certain amount of nutrients to develop. High nutrient availability favours the presence of fast-growing organisms such as macroalgae that compete with corals for light and space, to finally displace them (Wood, 1999). Nutrients also stimulate phytoplankton growth, reducing light penetration, and thereby limiting the depth distribution of zooxanthellate corals.

In the case of the temperate association, an excess of nutrients may only affect the coralline algae. The nutrient supply is usually related to river-discharge factors, with increased terrigenous input and salinity decrease, or to upwelling waters.

Nutrient availability is a very important factor in the development of carbonate factories in cold high-latitudes waters (Henrich *et al.*, 1997). In these settings, temperature can be excluded as a determining factor as it is by far lower than the temperature growth threshold of hermatypic corals (~18º C) and, hence, carbonate production, if it takes place, will be the foramol type. Nutrient supply is therefore the factor that controls the development of carbonates in subpolar and polar settings as long as terrigenous input remains relatively low. As cold waters are undersaturated in calcium carbonate, carbonate-secreting organisms need to expend more energy to continuously precipitate their calcareous skeletons and avoid carbonate dissolution: as a result, adequate nutrient input is necessary. Nutrient supply can be via ice-melting, local upwelling, and/or efficient benthopelagic coupling (i.e. rapid transfer of planktonic food to benthic communities) (Henrich *et al.*, 1997).

1.1.5.4. Luminosity

The euphotic zone is determined by the depth of light penetration in water. This light penetration is high in oligotrophic waters (up to 100 m) and decreases from mesotrophic to eutrophic environments. Therefore, hermatypic (zooxanthellate) corals and green algae (typical components of the tropical-chlorozoan-photozoan carbonate association), which are heavily dependent on light penetration, will develop in shallow water. In contrast, organisms of the non-tropical-foramol-heterozoan association (excluding the photodependent coralline algae) can develop in any range of water luminosity. Bryozoans, for instance, can live in waters from 15–20 m depth (Betzler *et al.*, 2000) to depths greater than 1000 m (McKinney and Jackson, 1989) and bivalves live from supratidal to abyssal settings. Water luminosity is a latitudinal-dependent factor as insolation is higher and more inclined (close to perpendicular) in low-latitude than in high-latitude settings. Special physiological adaptations of autotroph carbonate producers such as coralline algae are also needed for their development in high-latitude carbonate platforms that show extreme seasonality in solar radiation (Freiwald, 1998). Factors such as nutrients (see previous section) and terrigenous supply (see next section) can affect the depth

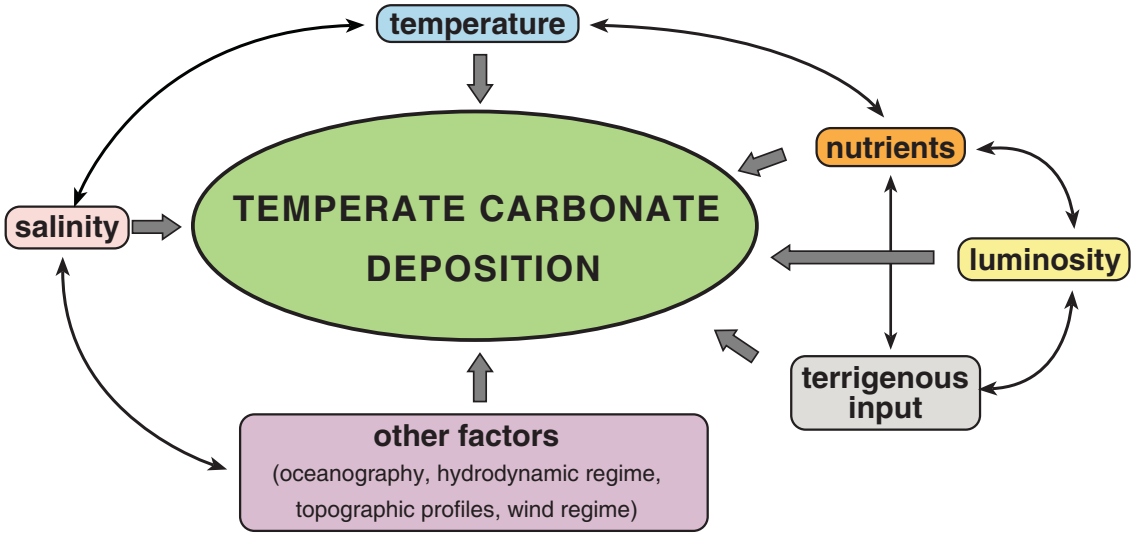

Fig. 5. Major controlling factors on temperate-carbonate deposition

of the photic zone, limiting the development of photozoan components. As a consequence, the seafloor in deeper (and commonly colder) waters in tropical areas can be dominated by organisms of the temperate-carbonate associations.

1.1.5.5. Terrigenous input

Terrigenous sediments can be supplied to shallow-water carbonate environments by rivers, hurricanes and storms, and as wind-transported dust. Chave (1967) highlighted that carbonate accumulation only takes place in shallow-water settings where terrigenous sedimentation is low or negligible, a fact also pointed out by Leonard *et al.* (1981). However, it should be borne in mind that what is really important is the balance between the rate of carbonate production and the rate of terrigenous sedimentation (James, 1997). If terrigenous input is sporadic and/or localized, carbonate-producer organisms can flourish (Martín *et al.*, 1989; Braga *et al.*, 1990; Gillespie *et al.*, 1998; Pufahl *et al.*, 2004). Moreover, carbonate accumulation can imply reworking and remobilization processes different from *in-situ* carbonate production, especially in the case of temperate carbonates (Martín *et al.*, 1996; 2004; Braga *et al.*, 2006a, Sections 4–8 in this study), sometimes resulting in a mixture of terrigenous and carbonate sediments.

Organisms in the different carbonate associations, such as hermatypic corals (chlorozoan/photozoan association), are able to remove low amounts of fine-grained particles deposited on the polyps, but they cannot grow if the clastic supply is high. Also important in the case of the photozoan association is water turbidity and decreased light penetration associated to terrigenous input. Suspension-feeding organisms of the foramol/heterozoan association are mainly affected by high rates of terrigeonus sedimentation due to clogging, but not affected by the subsequent light limitation. In general, the heterozoan association is more tolerant to terrigenous input than the photozoan association.

1.1.5.6. Oceanography, hydrodynamics and topography

Oceanography, hydrodynamics, and topography influence the distribution of carbonate types commonly modifying the normal (latitude-controlled) distribution of sea-surface water temperature. The importance of the global conveyor belt (thermohaline circulation) and surface ocean currents have been pointed out above (Section 1.1.5.1). Regional hydrodynamic conditions can also modify the distribution of carbonate types in relation to normal global distribution. For example, temperate carbonate deposition took place in the western Mediterranean during the Early Pliocene, a time of relatively warm global open oceans. This situation, prolonged to the present day, was related to the new current-circulation pattern established due to the opening of the Gibraltar Straits (about 4.9 Ma ago), which introduced Atlantic waters from a more northern (and cooler) source area (Martín *et al.*, *in press*).

The hydrodynamic regime and substrate type and palaeotopography can condition the location of carbonate factories (Betzler *et al.*, 2000; James *et al.*, 2001; Gläser and Betzler, 2002) and the redeposition processes (Martín *et al.*, 1996; Betzler *et al.*, 1997a), especially within small basins (Braga *et al.*, 2003a; Martín *et al.*, 2004).

1.2. Depositional models

The first well-established depositional models for temperate carbonates were defined for vast, open-ocean-facing, high-energy carbonate platforms in South Australia and New Zealand (Nelson *et al.*, 1988a; James and Bone, 1991; Boreen and James, 1993; James *et al.*, 1994). In the last fifteen years, the increasing contribution in facies models from modern and ancient examples of non-tropical carbonates around the world have brought to light the complexity and wide spectrum of environments where these carbonates form. Non-tropical carbonates can accumulate in beach systems (Merefield, 1984; Martín *et al.*, 1996; Betzler *et al.*, 1997a), at the toe of submarine cliffs (Betzler *et al.*, 2000; Titschack *et al.*, 2005), in straits/seaways (Anastas *et al.*, 1997; Martín *et al.*, 2001; Betzler *et al.*, 2006), spit platforms (Braga *et al.*, 2003a), estuaries (Clarke *et al.*, 1996; Pufahl *et al.*, 2004), sea-embayments (Martín *et al.*, 2004), tidal-dominated platforms (Farrow *et al.*, 1984), isolated ramps (Fornos and Ahr, 1997), epeiric ramps (Lukasik *et al.*, 2000), and in submarine canyons (Mitchell *et al.*, 2007a,b) and submarine fans and channels (Braga *et al.*, 2001; Vigorito *et al.*, 2005). In this section, the most representative depositional models from the most important temperate-carbonate regions (southern Australia, New Zealand, and the Mediterranean) and other areas are briefly described in order to introduce the reader to the temperate-carbonate depositional realm.

1.2.1. Southern Spain and modern western Mediterranean Sea

1.2.1.1. Neogene Betic basins in southern Spain

Neogene Betic basins in southern Spain formed as a result of the uplift of the Betic Cordillera during the Late Miocene (Braga *et al.*, 2003b). These intermontane, Mediterranean- or Atlantic-linked basins (Fig. 6) were partially infilled with temperate carbonate deposits ranging in age from the Late Miocene (early Tortonian) to the Early Pliocene (Zanclean) (Fig. 7). Temperate carbonate units in southern Spain, which alternate with tropical units, are characterised by a wide variety of sedimentary features related to variations in local conditions (mainly hydrodynamic and the topographic profile) within different depositional environments. As a consequence of this variation, there is no single depositional model of temperate carbonates for the Neogene basins of southern Spain (Braga *et al.*, 2006a) (Fig. 8). A synthesis of the main depositional models of temperate carbonate deposition in southern Spain based on several authors (Martín *et al.*, 1996, 2004; Betzler *et al.*, 1997a, 2000; Aguirre, 1998, 2000; Braga *et al.*,

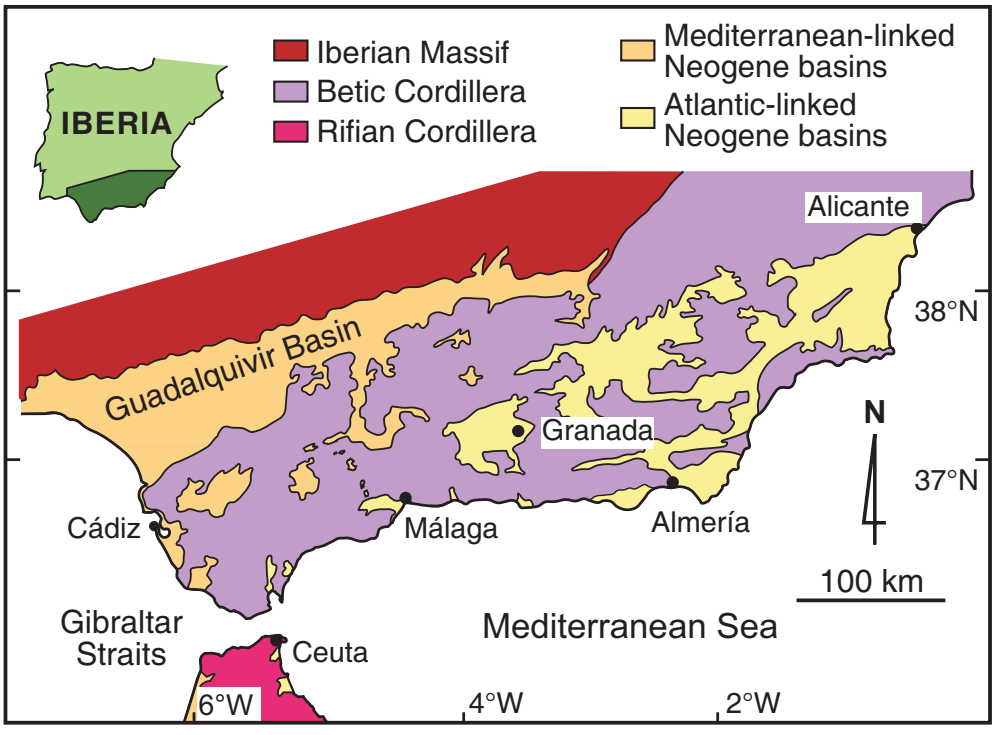

Fig. 6. Geographical and geological setting of the Neogene Betic basins showing distribution of Mediterranean-linked and Atlantic-linked basins.

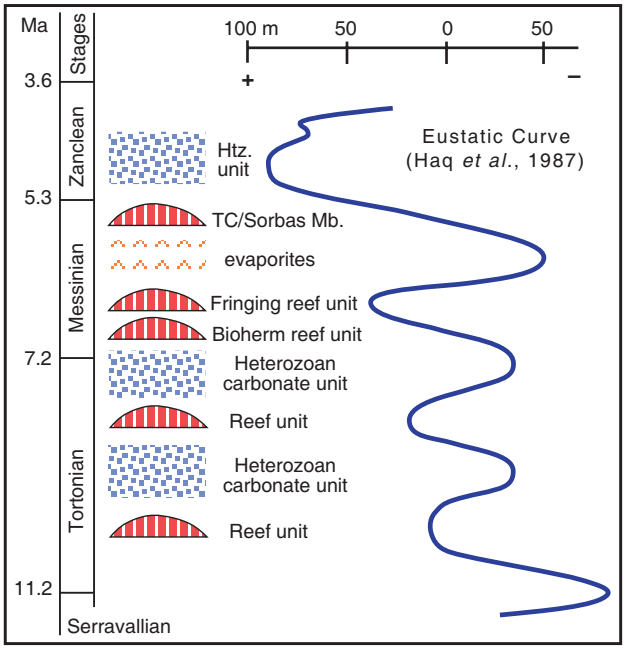

Fig. 7. Stratigraphic distribution of temperate and tropical sedimentary units from the Late Miocene to Early Pliocene in the Betic Cordillera (modified from Brachert *et al.*, 1996 and Braga *et al.*, 1996a). TC: Terminal Complex; Htz: Heterozoan.

2001; 2003a) is presented in Braga *et al.* (2006a). Skeletal components that form the temperate carbonates in these basins are mainly bryozoans, bivalves (primarily pectinids and oysters) and coralline algae, with benthic foraminifers (small and large), brachiopods, echinoids, barnacles, solitary corals, serpulids, and gastropods as accessory components in variable proportions. These preserved skeletal remains are essentially calcitic in origin or calcitic-replaced, with minor aragonitic components occurring as moulds.

Following the description scheme presented in Braga *et al.* (2006a), in a proximal to distal transect, the main depositional environments recognised in the Neogene Mediterranean-linked basins in southern Spain are the following:

Coastal belt. The coastal belt is characterised by a variety of sedimentary environments resulting from the specific hydrodynamic regime and paleotopography of the coastal setting. Beaches, rocky shores, rocky submarine cliffs, and spits were the main environments in coastal settings (Table 1) (Fig. 8).

Beach. The beach system is fully represented with backshore, foreshore, and shoreface subenvironments. Backshore settings can be represented by 1) aeolian dunes with high-angle, medium- to large-scale cross-bedding; 2) lagoon deposits consisting of massive to horizontally laminated silts and marls with plant remains; and/or 3) washover-fan deposits comprising landward-dipping bioclastic packstones and rudstones.

Rocky shore. In rocky shores, carbonate deposits accumulated at the foot of low-relief coastal cliffs. These shores were colonized by *Isognomon* shells and coralline-algal rhodoliths together with oysters, gastropods and barnacles, all mixed with blocks fallen from the cliffs and bored by sponge and *Lithophaga*.

Rocky submarine cliffs. The steep walls of submarine cliffs and adjacent areas were colonised by different types of organisms. Robust branching bryozoans were the main dwellers on submarine cliffs. These organisms grew attached to cliff walls and accumulated at the toe of cliffs after post-morten reworking, forming steeply dipping (up to 30º) rudstone aprons. Vermetid gastropods also colonised the submarine cliffs, forming a vermetid framework. Hard substrates on small depressions were occupied by barnacle patches. Gentle ramps on cliffs fronts presumably covered with seagrass patches were settled by nodular branching bryozoans, bivalves (including *Isognomon*), and coralline algae.

Spit. Spit-platform deposits are represented by bedded bioclastic packstones and rudstones accumulated by longshore currents several hundred metres away from the palaeoshoreline. Landward-dipping beds that change seawards to flat-lying trough-cross beds represent accumulation on the leeside of the spit of particles swept and removed from the top of the spit by storms. Sheltered carbonate factories developed between the spit and the shoreline.

Shoals. A shoal system formed by submarine dunes developing seawards from the coastal environments is well-represented in all the examples of Neogene temperate-carbonate ramps (Table 1). Shoal sediments consist of medium- to large-scale trough cross-bedded packstones to rudstones. These sediments were supplied from the factory areas seawards of the shoals (see below). Bioturbation of the shoal surface, especially by irregular echinoids (*Scolicia* burrows), is a common characteristic on the submarine bars.

Open platform. Carbonate ramps have two depositional profiles: gentle homoclinal and distally steepened (Fig. 8A). Carbonate factory zones (*sensu* Martín *et al.*, 1996), are areas of maximum carbonate (skeletal) production (*in-situ* growth of organisms), developed seawards of the shoals belt on both types of ramps. These areas were relatively calm environments located below the fair-weather wave base. Sediment from the factory areas consist of poorly

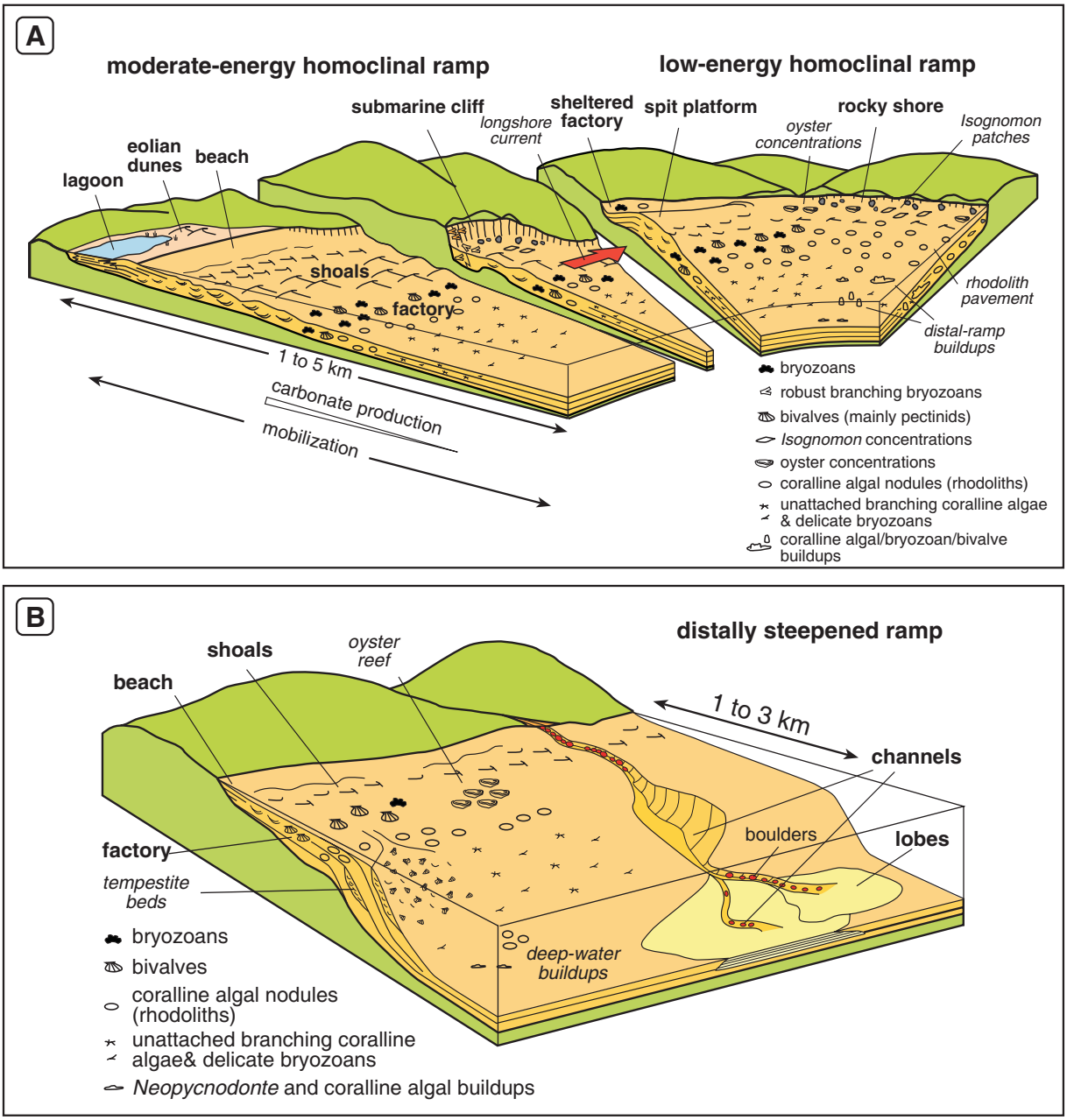

Fig. 8. Idealized depositional models of temperate carbonates in homoclinal (A) and distally-steepened (B) ramps in Neogene Betic (Mediterranean-linked) basins in southern Spain (from Braga *et al.*, 2006a).

bedded, coarse floatstones and rudstones. Bioclasts of the factory zones are well-preserved, with low fragmentation and abrasion of the skeletons. Fossil assemblages are composed of variable proportions of organisms such as nodular and branching bryozoans, bivalves, coralline algae (branching and rhodoliths), barnacles and other heterozoan components. Although mixed in different proportions, fossil groups tend to be spatially fractionated, commonly with bivalves and bryozoans in shallower settings and coralline algae in deeper waters. Seagrass meadows were presumably a common feature in the factory areas of the ramp.

In low-energy homoclinal ramps, background sediment in distal ramp settings consists of floatstone and rudstones of delicate-branching bryozoans and branching coralline algae with small coralline algal/bryozoan/bivalve build-ups and patches of *Neopycnodonte* (see Martín *et al.*, 2004 for further details). In moderate- to high-energy gentle ramps,

Table 2. Lithologies, textures, sedimentary structures, main skeletal components and other significant features of temperate carbonates formed in different depositional environments in the Mediterranean-linked, Betic intermontane basins (from Braga *et al.*, 2006a).

	Coastal belt							Shoal	Open platform			Toe slope and basin	
	backshore realm			beach	rocky shore	submarine cliff	spit platform		platform factory	outer platform (in gentle homoclinal ramps)	slope (in distally steepened ramps)	submarine lobes and channels	basin
	aeolian dune	lagoon	washover fan										
Textures and	Grainstone	siliciclastic silts and marls	packstone to rudstone	grainstone to rudstone	grainstone to rudstone	blocks of various sizes among grainstone-rudstone	packstone to rudstone	packstone to rudstone	pebble- to cobble-sized rudstone and floatstone	fine- to medium-grained floatstone to rudstone	medium-grained floatstone to rudstone	packstone to rudstone and mixed siliciclastics-carbonates	silty marls and marls
Sedimentary structures	high-angle, medium- to large-scale cross-stratification	horizontally laminated to massive	onland-dipping, parallel-laminated	low-angle parallel lamination (foreshore), small-scale trough cross-bedding (shoreface)	chaotic	inclined layers	landward-dipping beds with crude, parallel lamination	medium to large scale trough cross-bedding	poorly bedded to massive	well bedded, low-angle dipping layers to massive	well bedded, sigmoidal layers	parallel lamination in lobes; channels with lateral accretion and internal cut-and-fill structures	massive
Main skeletal components			bivalves, barnacles, bryozoans		*Isognomon* oysters, gastropods, rhodoliths and barnacles	vermetids, robust branching and nodular bryozoans	bivalves, coralline algae and nodular bryozoans	bivalves, coralline algae and bryozoans	nodular and branching bryozoans, coralline algae and bivalves (pectinids, oysters)	delicate bryozoans and branching coralline algae	delicate bryozoans, and branching coralline algae	coralline algae, bivalves and bryozoans	calcareous plankton, and benthic foraminifers
Other		land-plant remains	bioturbation (mainly *Scolicia*)	bioturbation (mainly *Scolicia*) in shoreface deposits	borings in carbonate blocks	short lateral continuity of beds (tens of metres) and rapid facies changes, borings in carbonate blocks		locally palaeosols, bioturbation (mainly *Scolicia*), high fragmentation	monospecific-paucispecific fossil assemblages, bioturbation (mainly *Scolicia*)	small build-ups made up of bryozoans, coralline algae, and bivalves	frequent intercalations of storm deposits		occasional intercalations of sediment gravity flows, bioturbation mainly *Thalassinoides*

the distal setting is formed by a fan-bedded zone made up of poorly sorted to parallel laminated floatstones and rudstones. Particles from the factory were removed and transported downslope by storm currents and accumulated in the distal ramp below the storm wave base. Redeposited beds also intercalate fine-grained background sediments deposited during fair weather.

Distally-steepened ramps are scarce in the Neogene Betic intermontane basins, and are only represented in the Carboneras Basin (Martín *et al.*, 2004). The ramp-edge was colonised by coralline algae forming rhodolith pavements and cut by channelised oyster-rich beds (Fig. 8B). The slope deposits consist of a medium-grained floatstone to rudstone with delicate branching bryozoans, bivalves and branching coralline algae that probably grew on the slope. This slope background facies intercalates bivalve-rich tempestite beds. *Neopycnodonte* and coralline algal build-ups developed at the base of the slope.

Toe of the slope and basin. These deep-water settings are poorly described within the temperate carbonate realm of the Neogene Betic basins. Distal-ramp carbonates commonly merge laterally into burrowed calcisiltites, silty marls, and marls deposited on basinal settings (Aguirre, 2000; Sánchez-Almazo *et al.*, 2001). The best example of slope-to-basin transition is represented by the submarine lobe and channel feeder system preserved in the Vera Basin (Braga *et al.*, 2001). Submarine channels up to several tens of metres wide probably developed as a continuation of river courses entering the sea, cross-cut the ramp sediments and the slope and graded into submarine fans up to 1 km wide on basinal settings. Sediments removed from the shallow-ramp and transported along submarine channels were finally deposited in the submarine fans (Fig. 8B).

To summarize, depositional models of temperate carbonates in southern Spain studied to date are gentle homoclinal and distally-steepened ramps typified by the presence of a carbonate factory zone (where organisms grew *in situ*) situated in relatively quiet waters (commonly below the fair-weather wave base or in sheltered zones in shallower waters) from which sediment was transported landwards and incorporated into shoals, spits and/or beaches, or seawards along the ramp, and accumulating as tempestites and/or fan-bedded deposits. Coastal settings landwards from the shoals are represented by a variety of environments related to local hydrodynamic and topographic conditions. The slope to basin transition consists of fine-grained sediments changing laterally to basinal sediments, or may be locally represented by a channel and submarine-fan system.

1.2.1.2. Neritic temperate carbonates in western Mediterranean Sea

The Project CARBMED led by Professor Christian. Betzler (University of Hamburg, Germany) was set to develop models of the neritic cool-water carbonate factories in three modern depositional systems of the western Mediterranean Sea. This was the major objective of the cruise Meteor 69/1 in August 2006, in which the Alborán-Ridge, the Oran Bay and the southern Mallorca Shelf were studied. In each of the working areas, seismic and parasound surveys were followed by grab sampling, box coring and vibrocoring. The recovered deposits are latest Pleistocene and Holocene in age. Occurrence of living red algae at the tops of the cores indicates that cores were retrieved from areas with an active carbonate factory.

The succession recovered at Alboran Ridge documents that there was no major carbonate production during the early transgression of the ridge, therefore indicating that carbonate factory started at a later stage of sea-level rise. Mixed carbonate–siliciclastic deposits with rhodoliths, bryozoans, and bivalves formed before pure carbonates. The carbonate factory is dominated by rhodoliths with only minor bryozoans and bivalves. Carbonates are calcarenites and calcirudites rich in red algal debris with minor to frequent mud. Smear slides reveal that calcareous mud is rich in calcareous nannoplankton.

Deposits in the Oran Bay are almost pure carbonates, rich in rhodoliths and red algal flakes. Other organisms are bivalves and minor bryozoans. Carbonates are calcarenites and calcirudites, in part rich in mud. Rhodoliths concentrate in layers up to 40 cm thick. Cores record a deepening upward trend, reflected in up-section decreasing grain size, and a change from smooth to warty rhodoliths (up to 6.5 cm large) in the lower part to small rhodoliths in the upper part of the succession. At the shallowest cores, this deepening trend is followed by shallower sediments, reflecting the filling of accommodation space.

Carbonate facies recovered in the Mallorca Shelf are more variable than in Oran Bay or Alboran Ridge. The eastern transects show a clear water depth-dependent zonation. Cores in shallow-water areas (<60 mwd) contain frequent branching rhodoliths and debris of rhodoliths, together with other bioclasts. In cores from greater water depths, there are lesser amounts of red algae and small bioclasts together with molluscs dominate the sediment. This zonation does not occur in the western transect, where rhodoliths and their fragments are a frequent component at all localities. Facies changes do not reflect a simple deepening-upward trend. In several cores, a 20–140 cm thick interval of facies dominated by the suspensivorous gastropod *Turritella* is indicative of a higher primary productivity.

1.2.2. South Australia

The southern margin of Australia is a passive continental margin formed by rifting processes that initiated in the late Mesozoic and separated the Antarctica and Australia plates (Veevers *et al.*, 1991). This margin has remained relatively stable since the late Eocene, although slow seafloor spreading continues in the present. Southern Australian shelves are the largest areas of modern cool-water carbonate deposition in the world, and inland exposures contain good examples of ancient Neogene non-tropical carbonates. Two examples are summarized here as representative of the depositional models for carbonate shelves in South Australia: the Late Pleistocene-Holocene sedimentation on the Eucla Shelf and an example of an Oligocene-Miocene epeiric cool-water carbonate ramp in the Murray Basin.

1.2.2.1. Eucla Shelf (Great Australian Bight): shaved-shelf model and bryozoan reef mounds (James et al., 1994, 2000, 2001, 2004)

The Eucla Shelf is an open-ocean carbonate shelf in a high-energy, swell-dominated oceanographic setting, the Great Australian Bight (GAB) (Fig. 9). Water circulation in the southern Australian margin is characterised by seasonality. The West Wind Drift (Flinders Current), the Leeuwin Current and the South Australian Current are the three dominant currents. The West Wind Drift is a cold circumpolar current that periodically intrudes into the outer shelf, whereas Leeuwin–South Australian Currents are low-salinity warm currents strong and well-defined in summer and weak and irregular in winter. The interplay of these currents leads to an overall downwelling situation in the Eucla Shelf (Fig. 9). The shelf has a gentle profile, with a very low relief, dipping less than 0.5º up to the shelf edge located at 160–200 m water depth. The shelf is bathymetrically divided into an inner platform that extends up to ~50 m depth, a large middle platform from 50–120 m, and a narrow outer platform from 120–160 m (200 m locally) (James *et al.*, 1994, 2001). The uppermost slope reaches 500 m water depth. Long-period swells (>12 s) in this setting place the fair-weather wave base at ~70 m water depth. Sediment on the seafloor shallower than 70 m (fair-weather wave base) is continuously swept by swells, and slightly mobilized up to 130 m water depth (storm wave base). Sediments deeper than 130 m are only moved during major storms.

Sediment on the shelf is composed of carbonate bioclastic particles, siliceous sponge spicules, lithoclasts, relict grains, quartz grains, and dolomite rhombs. Holocene sediments can be divided into three general facies types: basal rhodolith/bivalve gravel, nearshore bivalve-rich quartzose bioclastic palimpsest sand and offshore fine-grained bryozoan microbioclastic muddy sand. Carbonate production above the fair-weather wave base is active, but as grains are fragmented, abraded, and continuously moved due to swell action, net sediment accumulation is minimal. In deeper zones, muddy, bryozoan-rich and bioturbated sediment accumulates in the outer shelf and upper slope.

The hydrodynamic regime in the shelf conditions the zones of carbonate production, erosion and deposition. In this context, James *et al.* (1994) proposed the term "shaved shelf" for the Holocene carbonate-deposition

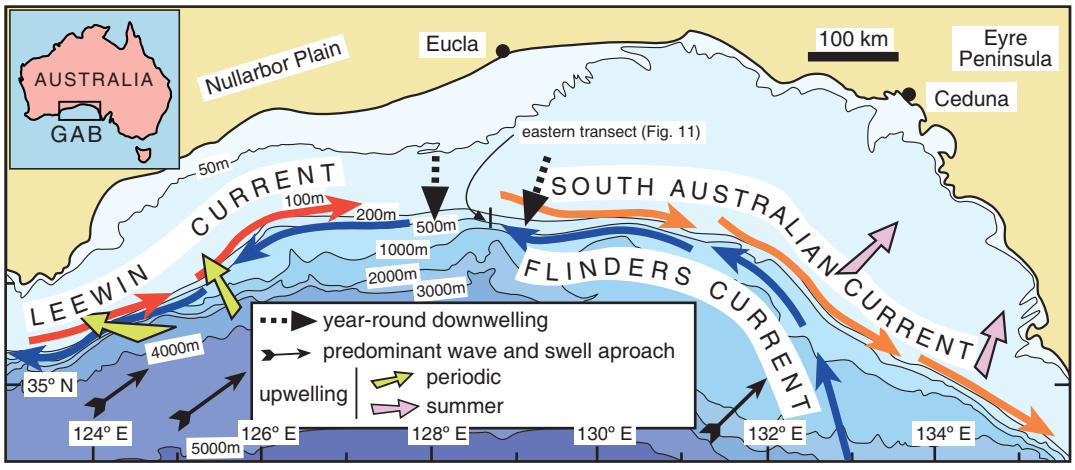

Fig. 9. Location and bathymetric map of the Great Australian Bight (GAB). Major currents are the Leeuwin Current, the South Australian Current and the Flinders Current. Main wave approach direction and overall positions of upwelling and downwelling are also shown (adapted from James *et al.*, 2001).

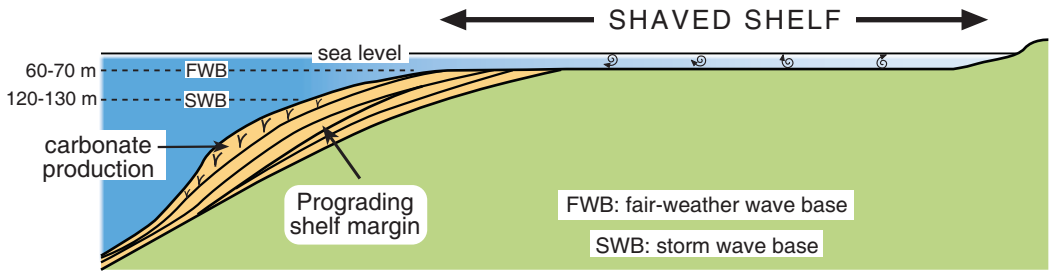

Fig. 10. Shaved-shelf depositional model (James *et al.*, 1994). Continuous action of large swells prevents significant sediment accumulation on the seafloor above the fair-weather wave base (60–70 mwd). Net carbonate production is limited to the outer shelf and upper slope, forming a prograding shelf margin.

style in continental shelves of southern Australia: Eucla Shelf (James *et al.*, 1994, 2001), Lincoln Shelf (James *et al.*, 1997), Lacepede Shelf (James *et al.*, 1992), and Otway Shelf (Boreen and James, 1993) (Fig. 10). Continuous wave action prevents significant sediment accumulation (less than 2 m) on the seafloor above the fair-weather wave base. This constant "shaving" is also enhanced by subaerial, submarine, and ravinement processes linked to sea-level changes. Consequently, net carbonate production only occurs in deep-water zones, producing as a result progradation of the outer shelf and upper slope.

General features of this depositional model can be applied to modern open-ocean temperate shelves in New Zealand (Nelson *et al.*, 1988a) and some ancient examples of cool-water carbonate deposits in southern Australia (James and Bone, 1991), and probably to other open ocean temperate regions.

Bryozoan reef mounds developed periodically on the outer shelf and uppermost slope at (100–240 m water palaeodepth) in the Great Australian Bight during the Pliocene–Pleistocene (James *et al.*, 2004) (Fig. 11). These

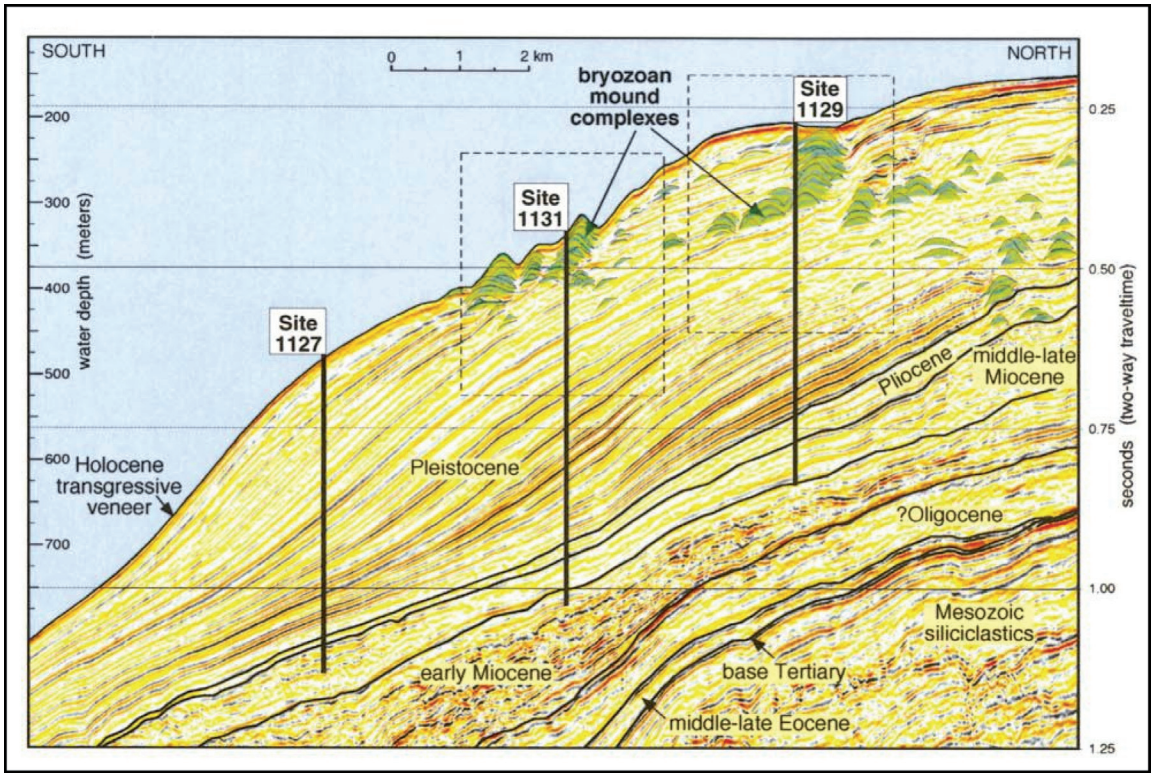

Fig. 11. South-north seismic profile (seismic line AGSO-169/05a) through the eastern transect of ODP Leg 182 (Sites 1129, 1131 and 1127) illustrating the spatial distribution of bryozoan mounds (from James *et al.*, 2004).

biogenic structures, which occur as single mounds or mound complexes, are up to 65 m thick, and they extend 10 km parallel to slope and up to 720 m normal to the slope (James *et al.*, 2000). Mound sediment consists of floatstones rich in well-preserved to fragmented bryozoan skeletons of diverse growth forms, with a packstone matrix made up of foraminifers, sponge spicules, coralline algae, tunicates, ostracods and pellets. Intermound facies contain similar components to those of the mounds but they are commonly fragmented, abraded and bioeroded.

James *et al.* (2000) first proposed that the bryozoan reef mounds in the Great Australian Bight flourished during sea-level lowstands. In these periods, the warm Leeuwin Current, responsible for the dominant downwelling situation in the shelf, weakened, thereby triggering an increase in the nutrient supply by upwelling currents along the continental margin, which promoted bryozoan mound growth. Further, in-depth, studies by James *et al.* (2004) showed that the development of the mounds during sea-level lowstands was due not only to possible local upwelling, but mainly to a general enhanced nutrient supply at the regional scale in the southern oceans (Nelson *et al.*, 1993) and to the northward displacement of the subtropical convergence zone. This situation led to high trophic resources at the palaeoshelf-edge and upper slope of the Great Australian Bight, which promoted the bryozoan mound development. Although bryozoan mound structures are also found in the old geological record, especially in the Palaeozoic (Wilson, 1975; Cuffey, 1977; James and Bourque, 1992; Wahlman, 2002, Webby, 2002), GAB mounds are the first described examples of Quaternary age.

1.2.2.2. Epeiric ramp (Murray Basin) (Lukasik et al., 2000)

The Murray Basin is a large Cenozoic basin located in southeast Australia. The southern part of this basin comprises a structurally elevated granitic and metasedimentary complex (Padthaway Ridge) that formed a string of islands and submerged highs. These reliefs configured an extensive, semi-protected, low-energy shallow sea behind them where an epeiric carbonate ramp developed during the Oligocene–Miocene (Fig. 12). Lagoonal, supratidal and non-evaporitic mudflat sediments were deposited to the north and east of the Murray Basin (Radke, 1987).

Four major sediment facies associations are recognized in the epeiric ramp: 1) A large foraminiferan-bryozoan facies association (FB) made up of photosymbiont-bearing foraminifers, bryozoans, serpulids (*Ditrupa*), bivalves, brachiopods, gastropods, echinoderms, and arthropods.

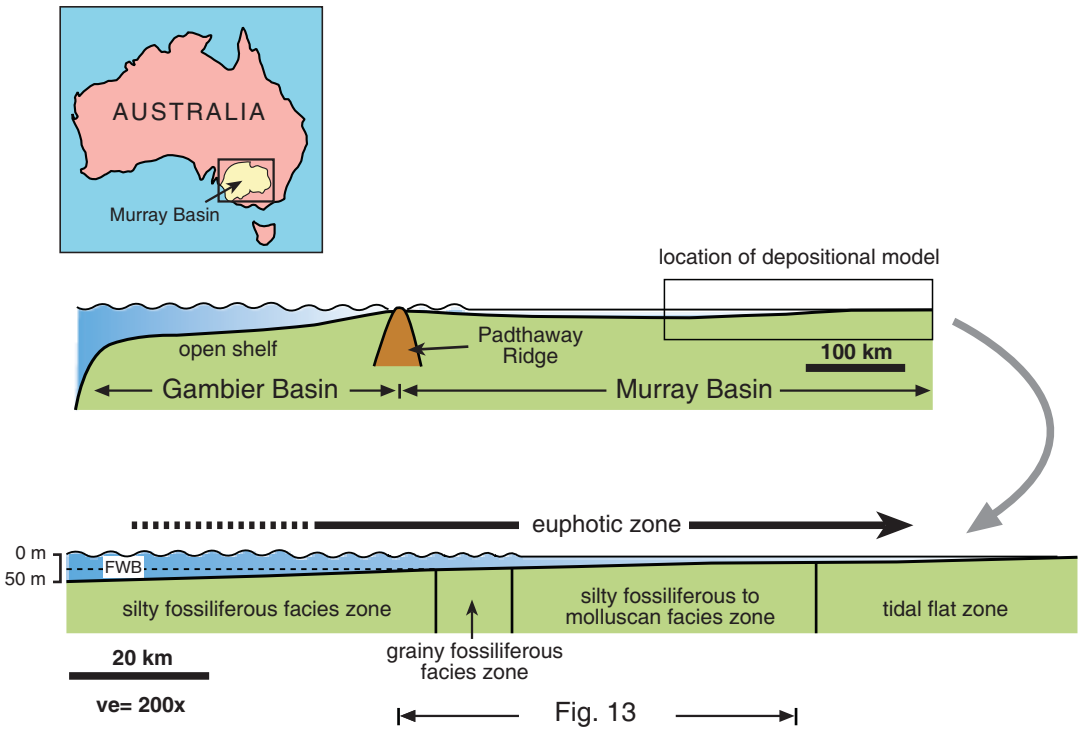

Fig. 12. Location of Murray Basin in South Australia (inset) and position of epeiric ramp depositional model (from Lukasik *et al.*, 2000) within Murray Basin, showing general facies distribution. FWB: Fair-weather wave base; ve: vertical scale.

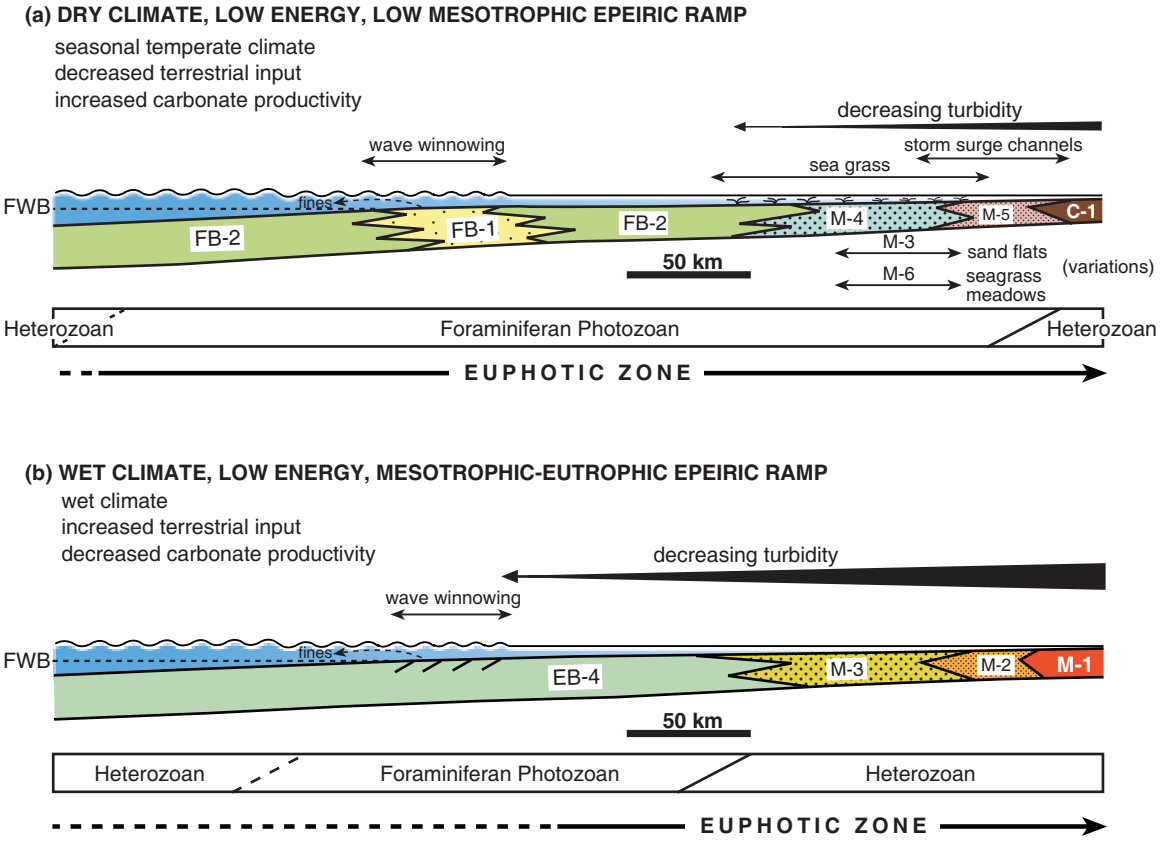

Fig. 13. Depositional facies models for the epeiric ramp in Murray Basin (from Lukasik *et al.*, 2000) illustrating distribution of main facies associations (FB, EB, M, and C). Two different sedimentary models developed depending on the regional climate and trophic resources in the ramp. Type and distribution of skeletal grain associations (heterozoan/photozoan) are also indicated. See Lukasik *et al.* (2000) for detailed subfacies description.

This association is divided into three facies: FB-1, FB-2 and FB-3. Facies FB-1 and FB-3 are grainy facies characterised by the presence of hardgrounds encrusted by bryozoans, oysters and coralline algae, and exhibiting high degrees of clast fragmentation and abrasion. Facies FB-2 is a bryozoan floatstone with excellent faunal preservation. 2) An echinoid-bryozoan facies association (EB) that comprises four facies types of echinoid rudstones and floatstones with up to 30% terrigenous clasts. 3) A mollusc facies association (M) with six facies types according to the dominant faunal components. 4) A clay facies (C) made up of green clay and molluscan floatstone beds that grade laterally and vertically into the mollusc facies association.

Lukasik *et al.* (2000) consider that organism diversity and abundance were related to trophic resource levels at the time of deposition. These authors interpreted the above facies associations as follows: sediments of the FB association, classified as a foraminiferan photozoan facies association, deposited under low- to high-energy, illuminated, relatively oligotrophic conditions; EB association deposited in slightly eutrophic to mesotrophic conditions at shallow to moderate depths; M association corresponds to sediments accumulated in shallow (<10 m), low- to moderate-energy, eutrophic to mesotrophic conditions; C facies were deposited in a shallow, low subtidal, nearshore setting.

Two depositional facies models for the Oligocene–Miocene epeiric ramp in the Murray Basin are inferred by Lukasik *et al.* (2000) depending on the regional climate and its influence on the trophic resource levels in the water (Fig. 13): (1) dry climate, low-mesotrophic conditions, during which little run-off to the sea resulted in low nutrient levels in the water column. This allowed high carbonate productivity and the subsequent development and spread of the foraminiferan photozoan facies association (FB), with sparse seagrass meadows and eutrophic facies (M and C) in nearshore settings. Hardgrounds formed under constant wave reworking that also produced abrasion and fragmentation of the bioclastic particles (FB); (2) wet climate, high-mesotrophic-eutrophic conditions during which the delivery of relatively high amounts of terrigenous sediments and nutrients into the

shallow sea produced an increase in turbidity and trophic resource levels in the water column. This rise led to the eutrophication of the nearshore waters, resulting in low rates of carbonate sedimentation with dispersed and patchy distribution of the flora and epifauna (M). Offshore facies rich in echinoids and gastropods (EB) reflect mesotrophic conditions.

1.2.3. North New Zealand

New Zealand is one of the most important temperate carbonate provinces in the world (Nelson *et al.*, 1988a). Despite being located in a tectonically active region (Australian-Pacific plate boundary) with relatively high terrigenous input into the sea, modern, cool-water carbonate deposition is taking place on shelves at different sites (Kamp and Nelson, 1988; Nelson *et al.*, 1988a; Gillespie and Nelson, 1996, 1997). Ancient counterparts (Oligocene to Pliocene) are even better represented in New Zealand, especially in the North Island (Nelson, 1978; Nelson *et al.*, 1994, 2003; Hayton *et al.*, 1995; Caron *et al.*, 2004a,b, 2005; Dix and Nelson, 2004). However, although temperate carbonates in New Zealand are abundant and well represented in modern and ancient basins, relatively few depositional models are inferred for these deposits (Nodder *et al.*, 1990; Hayton *et al.*, 1995; Nelson *et al.*, 2003; Caron *et al.*, 2004b), probably because studies focus mainly on aspects related to diagenesis (Nelson *et al.*, 1988b; Hood and Nelson, 1996; Nelson and Smith, 1996; Hood *et al.*, 2004a; Dix and Nelson, 2006), tectonics (Dix and Nelson, 2004), skeletal components and distribution (Nelson and Hancock, 1984; Nelson *et al.*, 1988a; Gillespie and Nelson, 1996, 1997), or sequence stratigraphy (Gillespie *et al.*, 1998; Caron *et al.*, 2004a, 2005).

This section summarises the depositional model proposed by Caron *et al.* (2004b) for Pliocene temperate carbonates in Hawke's Bay, northeast New Zealand and, in the absence of any model for modern carbonate deposition, the main characteristics of the recent, mixed carbonate-siliciclastic sediments in the Wanganui shelf (Gillespie and Nelson, 1996, 1997, Gillespie *et al.*, 1998) are listed below.

1.2.3.1. Pliocene temperate carbonates in the Hawke's Bay Basin (Caron et al., 2004b)

The Hawke's Bay Basin is a forearc basin located in the eastern North Island of New Zealand that has formed in response to the evolution of the convergent Australian/Pacific plate boundary zone since the Oligocene (Ballance, 1993). This forearc basin is a structural depression associated with an eastward subduction accretionary complex that consists of thrust fault-controlled anticlinal ridges and synclinal parallel basins, bounded to the east by a structural

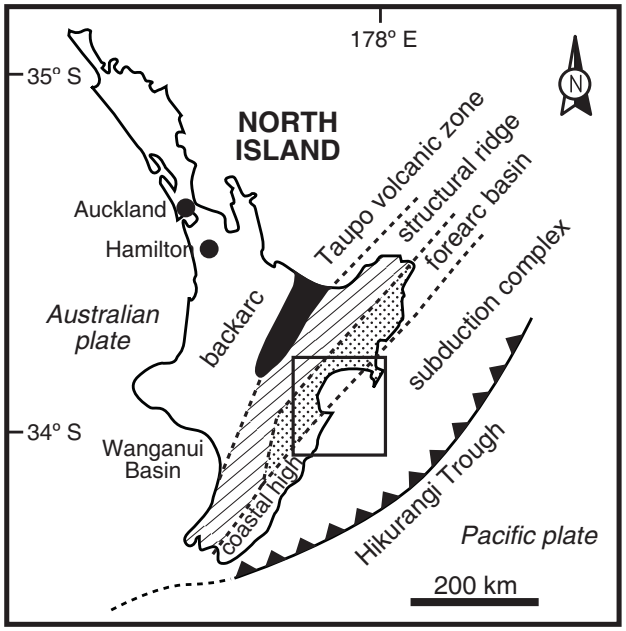

Fig. 14. Tectonic setting of the North Island of New Zealand. Inset marks the position of the Hawke's Bay.

ridge of Mesozoic basement (Caron *et al.*, 2004b) (Fig. 14). The Neogene basin fill comprises a sequence of marine sandstones, mudstones, flysch and carbonates up to 6 km thick, of which Pliocene carbonates (Te Aute limestones), though minor components, can be locally thick and quite extensive. Since the mid-Pliocene, the forearc basin has formed a seaway (Ruataniwha Strait of Beu, 1995) where carbonate units developed to the east as isolated banks on top of deforming anticlines and submarine highs, and were deposited on a land-attached ramp to the west (Fig. 15).

Caron *et al.* (2004b) proposed fourteen depositional facies grouped into three major facies assemblages: bioclastics (B), mixed carbonates-siliciclastics (M) and siliciclastics (S). These authors also distinguished three major skeletal associations: barnamol (barnacle -and bivalve mollusc-dominated), bimol (dominated by bivalves), and bryomol (bryozoan-dominated), and six petrographic microfacies with incorporated terrigenous clasts (see Caron *et al.*, 2004b for fully detailed description).

Two different depositional models were proposed for the middle- to early late-Pliocene temperate carbonates in the Hawke's Bay Basin: a continent-attached mixed carbonate-siliciclastic ramp to the west and land-detached isolated banks to the east (Caron *et al.*, 2004b) (Fig. 15). The ramp at the western margin was narrow, had a gentle profile and was swept by tidal and storm currents. Terrigenous basement-derived sediments by-passed the ramp preferentially along channels and incised valleys to deep-water settings of the Ruataniwha Strait.

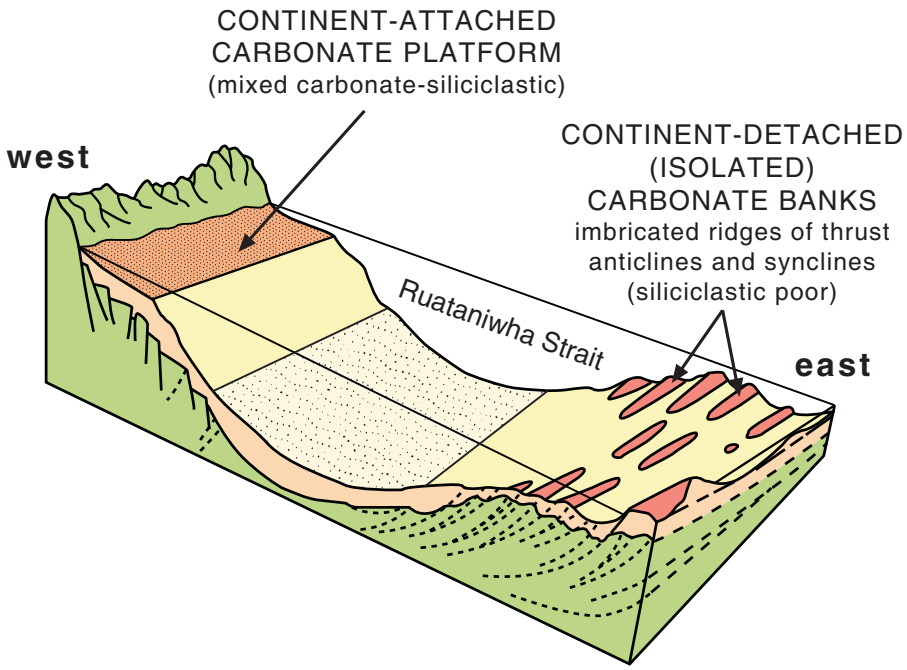

Fig. 15. Schematic palaeogeographic reconstruction of the Hawke's Bay forearc basin during the Pliocene. Two types of carbonate production sites developed: continental-attached carbonate platforms to the west and isolated banks on top of structural ridges of thrust anticlines to the east (from Caron *et al.*, 2004b).

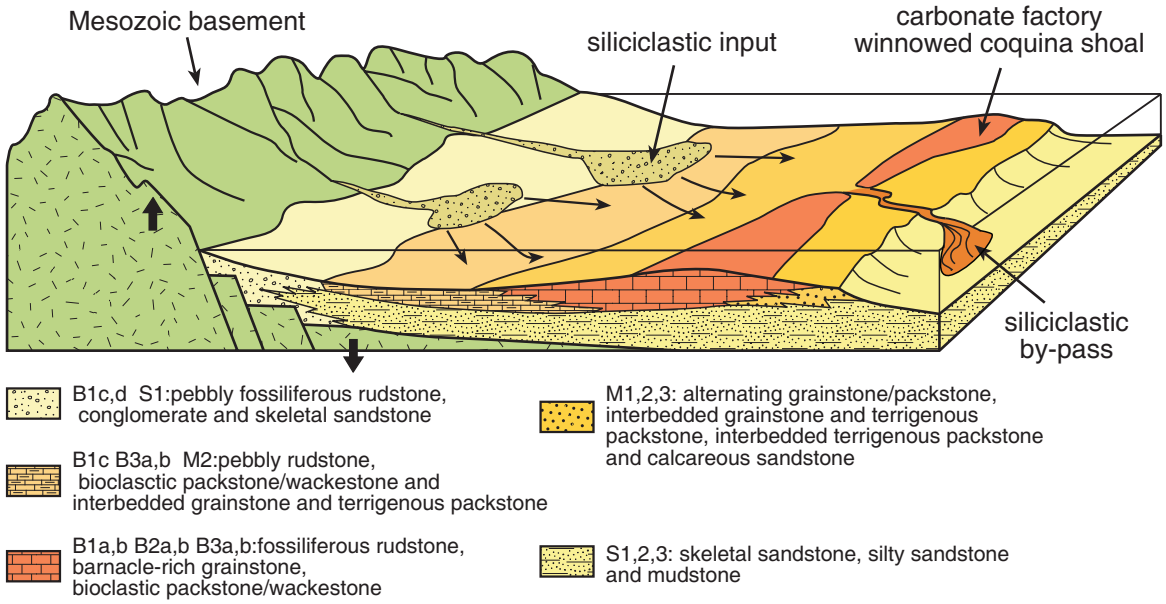

Fig. 16. Proposed depositional model for temperate-carbonate platform attached to a landmass at the western margin of the forearc basin in central Hawke's Bay (from Caron *et al.*, 2004b). See Caron *et al.* (2004b) for detailed facies description.

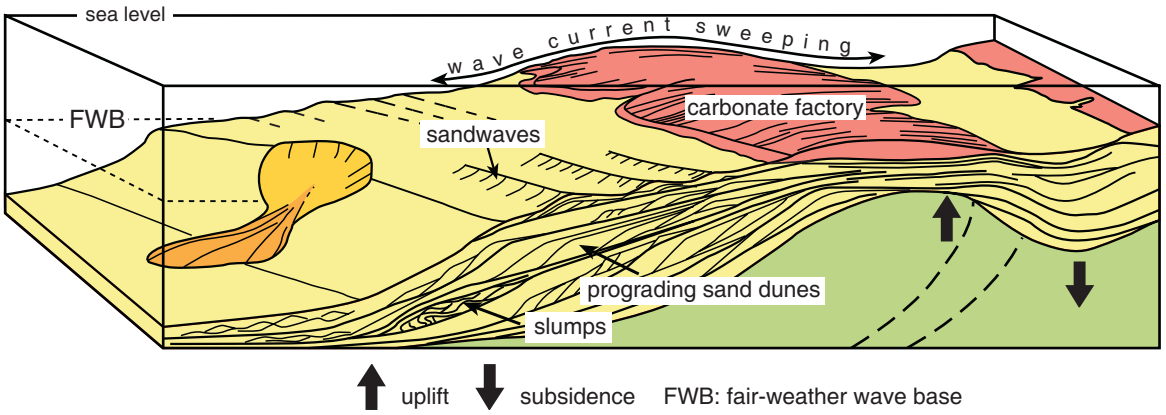

Fig. 17. Proposed depositional model of isolated carbonate banks at the eastern margin of the forearc basin in central Hawke's Bay (from Caron *et al.*, 2004b).

Bryozoan- and barnacle-dominated carbonate factories developed on rocky shores or on inner- to mid-ramp settings. Carbonate sediment was swept and winnowed by currents and accumulated as coquina shoals (Fig. 16). At the eastern margin, carbonate factories (barnacle- and bivalve-dominated) developed on syn-sedimentary tectonic highs (anticlines) cut by tidal-influenced channels. Bioclasts were shed from the factories by strong tidal and storm currents, and accumulated in the form of prograding dunes on the anticline flanks (Fig. 17).

These suggested depositional models of temperate carbonates show how inherited palaeotopography, hydrodynamics and terrigenous supply influence carbonate development and can help to interpret the occurrence of carbonate deposits in similar forearc basins (Caron *et al.*, 2004b).

1.2.3.2. Modern mixed carbonate-siliciclastic sediments in the Wanganui shelf (Gillespie and Nelson, 1996, 1997, Gillespie et al., 1998)

The Wanganui shelf lies within the South Taranaki and Wanganui bights, in the western central region of the New Zealand Greater Cook Straits (Fig. 18). This region forms part of the backarc system behind the present Australian-Pacific convergent plate boundary. The Wanganui shelf has a gentle profile (<1°), with water depths of less than 125 m and oceanic and storm-generated currents and tidal currents related to the tidally-swept Cook Straits Narrow to the south (Gillespie and Nelson, 1997). These currents put sediment into suspension at depths of ~70 m, reaching as far as 130 m during major storms.

Five surficial sediment facies are identified in the Wanganui shelf (Gillespie, 1992; Gillespie and Nelson, 1996) and are analogous to the subsurface facies (Gillespie and Nelson, 1997) (Fig. 19). *Facies 1* (bivalve-bearing gravelly sand) is divided into two subfacies: subfacies 1a (siliciclastic sand), in the inner shelf (<50 m depth), represents a modern prograding sand prism chiefly made up of fine sand derived mainly from North Island sediments, with interspersed skeletal fragments; subfacies 1b (bivalve-bearing volcaniclastic gravelly sand) comprises relict and palimpsest volcanic fragments, with bivalve shells, deposited in shallow-water settings on the northern part of the shelf.

Facies 2 (skeletal-dominated sandy gravel): is a temperate-carbonate facies whose development is controlled by low terrigenous input to the inner-middle shelf and the existence of suitable substrates for biogenic colonisation (bryomol association). It can be divided into three subfacies: subfacies 2a (bivalve-dominated sandy gravel) is immediately seawards of subfacies 1a on the inner-middle shelf (30–50 m water depth); subfacies 2b (bryozoan/bivalve-dominated sandy gravel) accumulates at 40–65 m water depth; and subfacies 2c (bryozoan/bivalve-dominated muddy sand) forms in deeper waters (50–90 m).

Facies 3 (bivalve-bearing muddy sand) is a mud-dominated facies present on the middle-outer shelf at depths of 80–100 m. Most of the bioclasts are fragmented and abraded and probably derive from Facies 2.

Facies 4 (siliciclastic mud) is deeper than Facies 3, although it also occurs in the middle-outer shelf (85–110 m). The terrigenous material comes from both the North and the South Island.

Facies 5 (micaceous sand) is a terrigenous-dominated facies supplied from the South Island that extends over areas of more than 100 m water depth.

Surficial carbonate deposits in the Wanganui shelf form a carbonate-rich lense zone (factory zone) (Facies 2)

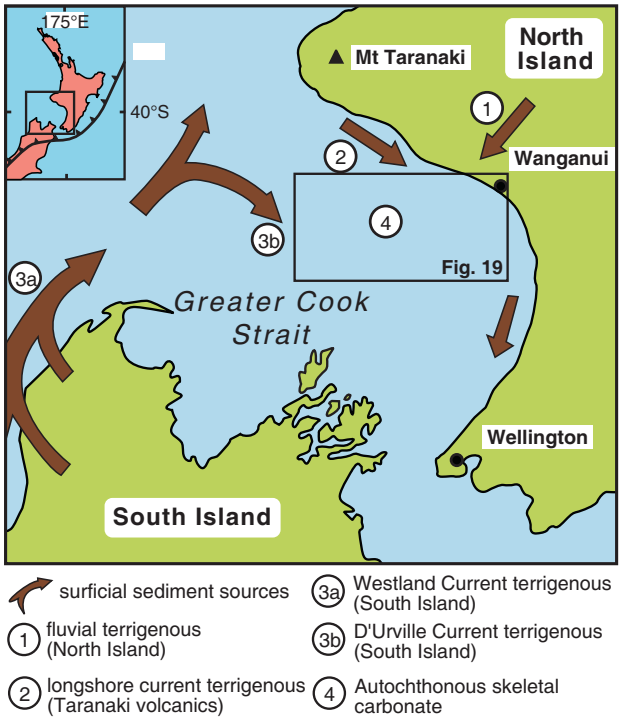

Fig. 18. Location of the Wanganui shelf (insets show area studied by Gillespie and Nelson, 1996, 1997, Gillespie *et al.*, 1998) within the Greater Cook Strait indicating main surficial sediment sources in the area (adapted from Gillespie and Nelson, 1996).

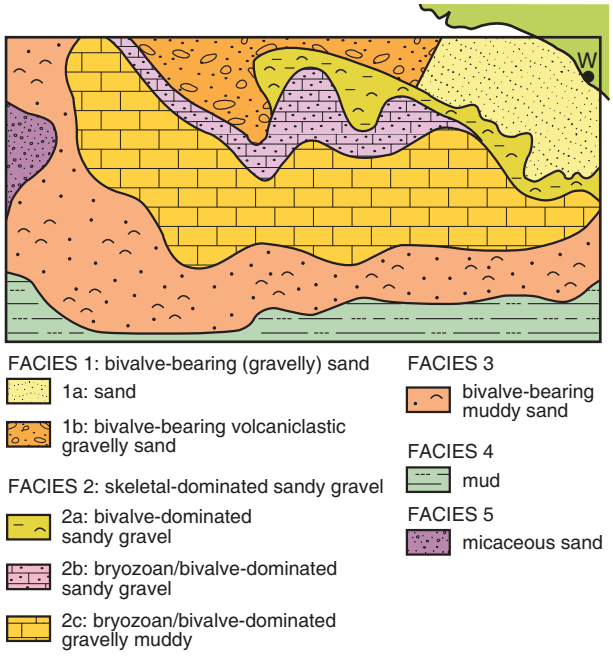

Fig. 19. Areal distribution of surficial sediment facies on the Wanganui shelf (from Gillespie and Nelson, 1997).

on the inner and middle shelf, surrounded by terrigenous sediments (Gillespie and Nelson, 1997) (Fig. 19). This sediment distribution (carbonates and terrigenous) results from the combination of three factors: the onland geology (terrigenous sediment sources provided by the active tectonic setting); the post-glacial sea-level rise that helped to trap terrigenous sediment along the shoreline and favoured the development of a bryozoan/bivalve-rich carbonate factory offshore (see Gillespie *et al.*, 1998 for further details about post-glacial history); and the hydrodynamic regime in the Greater Cook Straits, which no doubt influenced sediment distribution.

Wanganui shelf sediments differ from the open-ocean temperate platforms of southern Australia mainly in their higher mud content (both terrigenous and carbonate mud), higher sedimentation rates (5–10 cm/ky), more abundant aragonitic bioclasts (infaunal bivalves) and the type of substrate for the epifauna (large bivalve shells in the Wanganui shelf versus rocky surfaces in southern Australia shelves).

1.2.4. Other examples

1.2.4.1. Polar carbonates

Carbonate sedimentation in Polar Regions constitutes the end member of shallow-water carbonate deposition. Cold-water (<10°C) settings have traditionally been thought to be zones of inhibited carbonate deposition because of the higher solubility of calcium carbonate in cold waters and the subsequent slow biogenic precipitation rate. However, modern cold-water carbonate deposition does occur in high latitudes (Hosking and Nelson, 1969; Domack, 1988; Andruleit *et al.*, 1996; Henrich *et al.*, 1997; Freiwald, 1998; Rao *et al.*, 1998), usually in settings of minimum terrigenous sedimentation and high nutrient supply, and some ancient carbonate deposits are interpreted to have formed in such contexts as well (Beuchamp and Desrochers, 1997; Stemmerik, 1997; Rogala *et al.*, 2007). Two examples of cold-water carbonate depositional models, one modern (Spitsbergen Bank, Henrich *et al.*, 1997) and the other ancient (Lower Parmeener Supergroup, Rogala *et al.*, 2007), are exemplified here.

a) Spitsbergen Bank (Barents Sea) (Henrich et al., 1997)

Spitsbergen Bank is the largest open-shelf cold-water carbonate platform in the Arctic region (Barents Sea) (Fig. 20). This shallow-water bank is bordered by deep-water troughs (Bear Island and Storfjord Trough) (Fig. 21). Relatively warm Atlantic waters fill the trough, whereas the carbonate bank top is capped by cold Polar waters (Fig. 20). The Spitsbergen Bank is covered by sea ice for

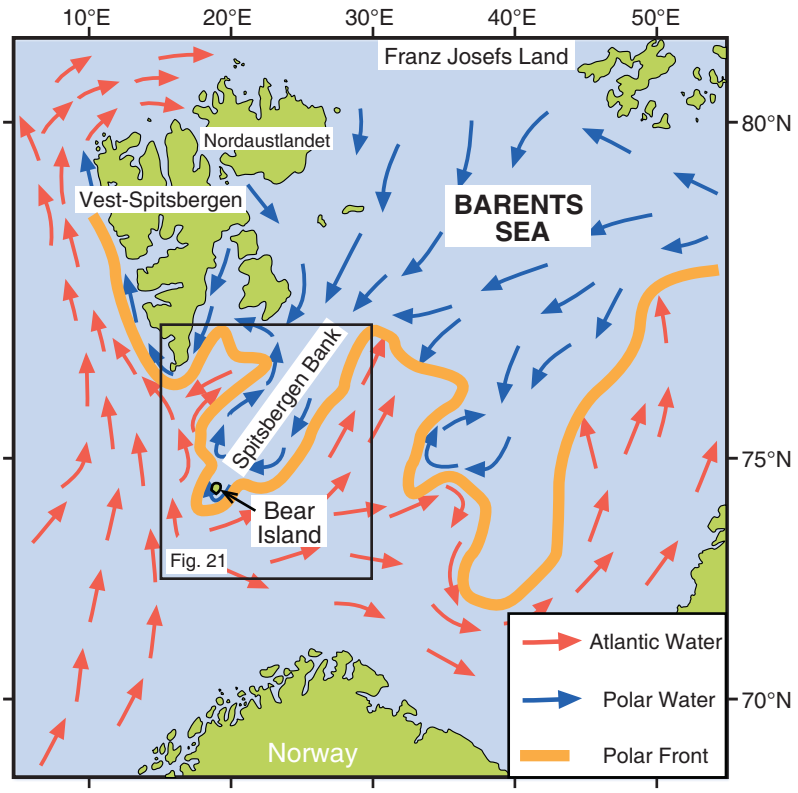

Fig. 20. Oceanographic setting in the Barents Sea. Troughs surrounding Spitsbergen Bank are dominated by warm Atlantic water, while cold Polar water prevails on the shallow-water bank. Location of the Polar Front and Fig. 21 are shown (from Henrich *et al.*, 1997).

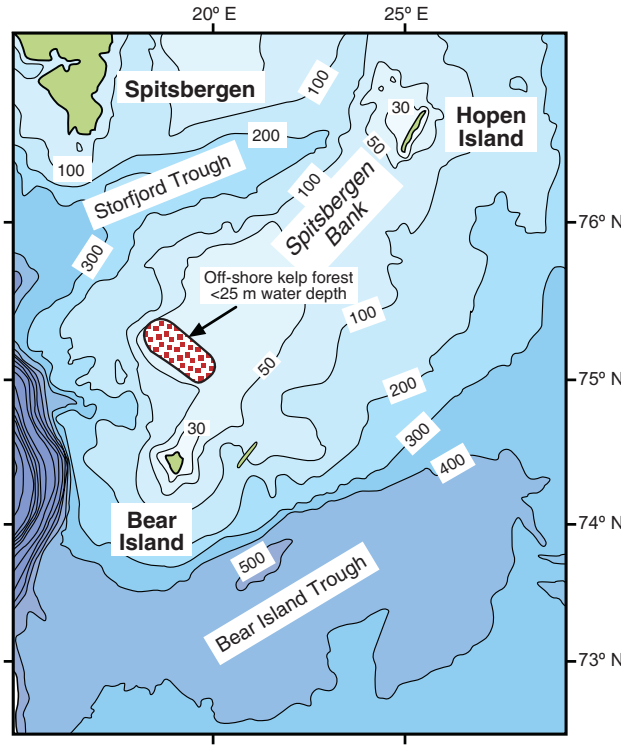

◀ **Fig. 21.** Bathymetry of Spitsbergen Bank between Bear Island and Hopen Island, illustrating position of Storfjord Trough to the north and Bear Island Trough to the south of the bank (from Henrich *et al.*, 1997).

6 months in winter. Summer ice melting results in salinity reduction at the surface but does not affect the water on top of the bank.

Lithoclasts on the Spitsbergen Bank consist of pebbles of the Mesozoic bedrock that are interpreted as glaciogenically reworked deposits from the underlying basement (Bjørlykke *et al.*, 1978). Bioclasts comprise abundant balanids, bivalves, benthic foraminifers, minor bryozoans, gastropods, echinoids, brachiopods, serpulids and ophiuroids. There is a bathymetric zonation of the biological constituents that occur in different facies belts (Fig. 22). Kelp forests (*Laminaria saccharina*) cover rocky substrates, including pebble and boulder pavements in waters shallower than 25 m. Balanids (*Balanus crenatus*) colonise as well the sea bottom between the kelp. Post-mortem, storm and current reworking of the balanid

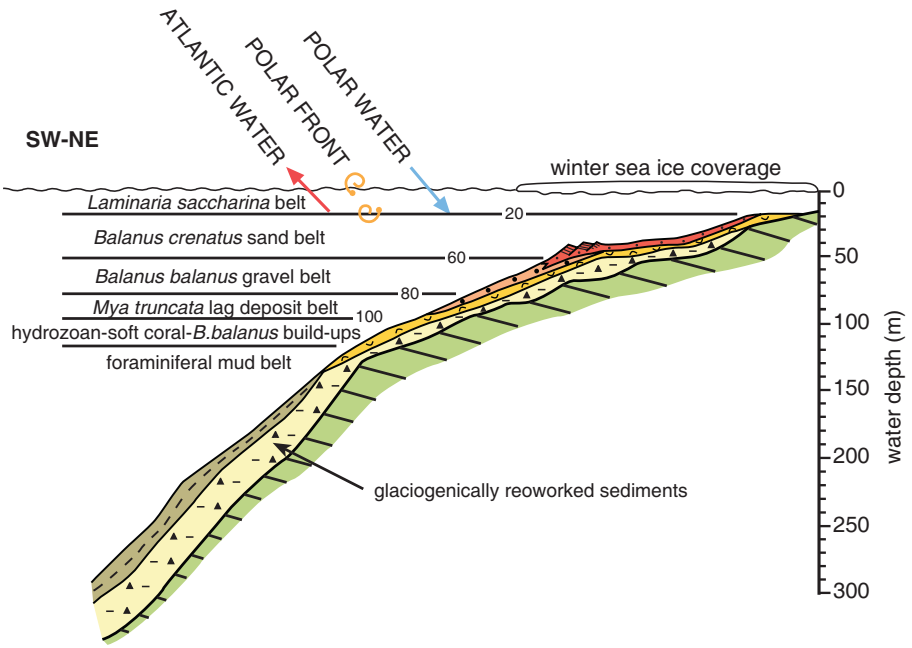

Fig. 22. Facies belt distribution along the southwestern margin of Spitsbergen Bank (from Henrich *et al.*, 1997).

remains produce sand-size particles that are transported to the bank margin forming submarine dunes. Gravels of fragmented and bio-eroded balanids (*Balanus balanus*) accumulate in the bank flanks in water depths of 50–80 m. Bivalves (*Mya truncata*) and echinoids are also important bioclastic components in the gravel. The sediment in the gravel belt is locally encrusted by bryozoans, ascidians and coralline algae. At ~80 m the seafloor is covered by a gravel lag deposit made up mainly of *Mya truncata* and reworked lithogenic particles. Small patch mounds composed of balanids (*Balanus balanus*), soft corals, bryozoans, and hydrozoans extend over the substrate at 100–120 m water depth. Below 120 m, the sediment consists of foraminifer-rich sandy muds and muds.

The depositional model inferred for the polar carbonate deposits in Spitsbergen Bank is shown in Figure 23. Two main carbonate factories developed at different positions within the bank, kelp forests associated with *Balanus crenatus* in the shallowest rocky parts of the bank and *Balanus balanus*-bryozoan-hydrozoan-soft-coral patch mounds on the bank slope, with high productivity conditions along the Polar Front between Atlantic and Arctic waters (Henrich *et al.*, 1997). Carbonate production is inhibited in zones where clastic discharge and seafloor erosion from icebergs occur and in the bank margins where strong currents pile the sediment into submarine dunes.

b) Lower Parmeener Supergroup: an Early Permian cold-water shelf in Tasmania (Rogala et al., 2007)

During the Permian, Tasmania was located at approximately 70ºS, forming part of the Pangaean supercontinent (Fig. 24). The Lower Parmeener Supergroup (latest Carboniferous–Middle Permian) comprises several facies associations that illustrate the transition from cold-water carbonate and mixed siliciclastic deposits to similar temperate deposits as a result of the northward movement of the Pangaean supercontinent. Facies associations are (Rogala *et al.*, 2007):

1) Diamictite, rhythmite, and glendonitic siltstones containing some marine bioclasts together with some *Tasmanites* (marine algae) oil-shale deposits. This facies association is interpreted to have been deposited in a glaciomarine, fjord-like environment.

2) Cross-bedded sandstones, mudstones and coals interpreted as stream floodplain deposits.

3) Sandstone and bioturbated mudstone facies accumulated in a peritidal setting, with tidal flats, intertidal channels, and a shoal system.

4) Pebbly sandstone, which overlies the Facies Association 3 and contains some bioclastic remains, is interpreted as a shoreface lag deposit.

5) Bioturbated mudstones and poorly fossiliferous siltstones that contain ostracods to the north and

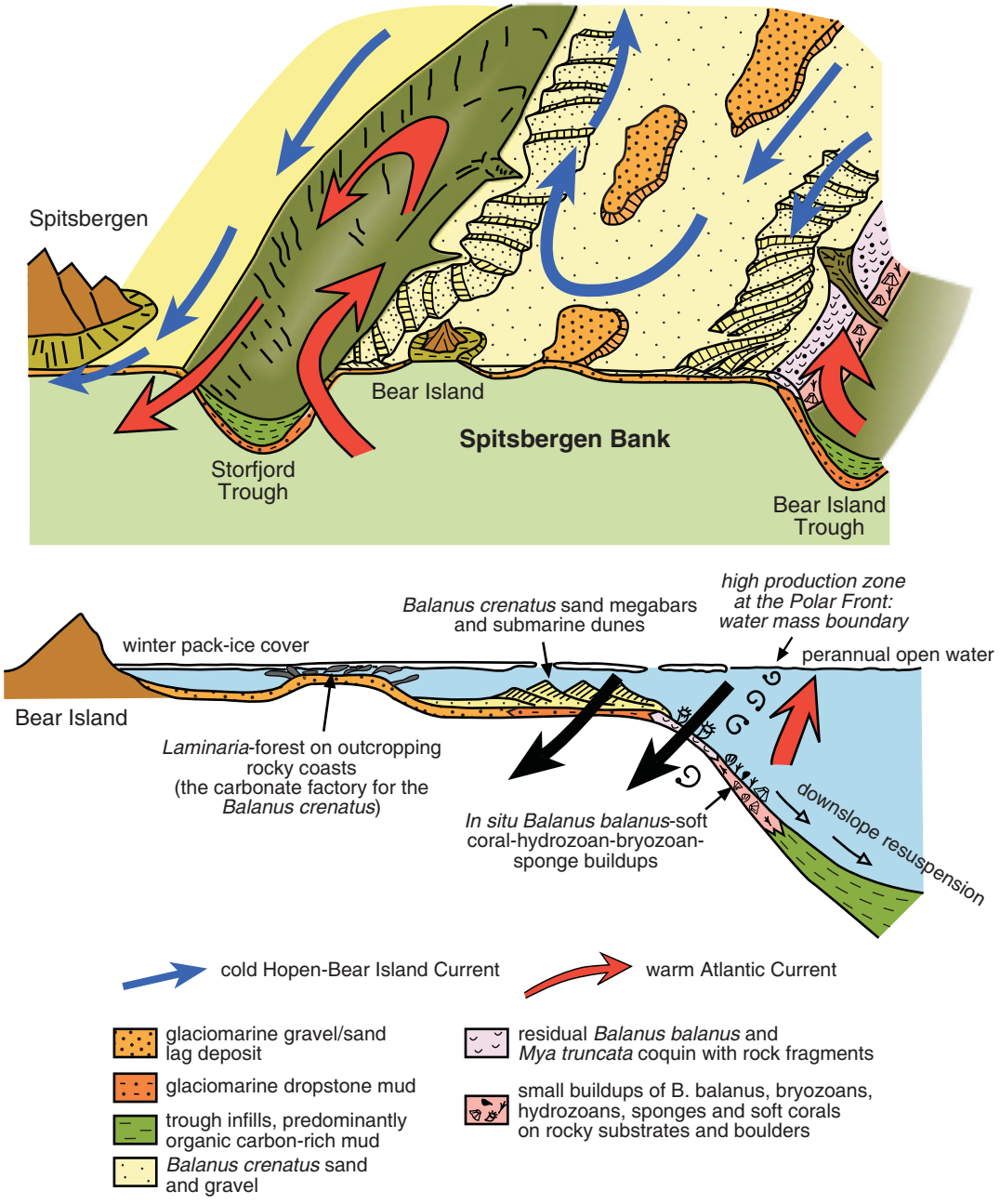

Fig. 23. Depositional model of the cold-water carbonates at Spitsbergen Bank. Distribution of main water currents on the bank is illustrated (from Henrich *et al.*, 1997).

brachiopods and bryozoans to the south. This facies association is interpreted to have formed in an inner-shelf palaeonvironment, with freshwater influence in the proximal part (north) and normal marine water basinwards (south).

6) Fossiliferous siltstone and limestone facies composed of fossiliferous siltstones, argillaceous limestones, pure limestones and spiculitic limestones. This essentially carbonate facies association contains abundant brachiopods, *Eurydesma* shells and sponge spicules, common bryozoans and crinoids, and lesser amounts of plant fragments. These sediments were deposited along mid-shelf settings.

7) Fossiliferous sandstones and siltstones and turdibitic sandstones. This facies association contains brachiopod and bryozoan skeletons and is interpreted to have been deposited in an outer-shelf environment.

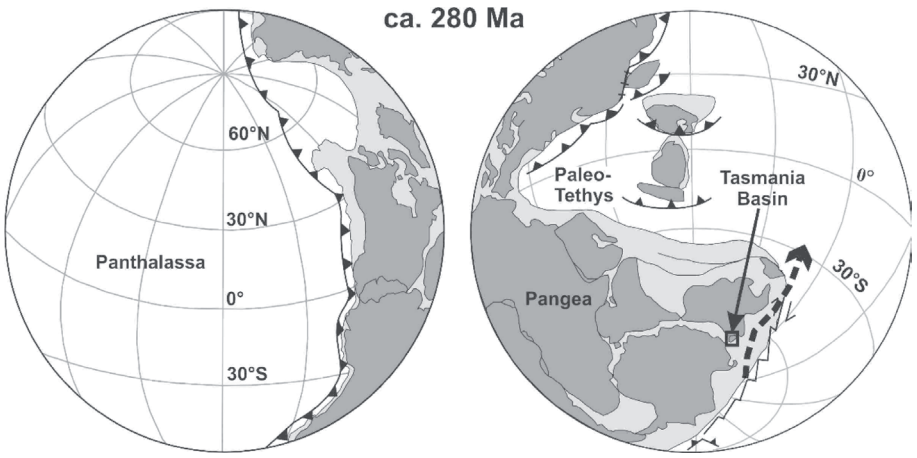

Fig. 24. Reconstruction of Pangaea (Ca. 280 Ma) (from Rogala *et al.*, 2007). Present-day continental land masses (including continental shelves) are shown in dark grey and Permian shelves in light grey. Dashed lines indicate the inferred direction of ocean currents.

Lateral and vertical changes of the previous facies association were divided by Rogala *et al.* (2007) into four time slides, covering the late Carboniferous to middle Permian, which represents the change from an ice-covered sea to an ice-free sea with isolated icebergs.

Phase 1) Latest Carboniferous-Asselian (~300–295 Ma) (Fig. 25). Sediment deposited during this period reflects regional deglaciation (Rogala *et al.*, 2007). The inner shelf was segmented due to irregular palaeotopography. U-shaped valleys were filled with glaciomarine diamictites and lacustrine rhythmites after glacier retreat. Siltstone-bearing glendonite deposits onlap the glaciogenic sediments and Tasmanite oil shales were deposited on the inner shelf.

Phase 2) Sakmarian (~295–286 Ma) (Fig. 26). Sparse fossiliferous siltstones extended over the still-segmented inner shelf, grading basinwards to fossiliferous siltstones with intercalated *Eurydesma* shoals and brachiopod-rich argillaceous limestones in the middle shelf. Plant remains, dropstones, and phosphates are especially common in the middle- to outer-shelf transition.

Phase 3) Late Sakmarian–early Artinskian (~286–283 Ma) (Fig. 27). During this time of lowered sea-level, alluvial and coastal sediments prograded along the basin. Carbonate deposits were limited to the inner shelf: ostracod-dominated sediments near the coast and brachiopod-rich in outboard settings. Glendonite and plant fragments also occur in the coastal sediments.

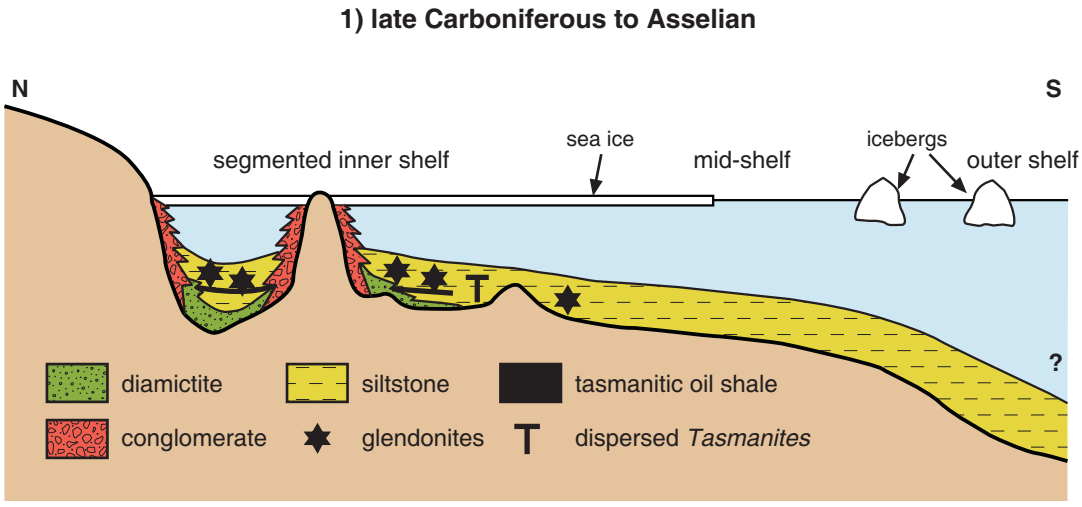

Fig. 25. Depositional model for the Tasmanian shelf during the latest Carboniferous–Asselian (~300–295 Ma) (from Rogala *et al.*, 2007).

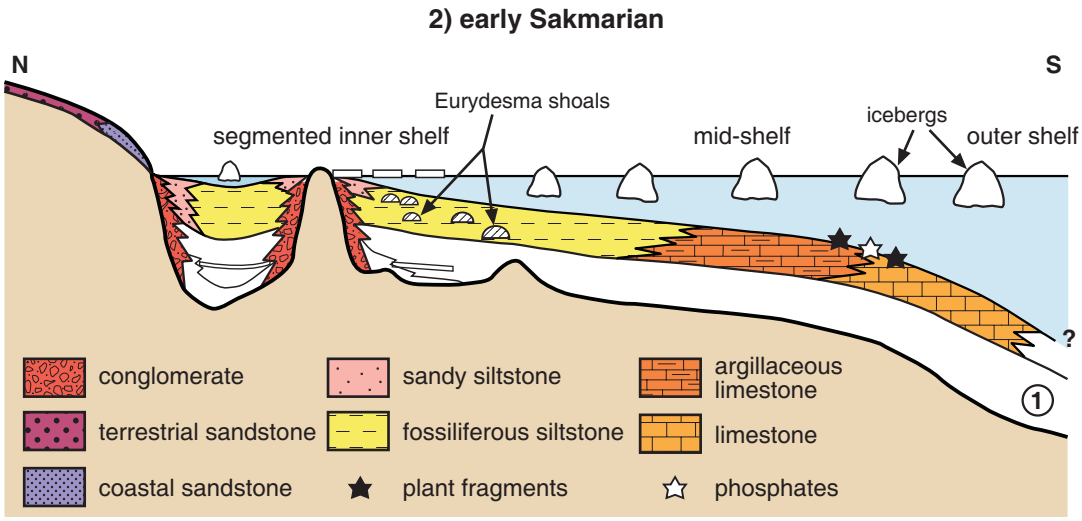

Fig. 26. Depositional model for the Tasmanian shelf during the early Sakmarian (~295–286 Ma) (from Rogala *et al.*, 2007).

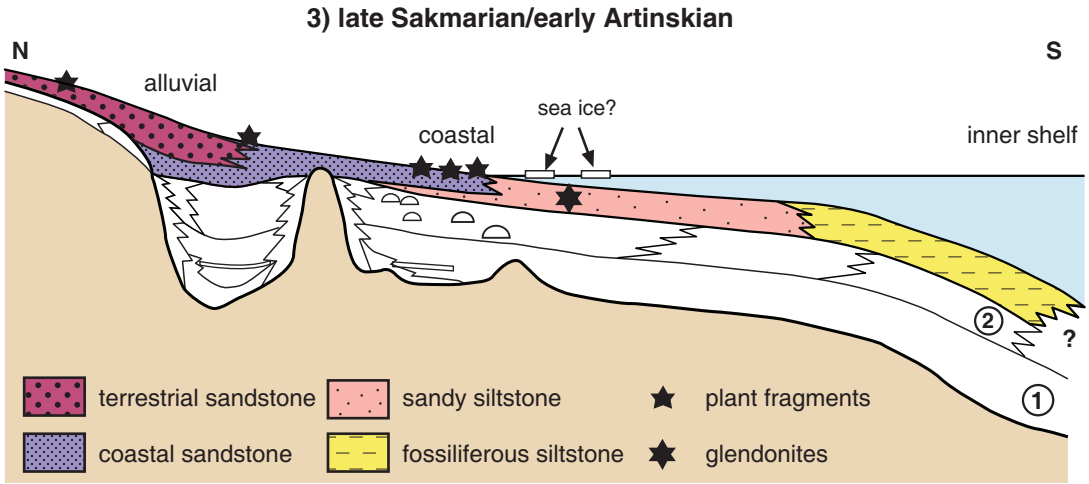

Fig. 27. Depositional model for the Tasmanian shelf during the late Sakmarian-early Artinskian (~286–283 Ma)(from Rogala *et al.*, 2007).

Phase 4) Artinskian (~283–276 Ma) (Fig. 28). Full marine conditions prevailed during this period of relative sea-level rise and highstand. Sandy and fossiliferous siltstones deposited in the inner shelf graded into argillaceous limestones and pure limestones in the middle shelf, where phosphates and plant remains were abundant. Sandstone turbidites were deposited in the basin from the outer shelf.

The interpretation of the Permian polar carbonates in Tasmania made by Rogala *et al.* (2007) shows that carbonate factories developed preferentially in outboard settings, far from the iceberg grounding line. Open-ocean settings supported the high trophic resources necessary for the maintenance of biogenic carbonate production in the carbonate-undersaturated cold waters supplied by upwelling currents (interpreted from the presence of phosphate deposits) and iceberg shedding. Tasmanian cold-water carbonates contain bioclastic components (mainly bryozoans, brachiopods and bivalves) that are characteristic of the heterozoan assemblage (James, 1997) but lack coralline algae and conodonts. These polar carbonates are associated with dropstones and glendonite, which indicate ice and cold-water conditions.

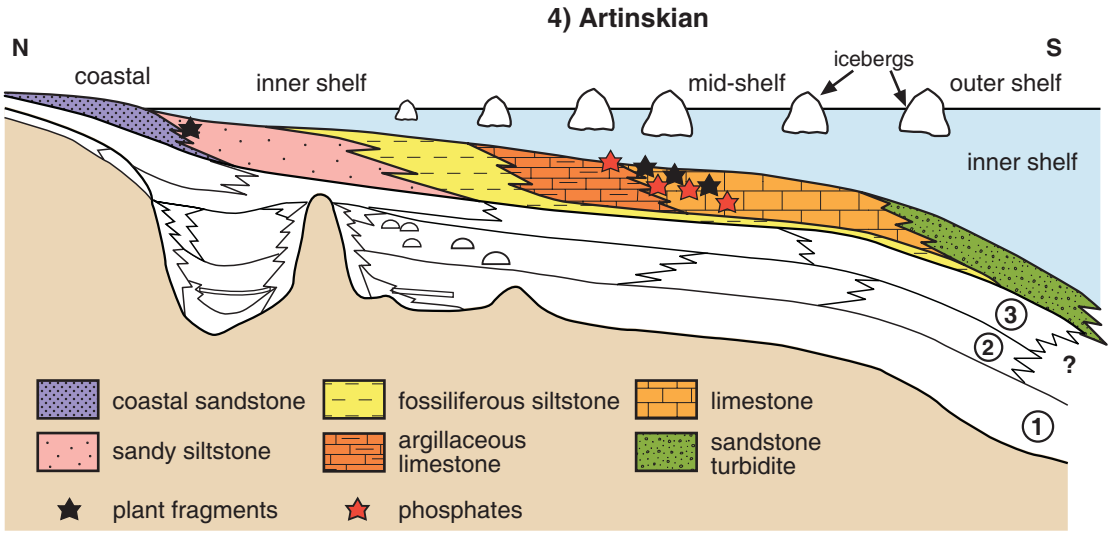

Fig. 28. Depositional model for the Tasmanian shelf during the Artinskian (~283–276 Ma) (from Rogala *et al.*, 2007).

1.2.4.2. Other occurrences of temperate carbonates worldwide

Some of the most significant depositional models of temperate carbonates described up to now have been summarized in the previous section, but there are some others as well studied that deserve mention.

a) Other Mediterranean temperate carbonates

Apart from southern Spain, most studies carried out on temperate carbonates in the Mediterranean region are from Italian and Greek basins.

Examples of submarine channel and fan deposits of Aquitanian to Serravallian age from Sardinia (Italy) are described by Vigorito *et al.* (2005, 2006). These authors recognised different architectural elements within large-scale (up to 4 km wide and 60–300 m deep) channels such as overbank deposits, levees, channel margins, lateral bars, and the channel thalweg. Channel infilling consists of several channel-fill units separated by erosional surfaces, which indicates multistory development of the main channel. Geometric features and spatial distribution of submarine fan deposits are controlled by the type and rate of sediment provided by the submarine channels at different times during sea-level changes. Recently, Bassi *et al.* (2006) focussed on the palaeoecology of the different depositional settings and palaeoceanographic controls on the development of a channel system.

Pedley and Grasso (2002, 2006) have studied the response of temperate carbonates to glacio-eustatically driven sea-level changes in Pleistocene outcrops of Sicily (Italy). The ramp model proposed (Pedley and Grasso, 2002) comprises an inner ramp with beach deposits, a middle ramp dominated by *in-situ Cladocora* (solitary corals) growths just below the fair-weather wave base, changing seawards to rhodolith pavements that extended below the storm wave base. A branching bryozoan carpet extends from the distal part of the middle ramp to the outer ramp. Ramp to basin sediments consist of pelagic (*Globigerina*-rich) wackestones. These authors pointed out the importance of the presence of inshore deposits and of a variety of shallow-water temperate carbonate factories in low-energy microtidal settings (Mediterranean Sea) in contrast to open-ocean platforms such as the cool-water carbonate shelves in southern Australia (see above). This difference was previously highlighted by Martín *et al.* (1996) and Fornos and Ahr (1997). Pedley and Grasso (2002, 2006) have also discussed some aspects of sequence stratigraphy as carbonate production takes place mainly during sea-level highstands and resedimentation during sea-level lowstands.

In the tectonically active region of Rhodes (Greece), Titschack *et al.* (2005) describe an example of temperate carbonate deposition mainly at the foot of submarine cliffs and micrograbens, and also in small depressions and within Neptunian dykes. The depositional model was influenced by a tectonically driven sea-level change (transgressive-regressive cycle) and steep palaeotopography. Two major carbonate production areas are inferred—one on shallow-water terraces above the fair-weather wave base and another in deeper terraces below the storm wave base. Autochthonous sediment was transported downslope by different gravitationally driven transport mechanisms, mainly rock falls and debris falls, but also grain flows, and

finally accumulated at the toe of the submarine cliffs, in micrograbens, and in small depressions. These authors also attempted to establish sedimentological criteria to recognize the above-mentioned mechanisms. They proposed that shell-inverse stacking patterns (concave-side up) are a potential proxy for debris falls.

b) Other Atlantic and Pacific temperate- to cool-water carbonates

The Gulf of California, western Canada, and western Scotland are other regions where temperate carbonate deposition takes place.

The Gulf of California is a N-S elongated embayment located between the tropical and temperate climate belts and it constitutes an important zone to study the transition between temperate and subtropical carbonate depositional settings (Halfar *et al.*, 2000, 2004, 2006). From north to south, heterozoan carbonates (bryozoan and mollusc dominated), deposited in temperate waters (average surface-water temperature of 20.4º C; Halfar *et al.*, 2006) and eutrophic conditions, are replaced by a photozoan association with small reefal structures growing in warm oligotrophic shallow waters (average surface-water temperature of 25º C; Halfar *et al.*, 2006). In an intermediate position, heterozoan carbonates (mollusc and coralline algal dominated) occur together with small coral patches, in small pocket bays, high-energy rocky and sandy shorelines, and mid-shelf settings (Halfar *et al.*, 2004).

Carey *et al.* (1995) describe Holocene non-tropical carbonates in the Hecate Strait, a high-latitude and tectonically active setting in the western continental margin of Canada. Water circulation is controlled by tidal and wind-driven currents that conditioned the distribution of the sediment. Carbonate deposition takes place in shallow-water settings (<50 m), generally on rocky and/or gravely substrates. The main skeletal components are of suspension-feeding bivalves, bryozoans and barnacles whose presence is favoured by strong currents that continuously supplied nutrients into suspension, and prevented the deposition of fine-grained sediment that can clog the feeding apparatus of these organisms. In any case, the supply of terrigenous sediment is almost negligible in these areas because most of it is trapped in the coastal fjords. Coarse-grained and hard substrates for colonisation by carbonate producers of glacial till and ice-rafted sediment outcrops formed during glacial periods and were subsequently inundated during the transgression.

The West Scottish tidal-dominated shelf is influenced by the relatively warm Gulf Current and it receives low terrigenous input as there are no major rivers entering the shelf. These conditions provide a favourable environment for the development of calcareous organisms. Scoffin (1988) recognised eight depositional settings on the modern shelf based on water depth, substrate type, and the degree of hydrodynamic exposure. The main carbonate factories are located on: rocky shallow substrates that are colonised by barnacles, molluscs, echinoderms, and serpulids; sandy substrates of shallow-water sheltered zones where carbonate producers are molluscs, echinoderms, and benthic foraminifers; and small banks formed by mussel shells and coralline algae that develop where tidal current is enhanced between islands.

2

OBJECTIVES AND CHOICE OF STUDY EXAMPLES

2.1. Objectives

In the last two decades, research on the temperate-carbonate depositional realm has significantly increased knowledge of these previously poorly-known type of carbonates, achieving a degree of comprehension comparable to that for the tropical carbonates. However, some aspects need further research, especially those concerning depositional models due to the high variability and number of controlling factors. One important issue is a better characterisation of outer-ramp and ramp- to -slope transitional settings as they are less studied than middle- and inner-ramp environments, especially in microtidal areas, such as the Mediterranean Sea. Due to the variety of topographic and hydrodynamic conditions in the ramps where temperate carbonates develop, carbonate factories are different in composition and sediment transport and deposition mechanisms can vary and so, consequently, can the resultant deposits. Cyclicity, especially in distal ramp settings, also needs better characterisation.

This thesis tackles the study of various depositional models of temperate-carbonate deposits in southern Spain, north New Zealand and south Australia in order to elucidate some of the afore-mentioned aspects and to achieve the following objectives:

1. To expand upon the spectrum of the temperate-carbonate depositional models, providing information about:

- Geometry of carbonate ramps
- Biogenic components of carbonate factories
- Facies belt distribution
- Relation with siliciclastic sediments
- Main controlling factors on depositional models
- Integration of proposed sedimentary models in the temperate-carbonate depositional realm

2. To clarify sediment-transport mechanisms and describe their resulting deposits, paying attention to:

- Sediment transport during fair-weather, storm, and high-energy conditions
- Transport and deposition in shallow- and deep-water settings
- Geometry and composition of resultant deposits
- Their relation with topographic and hydrodynamic conditions

3. To identify and analyse various aspects related to cyclicity and sequence stratigraphy in temperate carbonates, supplying information about:

- Recognition criteria
- Origin and time-constraints of cycles
- Response of temperate carbonates to sea-level changes

2.2. Study examples

In order to achieve the objectives presented in the preceding section, the study was carried out in the three most important regions in the world where temperate-carbonate deposition both occurs nowadays and took place in the past. These regions are the Mediterranean Sea, New Zealand, and southern Australia.

In the Mediterranean Sea region, southern Spain was chosen as the study area since the excellent exposures of temperate carbonate-bearing units in this area allow a detailed study of the sediments. Research on temperate carbonates in Neogene basins of southern Spain have brought to light new aspects of depositional models (see Section 1.2.1), sediment transport mechanisms, sequence stratigraphy, taphonomy, and controlling factors on non-tropical carbonate realm. These studies were performed mainly in Mediterranean-linked basins such as Agua Amarga Basin (Martín *et al.*, 1996; Betzler *et al.*, 1997a; Brachert *et al.*, 1998; 2001), Almayate Basin (Aguirre, 2000), Almería-Níjar Basin (Aguirre, 1998; Yesares and Aguirre, 2004), Cabo de Gata region (Franseen *et al.*, 1997; Betzler *et al.*, 2000; Johnson *et al.*, 2005), Carboneras Basin (Braga *et al.*, 2003a; Martín *et al.*, 2004), Sorbas Basin (Wood, 1996; Sánchez-Almazo *et al.*, 2001),Vera Basin (Braga *et al.*, 2001). Additional studies have also been carried out in Atlantic-linked basins and related seaways such as the Guadalhorce Corridor (Martín *et al.*, 2001), Guadix-Baza Basin (Betzler *et al.*, 2006), and Ronda Basin (Gläser and Betzler, 2002). The Sorbas Basin and Granada Basin were selected for the present work as they are the less-studied in terms of non-tropical carbonate deposition. Previous studies carried out in the Sorbas Basin dealt with a general description of the temperate carbonates (Martín and Braga, 1994; Wood, 1996) and the palaeonviromental context of temperate carbonates inferred from stable isotope studies (Sánchez-Almazo *et al.*, 2001), but no detailed depositional model was provided. However, these prior studies showed the occurrence of temperate shallow-water facies and ramp-to-basin transitions that could be used to elucidate some of the above-described issues. In the Sorbas Basin, the uppermost Tortonian–lowermost Messinian Azagador Member was the subject of study. In this case, the results could also be compared and contrasted with those from nearby Mediterranean-linked basins where the Azagador Member occurs as well. Despite the presence of temperate-carbonate units in the sedimentary infilling of the Granada Basin (an Atlantic-linked basin), no detailed studies concerning these temperate sediments have been made until now. The sites chosen are good exposures of Upper Miocene carbonate and mixed siliciclastic sediments that crop out in the surroundings of Alhama de Granada village (Fernández and Rodríguez-Fernández, 1991) showing complex facies relationships, abundant sedimentary structures and large-scale erosional surfaces.

Studies of ancient non-tropical carbonates in New Zealand have been carried out mainly in Oligocene and Pliocene-Pleistocene limestones distributed in different locations throughout the country (Nelson, 1978; Anastas *et al.*, 1997; Nelson *et al.*, 1994, 2003; Caron *et al.*, 2004b, 2005; Dix and Nelson, 2004; Hood *et al.*, 2004a). Modern examples of temperate-carbonate sedimentation are also well known from New Zealand's shelves (Nelson and Hancock, 1984; Nelson *et al.*, 1988a; Gillespie and Nelson, 1996, 1997; Gillespie *et al.*, 1998). Miocene carbonate occurrences are less common, probably due to dominantly terrigenous post-Oligocene sedimentation. Taranaki Basin margin was the chosen for investigation in New Zealand; in particular, the Middle Miocene temperate carbonates deposited in this basin. These limestones, regionally known as the Mangarara Formation, have remained poorly understood until recent times. The limestones occurs intercalated within siliciclastic sediments, and were mass-emplaced and deposited in deep-water settings.

Southern Australia has remained the largest sedimentary province of temperate-carbonate deposition in the world since the Eocene and therefore had to figure in an integrated work such as the one presented in this thesis. Numerous research studies dealing with cool-water carbonate depositional models have been performed in modern and ancient cool-water carbonates in southern Australia (James and Bone, 1991, 1994, 2007; Boreen and James, 1995; James *et al.*, 1997, 2000, 2004; Lukasik *et al.*, 2000; Pufahl *et al.*, 2004). Especially important are those works dealing with surficial sediments that better explain the facies distribution and hydrodynamic patterns along the shelves (Boreen and James, 1993; James *et al.*, 1992, 1994, 2001). As previously shown (see Section 1.2.2.1) carbonate sedimentation on the southern Australian shelves is mainly controlled by open-ocean hydrodynamic conditions. The selected area was, in this case, the Great Australian Bight because of the availability to access data from the Ocean Drilling Program Leg 182 (Great Australian Bight) and the chance to work with a research member that participated in that campaign (Dr. Christian Betzler, University of Hamburg, Germany). Pleistocene cool-water carbonates deposited in outer-shelf and upper-slope settings were the chosen subjects.

The thesis structure (see section below) is based on observations and results from the study carried out in all these basins by the author and other co-workers, which have been collected in different research papers (published, submitted and *in prep.*). These papers, each with distinctive goals, have been separated and organised into different chapters.

2.3. Thesis structure

The thesis is organized into four parts and comprises 14 chapters. In particular, the second part (Chapters 4–8) show the observations, results, and specific conclusions obtained from the study of temperate carbonates in outcrops from the Sorbas Basin, Granada Basin, Taranaki Basin, and from geophysical and lithological data from the Great Australian Bight obtained from the ODP Leg 182 data base. Part two is arranged as follows:

- *Chapter 4* shows the depositional models inferred for Upper Miocene carbonates (Azagador Member) in the Sorbas Basin and details the effects that a high-energy event(s) (tsunamis) had on ramp sediments and resulting deposits.

- *Chapter 5* also deals with the Azagador carbonates in the Sorbas Basin but concentrates on the study of high-frequency cycles in the temperate-ramp sediments. Removal and remobilization processes of bioclasts from the carbonate factories and resultant deposits are also presented in this chapter.

- *Chapter 6* describes a former submarine canyon (the Alhama Submarine Canyon) excavated in Upper Miocene temperate carbonates in the Granada Basin, detailing its morphology, infilling patterns and sediment composition, bed geometries, and origin.

- *Chapter 7* deals with the study of a carbonate-dominated submarine channel and fan system located in deep-water settings and developed during Middle Miocene times in the Taranaki Basin. In this chapter, description of the channel geometries and facies types as well as considerations about the carbonate source, sediment transport mechanisms, palaeogeography and palaeoceanographic aspects are given.

- *Chapter 8* presents the results of the research carried out from geophysical and lithological data from ODP Leg 182 (Great Australian Bight). These studies show the presence of sedimentary cycles in uppermost-slope sediments related with changing oceanographic conditions and oceanic current patterns during glacio-eustatic sea-level cycles.

In the third part of this thesis, an integrated discussion, general conclusions, and future perspectives on temperate-carbonates research are presented. This part is organized as follows:

- *Chapter 9* focuses on a comparison between the different depositional models studied herein and other models worldwide. Shared and distinctive patterns of the depositional models as well as new aspects are shown in the first two sections followed by a discussion of the main controlling factors that conditioned the characteristics of the temperate-carbonate depositional models developed in the studied basins.

- *Chapter 10* summarizes the most relevant results and their implications in the knowledge of the temperate-carbonate depositional realm.

- *Chapter 11* highlights some aspects of the investigation on temperate carbonates, that, in the opinion of the author, could be viable research lines on this topic in the future.

As mentioned, the main part of this thesis consists of the compilation of the published papers and submitted manuscripts by the author of this thesis and other co-workers. In order to keep the original structure of these studies, all the sections of the manuscripts are maintained except the references which, to follow a coherent format of the thesis volume, are put all together in the References section (Chapter 13). Index content (Chapter 14) is included to facilitate a quick search of interesting subjects.

3

METHODS

The work carried out in this study was essentially developed in the field for the southern Spain and New Zealand examples, and at the Universities of Hamburg and Granada in the case of southern Australia. Field work was completed and checked with laboratory analyses, essentially by thin-section study of the collected samples under the petrographic microscope. To illustrate the relationship among the different facies and the geometric features of beds in the outcrops, several photomosaics have been made.

3.1. Field work

The first step of the field work consisted in field trips to identify the different lithological units in the study areas and select the best localities for logging, as many outcrops of the temperate carbonate-bearing units comprised steep cliffs with difficult access that make logging of the study units challenging. General and detailed geological mapping was carried out in some outcrops to show the surface distribution of the units. In each outcrop, several stratigraphic sections were logged in order to study the vertical relations among the superimposed units and among the different facies types. In some locations, individual beds were laterally traced and lateral facies relationships were established from stratigraphic sections logged at different positions in the same unit. Data were obtained in all sections, together with a detailed sampling, of the following: bed geometry and thickness, lithology, colour, texture, sedimentary and biogenic structures, bioclastic content, skeleton types and taphonomic properties of bioclasts, matrix characteristics (type, size, relative abundance) terrigenous content, and, when possible, palaeocurrent measurements. Additionally, some marl samples were collected locally for dating purposes.

Due to the overall coarse grain size of the sediment, grain size was measured directly in the field with a graduated ruler for coarser rocks and a grain-size chart and lens for sand-sized sediments. Fine-grained rocks were studied in detail in the laboratory. Afterwards, these measurements were checked from the study of thin sections using a micrometer lens under the petrographic microscope.

Macrofossil characteristics (type, relative abundance and preservation) were qualitatively determined in the field. The analysis of the taphonomic attributes of the skeletons was performed (for appropriate bioclasts) following the taphonomic signatures used by Yesares and Aguirre (2004): geometry of the bioclast accumulations, size of bioclasts, packing, articulation, fragmentation, orientation (angle with respect to stratification), skeletal preservation, edge rounding, and biotic interactions (encrustations and borings). Taphonomic analysis was determined qualitatively, except one example analysed quantitatively (see Chapter 5).

3.2. Laboratory analysis

The laboratory analysis was carried out essentially with the petrographic microscope. More than 270 thin sections of the collected samples were studied in order to determine the components (type and relative abundance) and their microtaphonomic attributes (fragmentation, abrasion and biotic interactions), terrigenous content, porosity, matrix composition and cement types. Once all these features were determined, rocks were classified as indicated below. Results obtained from the laboratory analysis were verified against those carried out directly in the field (e.g. grain size, matrix type and content, or bioclast types).

The taxomonic classification of the coralline algae (an abundant bioclast in the study examples) was performed by Dr. Juan Carlos Braga Alarcón (University of Granada). Determination of benthic and planktonic foraminifers and age dating from marl samples of some outcrops was carried out by Drs. Isabel M. Sánchez-Almazo (CEAMA-University of Granada) and Julio Aguirre Rodríguez (University of Granada).

3.3. Other work

Work carried out prior to the field work consisted in the compilation and reading of the main published works dealing with temperate and cool-water carbonates in the last 30 years. Literature on specific topics (see Chapters 4–8) was extensively reviewed.

Additional work, carried out after the field and laboratory analysis, consisted basically in digitizing and vectorizing the geological maps and stratigraphic sections resulting from field work, taking photographs of the microfacies, and making photomosaics. Photomosaics were used to show an integrated view of the outcrops and those features (especially geometric ones) that may not be reflected with precision in the stratigraphic sections.

In the case of the southern Australia example (Chapter 8), the study, as mentioned above, was carried out essentially at the universities by studying Ocean Drilling Program Leg 182 published data (available online from www-odp.tamu.edu). For further details see Chapter 8 (Methods section, page 119).

3.4. Sediment and facies classification

As pointed out in the first chapter (Section 1.1), there are different classifications that can be used to differentiate the carbonate skeletal (and non-skeletal) associations (foramol/chlorozoan of Lees and Buller (1972) and heterozoan/photozoan associations of James (1997)) that characterise tropical and temperate carbonates. Temperate carbonates of the different studied examples are here classified using the James (1997) classification and thus considered as heterozoan. Other classifications derived mainly from the abundance of the dominant bioclastic components such as bryomol (Nelson *et al.* 1988a) and rhodalgal (Carannante *et al.*, 1988) are not generally used in this study. Only in some cases, when the temperate nature of the carbonate sediments is emphasized, is the foramol term also used. Similarly, the bryomol and rhodalgal terms are sometimes used to highlight the main bioclastic components of calcareous sediments. In this study, the term "rich" is preferentially used following the dominant bioclast(s) in the sediment to characterise the biogenic composition of some of the limestones.

Temperate-carbonate facies were classified following a double classification scheme. First, the facies was classified according to the grain size using a classification system similar to that employed for terrigenous sediments (Tucker, 1981). Carbonate sediments were termed calcisiltites when grain size was under 1/16 mm, calcarenites when grain size ranged from 1/16 to 2 mm, and calcirudites when grain size was greater than 2 mm. Within each grain-size group, the Udden-Wentworth grain-size scale (Wentworth, 1922) was used to define the grain-size ranges and names of the textural subgroups (e.g. very fine, fine, medium, coarse and very coarse for calcarenites). Finally, carbonate facies were classified using the Dunham (1962) classification of limestones according to depositional texture, as modified by Embry and Klovan (1971).

When terrigenous sediment is present in the carbonate sediments in significant amounts, the average percentage is given, and if necessary for further interpretation, composition, grain size, and characteristics of sphericity and roundness are also specified.

PART TWO

4

TSUNAMI-RELATED DEPOSITS IN TEMPERATE CARBONATE RAMPS, SORBAS BASIN, SOUTHERN SPAIN

Ángel Puga-Bernabéu*, José M. Martín, Juan C. Braga

Departamento de Estratigrafía y Paleontología, Facultad de Ciencias, Campus de Fuentenueva s.n., Universidad de Granada, 18002 Granada, Spain

**Corresponding author: Fax: +34 958 248528*

E-mail address: angelpb@ugr.es

Sedimentary Geology 199 (2007) 107–127

Received 3 May 2006; received in revised form 16 January 2007; accepted 16 January 2007

Abstract

Tsunami-related deposits occur in Upper Miocene (uppermost Tortonian-lowermost Messinian) temperate carbonates in the Sorbas Basin, SE Spain. These carbonates exhibit two distinct depositional models. At the northern margin, small, locally steepened ramps developed on an irregular palaeotopography. These ramps displayed bryozoan accumulations at the toe of submarine cliffs changing laterally to coralline algal rudstones to floatstones. A gentle homoclinal ramp extended along the southern margin of the basin. Bivalve (brachiopod/bryozoan)-rich carbonates formed in the mid-ramp, whereas coralline algal-rudstones spread over the outer-ramp, changing basinwards to packstones with planktonic foraminifers.

During the tsunami event large amounts of sediment were eroded from the carbonate ramps and redeposited. Two types of tsunami deposits are intercalated in outer-ramp sediments at both margins of the basin. In the steep outer ramps of the northern margin, some folded layers are eroded and overlain by convex upward, stratified megahummocks. In the southern ramp, an abnormal thick shell-debris bed (TSB) occurs. Distinctive sedimentary features of these tsunamites and the inferred inflow and backflow effects were controlled by different palaeotopographic profiles. At the northern margin, inflow tsunami wave(s) struck the steep ramps, causing folding of underlying beds and excavating a large, irregular erosive surface. Backflow surges filled the inflow scours with the removed sediment, producing the megahummocky sets. At the southern margin, incoming tsunami surge(s) crossed the gentle ramp and eroded the sediments, especially in the inner-ramp settings. Backwash transported part of the previously removed sediments basinwards, depositing them as a thick bioclastic bed on the outer-ramp.

The triggering mechanism of the tsunamis was probably related to seismic events recorded in the adjacent Tabernas Basin as several coeval seismites.

Keywords: tsunami, temperate carbonates, megahummocks, *maerl*, Sorbas Basin, SE Spain

1. Introduction

Tsunamis, among the most powerful events on Earth's surface, have a very high recurrence interval (Schnyder *et al.*, 2005). These "harbour waves" can be earthquake, volcanic, slide, or bolide-impact induced (Bondevik *et al.*, 1997; Carey *et al.*, 2001; Kelsey *et al.*, 2005; Lawton *et al.*, 2005). They erode and rework huge amounts of sediments from shallow marine and coastal settings and deposit them in either marine or continental environments. Tsunami-related deposits (tsunamites) have been referred to in numerous papers dealing with both Present and ancient examples (e.g. Clague and Bobrowsky, 1994; Dawson *et al.*, 1996; Hindson and Andrade, 1999; Dawson and Shi; 2000; Rossetti *et al.*, 2000; Cantalamessa and Di Celma, 2005; Schnyder *et al.*, 2005; Goff *et al.*, 2006).

Tsunami waves produce major effects on the seafloor in nearshore settings, but resulting deposits (scour-and-fill structures) are normally later eroded due to reworking by currents and waves (Einsele *et al.*, 1996). However, the effects of tsunami train waves (inflow and backflow surges) can also affect the platform in deeper positions (Pickering *et al.*, 1991), below the fair-weather and storm wave base. In these areas, preservation potential is higher as, after the tsunami event, normal sedimentation in calm-water conditions returns and the tsunami-generated deposits are buried and preserved.

In recent studies about tsunami deposits, one of the main concerns has been to determine significant sedimentary features of the tsunamites and their connection with landward flow and backflow (e.g. Massari and D'Alessandro, 2000; Rosetti *et al.*, 2000; Bussert and Aberhan, 2004; Cantalamessa and Di Celma, 2005). Only minor importance has been given, however, to the type of source-sediment (i.e. carbonate versus terrigenous). In the case of siliciclastic systems, sediments are always unlithified on the seafloor and, under tsunami conditions, particles of different sizes (silt to large boulders) are easily mobilized. Carbonate tsunamites in warm-water (tropical) settings, where seafloor cementation is very high, consist of large reef blocks swept by tsunami waves (e.g. Nott, 1997; Scheffers and Kelletat, 2004), or shell debris (van den Bergh *et al.*, 2003; Schnyder *et al.*, 2005). However, little attention has been paid up to now to tsunamites in non-

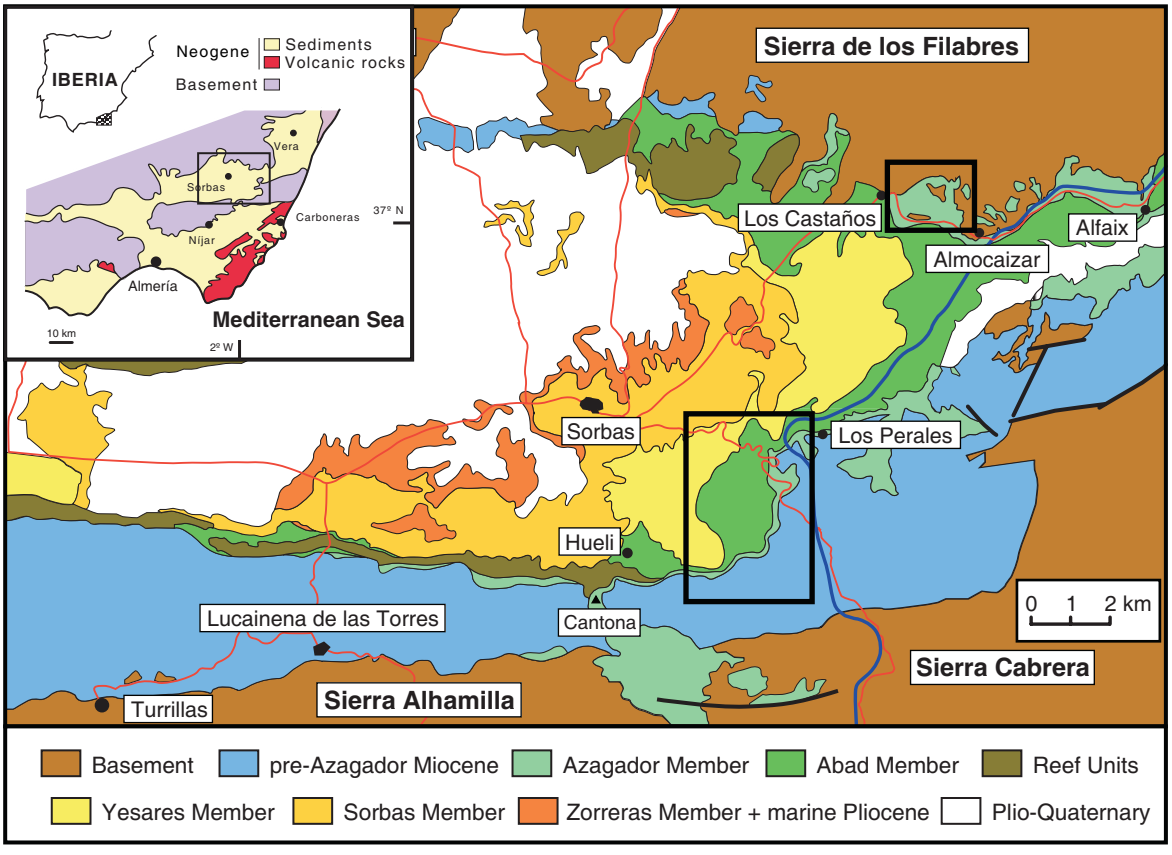

Fig. 29. Neogene basins in southeastern Spain and detailed geological map of the Sorbas Basin (modified from Montenat, 1990). Insets show location of the study areas.

tropical carbonate environments. Only a few examples, such as Mid-Pliocene carbonate deposits in South Italy studied by Massari and D'Alessandro (2000) and the "calcareous sandstones" referred to by Mastronuzzi and Sansò (2004) are presumably related to temperate carbonates. In shallow-marine, non-tropical carbonate environments, bioclastic particles remain loose on the seafloor due to a lack of early cementation (Nelson *et al.*, 1988a), thus favouring their mobilization and redeposition (Martín *et al.*, 1996, 2004; Betzler *et al.*, 1997a; Braga *et al.*, 2001). In this regard, non-tropical carbonates behave similarly to siliciclastics, as do, therefore, the tsunami-generated deposits.

This paper deals with abnormal thick beds in shallow-marine, temperate-carbonate ramps of late Miocene (latest Tortonian-earliest Messinian) age in the Sorbas Basin (southern Spain), which are thought to stem from large (tsunami) waves. The tsunami-related deposits that occur in this basin: (1) provide a sedimentary characterisation of outer-ramp tsunami deposits in temperate-carbonate environments; (2) show how the topographical profile of the ramp controls the type of tsunamite that develops within a given basin; (3) clarify the genesis of certain tsunami deposits with regard to landward flow and backflow; (4) complete the tsunamite spectrum from the deep-sea realm to marine-continental transitional environments.

2. Geological setting

The Sorbas Basin is a small intermontane basin in Almería (southern Spain) (Fig. 29) that formed as the Betic Cordillera was being uplifted during the Miocene (Braga *et al.*, 2003b). It is a small, E-W elongated basin bounded to the north by Sierra de Filabres and to the south by Sierra Alhamilla-Sierra Cabrera. These reliefs are made up of metamorphic rocks (phyllites, micaschists, quartzites, dolomites, marbles, and gneisses) that also constitute the basement of the basin. To the west it is linked to the Vera Basin and to the east to the Tabernas Basin.

Basin infilling extends from the mid-Miocene (?) to the Quaternary (Fig. 30), and comprises several stratigraphic units separated by unconformities (Martín and Braga, 1994). Older Miocene units consist of marine sediments: marly limestones, sandstones, conglomerates and marls that are poorly represented. Unconformably overlying these sediments are continental, presumably Serravallian, conglomerates and sandstones. The next unit, comprising shallow-marine calcareous sandstones and conglomerates, is early Tortonian in age. The following unit is from the late Tortonian. At that time, carbonate platform sediments, including coral-reef patches, and local fan-delta conglomerates and sands were deposited at the northern margin of the basin. Farther south, submarine fan deposits, consisting of conglomerates and turbidite sandstones, intercalate with basinal marls of the Chozas Formation of Ruegg (1964). Unconformably overlying the upper Tortonian sediments is the so-called Azagador Member of Ruegg (1964), which is latest Tortonian-earliest Messinian in age. It consists of non-tropical carbonate sediments (Martín *et al.*, 1999; Sánchez-Almazo *et al.*, 2001; Braga *et al.*, 2006b; Martín *et al.*, *in press*) deposited on carbonate ramps at both margins of the basin (Fig. 31). This carbonate unit contains the tsunami-related deposits studied in this paper and will be described in more detail below. Azagador carbonates grade upwards and laterally into marls (the Lower Abad Member marls of Ruegg, 1964; Martín and Braga, 1994). Unconformably overlying the Azagador carbonates at both margins of the basin is the first Messinian reef unit, the Bioherm Unit of Martín and Braga (1994). It contains coral and green algal (*Halimeda*) bioherms (Braga *et al.*, 1996b; Martín *et al.*, 1997). The second Messinian reef unit is the Fringing Reef Unit (Martín and Braga, 1994), which occurs on top of the Bioherm Unit; it consists of prograding coral-stromatolite fringing reefs (Riding *et al.*, 1991; Braga and Martín, 1996) at both margins of the basin. Basinwards, both Messinian reef-carbonate units change laterally to silty marls and marls with intercalated diatomites (the Upper Abad Member marls of Ruegg, 1964; Martín and Braga, 1994). A major, subaerial erosional surface can be traced from the top of the Fringing Reef Unit to the centre of the basin (Riding *et al.*, 1998, 2000). This surface is thought to be coeval with the Messinian Mediterranean desiccation (Martín and Braga, 1994; Riding *et al.*, 1998, 2000; Braga *et al.*, 2006b), starting at around 5.9 Ma (Gautier *et al.*, 1994; Krijgsman *et al.*, 1999). After the reflooding of the Mediterranean, and as a consequence of the tectonic uplift of the eastern margin, the Sorbas Basin became semi-isolated and selenite gypsum (Yesares Member of Ruegg, 1964) was deposited in its centre (Riding *et al.*, 1998, 2000). Evaporites are overlain by the Sorbas Member of Ruegg (1964), still Messinian in age, and comprising sands and silts together with oolites, stromatolite-thrombolite bioherms and coral-reef patches (Riding *et al.*, 1991, Martín *et al.*, 1993; Braga *et al.*, 1995). Fluvial and lacustrine sediments (Zorreras Member of Ruegg, 1964) overlie previous units. A thin shallow-marine unit, Pliocene in age, and an alluvial Plio-Quaternary unit complete the infilling of the Sorbas Basin (Mather, 1993, 2000).

3. Azagador carbonates

The tsunami-related deposits appear, as mentioned above, within the Azagador carbonates, which consist of bioclastic calcarenites and calcirudites with abundant

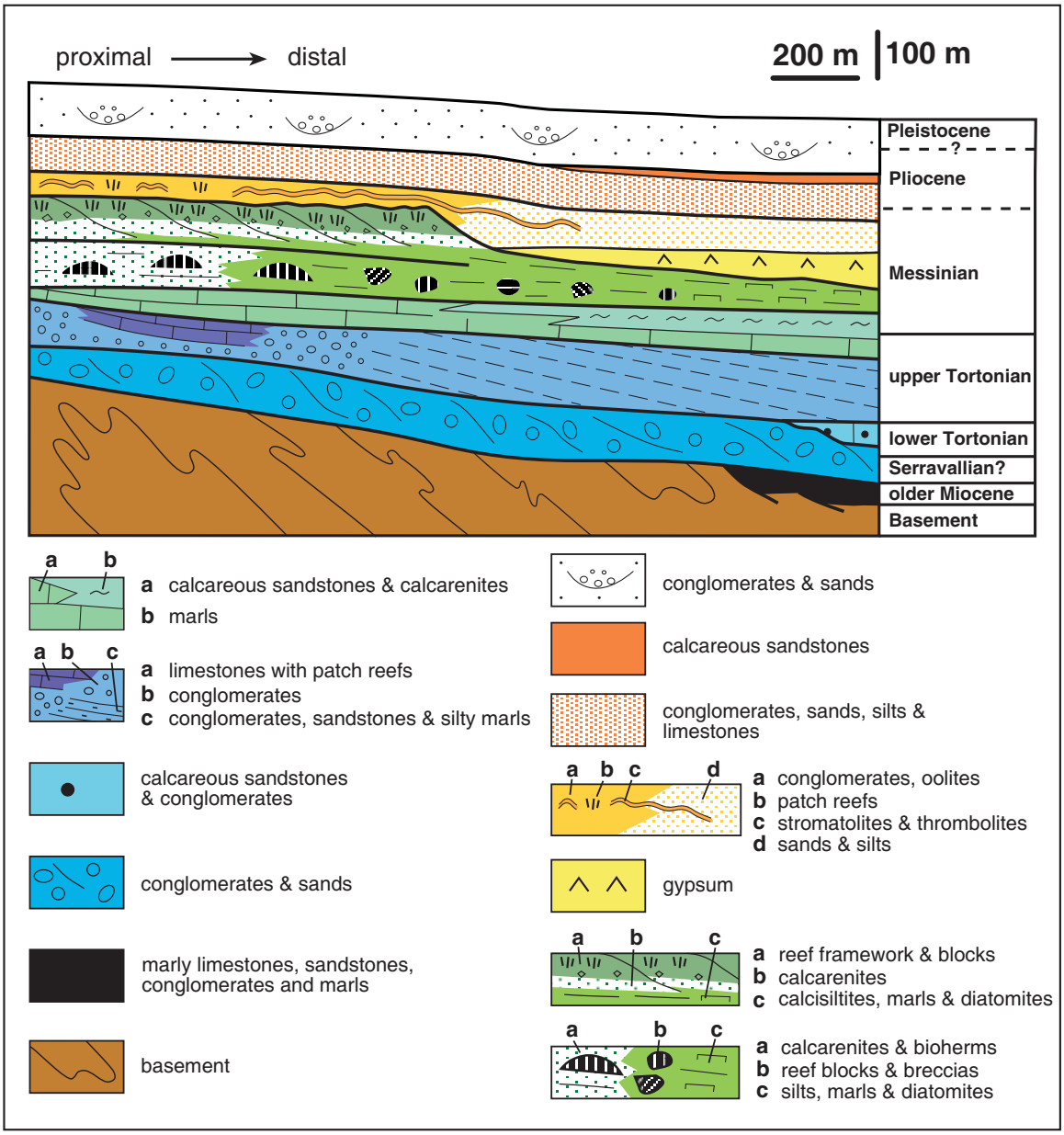

Fig. 30. Miocene to Quaternary stratigraphy of the Sorbas Basin (modified from Martín and Braga, 1994).

remains of coralline algae, bivalves, bryozoans, brachiopods, benthic foraminifers, and echinoderms. These bioclastic components belong to and are typical of the so-called foramol (Lees and Buller, 1972), rhodalgal (Carannante *et al.*, 1988), bryomol (Nelson *et al.*, 1988a), and heterozoan (James, 1997) non-tropical associations. Stable isotope studies carried out in the marls (the Lower Abad marls) laterally equivalent to the Azagador carbonates confirm the temperate nature of these carbonates (Martín *et al.*, 1999; Sánchez-Almazo *et al.*, 2001).

The Azagador carbonates were deposited on ramps at both margins of the basin (Wood, 1996) (Fig. 31). However, the topography of the underlying substrate caused differences in the facies types and sedimentary models at each margin, which in turn are reflected in the types of intercalated tsunamite deposits.

3.1. Northern margin

The Azagador carbonates at the northern margin of the Sorbas Basin were deposited on an irregular surface excavated on metamorphic rocks from the basement and/or upper Tortonian conglomerates and sands. The best outcrops are located at the "Bar Lemon" area, near the Los

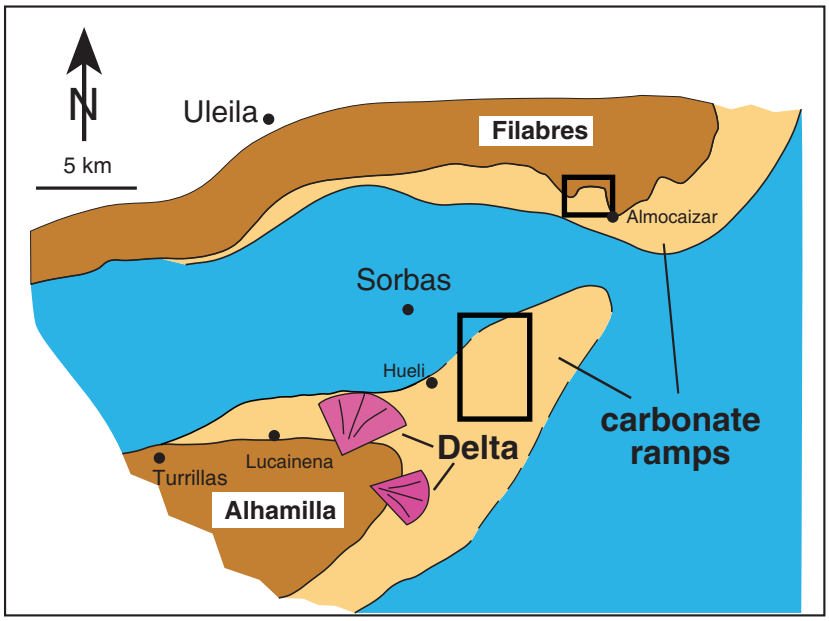

Fig. 31. Palaeogeography of the Sorbas Basin during the latest Tortonian-earliest Messinian (modified from Martín *et al.*, 1999). Insets mark the position of the areas studied in detail.

Castaños and Almocaizar villages. The most representative sequences and facies are presented in Figure 32.

The underlying substrate of metamorphic rocks and Tortonian conglomerates and sands shows a complex palaeotopography, with locally steep slopes. This irregular palaeorelief is directly overlain and onlapped by the Azagador carbonates (Fig. 32). To the south, these carbonates are covered by the Lower Abad marls.

3.1.1. Facies types

3.1.1.1. Robust branching bryozoan facies. This facies (up to 5 m thick) lies directly on either metamorphic basement outcrops or on upper Tortonian conglomerates and sands. It is arranged in wedge-shaped beds dipping 12–14º and extending laterally 50–100 metres.

Well-preserved, robust branching bryozoan (mainly *Myriapora truncata*) fragments, up to 7 cm in length, dominate this greyish calcirudite (rudstone) facies (Fig. 33A). Coralline algae, bivalves, echinoderms (regular echinoderms and *Clypeaster*), and benthic foraminifers (mainly *Elphidium* and *Heterostegina*) are also significant components. Nodular bryozoans (1–3 cm in diameter) are locally abundant. Terrigenous content (quartz and dolomite grains) is lower than 5%. This facies grades upwards and laterally into the branching coralline algal facies (Fig. 32), with bryozoan content progressively decreasing and red algal content simultaneously increasing in the transition zone.

3.1.1.2. Branching coralline algal facies. This facies is by far the most abundant and constitutes most of the palaeorelief infilling (Fig. 32). Calcarenite/calcirudite algal-rich beds adapt to the substrate topography, filling its irregularities. Individual layers, dipping 5–20º, range in thickness from 15 to 50 cm and have sharp to diffuse limits. The bulk of the sediment consists of a loosely to densely packed floatstone/rudstone with abundant branching coralline algal remains, up to 2 cm in size. *Lithophyllum* (*L.dentatum* (Kützing) Foslie and *L.incrustans* Philippi/ *L. racemus* (Lamarck) Foslie group), *Lithothamnion* and *Mesophyllum* are dominant genera. Small rhodoliths, 2–4 cm in diameter, are also locally present. Other bioclastic components are oysters (*Ostrea*), pectinids (*Chlamys* and *Gigantopecten*), bryozoans (delicate branching and nodular colonies), echinoderms (regular equinoids and *Clypeaster*) and benthic foraminifers. Siliciclastic content is always less than 10%.

3.1.1.3. Rhodolith facies. Densely-packed rhodolith pavements (Fig. 33B) occur in the deeper parts of small palaeorelief depressions. The rhodoliths are arranged in beds 100–150 cm thick, grading laterally into the branching coralline algal facies towards the depression margins (Fig. 32). The rhodoliths are ellipsoidal in shape and up to 10 cm in diameter. Their internal structure consists of small branching/columnar and encrusting plants of *Lithothamnion* and *Mesophyllum*. Loose coralline branches are locally abundant amid the rhodoliths. Oyster,

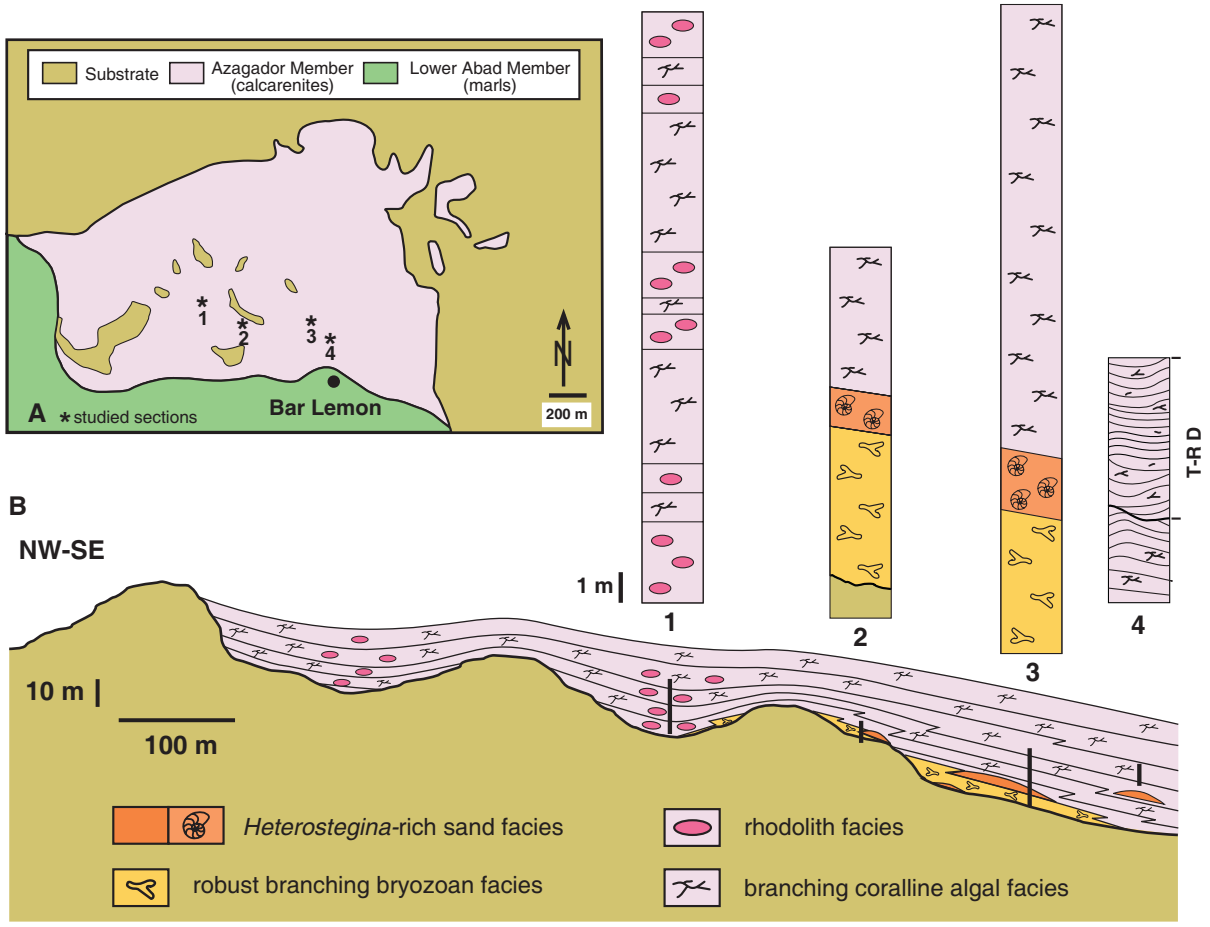

Fig. 32. (A) Simplified geological map of the Bar Lemon area and location of studied sections. (B) Synthetic scheme of the palaeorelief infilling and position of logged sections. Sediment distribution shows an overlapping (transgressive) infilling of the underlying topography. Robust branching bryozoan facies occur attached to and/or immediately on top of the irregular palaeorelief surface. They change laterally to and are covered by the branching coralline algal facies. Rhodoliths concentrate in the centre of small depressions. *Heterostegina*-rich sand facies exhibit a more erratic distribution and relate to areas of local, significant terrigenous supply. In section 4 the tsunami-related deposits (T-R D) (megahummocks) appear.

echinoderm, pectinid and rare nodular bryozoan remains also appear dispersed in this facies.

3.1.1.4. Heterostegina-rich sand facies. Sandy beds, rich in benthic foraminifers (*Heterostegina*), occur at different stratigraphic levels intercalated between robust branching bryozoan and branching coralline algal facies. They can also be found locally lying directly on conglomerates from the substrate. The sand bodies are wedge-shaped and consist of grey, medium-to-very coarse sand with quartz, dolomite, mica, and goethite grains. Sand beds are slightly undulated and vary from 70 to 350 cm in thickness.

Abundant *Heterostegina* tests, 5 mm average size, appear randomly orientated. *Heterostegina* content in the sediment is normally 20–30 %, although in some layers it reaches more than 50%. Densely-packed *Heterostegina* "patches" are locally present in thicker beds. Branching coralline algal fragments are also locally abundant. Fragments of pectinids, branching and nodular bryozoans, and echinoids are other minor constituents in this facies.

3.1.2. Facies interpretation

3.1.2.1. Robust branching bryozoan facies. Along the present-day Mediterranean coast of southeastern Spain, robust branching bryozoan deposits appear at water-depths of 15–20 m at the toe of submarine cliffs colonized by bryozoans (Betzler *et al.*, 2000). Well-developed Miocene counterparts have also been described by Betzler *et al.* (2000). Similarly, the submarine palaeorelief at the northern margin of the Sorbas Basin was colonized by robust branching bryozoans and their remains accumulated at the foot of the palaeocliffs in places where cliff slopes

were not overly steep (there are no bryozoan accumulations related to 70-90º slope-angle palaeoreliefs). Well-preserved bryozoan remains indicate minor reworking.

3.1.2.2. Branching coralline algal facies. This facies is interpreted as a fossil counterpart of *maerl* fields, which are widespread in shallow-water carbonate platforms from the Mediterranean Sea to the Artic Ocean (Bosence, 1983). In this fossil example, a depth-estimate of 15–40 m can be inferred from the overlapping bathymetric range in the common occurrence of the identified *Lithophyllum* species (*L. dentatum* and *L. incrustans/L. racemus*) and *Lithotahmnion* in the present-day Mediterranean Sea (Bressan and Babbini, 2003). This depth is below the current fair-weather wave base in the Mediterranean (Carannante *et al.*, 1988, based on Pérès and Picard, 1964).

3.1.2.3. Rhodolith facies. Rhodoliths in this facies are well preserved and exhibit growth-morphologies characteristic of low-energy environments (Braga and Martín, 1988; Aguirre *et al.*, 1993). These calm-water conditions are supported by depth estimates (>40 m), inferred from the depth distribution of similar modern Mediterranean coralline algal assemblages (*Lithothamnion and Mesophyllum* with no *Lithophyllum* plants) (Bressan and Babbini, 2003), and by the occurrence of this facies in the deepest parts of the small palaeorelief depressions

3.1.2.4. Heterostegina-rich sand facies. Heterostegina is a photodependent benthic macroforaminifer that lives attached to hard substrates (fixed or loose) in water depths ranging from 0 to 90 m (Langer and Hottinger, 2000). In our example, they are related to sand beds. The *Heterostegina* orientation in the sediment indicates an *in-situ* accumulation of the macroforaminifers after sand deposition. Red algal fragments and other bioclasts were probably transported together with the sand grains.

3.1.3. Depositional model

Azagador temperate carbonates at the northern margin of the Sorbas Basin were deposited over a palaeorelief shaped in metamorphic rocks from the Palaeozoic basement and/or upper Tortonian conglomerates. The highly irregular topography of the underlying substrate, with some local steep slopes, conditioned facies distribution and the sedimentary infilling. The latter took place during a transgressive stage with a relative sea-level rise (Fig. 34). Attached to submarine palaeocliffs, robust branching bryozoan grew prolifically, accumulating in small, cliff-toe aprons after dropping down post-mortem. Coralline algal facies interpreted as *palaeomaerl* colonized calm, deeper areas situated below fair-weather wave base.

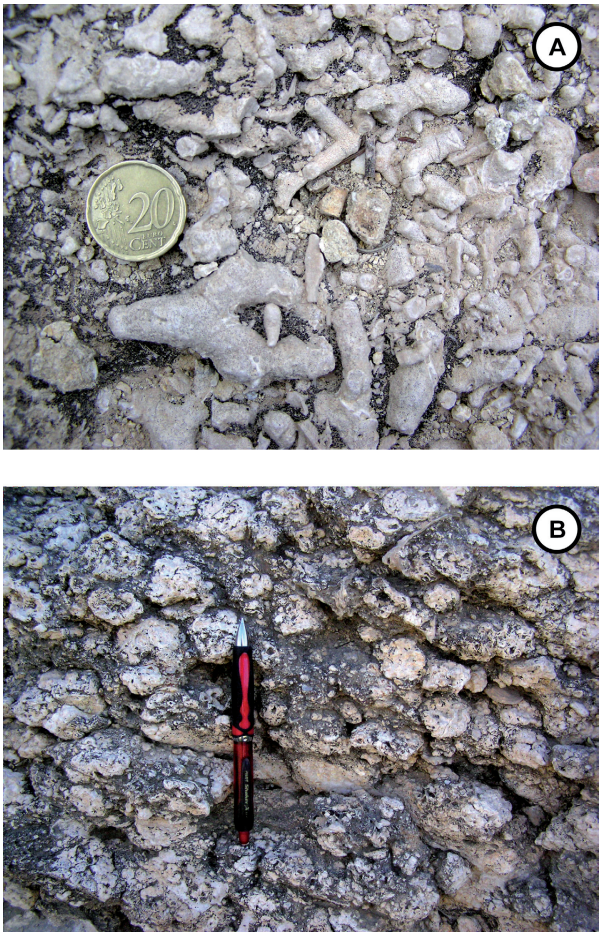

Fig. 33. Robust branching bryozoan facies at section 3. Coin is 2.2 cm in diameter. (B) Rhodolith facies at section 1. Pencil is 14.5 cm in length.

Rhodolith fields developed in the centre of small, deeper depressions (Fig. 34). Sand bodies, containing abundant *Heterostegina*, occur locally in areas where terrigenous input was higher.

3.2. Southern margin

The Azagador carbonates are well-exposed at the southern margin of the Sorbas Basin, extending from Cerro Cantona to Los Perales hamlet (Fig. 29). They lie unconformably on top of upper Tortonian marls and turbidite sandstones. They exhibit sheet-like geometry and are tilted to the north due to the Sierra Alhamilla uplift (Ott d'Estevou and Montenat, 1990; Martín and Braga, 1996**)**. The stratigraphic sections of the Azagador carbonates studied at this margin of the basin show similar vertical facies distribution (Fig. 35).

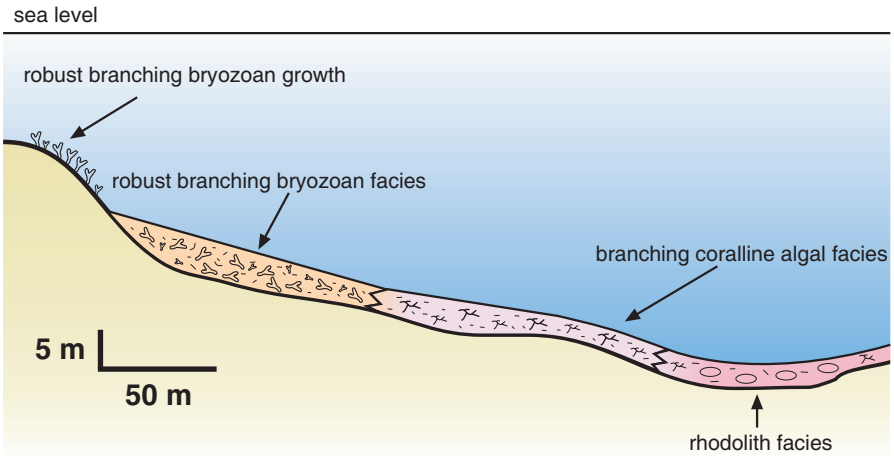

Fig. 34. Depositional model of the temperate-carbonate ramp at the northern margin of the Sorbas Basin. Prolific robust branching bryozoan growth took place on the walls of submarine cliffs and their remains accumulated at the base of the cliffs. In deeper ramp areas branching coralline algae proliferated, whereas rhodoliths concentrated in the centre of small depressions.

3.2.1. Facies types

3.2.1.1. Bivalve (oyster/pectinid) patches. Oyster (pectinid) patches, 1–5 m wide and up to 30 cm thick, are locally present at the base of the sequence in the El Cerrón section (Fig. 35). Most of the oyster and large pectinid shells are articulated or slightly disarticulated but still in life position. Smaller pectinid shells (*Chlamys*) are disarticulated and only slightly fragmented.

3.2.1.2. Branching coralline algal facies

This facies consists of a fine-to-coarse floatstone-rudstone, rich in coralline algal remains of *Lithothamnion* and *Mesophyllum and Lithophyllum (L.dentatum* and *L. incustans)* (Braga and Aguirre, 2001). Coralline growth-forms are mainly well-preserved loose branches (Fig. 36), although some minor encrusting growths and rhodoliths may appear as well. Other bioclasts present in this facies are pectinids (*Chlamys and Gigantopecten*), oysters, nodular and branching bryozoans, echinoids, and benthic foraminifers (*Elphidium* and miliolids). The matrix is a fine-to-medium calcarenite with abundant, macerated, red algal fragments. Packing ranges from loose to dense (*sensu* Kidwell and Holland, 1991). Terrigenous content is lower than 10%.

3.2.1.3. Bivalve beds. Shell beds occur intercalated within the branching coralline algal facies (Fig. 35). They can be oyster or pectinid layers depending on the major component. Oyster layers are up to 40 cm thick, with irregular limits. Loosely-to-densely packed oyster shells are disarticulated or slightly separated, disorganized and fragmented (especially in thinner layers). Pectinid layers are 1–30 m in length and up to 20 cm thick, have irregular (channelized) bases and are frequently amalgamated. Densely packed bioclasts in thicker beds are disarticulated and fragmented, with bimodal orientation. Concave-up and convex-up stacking biofabrics (*sensu* Kidwell *et al.*, 1986) are also present. Thinner layers are characterised by highly fragmented, orientated shells. The background sediment in both types of beds is made up of red algal fragments, nodular and branching bryozoans, echinoids, and benthic foraminifers.

3.2.1.4. Thick shell-debris bed (TSB). This layer is a 50–60 cm thick calcirudite bed with irregular limits characterised by a heterogeneous bioclastic content, with abundant pectinids, brachiopods, red algae, bryozoans, aragonitic bivalve moulds, oysters and minor echinoderms, balanids and benthic foraminifers. Details concerning this bed are given below when referring to the event (tsunami-linked) deposits.

3.2.1.5. Fine-grained carbonate facies. This facies, up to 6 m thick, consists of fine-grained calcarenites to calcisiltites grading upwards into silty marls and marls. It is mainly a bioclastic packstone/grainstone, rich in planktonic foraminifers and coralline algae, containing as well minor bivalve, bryozoan and echinoid fragments. Rare shark teeth and sponges are also present. Coarser bioclastic grains (coarse sand to granules) concentrate in its lower part, sometimes in small pockets. Sediment is highly bioturbated, with conspicuous *Thalassinoides* traces (Fig. 37). Siliciclastic content (mainly quartz) and glauconite grains are lower than 15 %.

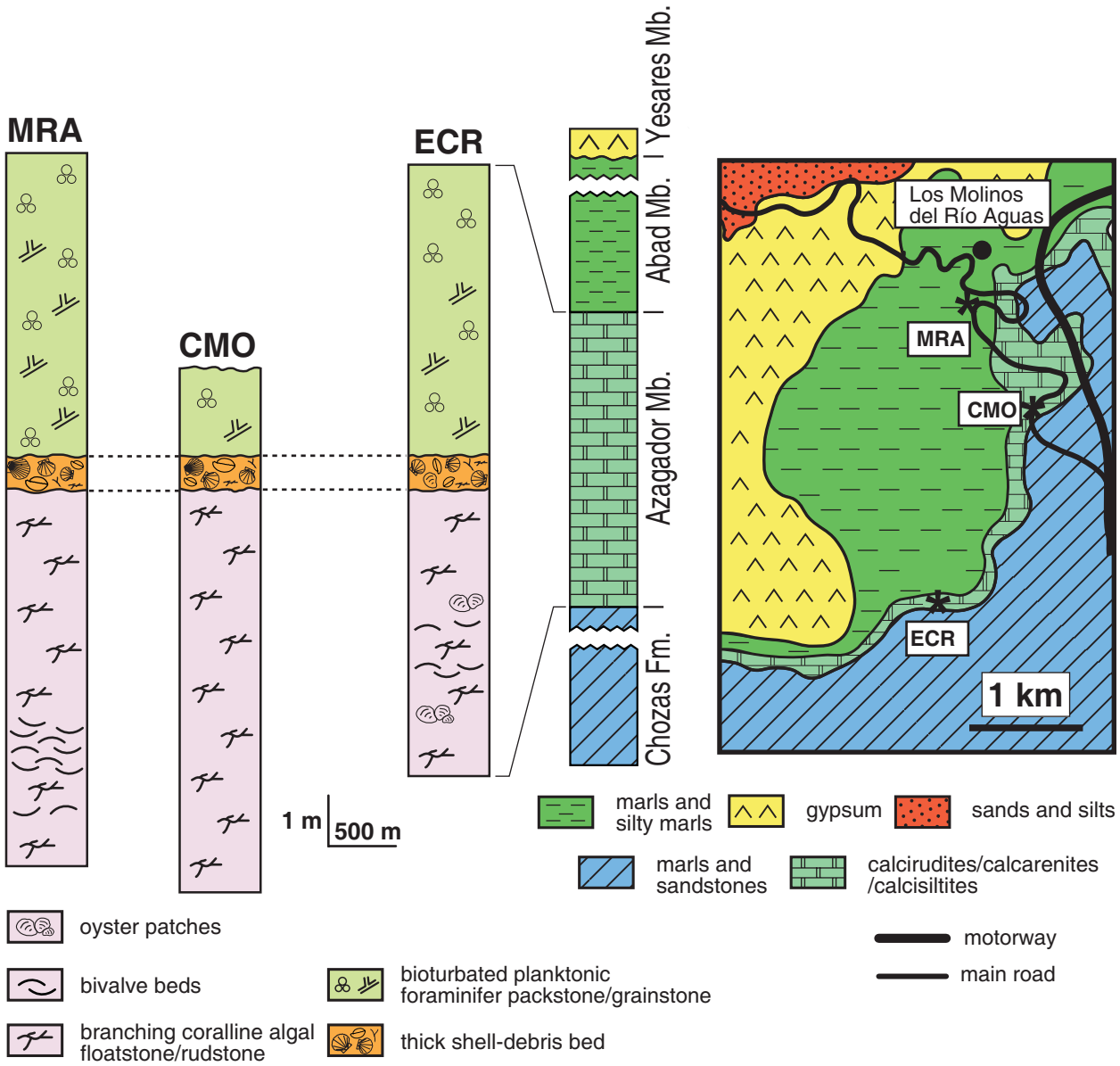

Fig. 35. Detailed geological map and stratigraphic scheme of the selected area in the southern margin of the Sorbas Basin. The logged sections, in a S-N transect (proximal to distal position), are the El Cerrón Section (ECR), the Cerro Molatas section (CMO) and the Los Molinos del Río Aguas section (MRA). The thick shell-debris bed (TSB), a tsunami-related event deposit, is shown as a marker bed.

3.2.2. Facies interpretation

3.2.2.1. Bivalve (oyster/pectinid) patches. Oyster/pectinid accumulations were common in mid-ramp settings. Oyster (pectinid) buildups appear to have colonized some areas of the platform at relatively shallow depths. Similar present-day and fossil examples of oyster growth in shallow-marine environments are well known (e.g. Norris, 1953; Herb, 1984).

3.2.2.2. Branching coralline algal facies. This facies, identical to its homonymous facies at the northern margin, also represents a *palaeomaerl* deposited in calm-water conditions. Coralline algal assemblages suggest a palaeodepth of 15–40 m in accordance with the present-day bathymetric distribution of similar modern Mediterranean assemblages (Bressan and Babbini, 2003).

3.2.2.3. Bivalve beds. Bivalve beds, with erosive, irregular bases, are interpreted as tempestites. Oyster beds show

Fig. 36. Branching coralline algal facies from section MRA (Los Molinos del Río Aguas). Coin is 2.3 cm in diameter.

Fig. 37. *Thalassinoides* traces in fine-grained carbonates from section MRA (Los Molinos del Río Aguas). Hammer is 33 cm in length.

redeposition signals (fragmented and disarticulated shells). In pectinid layers, the stacking biofabric (*sensu* Kidwell *et al.*, 1986), bimodal orientation and high fragmentation of shells indicate removal and redeposition of the shells.

3.2.2.4. Thick shell-debris bed (TSB). The interpretation of the deposition of this shell bed is given below when referring to the event (tsunami)-related deposits.

3.2.2.5. Fine-grained carbonate facies. Planktonic foraminifer abundance indicates a more open and deeper marine environment than in the previous facies. Abundant *Thalassinoides* feeding traces and glauconite grains point to a stable, low-energy environment with a low sedimentation rate.

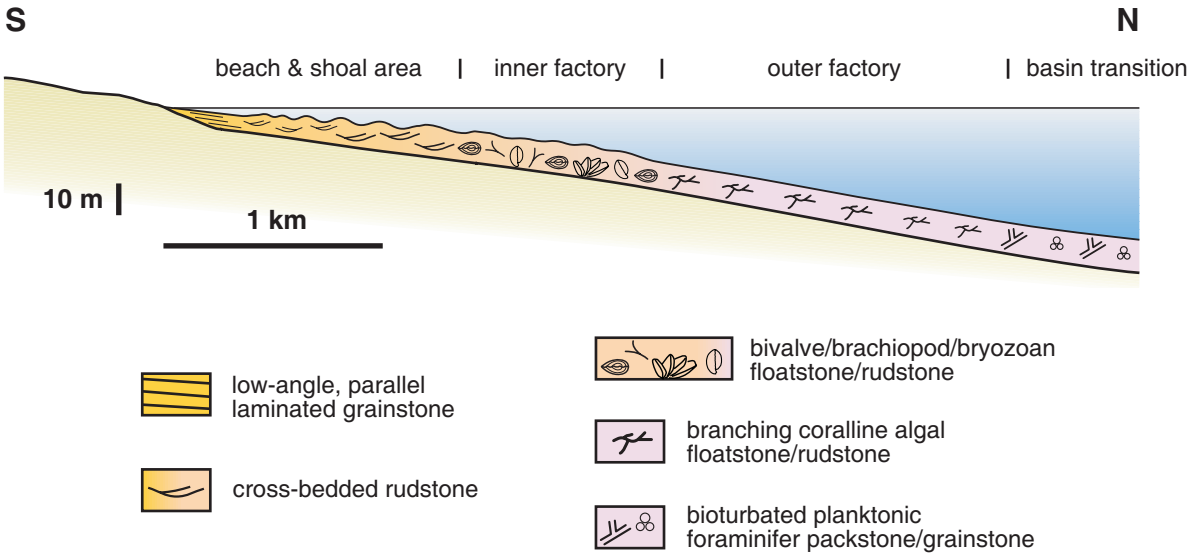

Fig. 38. Depositional model of the temperate-carbonate ramp at the southern margin of Sorbas Basin. *In-situ* carbonate production took place in middle (inner-factory) and outer (outer-factory) ramp positions.

3.2.3. Depositional model

At the southern margin of the Sorbas Basin, a gentle, shallow-water carbonate ramp (geometry deduced after counter-tilting of structural dip) developed, attached to Sierra Alhamilla. Stratigraphic sections show a deepening-upward sequence (Fig. 35), resulting from relative sea-level rise and transgression. Oyster (pectinids) patches appear at the base of the deepening-upward sequence and represent the shallowest deposits of the ramp preserved. Higher in the sequence, branching coralline algal facies dominate. They represent *palaeomaerl*s (branching coralline algal fields) that developed at depths of 15–40 m in an outer-ramp area. Tempestite layers, mainly composed of oysters and/or pectinids, intercalate within the *maerl* facies. Oysters and pectinids are minor components in outer-ramp facies (dominated by coralline algae), suggesting they were removed from mid-ramp areas and redeposited in deeper zones during storms. Downslope, red algal facies grade into fine-grained, foraminifer-dominated facies that are heavily-burrowed.

The depositional model inferred is that of a homoclinal ramp with two "factory" (carbonate production) zones: an inner factory (in a mid-ramp position), where bivalves (oysters and/or pectinids), brachiopods and bryozoans proliferated, and an outer production zone where branching coralline algal fields (*maerls*) developed (Fig. 38). Inner-ramp environments, are represented by a shoal area outcropping at Cerro Cantona (Puga-Bernabéu *et al.*, 2007a), presumably changing to landwards to a beach system as deduced by comparison with the Agua Amarga depositional model (Martín *et al.*, 1996).

4. Event-related deposits

4.1. Northern margin

In the exposures of the Bar Lemon area, there is a large erosive surface in the branching coralline algal facies (Fig. 39A). This surface likely formed as result of an exceptional event that caused considerable bed-erosion in the temperate-carbonate deposits of the northern margin of the Sorbas Basin.

To the north, this irregular surface is a top-lap surface that truncates 15–50 cm thick, branching coralline algal sheet-like beds (Fig. 39B). Some tens of metres to the south and inmediately below the erosion surface, the branching coralline algal beds are slightly folded (Fig. 39D).

On top of the erosive surface at this same location, large-scale undulated structures appear, forming a fining- and thinning-upward sequence up to 6 m thick (Fig. 39D). Individual beds from the undulated structures scour and drape each other. These beds are asymmetric, 40–200 cm thick, and have dipping angles ranging from 5º to 20º. An internal centimetric-to-millimetric lamination parallels bed undulations (Fig. 39G), with minor oblique cross-lamina (Fig. 39E). The sediment consists of a medium-to-coarse calcarenite, with a high terrigenous content (up to 20%) and strongly ground bioclasts (Fig. 39F) mainly of red algae and some bivalves. In a section perpendicular to the photomosaic in Figure 39A, a large (boulder-sized) calcirudite block appears (Fig. 39C) engulfed within the undulated beds. A more detailed, three-dimensional characterization of the large-scale, undulated

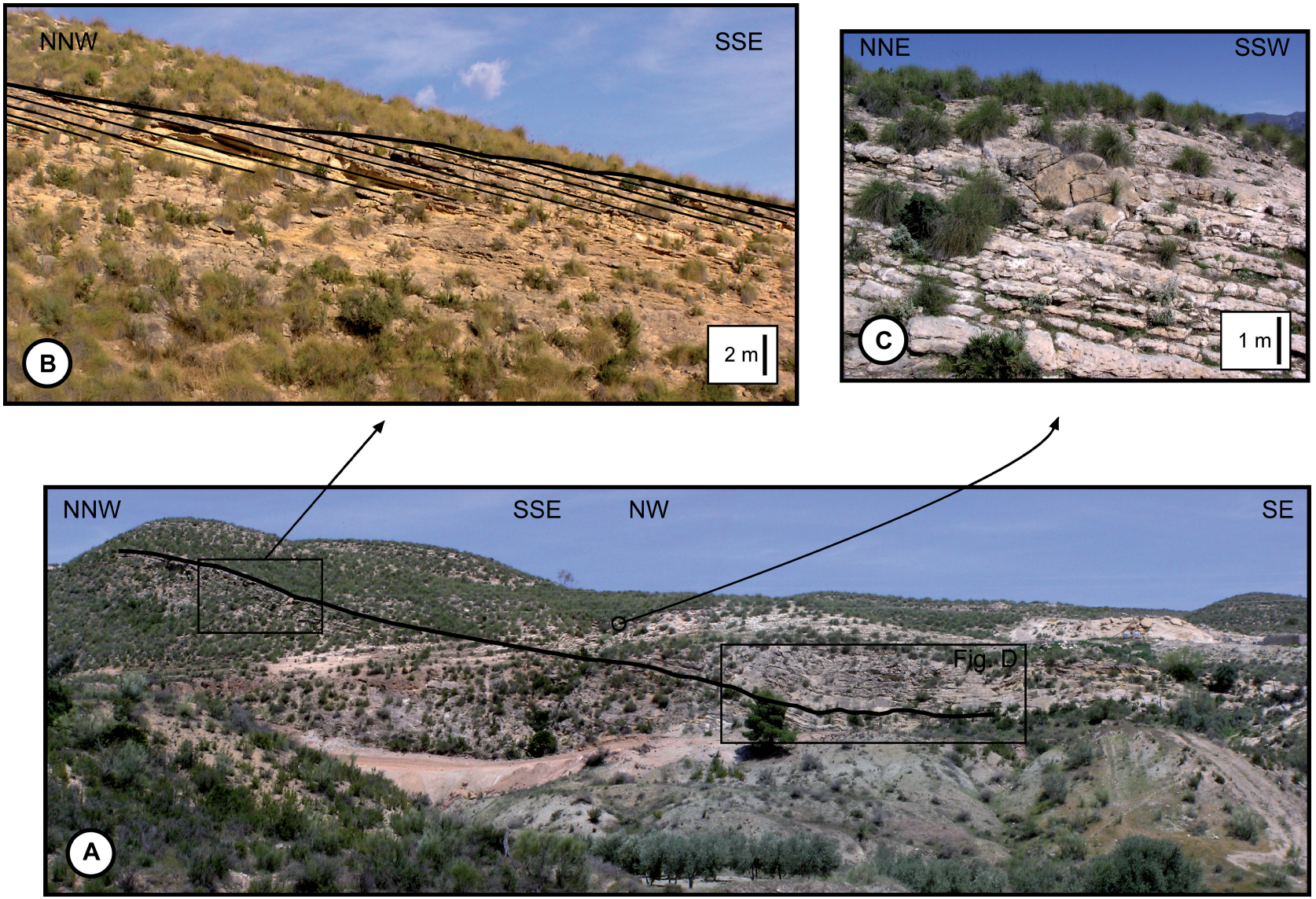

Fig. 39. Tsunami-related deposits at the northern margin of the Sorbas Basin. (A) Outcrop photograph exhibiting the large erosive surface (heavy line) within the branching coralline algal facies. (B) Detailed view of the top-lap surface. (C) Engulfed block within the megahummoks. (D) The erosion surface to the south. Slightly folded coralline algal-rich beds appear immediately below this surface. Megahummocky sets occur on top. (E) Detailed view of the erosion surface. The undulated, internal lamination in the overlying megahummocks stands out clearly. Hammer is 33 cm in length. (F) Microphotograph showing the megahummocky microfacies. Sediment is very poorly sorted. Major, irregular fragments are mainly coralline-algal branches. Bar is 1 mm length. (G) Detailed view of the megahummocky lamination draping the erosive surface. JMM is 1.75 m tall.

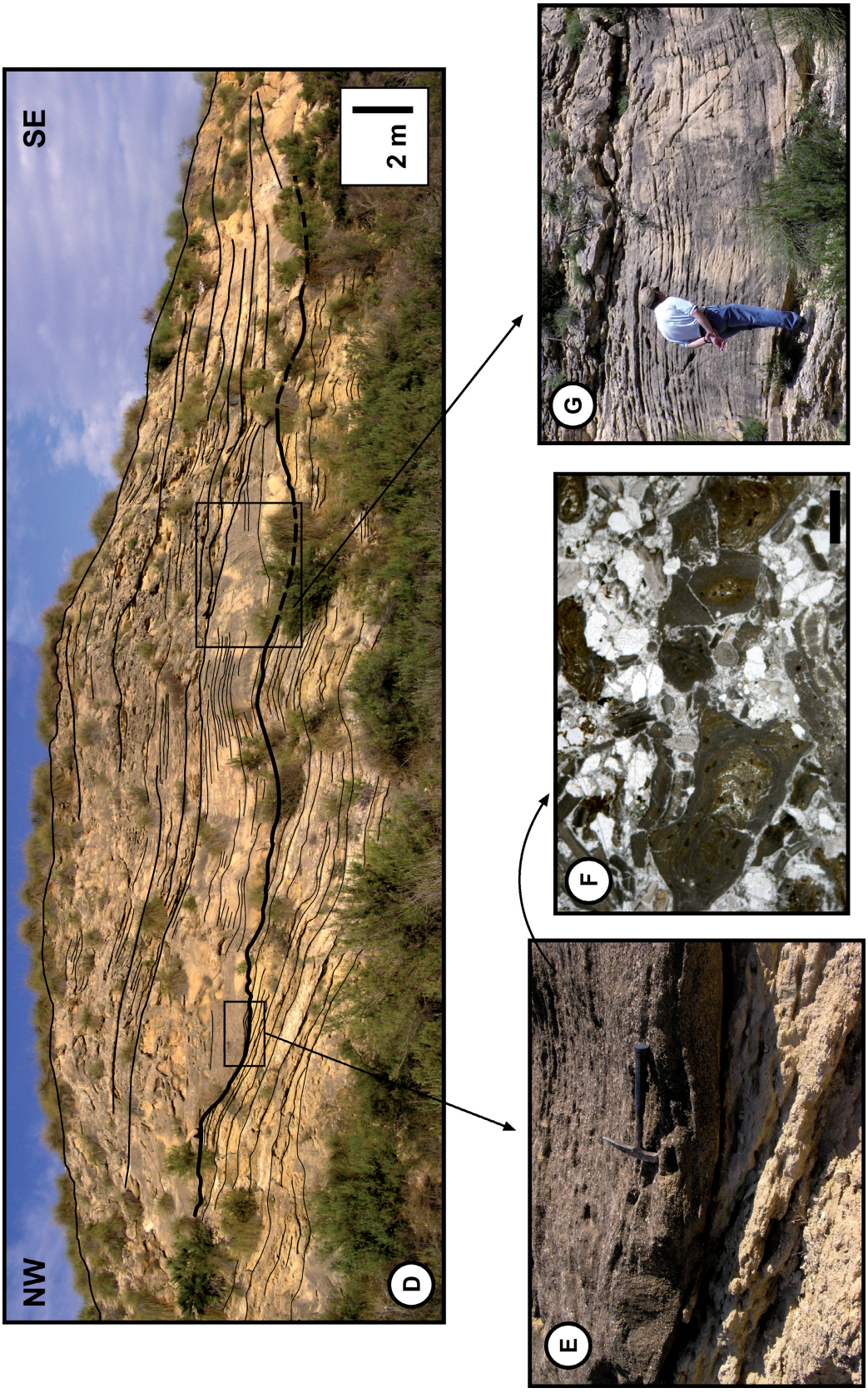

Fig. 39. (continued).

Fig. 40. Thick shell-debris bed (TSB). Close-up showing a heterogeneous bioclast mixing within this bed, with predominance of bivalve (pectinid) fragments. Pencil is 14.5 cm in length.

structures is not available, however, from the outcrop. These large-scale undulated structures are interpreted as megahummocks. Regardless of their scale, their sedimentary features are similar to those of hummmocks formed in shallow-water environments below fair-weather wave base as a consequence of combined flows during storm periods (Surlyk and Noe-Nygaard, 1986; Yagishita *et al.*, 1992; Li and Amos, 1999).

4.2. Southern margin

A singular shell bed (TSB) appears intercalated within outer-ramp deposits in the southern margin of the Sorbas Basin (Fig. 35). The major features of this bed are: (1) an irregular bottom and an irregular, but undulated, top; (2) lateral continuity, in a proximal-distal transect, of at least 3 km; and (3) a homogeneous thickness of 50–60 cm. This densely-packed, coarse rudstone bed consists of a heterogeneous mixture of bioclastic remains. The most abundant bioclasts are pectinids (*Chlamys*), mainly disarticulated and moderately fragmented (Fig. 40). Some large articulated pectinids vare also dispersed in the sediment. Concave-up and convex-up shell-arrangements occur. Second in abundance are brachiopods, whose articulated and disarticulated shells are always fragmented, but with peduncle valves still present. Other common bioclasts are coralline algae (branching forms and small rodoliths), bryozoans (nodular and branching colonies) and oysters. Aragonitic shell moulds, echinoderms (mainly spines) and minor balanids are also present. The interparticle matrix consists of a fine-grained, bioclastic calcarenite.

The geometric features and internal characteristics of this bed indicate strong erosion and bioclast transport and redeposition. This bed contains bioclasts from mid-ramp areas mixed with others from the outer ramp. In fact, most of the bioclasts are from the mid-ramp (see Depositional Model of the Southern Margin above). Bed geometry and taphonomic attributes of bioclasts suggest a single event. It seems that a high-energy process affected both the mid- and outer-ramp eroding and mixing bioclasts, which were later redeposited in deeper water as a single layer.

5. Discussion

5.1 Evidence of a tsunami-linked origin for the megahummocks and the thick shell-debris bed (TSB)

Advances in tsunami sedimentology in recent years have provided a full spectrum of sedimentological criteria to identify tsunami-related deposits (Massari and D'Alessandro, 2000; Takashimizu and Masuda, 2000; Bryant and Nott, 2001; Goff *et al.*, 2001; Schnyder *et al.*, 2005). However, these attributes may not be present in all tsunamites as they depend on such factors as the tsunami triggering-mechanism, the palaeogeographical context, shelf morphology, and position within the shelf. The sedimentary features of tsunami deposits also depend on properties related to the behaviour of the tsunami,

such as the number of tsunami waves, run-up height, back-flow energy and wave reflection. In addition, some characteristics are not exclusive of tsunami-related deposits, but are also shared by hurricane and typhoon (cyclone) deposits (Nott, 1997, 2004; Davies and Hasslet, 2000; Nanayama *et al.*, 2000; Goff *et al.*, 2004) leading at times to misinterpretation. Available data from the Sorbas Basin suggest that the event-related deposits described above (the megahummockites and the TSB) are tsunami-linked deposits in accordance with the following criteria:

1) Dimension of the structures

The megahummocks at the northern margin of the Sorbas Basin are larger (40–200 cm thick and 15–30 m wide) than normal, storm-associated hummocks (10–50 cm thick and 1–5 m wide). Although they probably formed in the same way (sea-bottom scouring and later infilling with sediment conformably draping the basal erosion surface), these megahummocks cannot be related to normal storm processes affecting the carbonate platform, as they imply stronger bed erosion and huge amounts of redeposited sediment. Consequently, we interpret these megahummocks as being the result of a tsunami wave(s). Deposits with similar structures, morphologies and scale, interpreted as tsunami-related deposits have been described by Massari and D'Alessandro (2000) and Rossetti *et al.* (2000).

The TSB (50–60 cm thick), cropping out at the southern margin of the Sorbas Basin, is in the thickness range (20–70 cm) of many tsunami sand-sheet deposits (Fujiwara *et al.*, 2000; Nanayama *et al.*, 2000; Bussert and Aberhan, 2004; Goff *et al.*, 2004). The TSB is also very persistent, extending for more than 3 km in a N-S transect within the outer ramp. Due to these characteristics, it cannot be considered a regular tempestite associated to normal or even major storms.

2) Components and geometry

Bioclasts in the TSB are from different source areas, located both in the mid- and outer-ramp (see Depositional Model Southern Margin above for details). The homogeneous mixture of bioclasts and taphonomic attributes indicate sediment remobilization and transport as a single flow, resulting in a uniform bed. The poor sorting is also a factor favouring a tsunami-linked origin. Storms usually generate well-sorted deposits, whereas grain sorting in tsunamites is generally poor (Goff *et al.*, 2004). Although true storm deposits appear intercalated in outer-ramp facies at the southern margin of the Sorbas Basin, the geometries, components and scale of these tempestites (see above) are not comparable with those of the TSB. Huge, embedded blocks found at the northern margin (see above) also imply strong sediment removal.

Tsunamite deposits at both margins show geometric features that clearly point to a large-scale erosive event that affected the carbonate ramps. At the northern margin, this erosion is reflected by the irregular surface found at the base of megahummocks and top-lapping branching coralline algal beds to the north. In the southern margin, the TSB exhibits an erosional base.

3) Palaeogeography

A high-energy event(s) clearly took place in the Sorbas Basin during the latest Tortonian-earliest Messinian. At that time, the Sorbas Basin was a small intermontane basin connected to the Mediterranean Sea (Martín *et al.*, 1999). The Mediterreanean, as today, was a semi-confined, marine basin with no significant oceanic influence, and thus sheltered from high-energy atmospheric processes such as hurricanes and typhoons. In this palaeographical context it is difficult to envision an exceptional atmospheric phenomenon as being responsible for the genesis of the TSB and the megahummocks in this basin.

5.2. Triggering mechanism

At the time of the deposition of the Azagador temperate carbonates (latest Tortonian-earliest Messinian), the Sorbas Basin was linked to the west to the Tabernas Basin, where a submarine-fan system developed (Kleverlaan, 1987, 1989). During this period, Kleverlaan (1987) makes reference to some megabeds, which he interprets as seismites. In particular, he describes a megabed called the "Gordo Megabed" (Fig. 41), which he considers to be a seismite associated with a major earthquake that caused the partial collapse of the slope at the northern margin of the Tabernas Basin. Such an earthquake (or the subsequent slide) might have produced a tsunami wave(s), which could have spread out to the adjacent Sorbas Basin, generating the tsunamites.

Available data do not allow us to assess whether the earthquake triggering the "Gordo Megabed" was the one responsible for the tsunamites in the Sorbas Basin. In any case, the "Gordo Megabed" is not the only megabed present in the Tabernas Basin (although it is the largest) whose sources could have generated tsunami waves that might have affected the shallow-water platforms in the Sorbas Basin.

The studied tsunami-linked deposits are located in the middle part of the stratigraphic sequence at both margins of the Sorbas Basin. Taking into account this similar stratigraphic position it is possible that both the megahummocks and the TSB could be related to a single tsunami event, albeit this attribution is not conclusive. In any case, although the TSB and the megahummocks

Fig. 41. Field view of the large seismite "Gordo Megabed" in the Tabernas Basin. JMM is 1.75 m tall.

might have been generated by different tsunamis (and in this respect could be linked to different megabeds in the Tabernas Basin), this possibility does not substantially modify our sedimentary interpretations.

5.3. Tsunami effects

Tsunami(s) train-waves (probably earthquake-induced) spread towards the Sorbas Basin sweeping the sediment in the carbonate ramps. In the northern margin, incoming wave(s) produced a sudden shock, increasing the pore pressure in the sediment on the sea bed which, as a result, was partly liquefied and subsequently folded. The exerted pressure was mainly vertical so that the resulting fold vergence is slightly downslope. Soft-sediment deformation on the sea floor is a frequent phenomenon associated to tsunamis (Rossetti *et al.*, 2000; Takashimizu and Masuda, 2000; Schnyder *et al.*, 2005). It is often earthquake-induced, although this is not the only possible mechanism (see discussion in Schynder *et al.*, 2005). The same or subsequent wave(s) "shaved" the steep ramp, generating a large, erosive surface. Tsunami back-flow transported part of the previously removed sediment in suspension into deeper zones, mostly filling the scours and building the megahummocks (Fig. 42).

In the southern margin, the tsunami presumably affected the whole ramp, eroding the sea bottom and incorporating the sediment into the wave on its way towards the coast. In-flow, nearshore tsunami deposits, if generated, have not been preserved (all inner-ramp deposits were removed by Quaternary erosion). The tsunami surge-ebb crossed back over the ramp, transporting basinwards part of the removed bioclastic sediment as a partially uniform sediment gravity flow ("densite" *sensu* Gani, 2004). The final result was the chaotic shell bed (TSB) deposited on the outer ramp (Fig. 43).

The response of the ramps to the tsunami shock (single or multiple events) was conditioned by the topographic profile. In the southern margin, the gentle profile of the ramp no doubt helped the tsunami inflow to cross the ramp and the tsunami backwash to introduce the eroded sediment back into the distal areas. Ramps at the northern margin underwent stronger bed-erosion than in the southern ramp as a result of the steeper ramp profile.

5.4. Tsunami-related deposit spectrum

Most of the reported tsunami-related deposits in Recent (Holocene) times and many ancient tsunamites occur in coastal and shallow-marine areas (Bryant *et al.*, 1992; Dawson and Shi, 2000; Smoot *et al.*, 2000; Luque *et al.*, 2002; van den Bergh *et al.*, 2003; Bussert and Aberhan, 2004; Scheffers and Kelletat, 2004; Cantalamesa and Di Celma, 2005)

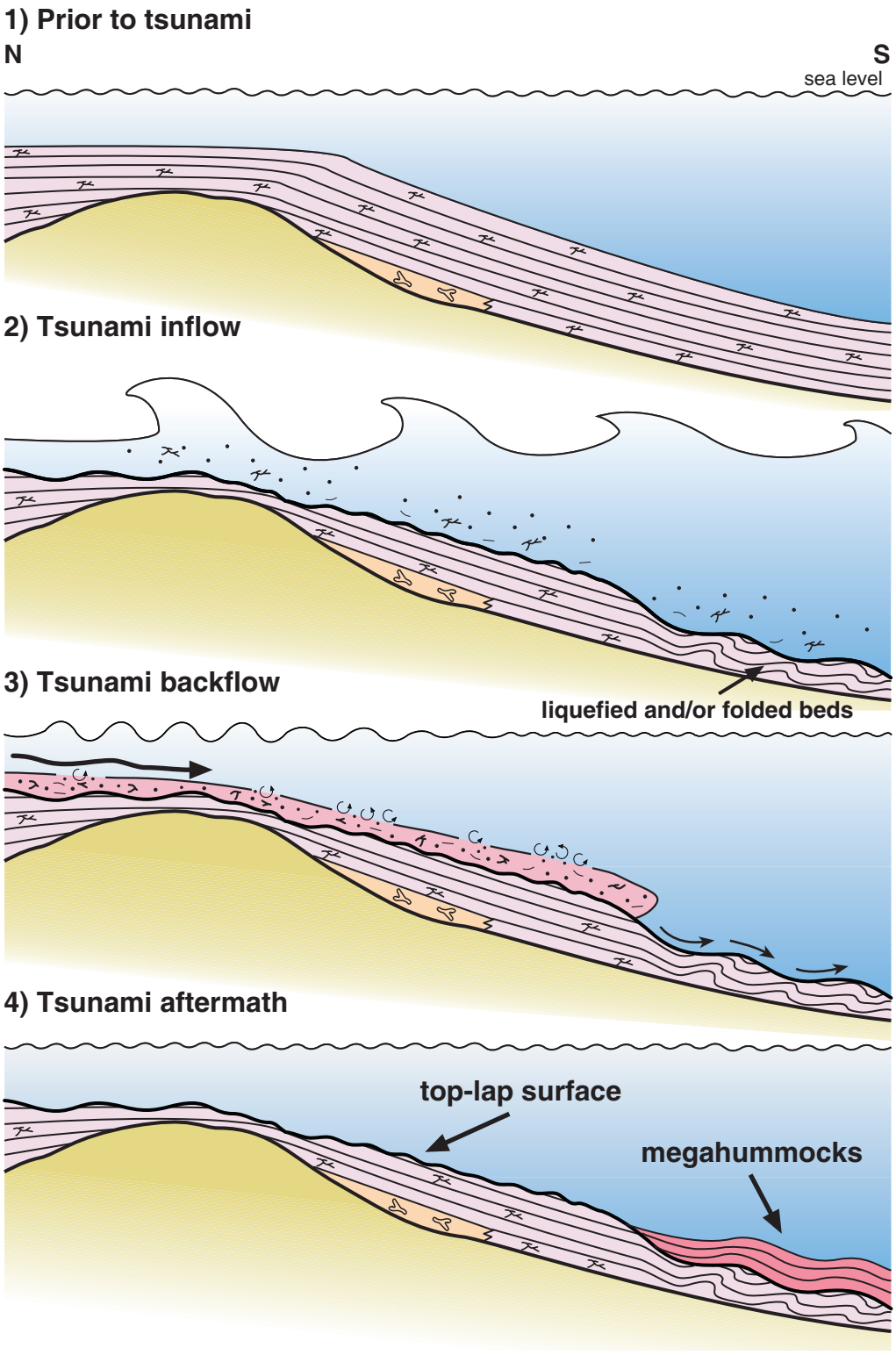

Fig. 42. Tsunami effects on the northern ramp of the Sorbas Basin. Steep slopes were strongly eroded by the incoming tsunami waves. The sediment brought back by the tsunami backflow was deposited in middle-outer ramp positions, on top of the irregular erosion surface, yielding the megahummocks.

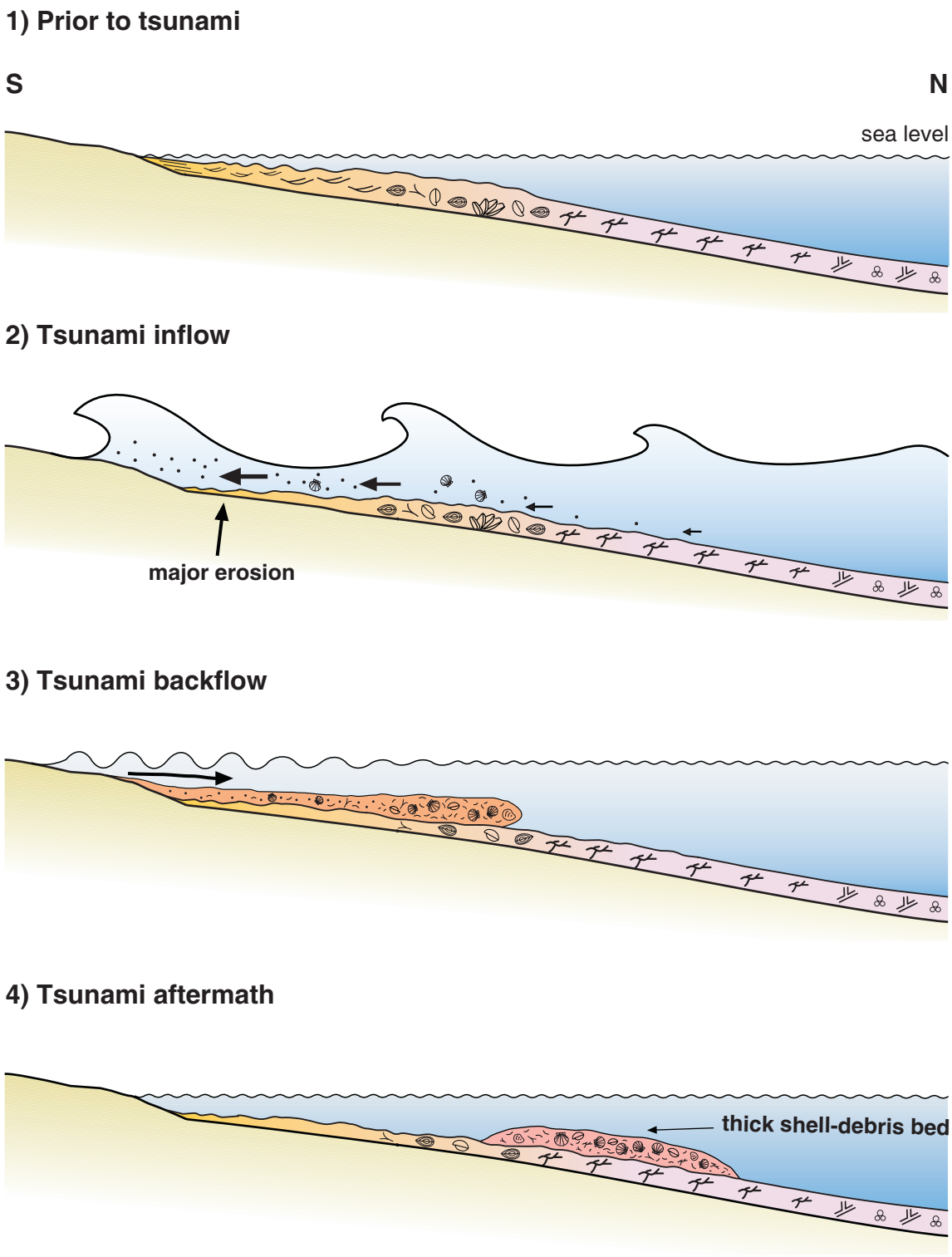

Fig. 43. Tsunami effects on the southern ramp of the Sorbas Basin. Tsunami inflow crossed the gentle ramp eroding the sea floor to some extent. Coarse bioclasts, derived mainly from the inner factory area, were removed and mixed with some finer-grained (sand-sized) carbonate sediment from the inner ramp (shoals and beaches), generating a debrite. The tsunami backflow took the debrite bioclastic sediments back to seawards depositing a thick, shell-debris bed in outer ramp settings.

Tsunami deposits in coastal areas commonly consist of coarse conglomerates with huge, often imbricated, blocks (Bryant *et al.*, 1992; Mastronuzzi and Sansó, 2000; Bryant and Nott, 2001; Scheffers and Kelletat, 2005). Tsunamites in coastal settings are also preserved as sand-sheets (including large washover fan deposits) (Andrade, 1992; Minoura *et al.*, 1996; Clague *et al.*, 2000; Luque *et al.*, 2002; Switzer *et al.*, 2006). Low-energy, marine-influenced coastal environments such as drowned valleys, coastal lakes, or protected bays are settings that may also be affected by tsunami waves, yielding sandy tsunamites of different geometries and scales (Minoura *et al.*, 1994; Bondevik *et al.*, 1997; Fujiwara *et al.*, 2000; Massari and D'Alessandro, 2000; Takashimizu and Masuda, 2000; Kelsey *et al.*, 2005; Ruíz *et al.*, 2005)

Tsunami-linked sediments that formed in high-energy, shallow-marine environments, situated above wave-base, are usually poorly preserved due to later sediment reworking by waves and/or currents. The scarce reported tsunamites consist, in these cases, of large scour and fill, giant swaley bedforms (Rossetti *et al.*, 2000).

The Tabernas and Sorbas basins in southern Spain provide some good examples that allow us to extend the tsunamite-related deposit spectrum from the well-known coastal areas to the deeper outer-ramp and slope realms (Fig. 44). We consider that the "Gordo Megabed", or other seismites described in the Tabernas Basin (Kleverlaan, 1987), and the tsunamites (TSB and megahummockites) of the Sorbas Basin were generated by the same event(s), and triggered by large earthquakes. Bearing this in mind, seismites, contemporaneously forming in deep-water settings, could be considered, in a very broad sense, as tsunami-related deposits, equivalent to outer-ramp tsunamites. Similar links are made by Cita *et al.* (1996)

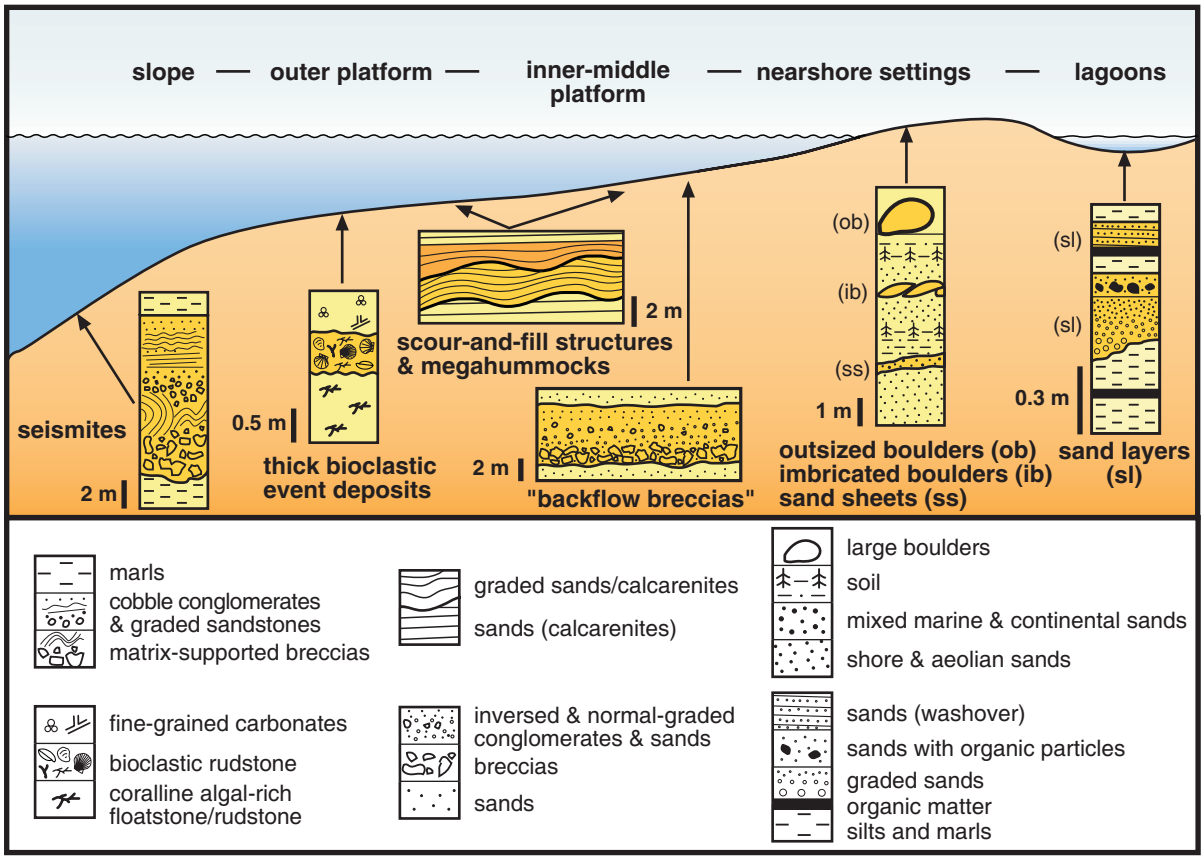

Fig. 44. Idealized tsunami-related deposit spectrum from continental to deep-water settings. Tsunami-related deposits stand out in a grey background. Selected examples and sections based on papers by several authors (Kleverlaan, 1987; Bondevik *et al.*, 1997; Rossetti *et al.*, 2000; Cantalamessa and Di Celma, 2005; Scheffers and Kelletat, 2005, Switzer *et al.*, 2006). Thick, bioclastic (shell debris) event deposit and megahummockite cases are those reported in this paper.

who consider that tsunami wave(s), induced by the collapse of the Santorini caldera (3500 years BP) in the eastern Mediterranean, produced megaturbidites and "homogenite" in deep-water settings, and correlate them with some coetaneous, coastal, tsunami-related deposits.

6. Conclusions

Sedimentological evidence from the Azagador Member carbonates indicates that a tsunami event(s) affected the Sorbas Basin in the latest Tortonian-earliest Messinian. At that time, temperate carbonate ramps developed at both margins of the basin. The underlying topography conditioned the development of two different depositional models: (1) a steepened ramp at the northern margin, representing a complex infilling of a highly irregular substrate, with robust branching bryozoan talus-facies at the toe of submarine cliffs changing to widespread *maerl* facies, consisting of branching coralline algal accumulations. Minor local facies include intercalated *Heterostegina*-rich sand bodies and rhodolith fields, located in small, deeper depressions; (2) a gentle homoclinal ramp, at the southern margin, with an inner (mid-ramp) carbonate factory rich in bivalves, brachiopods and bryozoans, and an extensive outer (outer-ramp) factory of coralline algae, changing basinwards to bioturbated sediments rich in planktonic foraminifers.

Two types of tsunami-related deposits, intercalated within outer ramp sediments, are recognised: megahummockites, at the northern margin, and a thick shell-debris bed at the southern margin. These two distinct tsunamites relate to different palaeotopographic profiles. Inflow and backflow surge effects can be inferred from the sedimentological and geometric features of the tsunamites. At the northern margin, the steep outer ramp facing the basin was strongly eroded by the incoming tsunami wave(s). The large erosive surface found at the base of the megahummocky sets and the folds in the underlying beds were generated during the tsunami inflow. The backflow surges transported in suspension the removed sediments, which infilled the scours, giving way to the megahummocks themselves. At the southern margin, the tsunami wave(s) crossed the gentle outer-ramp, eroding the seafloor to some extent, but major erosion focused on inner settings. The irregular base of the thick shell-debris bed indicates that incoming surges eroded the outer-ramp sediments to some extent, although this erosion was most intense in mid-and inner-ramp settings. The subsequent backflow removed and transported basinwards part of the previously eroded sediments. The resulting deposit is a shell-debris megabed, intercalated within outer-ramp sediments, rich in bioclasts removed from mid-and outer-ramp factories.

The triggering mechanism for this tsunami event(s) probably relates to a seismic event(s) resulting as well in the development of large-scale seismites (e.g. the "Gordo Megabed") in the adjacent Tabernas Basin during the same time interval.

Tsunamites in the Sorbas Basin contribute to characterise the poorly-known sedimentary record of tsunami deposits in outer-ramp environments, linking well-known shallow-water marine and continental tsunamites with tsunami-associated deposits (seismites and megaturbidites) in deep-water settings.

Acknowledgements

This work was funded by "Ministerio de Educación y Ciencia" (Spain), Proyect CGL 2004-04342 and by a doctoral F.P.U. grant (MECD-UGR) awarded to A. Puga-Bernabéu (AP2003-3810). J.M. Martín and J.C. Braga were also supported by Topo-Iberia Consolider Ingenio 2006 (CSD 2006-00041). We are grateful to Christine Laurin for correcting the English text. The constructive reviews by Peter J.J. Kamp and Kick Kleverlaan are greatly appreciated.

5

HIGH-FREQUENCY CYCLES IN UPPER-MIOCENE, RAMP TEMPERATE CARBONATES (SORBAS BASIN, SE SPAIN)

Ángel Puga-Bernabéu*, Juan C. Braga, José M. Martín

Departamento de Estratigrafía y Paleontología, Facultad de Ciencias, Campus de Fuentenueva s.n., Universidad de Granada, 18002 Granada, Spain

**Corresponding author: Fax: +34 958 248528*

E-mail address: angelpb@ugr.es

Facies 53 (2007) 329–345
Received 4 December 2006; accepted 8 March 2007

Abstract

Uppermost-Tortonian temperate carbonates occur at the southern margin of the Sorbas Basin (Almería, SE Spain). These carbonates, included in the Azagador Member, formed in a gentle, shallow-water ramp. Six facies cycles in ramp deposits comprise alternating bivalve-shell concentrations and coralline algal beds. The basic cycle reflects the landward advance, as relative sea level rose, of coralline algal deposits, which were the facies of the outer ramp, over bivalve biostromes, which grew in the shallower areas of the mid-ramp. Biostromes were mainly built by oysters and locally by *Isognomon*. In many cases, however, the removal of smaller shells by storms left only thin, discontinuous patches of large bivalves as residual remains of the oyster biostromes. Some original cycles might be missing due to complete removal of bivalve shells from the biostromes. The six cycles recognised, therefore, should be considered as the minimum number of original cycles in the Azagador carbonates. The available age constraints suggest these cycles were forced by orbital precession or some higher-frequency process. Lithological cycles forced by precession are characteristic of the basinal deposits laterally equivalent to the Azagador carbonates.

Keywords: temperate carbonates, oyster biostromes, cycles, taphonomy, Sorbas Basin, SE Spain

1. Introduction

Orbitally-controlled, high-frequency sedimentary cycles have been widely recognised and described in tropical peritidal carbonate deposits from a large number of localities of diverse geological ages (e.g. Fisher, 1964; Selg, 1988; Jiménez de Cisneros and Vera, 1993; Sami and James, 1994; Elrick, 1995). Likewise, slope and basinal fine-grained deposits laterally equivalent to carbonate platforms usually exhibit well-developed lithological cycles, which have been the subject of many cyclostratigraphic and astrochronological analyses (e.g. Kroon *et al.*, 2000; Prokoph and Thurow 2000; Gong *et al.*, 2001; Sierro *et al.*, 2001; Williams *et al.*, 2002; Elrich and Hinnov 2007). In contrast, reported examples of orbitally-forced sedimentary cycles within ramp carbonate rocks are very scarce (Aurell *et al.*, 1995; Badenas *et al.*, 2003). In all likelihood, the nature and degree of lithological and facies changes related to high-frequency oscillations are extremely unobtrusive in most cases or the original variations have been obliterated by later sedimentary and diagenetic processes.

The upper-Miocene Azagador carbonates in the Sorbas Basin, which formed in ramps along the basin margins, change laterally and upwards to fine-grained basin deposits showing outstanding orbitally-controlled cycles (Krijgsman *et al.*, 1999; Sierro *et al.*, 2003) The occurrence of clearly-defined cycles in coeval sediments suggests that these Azagador carbonates could provide good examples of the lithological and facies expression of orbital cycles in ramp carbonates. The aim of this work is to describe and interpret the background sedimentary processes and event-related modifications that shaped the appearance of these high-frequency cycles in the ramp deposits in the Azagador carbonates.

2. Geological setting

The Sorbas Basin is a small intermontane basin in southeastern Spain (Fig. 45) that developed as the Betic Cordillera lifted during the Late Miocene (Ott d'Estevou and Montenat, 1990; Braga *et al.*, 2003b). It is a small, E-W elongated basin bounded to the north by the Sierra de Filabres and to the south by the Sierra Alhamilla-Sierra Cabrera. These sierras, which are outcrops of the Betic basement, are mainly made up of metamorphic rocks and Lower-Miocene marine deposits.

Basin infilling extends from the Middle Miocene to the Quaternary (Fig. 46), and comprises several stratigraphic units separated by unconformities (Martín and Braga, 1994). Unconformably overlying the basement, continental red conglomerates and sandstones occur, presumably of Serravallian age. Lower-Tortonian, shallow-marine calcareous sandstones and conglomerates overlie the continental deposits. Upper-Tortonian carbonate platform sediments, including coral-reef patches, and local fan-delta conglomerates and sands occur at the northern margin of the basin. These deposits change laterally to submarine fan deposits, consisting of conglomerates and turbidite sandstones, intercalated within basinal marls (Chozas Formation of Ruegg, 1964). The Azagador Member of Ruegg (1964), which is the main subject of this study, unconformably overlies the upper Tortonian rocks. It consists of heterozoan carbonate sediments, latest Tortonian-earliest Messinian in age, deposited on carbonate ramps at both margins of the basin (Martín and Braga, 1994; Wood, 1996; Puga-Bernabéu *et al.*, 2007b). The Azagador carbonates grade upwards and laterally into marls–the Lower Abad Member marls of Ruegg (1964) and Martín and Braga (1994). Two Messinian reef units unconformably overlie the Azagador carbonates at both margins of the basin (Riding *et al.*, 1991; Braga *et al.*, 1996b; Braga and Martín, 1996; Martín *et al.*, 1997). Basinwards both Messinian reef-carbonate units change laterally to silty marls and marls with intercalated diatomites–the Upper Abad Member marls of Ruegg (1964) and Martín and Braga 1994. A major, subaerial erosional surface can be traced from the top of the Fringing Reef Unit to the centre of the basin (Riding *et al.*, 1998, 2000). This surface is thought to be coeval with the Messinian Mediterranean desiccation (Martín and Braga, 1994; Riding *et al.*, 1998, 2000; Braga *et al.*, 2006b). Selenite gypsum (Yesares Member of Ruegg, 1964**)** formed on top of this surface at the basin centre (Riding *et al.*, 1998, 2000). Evaporites are overlain by sands and silts together with oolites, stromatolite-thrombolite bioherms, and coral-reef patches (Riding *et al.*, 1991; Martín *et al.*, 1993; Braga *et al.*, 1995), late Messinian in age (the Sorbas Member of Ruegg, 1964). Fluvial and lacustrine sediments (the Zorreras Member of Ruegg, 1964) overlie the above units (Martín-Suárez *et al.*, 2000; Mather and Stokes, 2001). A thin, shallow-marine Pliocene unit and an alluvial Plio-Quaternary unit complete the infilling of the Sorbas Basin (Mather, 1993, 2000).

3. Methods

Three sections were selected in the Azagador Member outcrop at the southern part of the Sorbas Basin. This unit is well exposed at a south-facing cliff that is nearly continuous from Riscos de Sánchez to Collado de las Cabezas (Fig. 45). From the latter point, the unit can be traced to the Los Molinos del Río Aguas and Los Perales through less well-exposed outcrops. The three sections represent observation sites along a proximal-distal transect

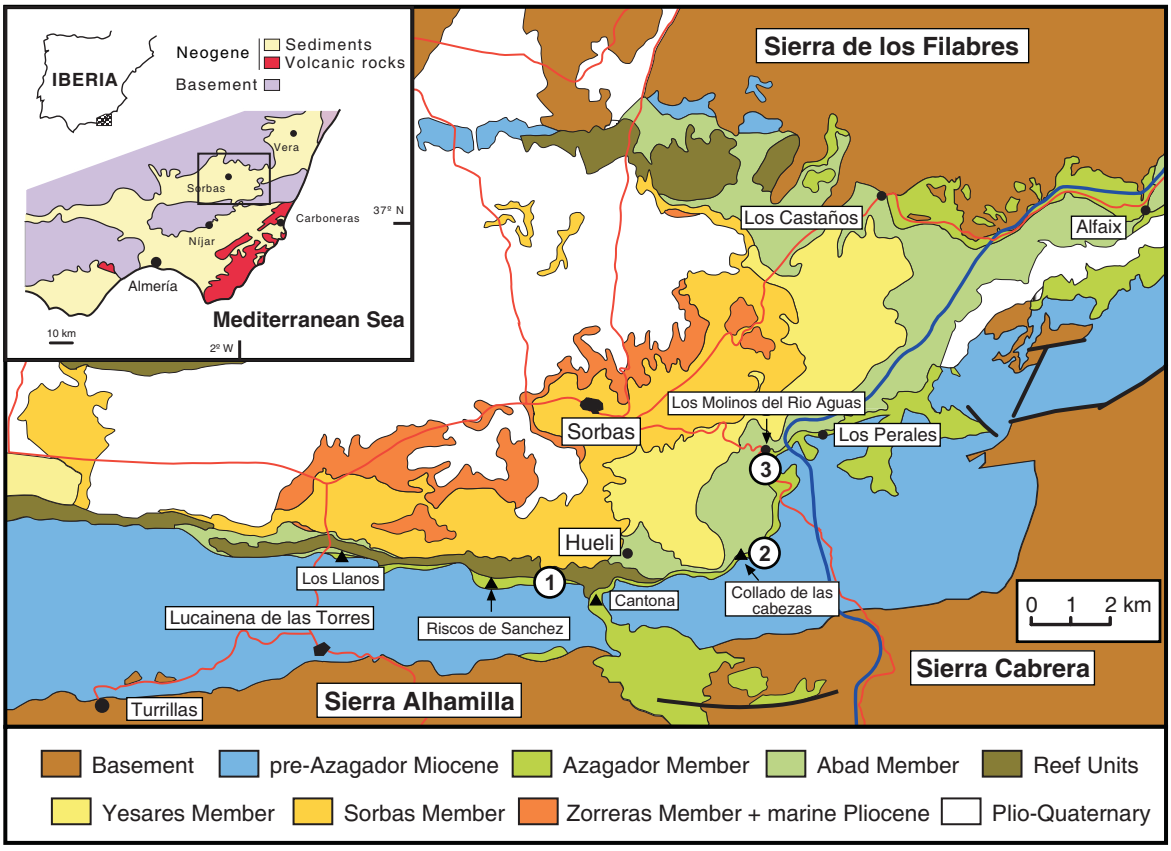

Fig 45. Neogene basins in southeastern Spain and detailed geological map of the Sorbas Basin (modified from Montenat, 1990). Numbers show location of the study sections: 1) Collado de Los Molinos; 2) El Cerrón; 3) Molinos del Río Aguas.

of the Azagador Member. The sections were logged and sampled for sedimentological analysis. Sixty-seven thin sections were cut from selected samples for characterisation of facies and identification of microfossils, especially coralline algae. Taphonomic attributes of individual beds were quantitatively analysed by observations in sampling quadrats 20 cm a side. Four to five quadrats were analysed per bed depending on the heterogeneity of the facies.

4. Azagador carbonates

The Azagador Member consists of platform carbonates mixed with diverse proportions of siliciclastics. The Azagador carbonates are bioclastic calcarenites and calcirudites with coralline algae, bivalves, bryozoans, brachiopods, benthic foraminifers, and echinoderms. These bioclastic components are characteristic of the Heterozoan skeletal association (James 1997). Stable isotope values of planktonic foraminifers in the marls (the Lower Abad marls) laterally equivalent to the Azagador carbonates indicate that these carbonates formed with surface-water temperatures similar to those of the present-day western Mediterranean (Sánchez-Almazo *et al.*, 2001). Siliciclastic sediments, concentrated at the basin margins in areas of river discharge, mainly occur as deltaic deposits with various degrees of reworking by marine processes.

The Azagador temperate carbonates formed on ramps at both margins of the basin (Wood, 1996). The topography of the underlying substrate controlled the facies types and distribution at each margin (Puga-Bernabéu *et al.*, 2007b). Azagador carbonates at the southern margin of the Sorbas Basin extend from Los Llanos to Los Perales hamlet, unconformably overlying upper Tortonian marls and turbidite sandstones (Fig. 45). The studied sections at the southern margin of the Sorbas Basin (Fig. 45) are described below in a proximal to distal transect.

4.1. Collado de los Molinos Section

The lower part of the Azagador Member in this section comprises conglomerate and bioclastic conglomerate clinobeds prograding westwards as they downlap the

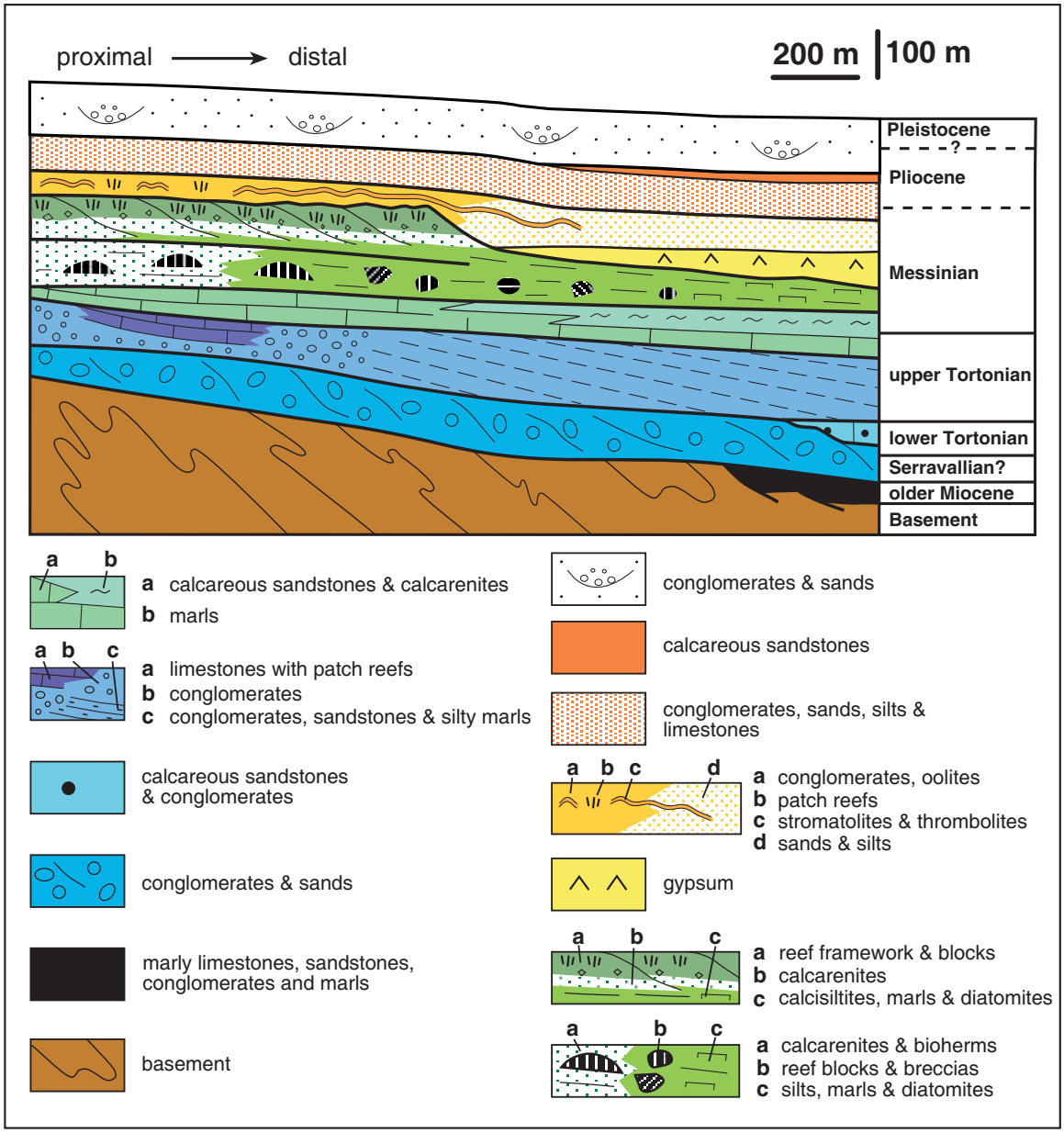

Fig. 46. Miocene to Quaternary stratigraphy of the Sorbas Basin (modified from Martín and Braga, 1994).

erosive surface on top of upper Tortonian marls and turbidite sandstones. Progradation of conglomerates continues laterally for 3 km to the Risco de Sánchez where it jogs to the north (Fig. 45). The Azagador carbonates overlie the toplap surface of the conglomerate beds and are in turn unconformably overlain by Messinian reef deposits (Fig. 47). The section exposure is roughly parallel to the strike of the northward-dipping Azagador carbonate beds.

4.1.1. Lower part

The lower part of the section consists of decimetre-scale beds of matrix-supported conglomerate. Total thickness is 12 m at the logged section, increasing laterally westwards up to 90 m. The matrix is made up of terrigenous sand with bioclasts. The terrigenous clasts are mainly pebbles and cobbles, made up of dark dolostone from the Triassic cover of the Betic basement cropping out in Sierra Alhamilla at the southern margin of the basin. Quartzite and micaschist pebbles from the Betic basement and clasts

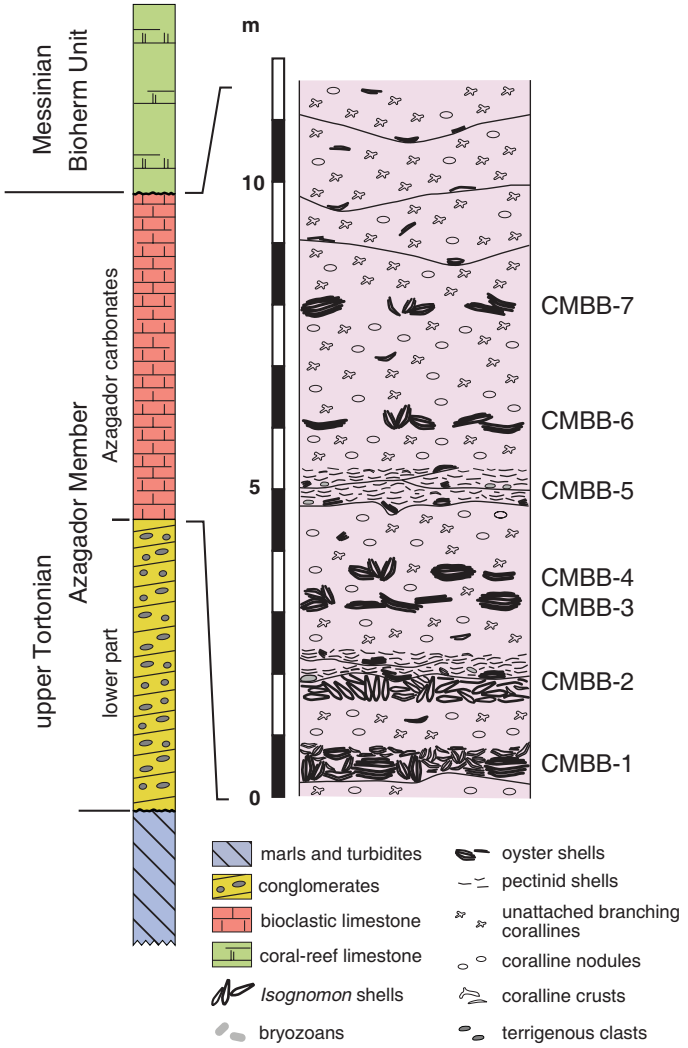

Fig. 47. Stratigraphic column of the Collado de los Molinos section (location shown in Fig. 45).

from the Tortonian turbidite sandstones also occur. The clasts are locally imbricated, pointing to current directions from the southeast. Non-graded beds dominate in the conglomerates, although some normally graded layers and crude planar lamination are observed locally. Identifiable bioclasts dispersed in the conglomerate are mainly oyster, pectinid, and coralline algal fragments. Some centimetre-scale layers show higher concentrations of bivalve shells parallel to bedding or with no preferred orientation. Large shells, up to 20 cm in size, of *Ostrea* and *Gigantopecten* tend to concentrate at the tops of conglomerate beds.

4.1.2. Interpretation

The conglomerate prograding clinobeds represent the foresets of a small delta of a river draining the Betic basement. Delta conglomerates and sands incorporated bioclasts, mainly from oysters that grew on the upper setting of the delta front.

4.1.3. Azagador carbonates

The limestone overlying the conglomerates, up to 12 m in thickness, comprises two main types of alternating deposits: bivalve and algal beds (Fig. 47). The taxonomic composition, taphonomic attributes and sedimentary structures of bivalve beds significantly change throughout the section and are described in detail below. The algal deposits are less diverse in components and structures.

4.1.3.1. Bivalve beds. CMBB-1) The lowest bivalve bed is mostly made up of densely-packed, articulated, whole

Table 2. Average values of taphonomic attributes measured in the Collado de los Molinos section

Bivalve bed	Articulation		Shell size (cm)				Angle (°)		Orientation			Fragment			Interaction	
	A	D	Max	Min	Ave	SD	Ave	SD	Up	Down	Other	Int	Edge	Frag	Bor	Enc
CMBB-1	18.7	81.3	16.5	0.6	5.0	3.0	68.6	51.6	24.7	29.7	45.6	17.6	29.7	52.7	26.9	0.55
CMBB-2	47.0	53.0	17.0	0.7	7.5	4.5	64.2	61.2	19.7	12.1	68.2	62.1	1.5	36.4	3.0	0.0
CMBB-3	20.0	80.0	16.0	1.5	8.8	5.1	68.9	55.9	31.4	31.4	37.2	20.0	25.7	54.3	57.1	0.0
CMBB-4	23.1	76.9	22.0	1.5	8.5	4.5	84.4	46.3	26.9	28.8	44.3	17.3	34.6	48.1	61.5	1.9
CMBB-5	0.0	100.0	18.0	0.6	2.1	1.9	78.8	58.4	62.4	15.3	22.3	0.0	0.0	100.0	0.0	0.0

Values are expressed as the average percentages obtained from the five squares (20 cm a side) distributed in each bivalve bed.

A: articulated; D: disarticulated, Max: largest shell size; Min: smallest shell size; Ave: average; SD: standard deviation; Fragment: fragmentation; Int: intact; Frag: fragmented; Bor: boring; Enc: encrusting.

and unabraded shells of *Ostrea edulis*. They grew on and around sand lenses, rich in coralline algae, echinoid spines, and bryozoans that formed at the top of the underlying deltaic conglomerate. The shell concentration filled the uneven seafloor and, consequently, its thickness varies from 15 to 55 cm. Oysters mostly occur in life orientation, with the plane of the commissure oriented from vertical to parallel to the bedding as most individuals grew on and adapting to pre-existing specimens. Shell-size range (from 0.6 to 16.5 cm, Table 2) reveals a wide age spectrum of individuals in the assemblage. The shells show *Entobia* borings (made by clionid sponges) and a few are partially encrusted by unilaminar bryozoans. *Pecten dunkeri* Mayer and *Gigantopecten* sp. are accessory components. Inter- and intraskeletal spaces were filled by bioclastic calcarenite-calcirudite or remained open.

CMBB-2) The lower part of this bed (up to 90 cm in thickness) consists of densely packed, mainly articulated specimens of *Isognomon* (*Hippochaeta*) *maxillatus* with varying degrees of dissolution of the original shell. Many *Isognomon* specimens are actually preserved as inner moulds with very little or no shell remaining. Although most individuals occur subhorizontally, locally a few specimens are preserved in life orientation with a subvertical commissure plane. Size of specimens ranges from 5 to 15 cm. *Ostrea*, *Spondylus*, *Pecten*, and *Chlamys* are accessory components of the bivalve assemblage. Echinoids, bryozoans and coralline algae appear in the calcarenite-calcirudite matrix filling the original inter- and intraskeletal open spaces of the shell concentration.

The *Isognomon* concentration is incised by an irregular erosive surface overlain by a rudstone of bivalve shells, coralline algae, and terrigenous clasts, up to 10 cm in size. Bivalves are mainly large (up to 20 cm), disarticulated, and broken *Ostrea* and pectinid shells, including very large (up to 25 cm) disarticulated *Gigantopecten* valves. Shell orientation shows high variance. Coralline algae occur as rhodoliths and broken branching thalli. The total thickness of this overlying layer varies from 40 to 60 cm.

CMBB-3 and CMBB-4) These two beds consist of thin (up to 25 cm), laterally discontinuous patches of thick, large oysters (*Ostrea* and minor *Hyotissa*). Oyster valves, mostly >10 cm in size, are articulated and disarticulated with high variance in orientation and low fragmentation. Some specimens form small clusters. Large articulated and disarticulated *Gigantopecten* shells, and broken valves of *Pecten*, *Chlamys,* and *Spondylus* occur among the oyster shells together with coralline algae and scarce terrigenous pebbles.

CMBB-5) This bed is a rudstone with an irregular erosive base and variable thickness up to 70 cm. Identifiable bioclasts are mainly stacked, concave-up valves of *Chlamys* (and *Pecten*) with variable fragmentation (Fig. 48). Large fragments of *Ostrea* and *Gigantopecten* with no preferred orientation tend to concentrate at the base of the bed, together with terrigenous pebbles up to 3 cm in size. Coralline algal and bryozoan fragments occur among the bivalve shells.

CMBB-6 and CMBB-7) The two upper bivalve beds are similar to the afore-described CMBB-3 and CMBB-4.

4.1.3.2. Algal beds. Calcirudite-calcarenite intervals with coralline algae as main components alternate with the bivalve beds. The algae mostly occur as rhodoliths, up to 5 cm in size, with unattached branching thalli engulfed in a matrix of algal, bryozoan, mollusc, echinoid, and foraminifer fragments and few terrigenous grains. Rhodoliths are made up of encrusting, warty, and fruticose plants that grew on bioclastic nuclei, commonly branching bryozoan colonies. *Lithothamnion* (mainly *Lithothamnion philippii* Foslie and *Lithothamnion ramossisimum* (Reuss) Piller), *Mesophyllum* (*Mesophyllum lichenoides* (Ellis) Lemoine and *Mesophyllum alternans* (Foslie) Mendoza

Fig. 48. Stacked pectinid shells in a storm shell concentration (bivalve bed CMBB-5) of the Collado de los Molinos section. Some large bivalves (*Gigantopecten*) are also present. Coin is 2.3 cm in diameter.

and Cabioch), *Lithophyllum* (*Lithophyllum incrustans* Philippi-*Lithophyllum racemus* (Lamarck) Foslie group and *Lithophyllum dentatum* (Kützing) Foslie) are the major components of the coralline algal assemblages. *Elphidium* is the most common foraminifer. Some shells at the top of the bivalve concentrations are encrusted by thin veneers, up to a few centimetres thick, of coralline algae with minor nodular bryozoan colonies (Fig. 47).

Above the uppermost bivalve concentration (CMBB-7), in the last 2 m of the section, the algal beds show cross-cutting erosive bases. Pectinid fragments concentrate on top of these erosive surfaces.

4.1.4. Interpretation

4.1.4.1. Bivalve Beds. The high proportions of articulated whole shells of *O. edulis* in life position, together with the wide size spectrum in the oyster assemblage suggest that CMBB-1 is the result of *in-situ* growth of gregarious oysters with little or no reworking of shells. Relatively few pectinids dwelt on the build-up. The oysters colonised an undulated bioclastic bottom and built a biostrome for several generations with a very low sedimentation rate, as indicated by the abundant empty spaces between shells. The matrix partially filling the voids between shells is most probably the result of percolation from the red algal deposits that buried the oyster biostrome. Similarly, the lower part of CMBB-2 is an authochtonous concentration of articulated *Isognomon* specimens locally preserved in their original vertical growth habit (Savazzi, 1995), but mostly fallen down to lie on one of the valves. Oysters and *Spondylus* settled on the bottom or directly on *Isognomon* shells, contributing to construction of the bivalve biostrome. The dissolution of *Isognomon* shells is a later diagenetic feature.

In contrast, the upper part of CMBB-2, as well as CMBB-5, can be interpreted as event shell concentrations. Clear-cut erosive bases, rough fining upward grading of clasts (including large terrigenous pebbles), and stacking of fragmented valves are prominent features characteristic of proximal tempestites.

The occurrence of only large specimens of oysters and pectinids in discontinuous thin patches suggests that CMBB-3, -4, -6, and -7 are lag-shell concentrations. We interpret these beds as "residual" oyster biostromes such as CMBB-1, after selective removal of small- and medium-sized shells of builders and dwellers (Fig. 49). Storms affected the original biostromes leaving only the heaviest shells *in situ* or slightly displaced. This process favoured the concentration of shell clusters that withstood removal better than isolated specimens.

4.1.4.2. Algal beds. The alternating algal facies formed by the autochthonous/parautochthonous accumulation of

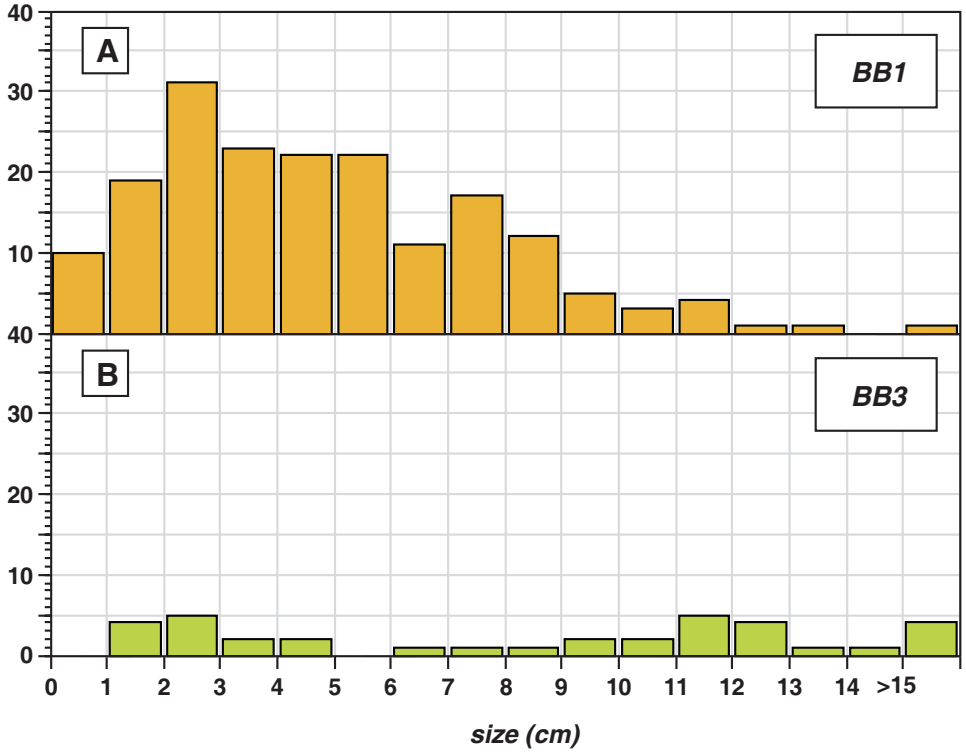

Fig. 49. Shell-size distribution in A) an unaltered biostrome (CMBB-1), and B) a bed of thin discontinuous patches of large shells (CMBB-3). The analysed surface was the same in both beds: five quadrats measuring 20 cm a side. The histograms clearly show the selective disappearance of small shells and a general reduction in the number of specimens when the original biostromes (A) were washed by storms and only large and clustered shells remained (B).

coralline algal skeletons. Within this algal factory, part of the plants encrusted hard substrates such as bivalve shells, but most plants grew unattached, producing loose carbonate particles of various sizes, from just millimetres to a few centimetres. The majority of identified components of the algal assemblages are extant species in the Mediterranean Sea (Braga and Aguirre, 2001). In present-day Mediterranean platforms, they show depth distributions that can be applied to interpret the palaeodepth for the formation of the late-Miocene algal beds (Bressan and Babbini, 2003). The occurrence of *Lithophyllum incrustans-Lithophyllum racemus* and *Lithophyllum dentatum* with *Lithothamnion philippi* and *Mesophyllum* species suggests palaeodepths of 15–40 m for the algal factory. This depth is below the current fair-weather wave base in the Mediterranean (Pérès and Picard, 1964). The abundance of the epiphytic foraminifer *Elphidium* points to the presence of sea-grass meadows or patches on the algal gravel that covered the sea floor. Biological and storm reworking caused fragmentation of bioclasts, especially bivalve shells. The amalgamated erosive surfaces with shell lags in the upper part of the section indicate repeated reworking by storms of the uppermost algal deposits.

4.2. El Cerrón Section

In this section the Azagador carbonates, which unconformably lie on top of upper Tortonian marls and turbidite sandstones, consist of alternating bivalve and algal beds in the lower half (Fig. 50). As in the previous section, algal beds are monotonous in composition and structure while bivalve beds show strong variations in their features and are described in detail in the following from bottom to top.

4.2.1. Bivalve beds

ECBB-1 and ECBB-2). The bivalve beds are thin (up to 15 cm), laterally discontinuous patches of thick, large, articulated and disarticulated *Ostrea* valves, ranging in size from 10 to 20 cm. The degree of fragmentation of valves is low with a high variance in orientation. Large fragments of *Gigantopecten* shells, and broken valves of *Pecten*, *Chlamys,* and *Spondylus* also occur. Large shells are encrusted by coralline algae and bored by *Entobia* (sponge borings).

ECBB-3). This is an *O. edulis* shell concentration, up to 40 cm in thickness, with an irregular erosive base. The

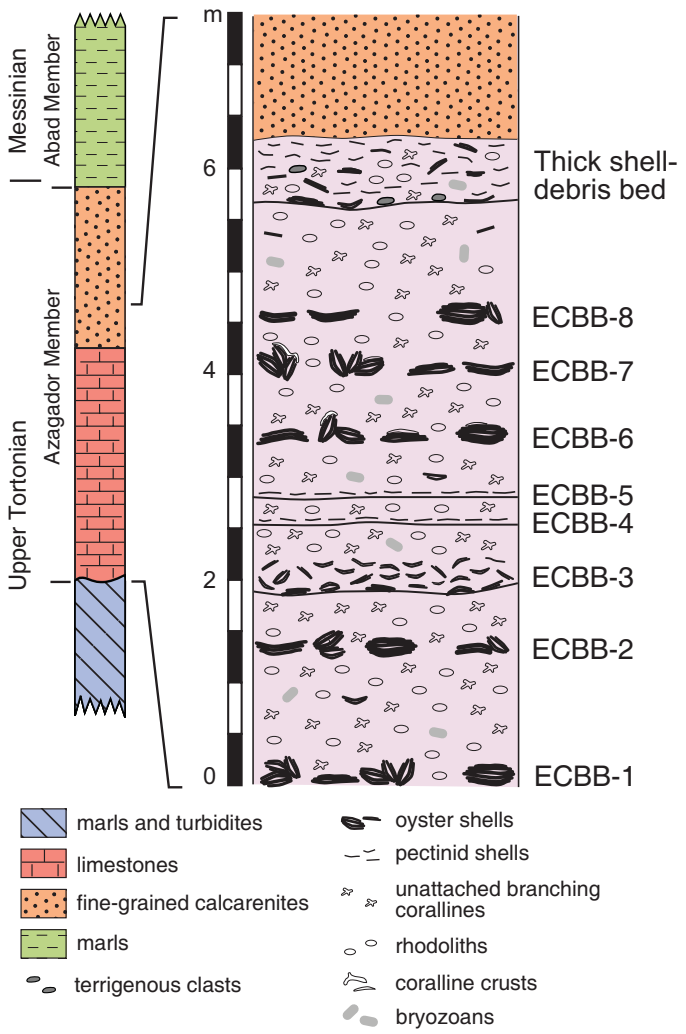

Fig. 50. Stratigraphic column of the El Cerrón section (location shown in Fig. 45).

largest shells, up to 22 cm in size, are concentrated at the base. Pectinid shells, echinoids, and coralline algae also occur in the calcirudite matrix. Most oyster valves are disarticulated and fragmented, although the fragments are relatively large. A preferred concordant orientation of valves is patent, particularly of flat right valves of *Ostrea*. *Entobia* borings and encrusting bryozoans are observed, but bioerosion and encrustation are not intense.

ECBB-4 and ECBB-5). These beds comprise relatively thin, up to 10 cm, shell concentrations with an irregular wavy base. Shells are disarticulated and fragmented valves of pectinids and oysters ranging in size from 2 to 8 cm. Most shells are concordant with convex-up and -down orientations in the case of curved valves. Coralline algal and bryozoan fragments occur in the calcarenite matrix.

ECBB-6 to -8). These beds are similar in geometry and composition to beds ECBB-1 and -2. Encrustation of oyster shells by coralline algae is particularly extensive in beds ECBB-6 and ECBB-7 (Fig. 51).

4.2.2. Algal beds

Calcirudite-calcarenite intervals mainly composed of coralline algae alternate with the bivalve beds. The features and components of these algal beds are similar to those of the algal intervals intercalating bivalve beds in the Azagador limestones at the Collado de los Molinos section described above.

The uppermost coralline algal interval is overlain by a bioclastic calcirudite, 50–60 cm thick, with an erosive base and undulated top. The bed is a concentration of densely packed fragments of pectinids, brachiopods, coralline

Fig. 51. Oyster shell encrusted by coralline algae. Discontinuous bivalve patch (ECBB-6) in the El Cerrón section. Coin is 2.3 cm in diameter.

algae, aragonitic shell moulds, oysters, echinoderms (mainly spines), and rare balanids. This thick shell-debris bed (TSB) is described in detail in Puga-Bernabéu *et al.* (2007b). Curved bivalve shells are stacked with convex-up and -down orientations and the matrix is a bioclastic calcarenite.

Fine-grained calcarenites to calcisiltites, 6 m thick, rich in planktonic foraminifers, form the upper part of the Azagador carbonates in this section. These deposits are bioturbated by conspicuous *Thalassinoides* traces. Siliciclastic content, mainly quartz and glauconite grains, is lower than 15%. The fine-grained calcarenites grade upwards into silty marls and marls.

4.2.3. Interpretation

Bivalve beds ECBB-1, -2, -6, -7, and -8, like similar deposits in the Collado de los Molinos section, can be interpreted as lags of large shells and shell clusters after removal by storms of smaller and lighter components of original oyster biostromes.

Several sedimentary and taphonomic features suggest that ECBB-3 is a tempestite: an erosive base, rough fining-upwards of bioclasts, and disarticulated and fragmented valves with preferred concordant orientation. The high proportion of oyster shells indicates that this bed is the result of reworking by a storm of an oyster biostrome with little mixing of bioclasts from other sources within the platform.

Undulated bases, disarticulation, and fragmentation of valves, together with the preferred concordant orientation of shells, indicate that ECBB-4 and ECBB-5 are tempestites as well. The lack of deep incisions at the base, lesser thickness, and better size sorting suggest these storm concentrations are more distal than those in ECBB-3.

The algal intervals can be interpreted, as in the Collado de los Molinos, as autochthonous/parautochthonous accumulations of coralline algal skeletons either encrusting bivalve shells or as unattached particles. A certain degree of reworking is mainly evidenced by fragmentation of invertebrate shells included in the algal gravel. Coralline algal components, and consequently their palaeobathymetric significance, are similar to those at the Collado de los Molinos section.

Geometric features and internal characteristics of the TSB, which can be traced for more than 3 km N-S across the Azagador carbonates, indicate strong erosion and bioclast transport and redeposition in a single event. The high-energy process required for such huge sediment remobilisation and transport in a single flow has been related to a tsunami event (Puga-Bernabéu *et al.*, 2007b).

Planktonic foraminifer abundance in the fine-grained calcarenites to calcisiltites indicates an open, deeper, and low-energy marine environment with a low sedimentation rate that favoured the formation of glauconite and the development of abundant *Thalassinoides* traces.

4.3. Molinos del Rio Aguas Section

4.3.1. Description

The Azagador carbonates unconformably overlie upper Tortonian marls. The lower 4.5 m of the section consist of laterally discontinuous, amalgamated beds with irregular, erosive bases and maximum thicknesses of about 50 cm. Fragments of oysters, up to 10 cm in size, and minor pectinid shells concentrate at the base of the beds (Fig. 52). Shell fragments are oriented parallel to the bed base. Two clusters of several relatively large, up to 12 cm, *Ostrea* specimens, a few of them articulated, are observed. The bulk of the deposit, however, is a rudstone of coralline algal bioclasts. These include rhodoliths (up to 4 cm in size), rhodolith and branching coralline fragments, and unattached open-branching plants. The overlying 3 m are flat-bedded rudstones with irregular erosive bases, composed of densely packed open-branching, unattached coralline algal thalli. *Lithothamnion* and *Mesophyllum* are the major genera in the algal assemblages throughout the section, with *Lithophyllum* (*Lithophyllum dentatum* and *Lithophyllum incrustans-Lithophyllum racemus*) as a secondary component. Concentrations of fragments of thin laminar thalli of *Mesophyllum lichenoides* occur locally.

The coralline algal deposits are overlain by a bioclastic calcirudite, 50–60 cm thick, which can be traced to the similar bed (TSB) overlying the algal rudstones at El Cerrón section. The section ends with 2.5 m of fine-grained calcarenites to calcisiltites rich in planktonic foraminifers and *Thalassinoides* traces, which grade upwards into silty marls and marls.

4.3.2. Interpretation

In this section, bivalve shell concentrations only occur as lag deposits on the erosive surfaces at the base of amalgamated algal beds. These can be interpreted as

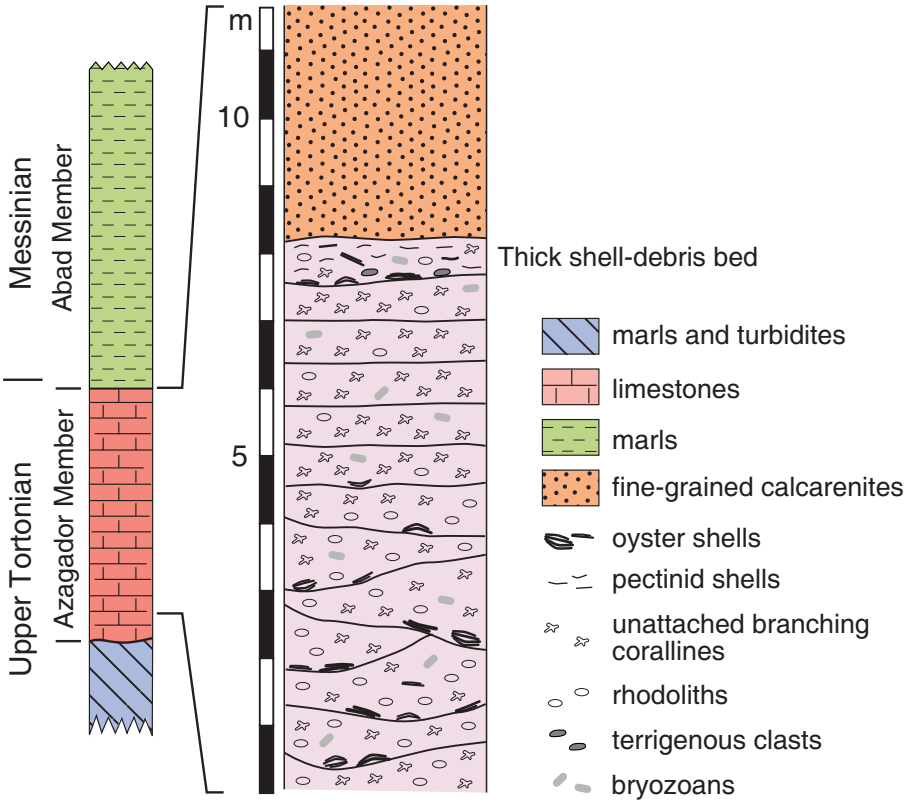

Fig. 52. Stratigraphic column of the Molinos del Río Aguas section (location shown in Fig. 45).

amalgamated storm deposits, resulting from reworking of algal and bivalve factories. See El Cerrón Section for a description and interpretation of the overlying TSB and fine-grained calcarenites to calcisiltites.

5. Depositional model

Based on the geometry of the deposits and facies distribution, it can be inferred that the Azagador carbonates formed in a gentle, shallow-water carbonate ramp extending to the south-southwest on the abandoned lobes of a delta. Autochthonous bivalve concentrations alternate with coralline algal facies in the most proximal section (Collado de los Molinos section), whereas algal facies are more abundant in the more distal sections (El Cerrón and Molinos del Río Aguas sections). This suggests that bivalve patches formed in the shallowest parts of the ramp while coralline algae thrived seawards of the bivalve autochthonous concentrations (Puga-Bernabéu *et al.*, 2007b).

Inner-ramp environments were represented by a shoal area, the remains of which crop out at Cerro Cantona, 0.75 km to the southeast of Collado de los Molinos section. There was an inner carbonate factory in a middle-ramp position, dominated by bivalves (oysters, *Isognomon*, *Spondylus*, pectinids) and an outer production zone where coralline algal fields developed (Fig. 53). *O. edulis* is widely distributed in shallow settings of temperate seas around Europe and North Africa (Stenzel, 1971); *Isognomon maxillatus* also lived in shallow subtidal settings (Savazzi 1995). The development of bivalve biostromes is probably associated with productive waters (Wood, 1993) and the river discharge evidenced by delta deposits from the Collado de los Molinos section to Riscos de Sánchez may account for high nutrient levels on the southern margin of the Sorbas Basin.

The present-day depth distribution in the Mediterranean Sea of the species recognised in the algal assemblages indicates that *in-situ* algal growth took place at palaeodepths of 15–40 m. Coralline crusts on bivalve shells in biostromes and rhodoliths with no evidence of reworking are representative autochthonous coralline remains while the algal fragments in the tempestite beds are obviously reworked and removed down ramp. The common occurrence of *Elphidium*, epiphytic foraminifer that lives on seagrass, points to the existence of seagrass patches or meadows on the sea floor covered by coralline algal nodules and loose plants.

The relative increase in algal facies upsection suggests a deepening-upward pattern in the Azagador carbonates, which is confirmed in the El Cerrón and Molinos del Río Aguas sections by the vertical change from algal calcirudites to finer-grained calcarenites and marls with planktonic foraminifers. This suggests that downslope red algal facies graded into fine-grained, heavily-burrowed, foraminifer-dominated facies (Fig. 53), which in turn passed laterally to deep-water marls.

Tempestites occur among the bivalve and algal factory deposits. Storm-concentrated bivalve-shell beds appear in the lower part of the Collado de los Molinos and El Cerrón

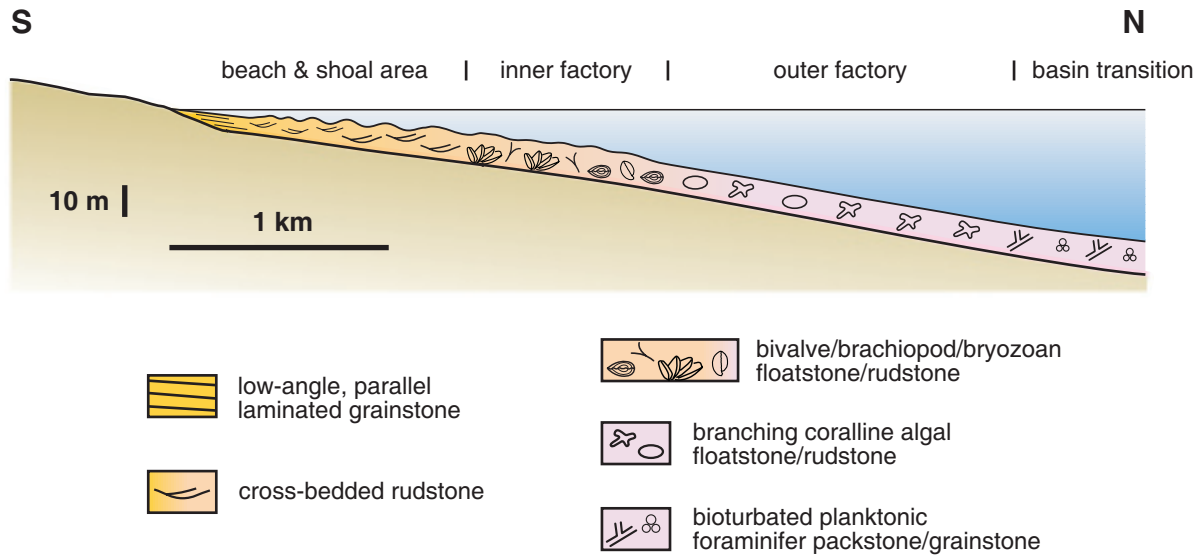

Fig. 53. Depositional model of the temperate-carbonate ramp at the southern margin of Sorbas Basin. *In-situ* carbonate production took place in middle (inner-factory) and outer (outer-factory) ramp positions (after Puga-Bernabéu *et al.*, 2007b).

sections while the upper parts of these two sections and the Molinos del Río Aguas section (the most distal one) consist of storm-related deposits comprising amalgamated beds of algal calcirudites with erosive, irregular bases. In this section, bivalves only occur as lag fragments on the erosive surfaces. The vertical and lateral distribution of the algal-dominated storm deposits indicates that the algal factory changed basinward to a facies belt dominated by tempestites mainly fed by reworked algal skeletons displaced downslope from their production area.

6. Cycles

In the lower part of the Azagador carbonates at the Collado de los Molinos section, bivalve biostromes of shells preserved in life position or tilted down alternate with algal levels composed of algal nodules and loose branches, corresponding to the carbonate factory dominated by algae. According to the proposed depositional model, this alternation represents cyclic development of relatively shallower facies (bivalve biostromes) and deeper facies (algal-factory intervals). This sequence can be interpreted as having been caused by fluctuations in relative sea level driving fluctuating shoreward and basinward displacement of facies belts.

We suggest that the same type of cyclicity is reflected by the alternation of thin and discontinuous patches of large bivalves and algal beds. According to our interpretation, these discontinuous patches are the residual deposit left after removal by storms of smaller shells from original bivalve biostromes (Fig. 54). The strong taphonomic modification of the original bivalve biostromes by storm events and later fair-weather processes affects the expression of the sedimentary cycles, but the background process, that is, the cyclic alternation of shallower and deeper facies driven by relative sea-level fluctuation, was essentially the same in cycles with a well-developed bivalve bed and in those in which only a thin and discontinuous bivalve layer remained.

At El Cerrón section, most cycles consist of couplets of thin, discontinuous patches of large shells and algal intervals. The bivalve bed in the second cycle is an original oyster biostrome modified by reworking with relatively little modification of original features. The shells were displaced from their life position, disarticulated and broken, but the degree of removal from small shells and fragments is not as pronounced as in the rest of the bivalve beds. This is an additional variant of the recorded expression of the original cyclity of bivalve biostromes and algal factory facies.

In the Collado de los Molinos and El Cerrón sections, storm-concentrated beds disrupt the regular alternation of bivalve biostromes and algal factory facies. These storm-shell beds can overlie both bivalve biostromes and algal facies, suggesting that they accumulated over large areas of the ramp.

At the most distal section, the Molinos del Río Aguas section, the bivalve biostromes/algal facies cycles are not recorded. The distal position of the section may account for the lack of the shallower bivalve concentrations. The bivalves occur as shell lags on the erosive surfaces of the successive amalgamated beds as components of storm-event deposits. There is no record of any background cyclicity such as that observed in more proximal sections.

The TSB at the transition from the algal rudstones to finer-grained calcirudites that extends from El Cerrón to the Molinos del Río Aguas section is an event deposit related to a high-energy process, probably a tsunami (Puga-Bernabéu *et al.*, 2007b). Like the storm shell beds, it constitutes a perturbation of the background cyclicity caused by an episodic process.

The lag nature of the thin discontinuous patches of large bivalves, which are the only remnants of the original bivalve biostromes, suggests that the actual number of recorded cycles cannot be an accurate reflection of the original number of fluctuations in sea level. The number of preserved cycles may be less than originally occurred if the removal of shells from bivalve biostromes by storms extended to the point of not leaving any residual specimens. The intercalation of event deposits (tempestites and tsunamite) in the background cycles further contributes to altering the cyclic pattern of the ramp deposits. Taking this into account, the six cycles recognisable both at Collado de los Molinos and El Cerrón should be considered as the minimum number of original cycles in the Azagador carbonates at the southern margin of the Sorbas Basin.

The available biostratigraphic data from the underlying and overlying marls accurately constrain the age of the the Azagador carbonates in the study area. According to Sánchez-Almazo *et al.* (2001), the top 38 m of the underlying upper Tortonian marls and turbidites at the Collado de los Molinos section formed after the planktic foraminiferal event PF-1 of Sierro *et al.* (1993), dated at 7.51 Ma by Hilgen *et al.* (1995). The planktic foraminiferal event PF-3 of Sierro *et al.* (1993), dated at 7.24 Ma by Hilgen *et al.* (1995), has been recorded in the marls immediately overlying the Azagador carbonates, 2 m above the contact at the Molinos del Río Aguas section. This chronological bracketing implies a time span of 270 ky for the deposition of nearly 40 m of marls and turbidites, the development of the erosional unconformity surface underlying the Azagador Member and the deposition of the Azagador carbonates plus the deltaic deposits. The narrow time interval left for the formation of

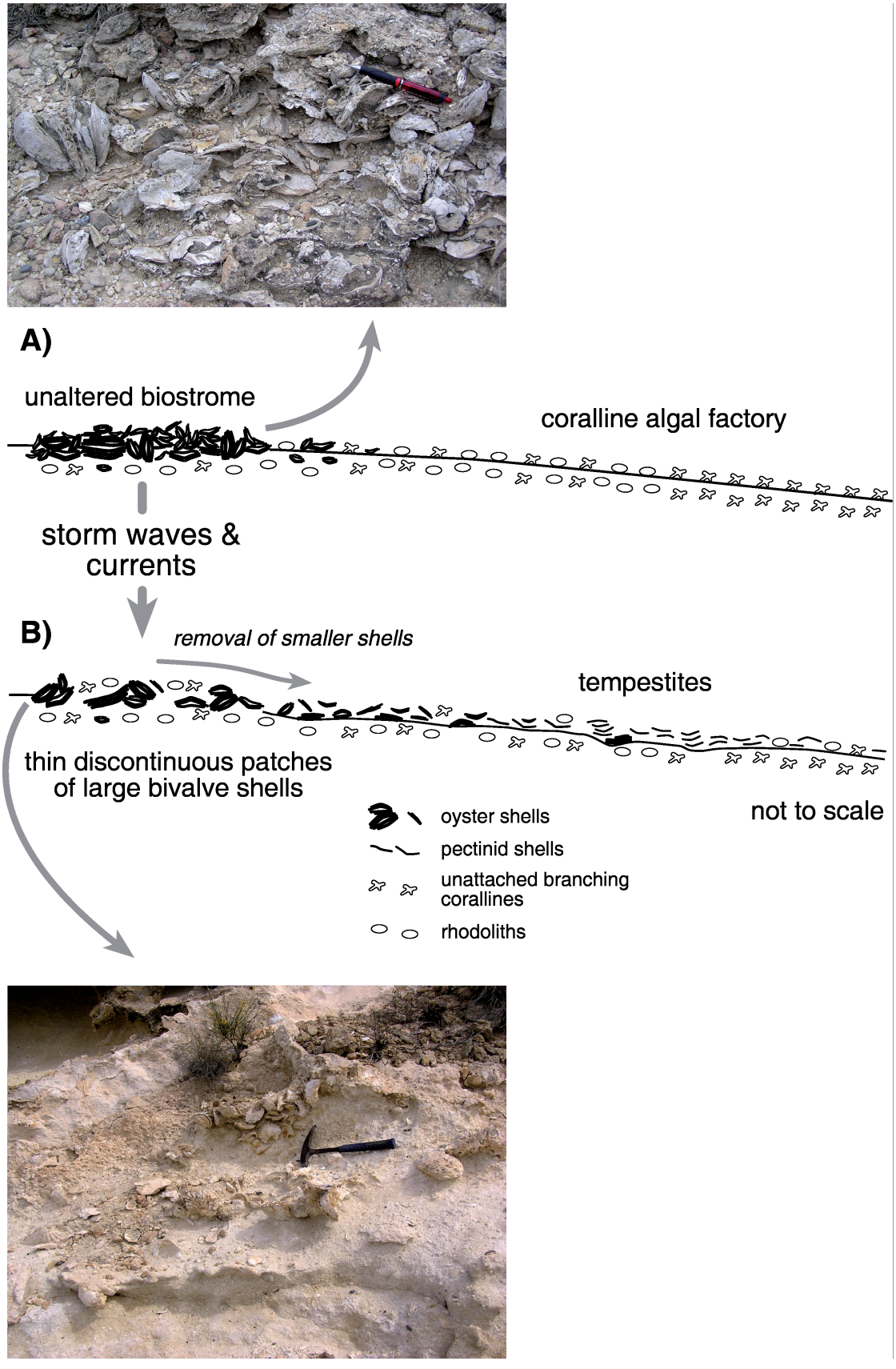
A)
unaltered biostrome
coralline algal factory
storm waves &
currents
B)
removal of smaller shells
tempestites
thin discontinuous patches
of large bivalve shells
not to scale
oyster shells
pectinid shells
unattached branching
corallines
rhodoliths

◀ **Fig. 54.** Model of the formation of thin discontinuous patches of large bivalve shells. A) Unaltered oyster biostromes included many articulated shells in growth position with a wide size (age) spectrum. B) Storm waves and currents removed small, lighter shells, leaving a lag of large, heavy shells and clusters of shells cemented one upon the other. The detached shells, together with other bioclasts, then accumulated as tempestites within the ramp. Pencil in A) field view is 14.5 cm in length; hammer in B) field view is 33 cm in length.

Azagador carbonates suggests that the recorded cyclicity was controlled by orbital precession or by some other cyclic process frequency higher than the one of orbital precession.

Precession-controlled cycles are the most outstanding lithological feature of the basinal deposits (Lower Abad marls) to which the Azagador carbonates grade laterally and vertically. The cycles in the Lower Abad consist of alternating grey homogeneous marls and indurated, opal-rich marls (Krijgsman *et al.*, 1999; Sierro *et al.*, 2001, 2003). Oscillations in planktic foraminiferal assemblages associated to lithological cycles have been interpreted as the result of climatic fluctuations with cooler and warmer periods related to precession maxima and minima, respectively (Sierro *et al.*, 2003). The lithological and palaeontological data obtained from the basinal sediments, however, are not sufficient to provide any indications about sea-level changes associated to climatic fluctuations. In the cycles described in this paper, taking into account that the upper limit for the algal factory belt is at about 15 m and its lower limit is at about 40 m, changes in sea level driving the onlapping of the algal factory on bivalve biostromes might represent sea-level oscillations of a few metres up to a few tens of metres.

Similar cycles involving high-frequency sea-level changes were described in the inner-ramp deposits of the Azagador Member in the Agua Amarga Basin, a Betic intermontane basin, some 20 km southeast of the Sorbas Basin. Five cyclic alternations of shallower and deeper facies within one of the sedimentary packages making up the Azagador Member in the Agua Amarga Basin were interpreted as driven by sea-level oscillations of a few metres to tens of metres controlled by orbital precession (Martín *et al.*, 1996).

7. Conclusions

The uppermost-Tortonian, temperate carbonates of the Azagador Member formed in a gentle, shallow-water carbonate ramp at the southern margin of the Sorbas Basin. Bivalve biostromes, mainly comprising oysters, developed in the mid-ramp, basinwards of a shoal belt, while coralline algae were the main sediment producers seawards of the bivalve autochthonous concentrations.

The alternation of bivalve-shell concentrations and coralline algal beds in the Azagador carbonates primarily is interpreted to reflect a cyclicity involving sea-level changes. The fluctuations in sea level controlled landward and seaward displacements of facies belts. The basic cycle represents the landward onlapping of coralline algal deposits (facies of the outer ramp) over bivalve biostromes (shallower facies of the mid-ramp) as relative sea level rose. The relatively restricted palaeodepth for the deposition of the algal beds (15–40 m; estimated from the depth distribution of extant coralline species) suggests sea-level fluctuations of a few metres up to a few tens of metres in each cycle. No cycles are recorded in the most distal section, the Molinos del Río Aguas, despite sea level changes, this section remained too deep for bivalve-biostrome development throughout the depositional interval of the Azagador carbonates.

The bivalve biostromes in many cycles, however, were strongly modified by taphonomic processes. The almost unaltered build-ups consist of bivalve biostromes, including many articulated shells in growth position with a wide size (age) spectrum. In contrast, thin discontinuous patches of large shells can be interpreted as the remains of the original bivalve biostromes, from which the smaller and lighter components were removed by storms. Some original cycles might not have been preserved if all the shells in the biostromes were removed. The six cycles recognised both in the Collado de los Molinos and El Cerrón sections, therefore, should be considered as the minimum number of original cycles in the Azagador carbonates.

The available age constraints indicate that the Azagador carbonates formed during an unknown portion of a 270 ka interval. This suggests that these described cycles were forced by orbital precession or some other higher-frequency process. Forcing by orbital precession has been well documented in lithological cycles in the basinal deposits to which the Azagador carbonates laterally change.

Acknowledgements

This work was funded by "Ministerio de Educación y Ciencia" (Spain), Proyect CGL 2004-04342/BTE and by a doctoral F.P.U. grant (MECD-UGR) awarded to A. Puga-Bernabéu (AP2003-3810). J.C. Braga and J.M. Martín were also supported by Topo-Iberia Consolider Ingenio 2006 (CSD 2006-00041). Constructive comments by A.M. Smith (University of Otago) and an anonymous reviewer are greatly appreciated. We are indebted to Christine Laurin for correcting the English text.

6

SEDIMENTARY PROCESSES IN A SUBMARINE CANYON EXCAVATED INTO A TEMPERATE-CARBONATE RAMP (GRANADA BASIN, S. SPAIN)

Ángel Puga-Bernabéu*, José M. Martín, Juan C. Braga

Departamento de Estratigrafía y Paleontología, Facultad de Ciencias, Campus de Fuentenueva s.n.,

Universidad de Granada, 18002 Granada, Spain

**Corresponding author:*

Fax: +34 958 248528

E-mail address: angelpb@ugr.es

Sedimentology
Submitted 18 May 2007; accepted with minor revision 22 August 2007; under review October 2007

Abstract

During the Late Tortonian, shallow-water temperate carbonates were deposited in a small bay on a gentle ramp linked to a small island (Alhama de Granada area, Granada Basin, S. Spain). A submarine canyon (the "Alhama Submarine Canyon") developed close to the shoreline, cross-cutting the temperate-carbonate ramp. The Alhama Submarine Canyon had an irregular profile and steep slopes (10-30º). It was excavated in two phases reflected by two major erosion surfaces, the lowermost of which was incised at least 50 m into the ramp. Wedge- and trough-shaped, concave-up beds of calcareous (terrigenous) deposits overlie these erosional surfaces and filled the canyon. A combination of processes connected to sea-level changes is proposed to explain the evolution of the Alhama Submarine Canyon. During sea-level fall, part of the carbonate ramp became exposed and a river valley was excavated. As sea level rose, river flows continued along the submerged, former river-channel, eroding and deepening the valley and creating a submarine canyon. At this stage, only some of the transported conglomerates were locally deposited. As sea level continued to rise, the river mouth became detached from the canyon head; littoral sediments, transported by longshore and storm currents, were now captured inside the canyon, generating erosive flows that contributed to its excavation. Most of the canyon infilling took place later, during sea-level highstand. Longshore-transported well-sorted calcarenites/fine-grained calcirudites derived from longshore-drift sandwaves poured into and fed the canyon from the south. Coarse-grained bioclastic calcirudites derived from a poorly-sorted, bioclastic "factory facies" cascaded into the canyon from the north during storms.

Keywords: submarine canyon, incised valley, infilling patterns, internal cyclicity, temperate carbonates, Granada Basin.

1. Introduction

Submarine canyons are common features on the seafloor in most continental margins worldwide. They are major erosional morphological incisions that funnel coarse-grained sediment from the shelf into deep-water settings to form submarine fans (Piper, 1970; Inman *et al.*, 1976; Klaucke *et al.*, 2004; Satur *et al.*, 2005). Some submarine canyons are connected to river valleys, either physically linked to or slightly detached from the shelf-edge (Nelson *et al.*, 1970; Goodwin and Prior, 1989; Curray *et al.*, 2003; Puig *et al.*, 2003; Liu and Lin, 2004). Others have a confined head located at the shelf-edge (some with feeder gullies and tributaries) (McAdoo *et al.*, 1997; Bertoni and Cartwright, 2005; Drexler *et al.*, 2006) or in shallower water, near the coastline (Beer and Gorsline, 1971, Lewis and Barnes, 1999; Smith *et al.*, 2007). The canyon head collects sediments provided by longshore and/or storm currents (Beer and Gorsline, 1971; Herzer and Lewis, 1979; Lewis and Pantin, 2002, Puig *et al.*, 2003). The largest submarine canyons and related submarine fans are located in passive margins (Pirmez and Imran, 2003; Babonneau *et al.*, 2002) whereas smaller canyons are found in active margins (Normark *et al.*, 1979, 1998; Alonso and Ercilla, 2003).

Sedimentary processes, bed geometries, and sediment-distribution patterns are well established for submarine canyons fed by siliciclastic sediments, mainly in those Pleistocene to Holocene in age (Andrews and Hurley, 1978; Popescu *et al.*, 2004; Normark *et al.*, 2006). Sediment gravity flows, produced by slumps (canyon flank failures) or by littoral drift and storm currents seem to be the most frequent transport mechanisms down-canyon. Infilling geometries depend on the sedimentary phase considered (erosion, bypass, deposition and infilling) and the sedimentary processes acting in the canyon. Grain-size distribution usually fines downward.

Classic models of sequence stratigraphy have postulated that submarine canyons were active during sea-level lowstands (Posamentier and Vail, 1988; Vail *et al.*, 1991), when shelves were exposed and rivers were able to erode the platform and upper slope. During rising sea-level and highstands, submarine canyons become detached from the sediment source-area and sediment supply diminishes. Although these types of eustatic responses are inferred for many submarine canyons (Kenyon *et al.*, 2002; Fildani and Normark, 2004; Normark *et al.*, 2006), active sediment deposition in submarine canyons also occurs during sea-level rise and highstand stages (Weber *et al.*, 1997; Piper *et al.*, 1999; McHugh and Olson, 2002; Smith *et al.*, 2007). Moreover, several authors have suggested that local factors, such as shelf and slope morphology, subsidence and sediment supply may be more significant than global eustatic changes (Galloway *et al.*, 1991; McHugh *et al.*, 2002).

Shelf- to basin sediment transport forming submarine fans is not an exclusive feature of siliciclastic systems as it can take place as well in carbonate (tropical and non-tropical) systems (Ruíz-Ortíz, 1983; Wright and Wilson, 1984; Payros *et al.*, 2007). In particular, a few examples of channelized deposits involving non-tropical (temperate- to cool-water) carbonates have recently been described by Braga *et al.* (2001) and Vigorito *et al.* (2005). As pointed out by several authors, non-tropical carbonate sediments are easily mobilized due to the lack of early marine cementation (Nelson *et al.*, 1988a; Martín *et al.*, 1996, 2004; Betzler *et al.*, 1997a; Braga *et al.*, 2001), forming deposits equivalent to those observed in the siliciclastic realm. Studies of fossil, canyon-related, non-tropical carbonates from the western Mediterranean region, however, deal with submarine lobe and feeder-channel deposits (Braga *et al.*, 2001; Vigorito *et al.*, 2005). Only in one of them (Braga *et al.*, 2001) is the connection between the submarine fan system and the inner sediment source-area detailed. In that example, small canyons (probably connected to landward with rivers) cut the carbonate platform acting as sediment transport paths into deep-water settings.

Outcrops of ancient submarine canyons in carbonates are scarce (Watts, 1988; Braga *et al.*, 2001; Ruíz-Ortíz *et al.*, 2006), and examples of ancient siliciclastic counterparts are not very common either (Stanley, 1967; Druckman *et al.*, 1995, Anderson *et al.*, 2006), probably due to their large scale (Normark 1983/84). The few examples of sub-Recent to Present submarine canyons in non-tropical ramps described until now are all southern Australian basins (Leach and Wallace, 2001; Mitchell *et al.*, 2007b); the most representative example is the Bass Canyon (Pliocene to Recent) (Conolly, 1968; Mitchell *et al.*, 2007a). In this paper we present an example of a small ancient (Upper Miocene) submarine canyon cutting through a temperate-carbonate ramp in the Granada Basin in southern Spain (the Alhama Submarine Canyon). The 3D outcrop of this submarine canyon provides a unique opportunity for detailed analysis of its sedimentary fill that may help to interpret submerged and subsurface examples with similar features. We propose a model for this type of poorly known canyon, and provide details about its morphology, infilling patterns, sediment composition, bed geometries, and origin.

2. Geological setting

The Granada Basin is a Neogene intermontane basin located in the central part of the Betic Cordillera (Fig. 55). Its Neogene-Quaternary sedimentary infill unconformably

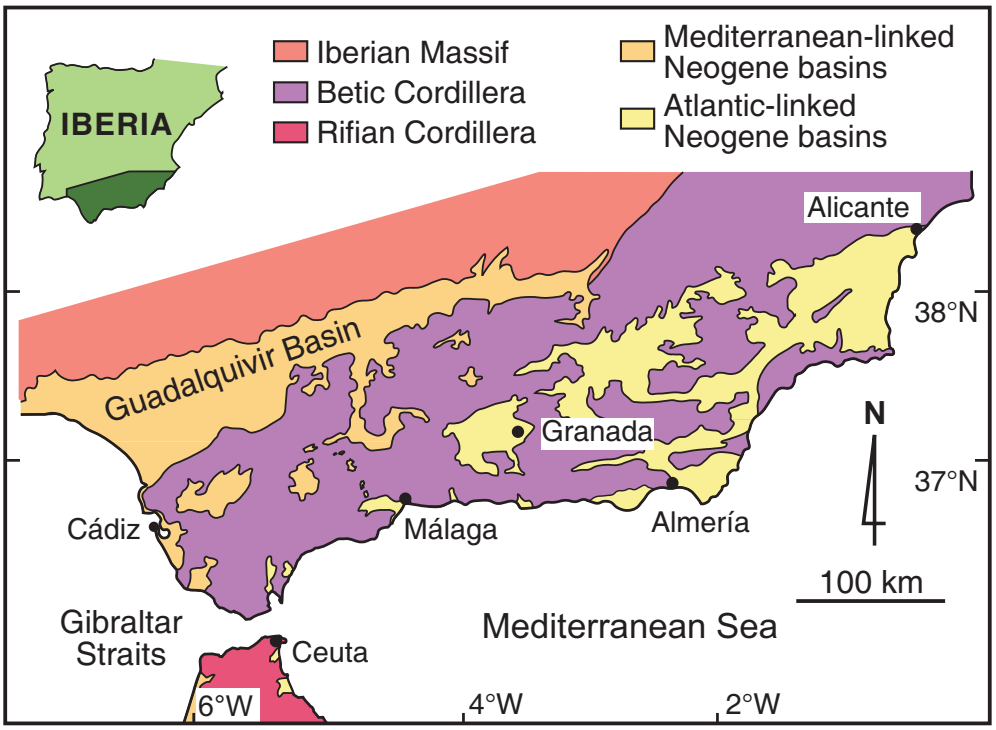

Fig. 55. Geographical and geological setting of the Granada Basin (S. Spain). Inset shows precise location of Alhama de Granada area.

overlies an irregular basement paleorelief and comprises several units separated by unconformities (Martín *et al.*, 1984; Braga *et al.*, 1990, 2003b) (Fig. 56).

Although Neogene sedimentation started earlier in the area, the Granada Basin was delimited as such in the Late Tortonian (Braga *et al.*, 2003b). At that time it was a marine bay, open to the west and flanked to the south by various small islands (Fig. 57). During the Late Tortonian there was a major transgressive–regressive cycle (Rodríguez-Fernández, 1982) that could be correlated with the TB 3.3.2 eustatic cycle of Haq *et al.* (1987). The transgressive Upper Tortonian sediments are bioclastic carbonates and sands and conglomerates deposited in shallow-marine platforms, changing laterally to deep-water marls (Fig. 56). The regressive Upper Tortonian sediments are coarse-grained conglomerates and sands related to fan deltas, prograding on top of deep-water marls (Dabrio *et al.*, 1978; Braga *et al.*, 1990). In the latest Tortonian the Granada Basin was isolated from the sea when its western and southern margins uplifted and emerged (Dabrio *et al.*, 1982). The isolation of the marine basin and its final desiccation led to deposition of evaporites, including halite, in its centre (Dabrio *et al.*, 1982; Martín *et al.*, 1984) (Fig. 56). Since then the Granada Basin has been continental with alluvial-fan, fluvial and lacustrine sedimentation (Braga *et al.*, 1990, 2003b; Fernández *et al.*, 1996) (Fig. 56).

The studied sediments belong to the lowermost Upper Tortonian unit (Rodríguez-Fernández and Sanz de Galdeano, 2006). Serravallian (Martín-Suárez *et al.*, 1993) and Lower Tortonian (Rivas *et al.*, 1999) deposits underlie this unit locally (Fig. 56). The study unit can be divided into two subunits, the lower terrigenous and the upper carbonate, both of which are well represented around the village of Alhama de Granada. The deposits in the basal siliciclastic subunit most likely accumulated in coastal and shallow-marine platform areas within a small bay (Fernández and Rodríguez-Fernández, 1991). The submarine-canyon deposits dealt with in this paper are found within the upper carbonate subunit. The presence of *Neogloboquadrina humerosa* (Blow) in marl samples laterally equivalent to the upper part of the carbonate subunit (~1 km north of Alhama de Granada) indicates a maximum age of 8.5 Ma (Upper Tortonian) for the carbonate subunit, which is in accordance with Rodríguez-Fernández and Sanz de Galdeano's (2006) datings. A lower Tortonian age for the basal siliciclastic subunit cannot be discarded in absence of any biostratigraphical data.

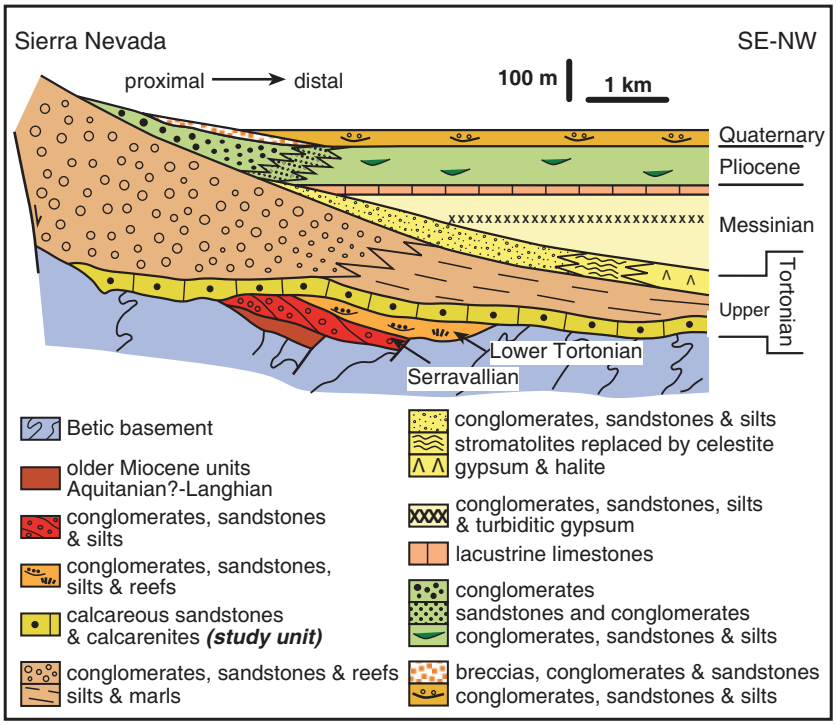

Fig. 56. Miocene to Quaternary stratigraphy of the Granada Basin (after Braga *et al.*, 1990). Studied sediments belong to the lowermost Upper Tortonian unit (calcareous sandstones and calcarenites).

Fig. 57. Late Tortonian palaeogeography of the Granada Basin. Study area (inset) corresponds to the small bay located at the eastern side of the southwesternmost island.

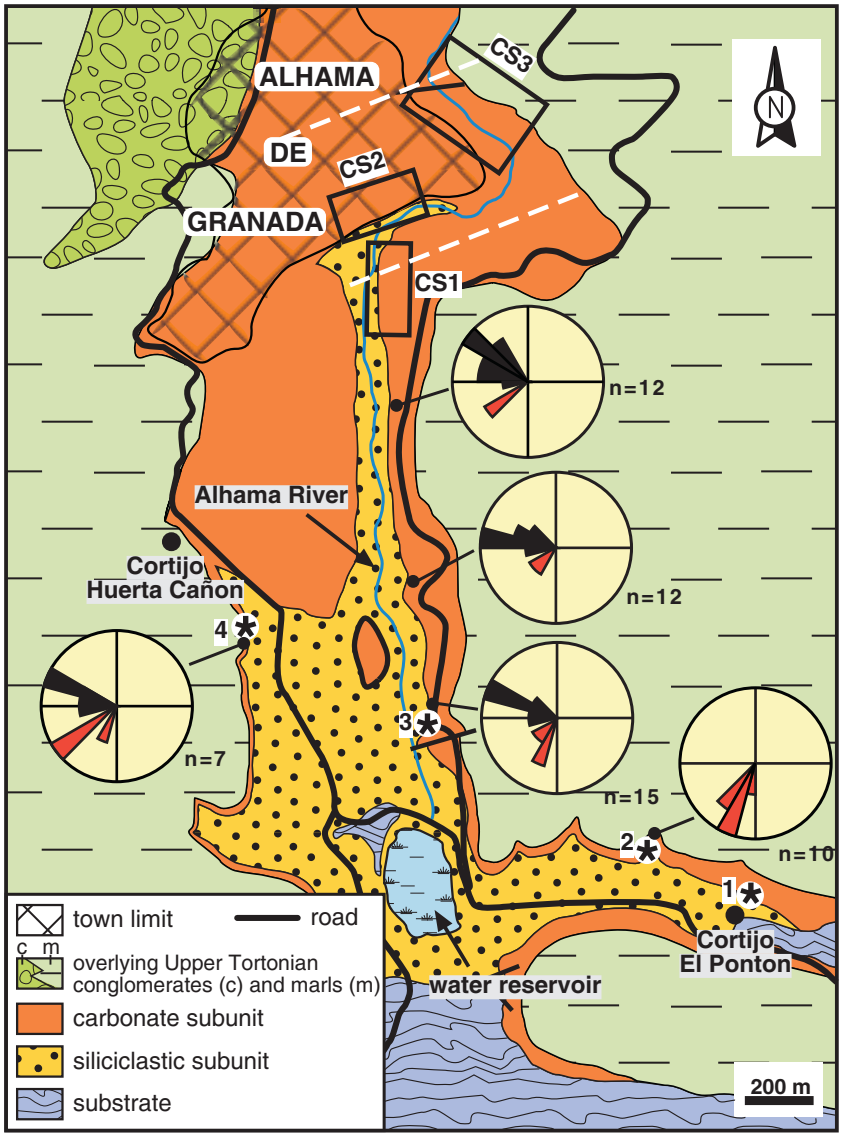

Fig. 58. Detailed geological map of Alhama de Granada area, indicating precise position of the sections. 1 and 2: Cortijo El Pontón sections; 3: Alhama River section; 4: Cortijo Huerta Cañón section; CS1: Canyon section 1; CS2: Canyon section 2; CS3: Canyon section 3. Rose diagrams (n= number of measurements) show palaeocurrent directions of longshore-drift- (black) and wave- (red) induced cross-bedding. White dashed line marks preserved area of Alhama Submarine Canyon.

The study carbonates contain abundant remains of bryozoans, bivalves, echinoderms and coralline algae. These components are typical of the bryomol association of Nelson *et al.* (1988a) and the heterozoan association of James (1997), which characterise most temperate-cool water carbonates. The absence of large benthic foraminifers in the heterozoan carbonates of Alhama de Granada suggests that they formed in waters cooler than the ones in which the lower and upper Tortonian heterozoan carbonates of the Almería basins, to the southeast, were deposited. Fossil assemblages in the latter carbonate units, and stable oxygen isotopes of planktonic foraminifers from laterally equivalent pelagic deposits, indicate mean annual sea-surface water temperatures of 16-20 ºC (Brachert *et al.*, 1998; Sánchez-Almazo *et al.*, 2001). The detailed palaeogeography of the Alhama de Granada area at the time of deposition of these carbonates was that of a small bay, linked to an island located on the southwestern side of the Granada embayment (Fig. 57).

3. Ramp carbonates: stratigraphy, facies and depositional model

3.1. Study sections

3.1.1. Cortijo El Pontón sections

The Cortijo El Pontón sections (numbers 1 and 2 in Figs. 58 and 59) are located at the southern part of the study area. In this zone, carbonate and mixed siliciclastic-carbonate sediments overlie sands and conglomerates of the underlying siliciclastic subunit, and pinch out and onlap the basement to the south. Deposits close to the basement consist of calcarenites and calcirudites with high terrigenous content and intercalated conglomerates (Section 1 in Fig. 59). Fragments of bivalves (mainly pectinids), bryozoans (branching and nodular colonies) and echinoderm spines are the main bioclastic components. These sediments exhibit crude low-angle lamination dipping north. They laterally merge to the north and northeast into carbonates in section 2.

The carbonates in section 2 also have conglomerate beds intercalated (Fig. 59) and consist of grainstones and rudstones rich in bivalves, bryozoans and echinoderms with lesser amounts of coralline algae and benthic and planktonic foraminifers. Bioclasts are fragmented and abraded and terrigenous content is less than 5%. The carbonates are mostly horizontally bedded and laminated, although small-scale cross-bedding also occurs in some beds (Fig. 59). Rudstones, with coarse bioclasts, compose the tabular beds whereas the cross-bedded layers are made up of fine- to medium-grained grainstones.

In the two sections the intercalated conglomerates vary from matrix- to clast-supported and mainly comprise pebbles and minor cobbles. Boulders up to 40 cm in size also occur locally. Clasts are from Palaeozoic metamorphic rocks (micaschists and gneisses together with some quartzites) and Triassic and Jurassic (marly) limestones-dolostones. Clasts are subangular to well-rounded with no preferred orientation. Some dolomite clasts show *Lithophaga* borings. The matrix is medium-grained sand with variable amounts of bioclasts (bryozoans, pectinids, echinoderms and oysters). The lower conglomerate beds can be traced from section 1 to section 2. Higher in the sequence, conglomerate beds only occur in section 2 (Fig. 59).

3.1.2. Alhama River section

Calcarenites/calcirudites, up to 45 m thick, compose most of the vertical cliffs along the Alhama River valley. In this section (number 3 in Figs. 58 and 59), cross-bedded, coarse sands to pebbles in the underlying siliciclastic subunit, change upward into carbonates. Although steep cliffs and faulted blocks make logging of the carbonate subunit difficult, two different types of carbonate facies are recognised (Fig. 60). The first type is a medium-grained grainstone to fine-grained rudstone made up of fragmented and abraded bioclasts (mainly bivalves and bryozoans) with up to 10% terrigenous grains. Trough cross-bedding pointing to WNW and SW (Fig. 58) is the most conspicuous sedimentary structure (Fig. 60A). Trough cross beds range from 4 to 20 m in length, and from 1 to 2 m in height. Some layers are intensively burrowed by *Scolicia* traces. The second facies type, which is intercalated with the first type (Fig. 60A), is a horizontally to low-angle laminated, coarse-grained (granule- to pebble sized) rudstone with abundant, highly-irregular fragments of bivalve shells and bryozoans, and minor echinoderm remains (Fig. 60B). In the uppermost part of the section, a thick, matrix-supported conglomerate bed, up to 7 m thick, is intercalated between the carbonates (Fig. 59). Conglomerate clasts, pebble- to cobble-sized, are mainly of limestones and marly-limestones, with lesser amounts of metamorphic rocks. No grading is observed. Bioclasts of bivalves and bryozoans are dispersed within the sandy matrix.

3.1.3. "Cortijo Huerta Cañón" section

This section is located at the eastern margin of the study area (number 4 in Figs. 58 and 59). In the underlying siliciclastic subunit the most common sedimentary structure is hummocky-cross stratification, locally interrupted by biogenic escape-traces 30 to 50 cm height. The overlying subunit consists of an alternation of millimetre- to centimetre thick siliciclastic- and carbonate-rich layers at the base. Clasts in the siliciclastic layers are pebble-sized rounded schist, dolomite, quartzite and limestone fragments. Calcareous layers consist of calcarenites and calcirudites rich in fragmented and abraded bivalve and bryozoan and minor echinoderm bioclasts. Higher in the sequence the unit is predominantly carbonate. Sedimentary structures change from bottom to top of the unit. At the base, low-angle, centimetre-thick bedding is present, as well as some small-scale cross-bedding pointing to SW. Higher in the section, trough cross-bedding, pointing to WNW (with a subordinate SW direction), is the dominant structure (Fig. 58). A conglomerate bed similar to those described above is intercalated in the middle part of the sequence; this bed is laterally discontinuous, with a maximum thickness of one metre.

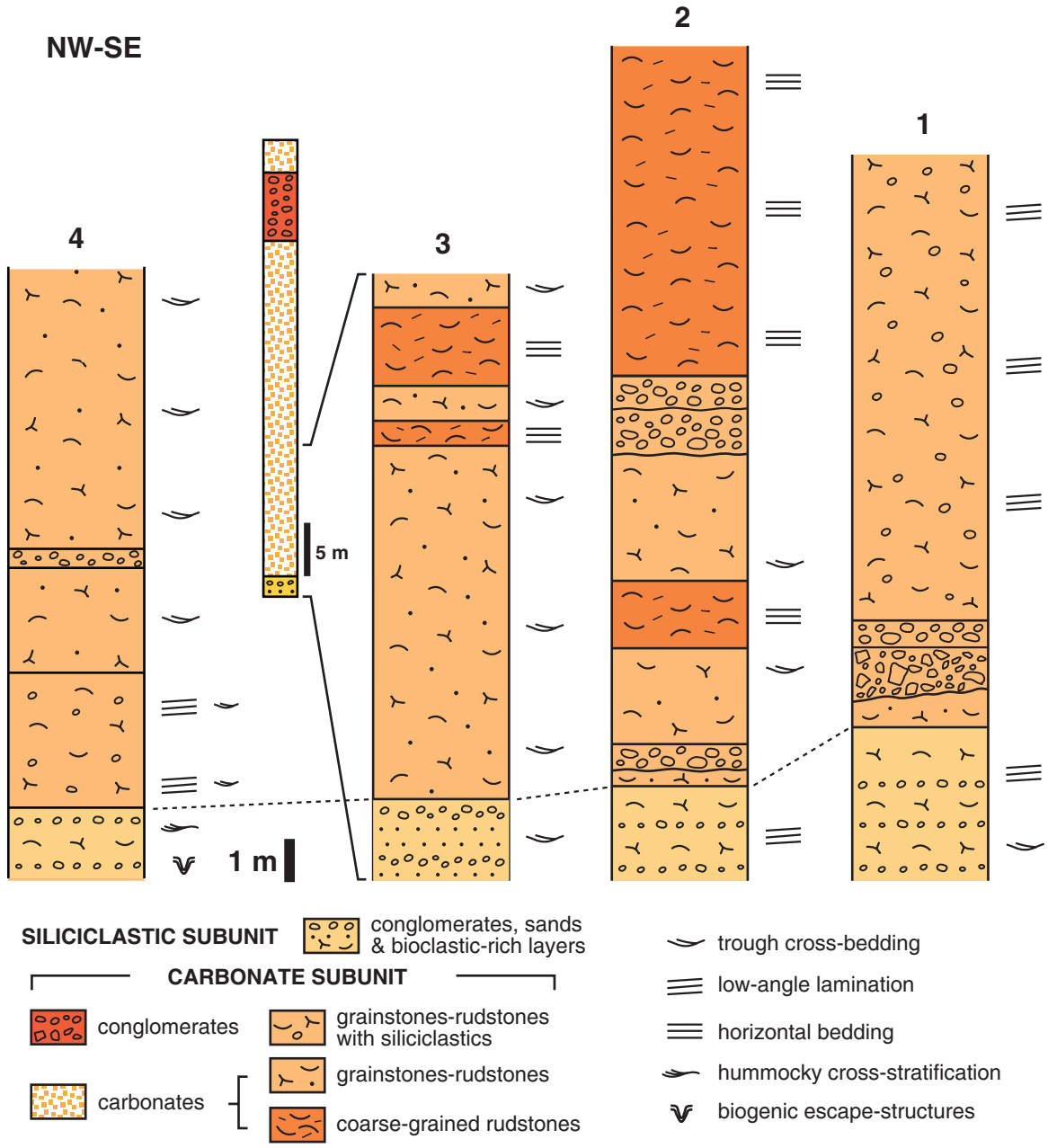

Fig. 59. Stratigraphic columns of the carbonate-subunit sections. 1 and 2: Cortijo El Pontón sections; 3: Alhama River section; 4: Cortijo Huerta Cañón section. See Fig. 58 for location.

3.2. Depositional model

The depositional model inferred for the carbonate subunit is that of a gentle ramp within a bay opening to the NE (Fig. 61A). A beach system comprising foreshore to shoreface subenvironments is deduced by the presence of low-angle bedding in sediments lining the substrate in the Cortijo El Pontón sections (see Fig. 59, columns 1-2) passing laterally into carbonate-rich sediments with cross and horizontal bedding.

Seaward of the beach a shoal system developed (Fig. 61A). Trough cross-bedded sediments cropping out mainly in the Alhama River and the "Cortijo Huerta Cañón" sections resulted from the migration of submarine dunes and sandwaves. Smaller dunes (up to 0.5 m high) were moved towards the coast, presumably by waves, while large dunes and sandwaves (2-5 m high) were mobilized from SE to NW, parallel to the coast, by longshore currents (Figs. 58 and 61A). Sets with abundant *Scolicia* burrows indicate that migration of these bedforms alternated with

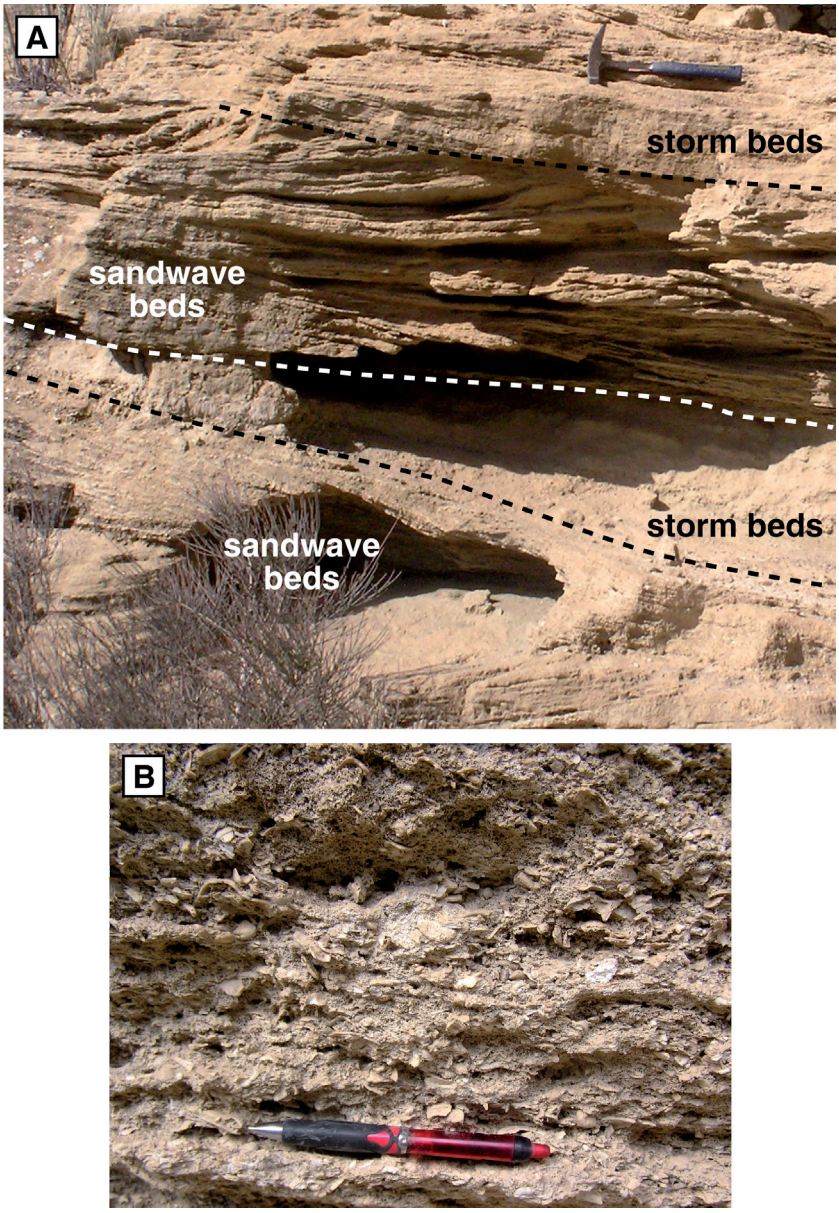

Fig. 60. Main facies types in Alhama River section (see Fig. 58 for location). (A) Sandwave cross-stratified beds, consisting of grainstones and fine-grained rudstones, alternate with storm-related, horizontally (to low angle)-laminated, coarse-grained rudstones. Hammer is 33 cm in length. (B) Close-up of storm beds exhibiting abundant, coarse bioclastic remains (mainly from bivalves and bryozoans). Pencil is 14.5 cm in length.

calm periods in which the sediment was bioturbated by echinoderms.

Seaward of the shoal area, coarse bivalve/bryozoan bioclasts accumulated in a "factory area" (sensu Martín *et al.*, 1996) (Fig. 61B). Most bioclasts however, were reworked and remobilized during storms and re-deposited landwards as horizontally-bedded to gently-dipping, coarse-bioclastic tempestite-layers cross-cutting and alternating with the shoal, cross-bedded layers (Figs. 60 and 61B). Bivalve shell fragments in these tempestite deposits have sharp edges and bryozoan remains are less abraded than those of the dunes. These taphonomic attributes indicate that tempestite bioclasts were rapidly buried with no later reworking by wave action.

Inferred hydrodynamic conditions are thought to have been similar to those occurring in southern Spain coastal

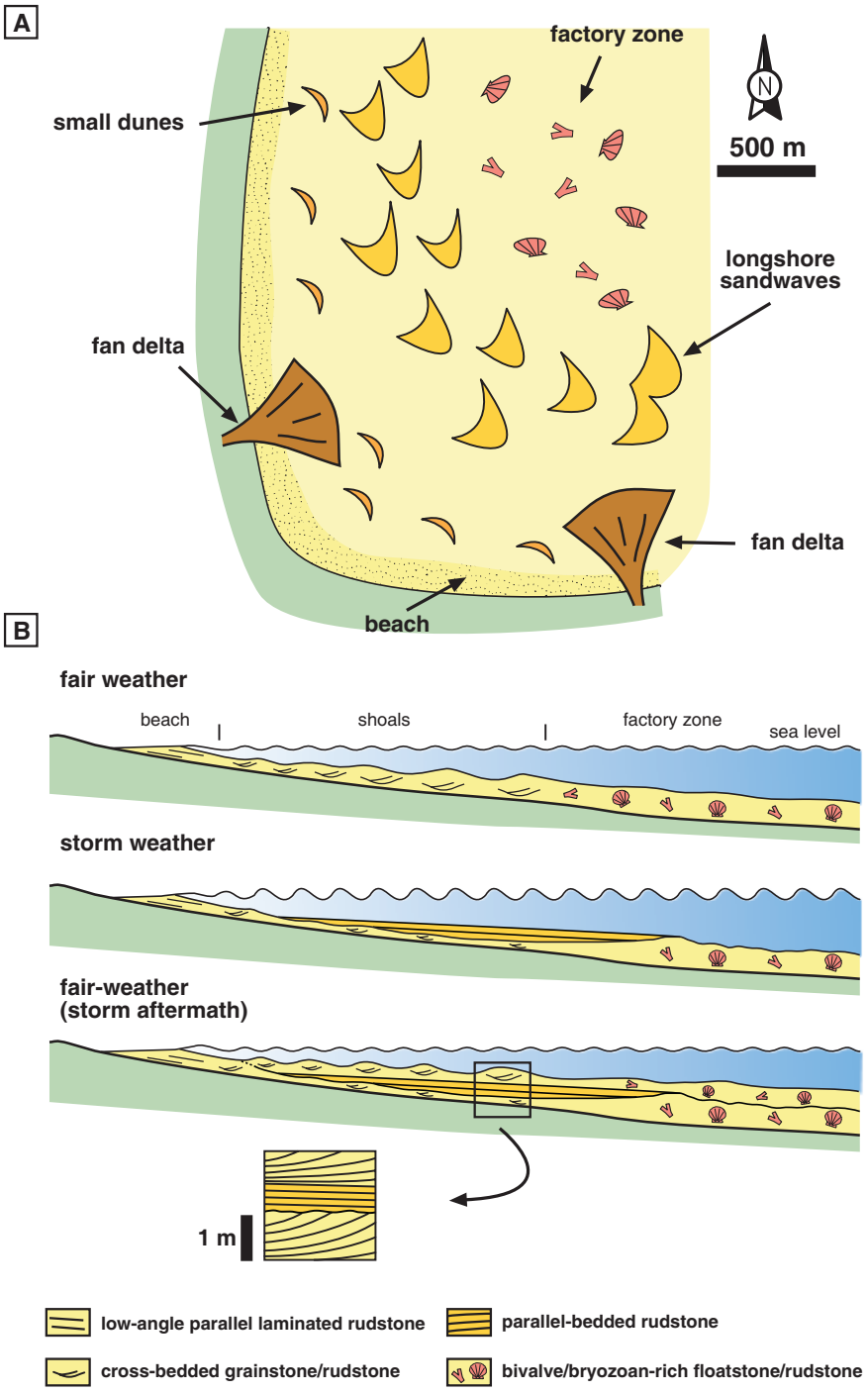

Fig. 61. Late Miocene palaeoenvironmental reconstruction of Alhama de Granada area (A). The area was a small bay with a coastal beach system changing seawards to a shoal system with two types of sedimentary bodies; small dunes closer to the beach and large sandwaves, more to seaward. The small dunes migrated landwards, probably moved by waves, while longshore currents mobilised sandwaves from SE to NW, parallel to the coast. Seawards of the shoals, a bivalve- and bryozoan-rich factory zone developed. Locally, small fan deltas entered the bay. (B) Cross-section of carbonate ramp showing effects of storms. During fair-weather periods, beach, shoal, and factory-zone systems developed on the carbonate ramp. During the stormy weather periods, bioclasts from factory zone were scoured and mobilised to be deposited landwards as horizontal- to gently dipping beds on top of eroded submarine dunes. After storm period, storm beds were covered by shoals. Repetition of these processes resulted in sandwave deposit/storm deposit alternation shown in Fig. 60A.

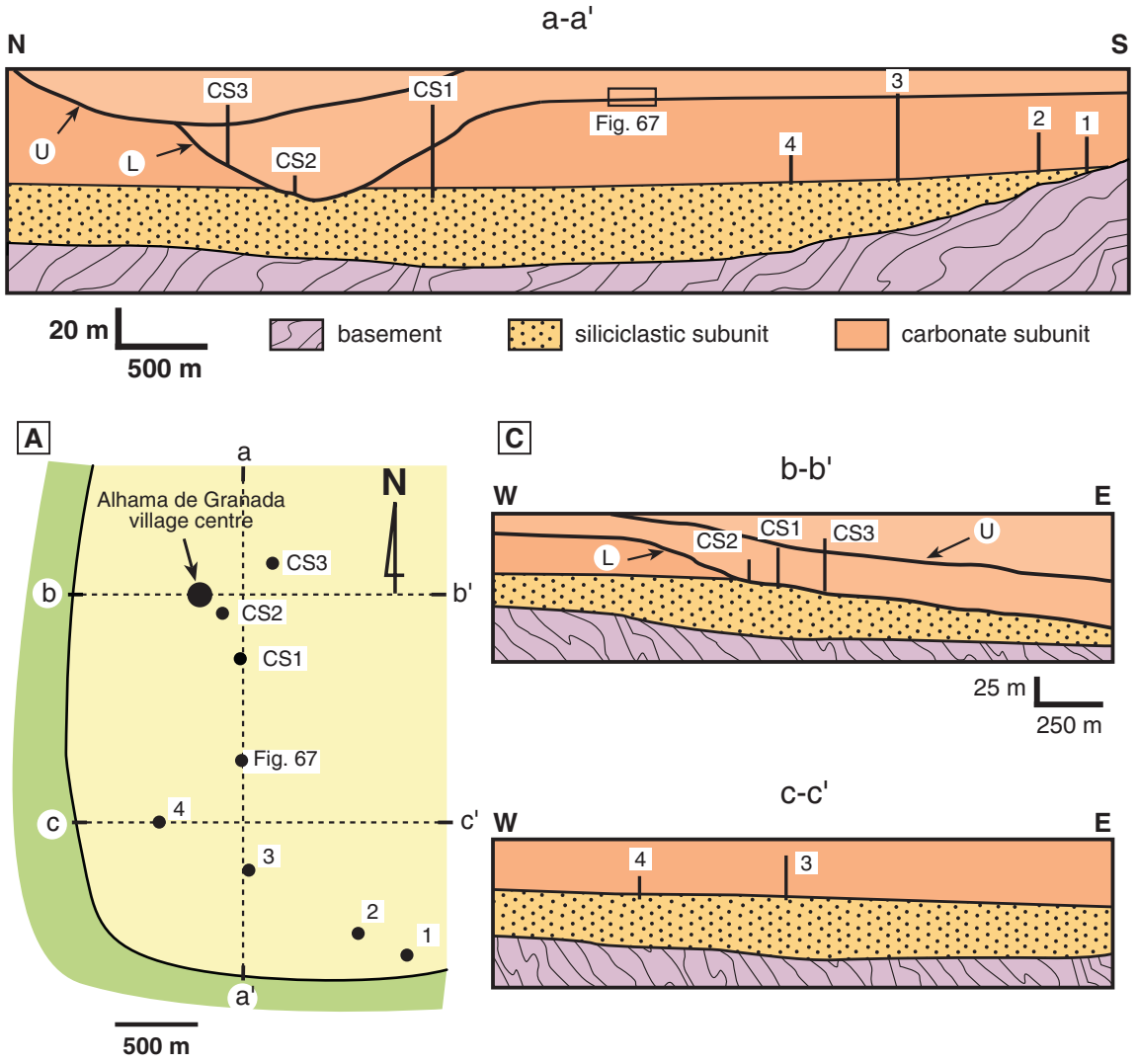

Fig. 62. (A) Schematic map, based on the palaeogeographical reconstruction shown in Figs. 61A and 66C, D, illustrating position of study sections. Location of Alhama de Granada village centre is given as reference. (B) North-South transect showing geometric relationships among different sedimentary units. Position of Fig. 67 is marked for a better understanding of description given in the text. (C) West-East transects in two different positions along the ramp. 1 and 2: Cortijo El Pontón sections; 3: Alhama River section; 4: Cortijo Huerta Cañón section; CS1: Canyon section 1; CS2: Canyon section 2; CS3: Canyon section 3. L: Lower erosional surface; U: upper erosional surface.

areas at Present as well as during Pliocene times (Martín *et al.*, 2004). Longshore currents were probably induced by deflected westerly storms, which are dominant in the area. Easterly storms are thought to have been responsible for the formation of the tempestite deposits.

Intercalated conglomerate beds in sections 1, 2, and 4 (Fig. 59) are interpreted as fan-delta lobe deposits, an indication that small fan deltas entered the bay at certain points (Fig. 61A). Part of the fan-delta sediments were locally reworked by waves and currents and the clasts incorporated to the beach and/or to the shoals. Clast composition points to a basement source-area to the south.

4. The Alhama Submarine Canyon

Two large incision surfaces are recognized in the Alhama River-cliff outcrops near the village of Alhama de Granada (Fig. 62). The lower one was excavated into the

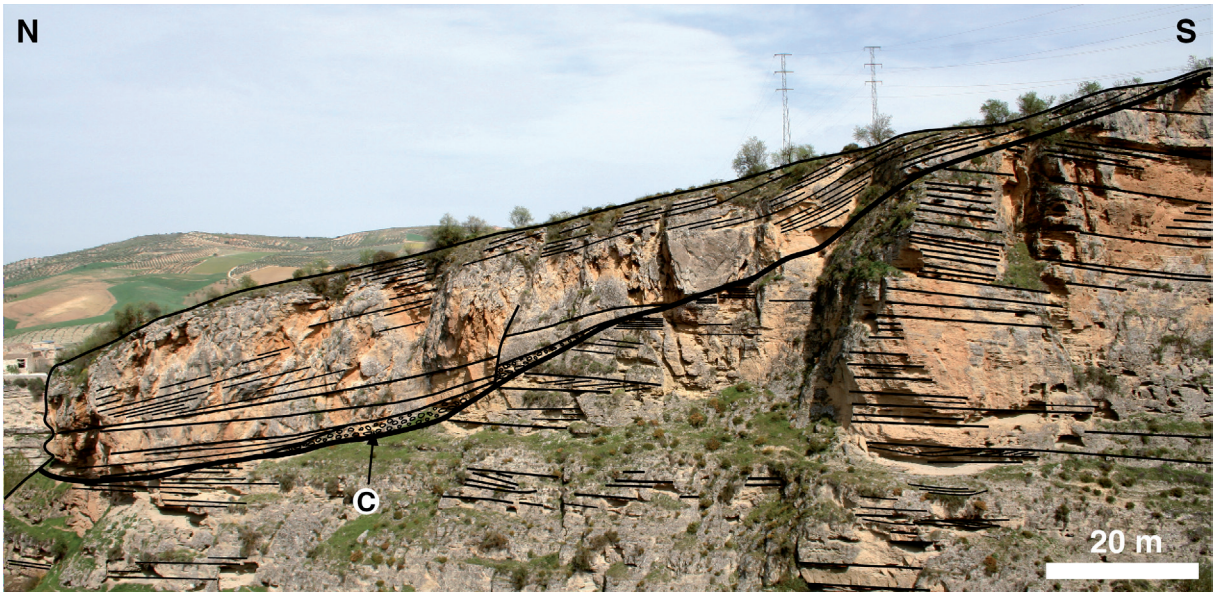

Fig. 63. Outcrop photograph of the southern margin of the Alhama Submarine Canyon (Canyon section 1). Large erosion surface marking base of submarine canyon stands out clearly. Note "perched" conglomerate bed lying directly on this surface (c: conglomerates). Overlying beds progressively onlap conglomerates to cover them completely. Also note synsedimentary fault and draping geometry of uppermost beds on canyon margin (right side of picture), conforming to underlying topography.

above-described sediments. Calcareous and terrigenous deposits with different geometries overlie these erosional surfaces and compose the "canyon sequence". The 3-D outcrops extend over an area of 0.4 km^2 (~800 m in length and ~500 m width). Selected sections of the canyon infilling, illustrated with photomosaics (see Figs. 58 and 62 for location) are described below.

4.1. Canyon section 1 (CS1)

Canyon section 1 is located in the middle of the N-S panoramic view shown in Fig. 63. The most striking feature in this exposure is the occurrence of a large incision surface, up to 50 m deep (Fig. 63), excavated into the carbonate-ramp sediments and the underlying terrigenous subunit. This surface dips northwards, with dipping angles diminishing from 20-30º to 10º downslope.

The first deposit on top of this surface is a discontinuous conglomerate bed up to 2 m thick. Conglomerate clasts, all from the basement, are mainly of micritic limestones and marly limestones, minor metamorphic rocks and chert nodules. They are cobble-sized on average, although some boulders may also appear. A mixed bioclastic/siliciclastic matrix fills the interparticle space.

A thick deposit (~7 m) of convex-upward, semi-lenticular calcarenite/fine-grained calcirudite bodies onlaps the conglomerate bed (Fig. 63). These bodies pinch out laterally to the north and/or to the south. The three lowermost beds (including the conglomerate bed) are cut and displaced by a normal synsedimentary fault (Fig. 63). Successive beds filled in the irregularities of the underlying beds thus progressively smoothing the palaeotopography of the underlying incision-surface. The smoothing is especially noteworthy at the southernmost corner, where sigmoidal beds occur (Fig. 63). Sigmoidal beds pass laterally downslope to sheet-like beds up to 60 cm thick.

4.2. Canyon section 2 (CS2)

This section is located immediately south of the village of Alhama de Granada (Figs. 58 and 62). Most deposits in this section belong to the terrigenous subunit underlying the carbonate subunit. A large, nearly flat surface cross-cuts the siliciclastics (Fig. 64A). This surface is overlain by a 3 metre-thick conglomerate bed that can be traced laterally ENE for 250 m before it pinches out. It crops out again some 30 m to the east, extending for at least another 250 m. Conglomerates consist of pebbles, cobbles and minor boulders of limestone and marly-limestone, and some minor metamorphic rocks, floating in a mixed terrigenous-carbonate matrix, medium sand to granule in size. Centimetre-sized (up to 10 cm) bioclasts occur in the matrix, comprising pectinids, bryozoans (branching and nodular colonies), echinoderm spines and oyster shells. Locally, inverse grading is observed at the base of the bed. The rest of the sequence, up to 7 m thick, is carbonate-dominated. It consists of centimetre–thick, parallel-bedded,

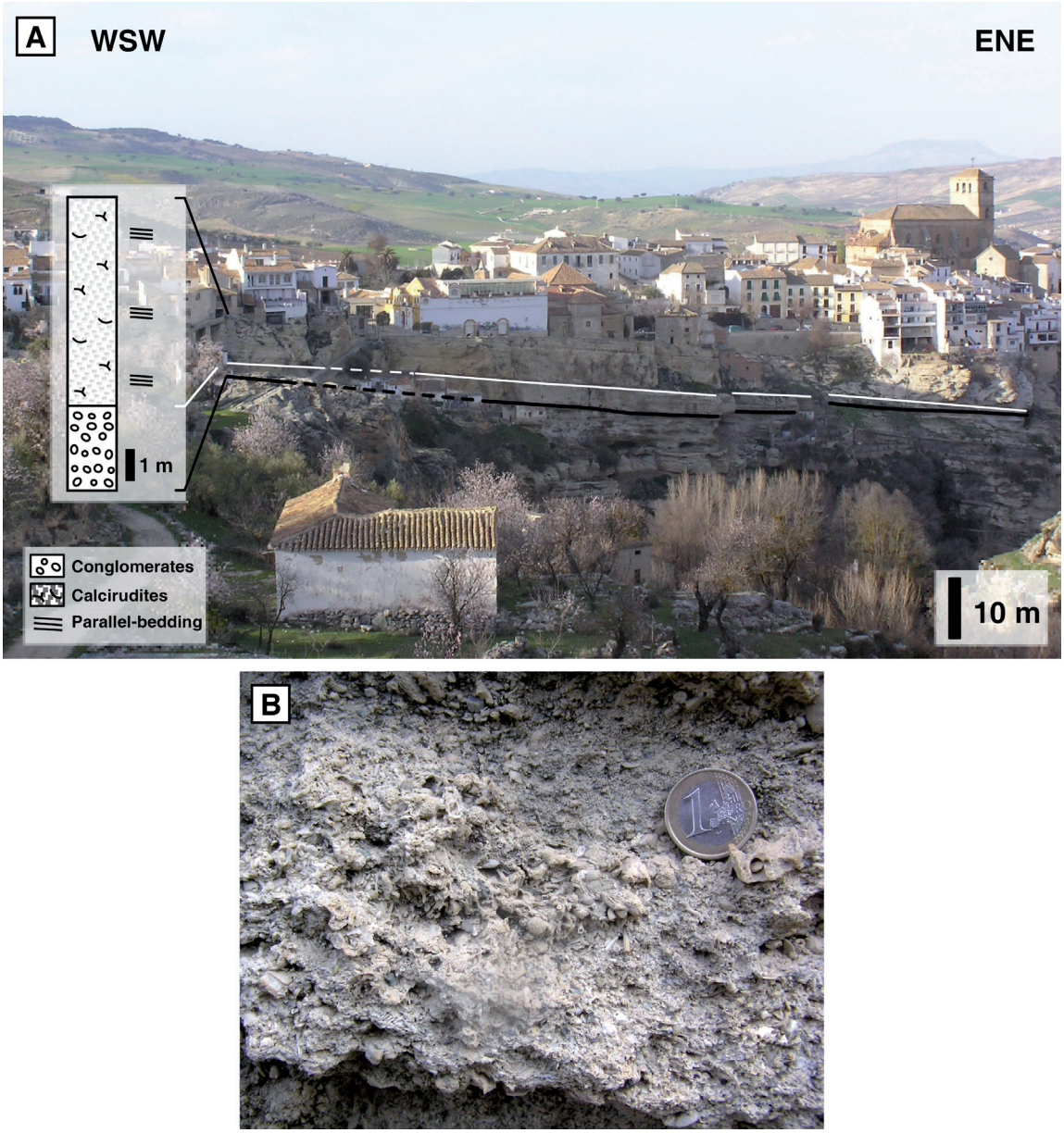

Fig. 64. (A) Panoramic view of northern margin of the Alhama Submarine Canyon (Canyon section 2). Black line marks canyon base. White line traces top of the conglomerate bed that appears directly on top of canyon-base surface. (B) Close-up view of overlying beds of canyon infilling consisting of coarse bioclastic (bivalve/bryozoan–rich) calcirudites. Coin is 2.3 cm in diameter.

coarse-grained grainstones and rudstones, with bioclasts up to 2 cm in size, dipping slightly northeast. Abundant abraded and fragmented bryozoan skeletons are the main components, followed by bivalve shells (Fig. 64B). Minor amounts of coralline algae and echinoderms also appear.

4.3. Canyon section 3 (CS3)

Two irregular erosional surfaces are present in the Alhama River cliffs, on the northeastern side of Alhama de Granada (see Figs. 58 and 62 for location). The basal surface crops out only at the bottom of the river valley. The sediment underneath this surface is a fine-grained bioclastic calcarenite. A discontinuous conglomerate bed up to 3 m thick lies on top of the erosional surface. It is made up of rounded pebbles, cobbles and boulders (up to 60 cm) of micritic limestones, marly limestones, and some chert nodules. The overlying sediment infilling,

25 m thick, consists of large (up to 100 m in length) wedge- and trough-shaped, concave-up calcarenite/calcirudite sedimentary bodies (Fig. 65A, B), with some *Scolicia* burrows. Some cross-bedded deposits, pointing to the north-northeast, are intercalated between them (Fig. 65D, E). The large concave-up sedimentary bodies are cut by another erosional surface (Fig 65A, B). A discontinuous conglomerate including some well-cemented Miocene carbonate (calcarenite/calcirudite) boulders, up to 2 m in diameter, lies directly on top of the upper erosion surface (Fig 65C). The overlying beds, up to 15 thick, are from horizontal (Fig. 65A) to slightly concave-up (Fig. 65B). The latter sediments consist of a medium- to coarse-grained, bioclastic calcarenite/calcirudite, similar to that described in canyon section 2.

4.4. Interpretation

The two large incision surfaces found in Alhama de Granada were produced by significant erosion, affecting both siliciclastic and carbonate shallow-marine sediments. The excavated relief in the lower incision was at least 50 m deep. This relief was subsequently infilled. We consider that these erosional features and associated fill are the result of the different phases of formation, abandonment, and infilling of a submarine canyon that developed close to the shoreline and cross-cut shallow-marine, platform sediments. This canyon (the "Alhama Submarine Canyon") constituted a major geomorphic feature in the carbonate ramp. The canyon margins had an irregular profile and the canyon walls had steep slopes (10-30º). These characteristics are recorded in other submarine canyons (channel-margin slopes of >10º have been described by Stanley (1967), Lewis and Pantin (2002), Popescu *et al.* (2004), and Elliott *et al.* (2006) among others). Relatively high axis gradients (3-7º in the case of the Alhama Submarine Canyon) are also common features in certain submarine canyons (Stanley, 1967; Lewis and Barnes, 1999; Elliott *et al.*, 2006), although axis gradients may be as low as ~1º (Danubio Canyon and Astoria Canyon (Nelson *et al.*, 1970; Popescu *et al.*, 2004).

5. Discussion

5.1. Genesis of the Alhama Submarine Canyon

One of the major questions concerning submarine canyons is their origin. This topic was intensively debated in the past (Winslow, 1966; Gorsline, 1970; Shepard 1972) and still remains uncertain.

In the study example, the sedimentological data suggest that at a given moment part of the carbonate ramp became exposed. As a result, erosion significantly increased and a small river valley was excavated in the Alhama de Granada area (Fig. 66A). At this time significant fan-delta progradation took place approximately 2 km south of Alhama de Granada village. The thick and extensive uppermost conglomerate bed in the Alhama River section represents a major fan-delta lobe deposit spread over the carbonate-ramp sediments in that area. This conglomerate bed is much thicker (~7 m) than those intercalated within the carbonate-ramp sediments occurring underneath. It is laterally equivalent to the lowermost erosional surface seen in Canyon sections 1 and 2 (CS1 and CS2), which means that the two processes, fan-delta progradation and initiation of canyon excavation, happened at the same time.

As sea level rose, the distal reaches of the former river valley became inundated. In this situation it is presumed that some river flows continued along the submerged, former river-channel, once they entered the sea, eroding and deepening the valley and turning it into a submarine canyon (Fig. 66B). This canyon acted, at this stage, mainly as a by-pass area although some of the transported conglomerate sediments were locally abandoned and accumulated inside the canyon (Fig. 66B). Major excavation of submarine canyons connected landward with rivers is considered to occur mainly at this stage (Nelson *et al.*, 1970; Antobreh and Krastel, 2006; Normark *et al.*, 2006), when rivers incise into the platform and provide large amounts of sediments. Hyperpycnal (near bottom) flows, produced at the river mouths mainly during flood periods (Piper *et al.*, 1999; Popescu *et al.*, 2004; Baztan *et al.*, 2005), provide the erosion mechanism (turbidity currents and/or mass flows) to maintain and enlarge the canyon profile.

As sea level continued to rise, the river mouth became detached from the canyon head and, consequently, lesser amounts of river sediment fed the canyon. By now, the canyon stood out as a prominent feature cross-cutting the carbonate ramp (Fig. 66C). In this ramp, submarine dunes, formed by loose carbonate sand and gravels, were moved SE to NW by longshore currents until they collapsed into the canyon at its southern side, close to the canyon head. At the same time, storm action from time to time mobilized sediment from the "factory area" to the northern side of the canyon. Both processes could have generated erosive flows (turbidity currents *sensu lato*) (Inman *et al.*, 1976; Fukushima *et al.*, 1985; Gaudin *et al.*, 2006), converging and being channelized into the canyon, which could have contributed to its excavation. This is well exemplified in some modern examples where canyon heads collect sediments provided by longshore and/or storm currents (Beer and Gorsline, 1971; Herzer and Lewis, 1979; Lewis and Pantin, 2002, Puig *et al.*, 2003; Normark *et al.*, 2006). Erosion by sediment flows is proposed for the maintenance of many submarine canyons close to the shoreline,

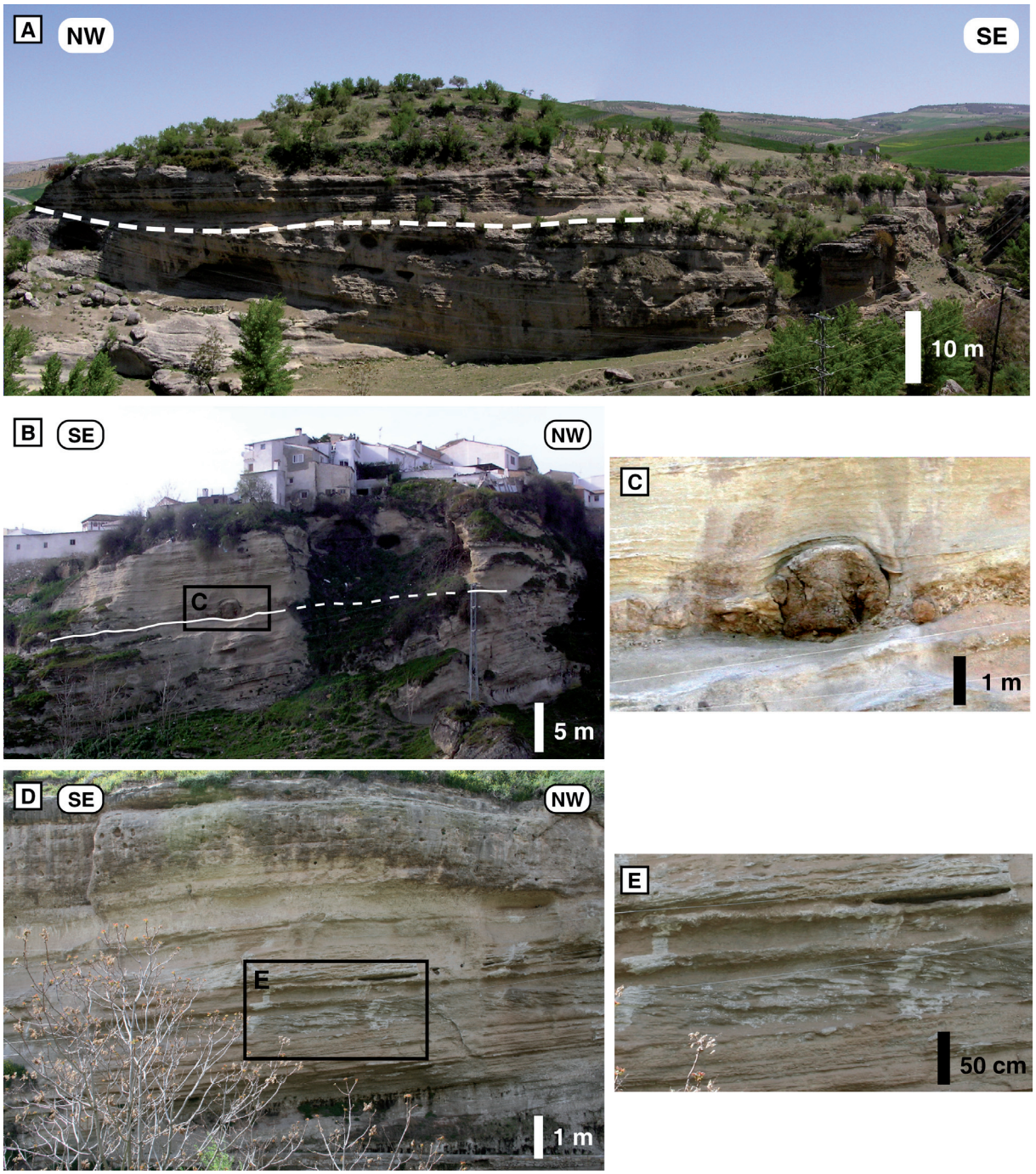

Fig. 65. (A) Northern side of Alhama River valley at Canyon section 3. Panoramic view showing deposits corresponding to two different stages of infilling of Alhama Submarine Canyon. White dashed line delineates position of erosion surface separating both episodes and generated during re-excavation phase of canyon. Note large size of trough-shaped, concave-up infill. (B) Southern side of Alhama river valley at canyon section 3 showing a comparable view. Note huge calcarenite block (inset) on top of intra-canyon erosional surface. (C) Detailed view of conglomerate bed incorporating huge calcarenite block, and other minor ones, resting on top of intra-canyon erosional surface. (D) Cross-bedding structures inside the concave-up beds from lower phase of canyon infilling. (E) Close-up view of cross-bedded sets.

such as the ones in the California Continental Borderland (Beer and Gorsline, 1971; Shepard and Marshall, 1973; Shepard *et al.*, 1974; Puig *et al.*, 2003).

In this phase, the canyon-axis gradient was high enough to transport (bypass) basinward the sediment supplied by longshore and storm currents captured in the canyon margins (Fig. 66C) and probably also in the canyon head, which is not preserved. Currents generated during storm periods are demonstrated to be important for transporting sediment down-canyon (Shepard *et al.*, 1974; Inman *et al.*, 1976; Fukushima *et al.*, 1985; Puig *et al.*, 2003). Slope failures and subsequent mass flows, concomitant to and resulting from canyon excavation (Galloway *et al.*, 1991; Normark *et al.*, 1998), could also have occurred. Evidence of synsedimentary faulting, which could be related to slope failures, is found locally in the canyon flanks (Fig. 63). All these mechanisms contributed to the enlargement of the canyon prior to its infilling. The maintenance and enlargement of submarine canyons by submarine processes is widely accepted nowadays (Popescu *et al.*, 2004; Baztan *et al.*, 2005; Elliot *et al.*, 2006).

All the transported sediments moved along the canyon and were presumably exported downslope. Submarine canyons in different continental margins around the world merge into a submarine fan system (Coronado canyon, Normark *et al.*, 1979; Hueneme Canyon, Piper *et al.*, 1999; Almería Canyon and Guadiaro Canyon, Alonso and Ercilla, 2003; Monterey Canyon, Fildani and Normark, 2004; Petit Rhône Canyon, Bonnel *et al.*, 2005; Bass Canyon, Mitchell *et al.*, 2007a) or into a meandering or braided channel system (Lewis and Pantin, 2002; Ó Cofaigh *et al.*, 2006) that might also end in submarine fans. Any of these transitions might have occurred in the Alhama Submarine Canyon. Neither channel nor fan deposits have been identified in the study area or crop out in the surrounding zone as they are almost certainly covered by thick, Miocene-Pliocene, marine and continental (lacustrine) younger deposits. A complete transition from canyon to submarine fan deposits, through a meandering channel system, can be observed in a comparable Miocene example, in outcrops from the Vera Basin in southern Spain (Braga *et al.*, 2001).

5.2. Infilling of the Alhama Submarine Canyon

Seismic and acoustic profiles provide useful tools to study the infilling geometries of present-day, large submarine canyons (Lewis and Barnes, 1999; Gardner *et al.*, 2003a; Bertoni and Cartwright, 2005). However, as a result of the low bed resolution of these methods, details of the infilling (such as individual bed geometries or the presence of some sedimentary structures) remain obscure and can be unravelled solely in a few examples (Popescu *et al.*, 2004; Baztan *et al.*, 2005; Cronin *et al.*, 2005), often only when completed with core sample studies (McHugh *et al.*, 2002, Drexler *et al.*, 2006). In the case of the ancient Alhama Submarine Canyon, however, good outcrop conditions favour direct detailed sedimentary observations and interpretations.

As mentioned above, conglomerates on top of the erosion surfaces are thought to have been transported and deposited along the canyon axis by density currents linked to rivers entering the sea during the early stages of canyon formation. They appear now as discontinuous beds, hanging on the canyon walls, where they remained as a residual lag (Fig. 63).

Most of the canyon sediment infilling (large, wedge- and trough-shaped, concave-up carbonate sedimentary bodies) (Figs. 63, 64 and 65) was nonetheless supplied much later, laterally to the canyon by longshore and storm currents, once the profile along the canyon axis smoothed enough to favour sediment deposition. In the Alhama Submarine Canyon, longshore-transported sediments, feeding the canyon from the south, are made up of calcarenites/fine-grained calcirudites. They derived from longshore-moved sandwaves, collapsing into the canyon (Figs. 66D, 67), with sediments consisting of relatively well-sorted and ground bioclastic grains. Storm-related sediments, which poured into the canyon from the north, are mostly made up of coarse-grained bioclastic calcirudites, derived from the poorly-sorted, bioclastic factory facies (facies from main carbonate production areas, *sensu* Martín *et al.*, 1996). At this stage, sediment from the ramp was successively dropping into the canyon, filling in the bottom irregularities. Wedge-shaped sedimentary bodies, probably fed from the canyon margins, have also been observed in other canyon infillings (Galloway *et al.*, 1991; Baztan *et al.*, 2005). The Alhama Submarine Canyon worked in a similar way to some present-day submarine canyons of the eastern California coast, which are detached from rivers and sediment-fed by littoral drifts and storms currents (Dume Canyon, Piper *et al.*, 1999; La Jolla Canyon, Shepard and Marshall, 1973; Redondo Canyon, Beer and Gorsline, 1971).

The cross-bedded deposits that appear at Canyon Section 3 (Fig. 65D, E) are the result of submarine dunes migrating along the canyon-axis at its deepest reaches. They testify to local sediment removal and transportation downcanyon by traction currents. The occurrence of sandwaves migrating along the canyon axis has been reported in modern submarine canyons (Satur *et al.*, 2005; Anderson *et al.*, 2006; Mitchell *et al.*, 2007a; Smith *et al.*, 2007). Currents along submarine canyons can reach flow velocities of 31.6 cm/s (Shepard *et al.*, 1974), 50 cm/s (Shepard and Marshall, 1973), 78 cm/s (Puig *et al.*, 2003)

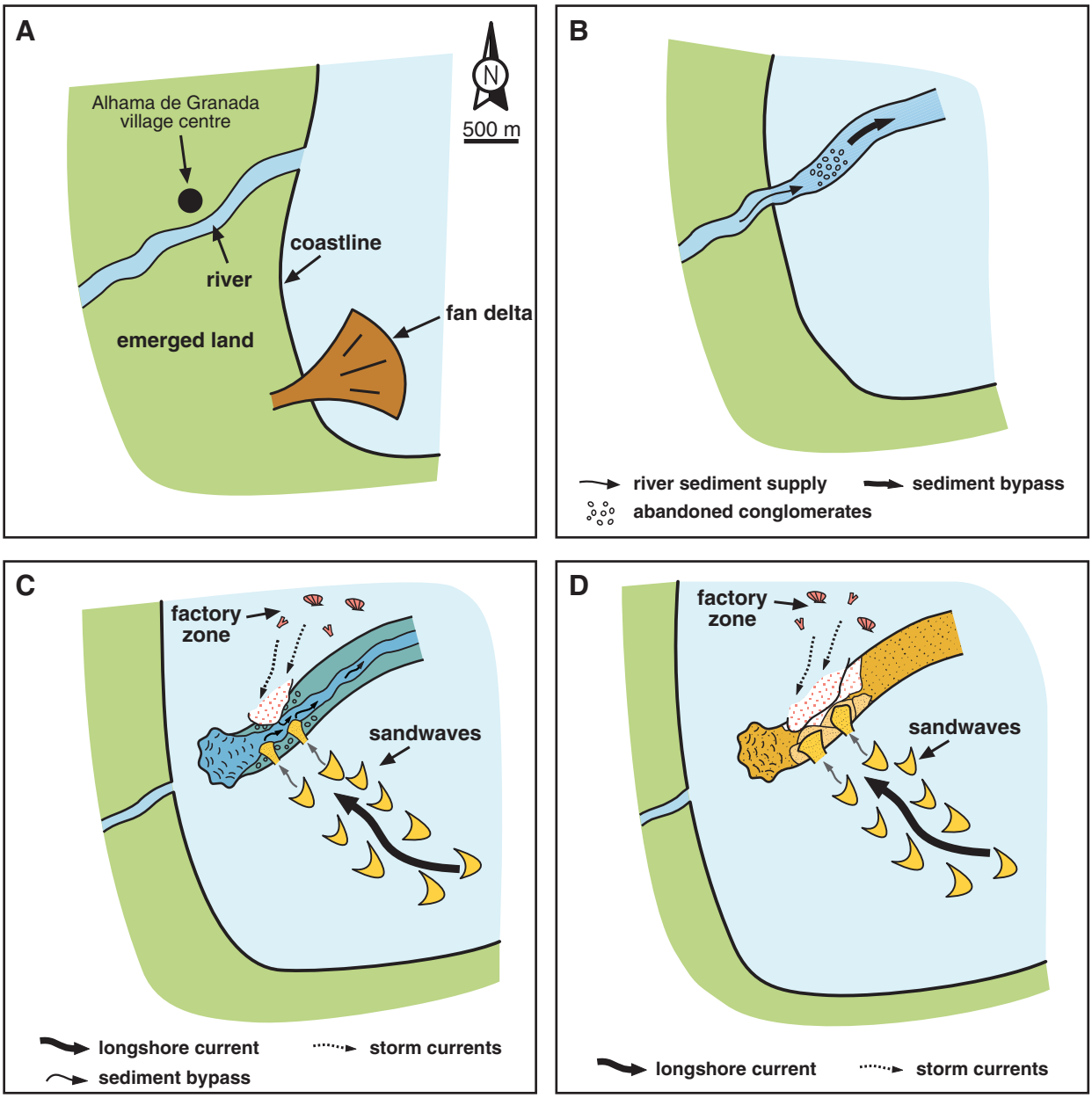

Fig. 66. Synthetic schemes showing genesis and sequential evolution of the Alhama Submarine Canyon. (A) Part of ramp is exposed during a sea-level fall. A major river existed in the area of Alhama de Granada. A small fan delta, linked to another river, formed 2 km to the south. (B) When sea-level rose, main river valley partially inundated and an incipient submarine canyon began formation. River sediment flows entering canyon mainly bypassed the area and contributed, as erosive flows, to enlargement and deepening of the canyon. At this stage only some coarse conglomerate deposits were abandoned and accumulated inside the canyon. (C) As sea level continued to rise, submarine canyon became detached from river valley. Sediment supply into canyon was now provided by longshore and storm currents. Canyon still persisted mainly as a bypass area, funnelling sediments downslope. (D) At this stage, the submarine canyon is abandoned and progressively infilled with the sediment supplied by longshore currents (collapsed sandwaves), on southern side and storm currents (removed factory facies) on its northern side.

and even up to 190 cm/s (Xu *et al.*, 2004). Those velocities, as reported in the Kaikoura Canyon (Lewis and Barnes, 1999), are able to generate megaripples in coarse sands (0.20 m/s) and pebbles (0.51 m/s), which are common grain sizes for carbonate particles in the Alhama Submarine Canyon infilling.

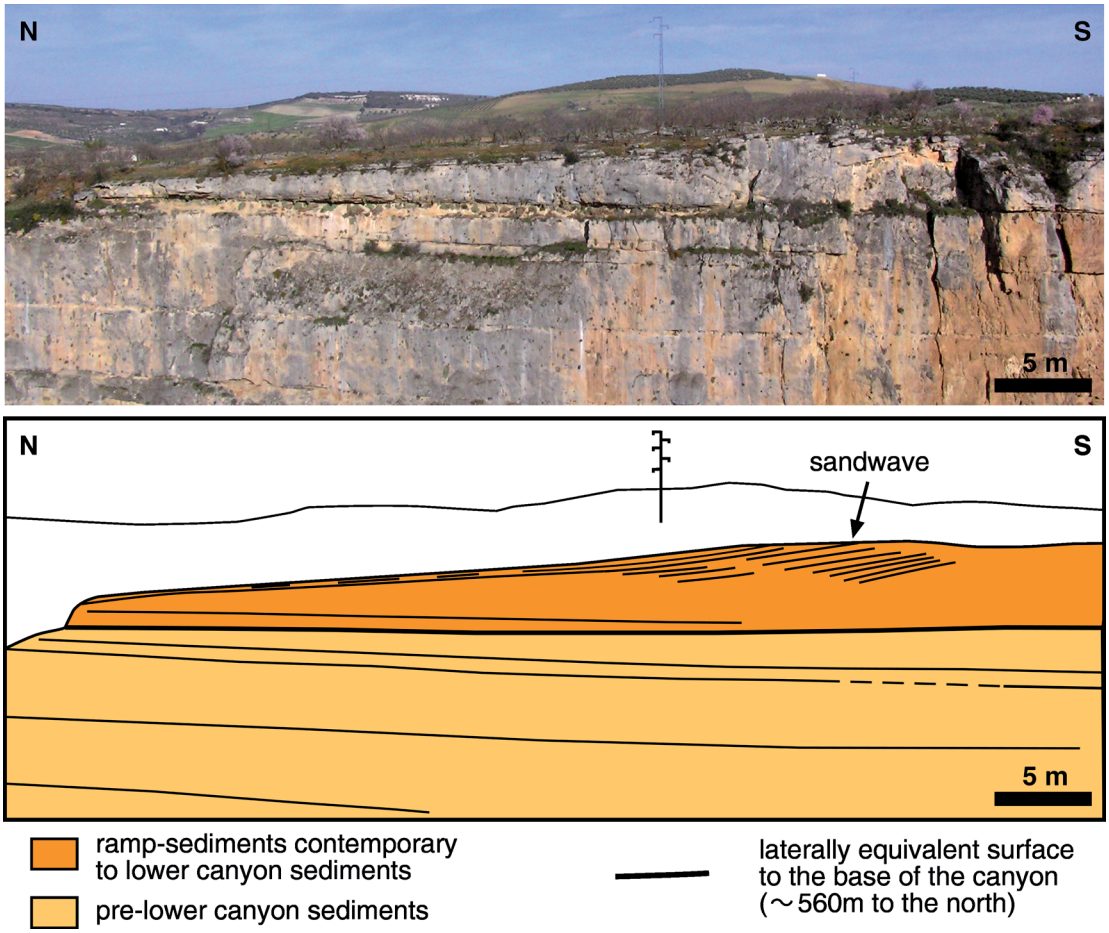

Fig. 67. Field view and interpreted diagram of a sandwave migrating towards the Alhama Submarine Canyon. The most outstanding surface (thick black line) is laterally equivalent to canyon-base erosion surface in Fig. 63. Some sandwaves, moved by longshore currents, collapsed along southern canyon margin, supplying sediment into the canyon at different stages (Fig. 66C, D).

5.3. Re-excavation of the canyon

Temperate carbonates usually remain uncemented on the sea floor (Nelson *et al.*, 1988a) but become easily cemented when they are subaerially exposed. The existence of well-lithified, Miocene carbonate blocks on top of the uppermost erosional surface therefore clearly indicates local emersion prior to and/or during re-excavation of the canyon. This reactivated canyon was infilled by sediments similarly to as the described above. Several phases of fill and erosion are common characteristics in the growth pattern of submarine canyons (Galloway *et al.*, 1991; Pratson *et al.*, 1994; Braga *et al.*, 2001).

5.4. The Alhama Submarine Canyon. An integrated model

The history of generation and infilling of the Miocene Alhama Submarine Canyon comprises a major erosion event, responsible for the development of the lowermost incision surface, followed by infilling, and a new erosion event, resulting in the formation of the uppermost incision surface, with a final infilling of the reactivated canyon. This sequence of events must be taken into account when reconstructing its history.

To explain the evolution of the Alhama Submarine Canyon we propose a combination of processes linked to sea-level changes (Fig. 68). In general, the relationship of submarine canyons with sea-level changes (and/or tectonics) is poorly understood and different hypotheses have been proposed (Schwalbach *et al.*, 1996; McHugh *et al.*, 2002; Baztan *et al.*, 2005, Bertoni and Cartwright, 2005; Antobreh and Krastel, 2006; Normark *et al.*, 2006). In our case the sequence of events seems to have occurred in the following way:

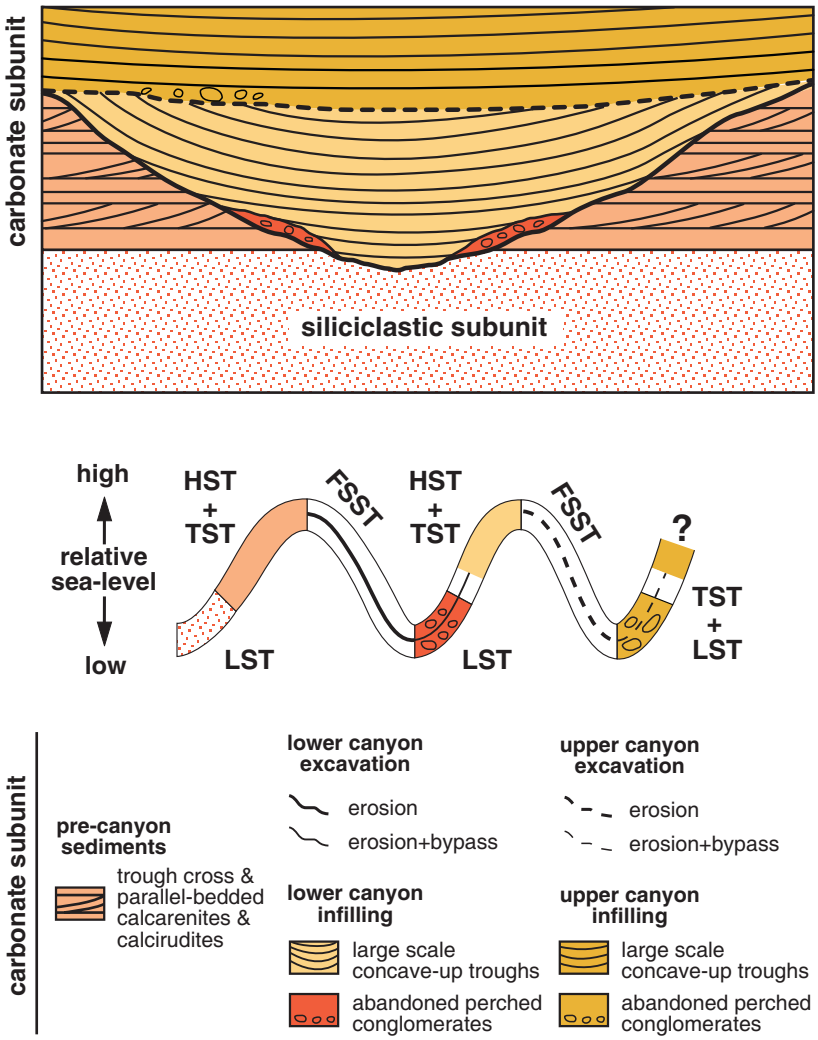

Fig. 68. Sequence stratigraphy of carbonate subunit and cyclical evolution of Alhama Submarine Canyon in relation to sea-level changes. FSST: falling sea-level system tract; LST: lowstand system tract; TST: transgressive system tract; HST: highstand system tract. Major erosion events (resulting in canyon genesis and re-excavation) took place (linked to rivers) during sea-levels falls, when part of the carbonate ramp became exposed. During lowstand and transgressive stages, erosion and sediment bypass were the dominant processes. Only some conglomerates, abandoned in the canyon floor during the lowstand, remain preserved as "perched" sediments on top of erosion surfaces. Canyon infilling took place mainly during highstand stages, at times when the submarine canyon was temporarily abandoned.

1) Falling sea-level

During falling sea level, part of the carbonate ramp became exposed and river erosion was very active. As a consequence, a small river valley was excavated in the Alhama de Granada area and a channelized feature formed in the exposed ramp.

2) Sea-level lowstand

The former river valley started to be inundated. Once an incipient submarine canyon was generated, a feedback mechanism promoted its growth. River flows continued along the submerged channel as they entered the sea, contributing to excavate and enlarge the canyon.

3) Sea-level rising

Littoral sediments were increasingly captured inside the canyon once the river mouth became detached from the canyon head. Longshore and storm currents provided large amounts of sediments for canyon incision. Erosive flows, confined along the canyon axis, excavated the canyon floor, eventually producing instabilities in the canyon walls that led to sediment failures, which likely also generate erosive flows downward.

4) Sea-level highstand

At highest sea-level, the dominant processes were sedimentation and infilling of the canyon. Longshore and storm currents poured sediment into the canyon, slope was progressively smoothed and, subsequently, the erosive flows generated lost their capacity to transport sediment downcanyon. The submarine canyon was no longer being excavated along its axis and was therefore being infilled.

This 4-stage sequence of events was repeated a second time. As indicated above, the sedimentary unit studied herein was presumably deposited during the transgressive part of cycle TB3.3.2 of Haq *et al.* (1987). The described internal cyclicity, however, must have been controlled by higher-frequency processes. Unfortunately, we do not have enough data to constraint precisely the time involved and the cyclicity order. Late Pleistocene submarine canyons exhibiting a comparable sequence of incision–infilling–re-excavation driven by eccentricity sea-level changes have been reported from the Gulf of Lion (France) (Baztan *et al.*, 2005).

5.5. Comparison with siliciclastic systems

The key difference between the Alhama Submarine Canyon and most of siliciclastic submarine canyons is the provenance of the sediment. In siliciclastic (canyon) systems, sediment comes from inland settings and it is mainly supplied by rivers. On the contrary, in the case of the Alhama Submarine Canyon, sediment is produced in the ramp. Sediment supply into the canyon, however, seems to be controlled by similar mechanisms in both cases. As discussed above, in the Alhama Submarine Canyon, sediment was mostly supplied by longshore (sandwaves-moved) and storm currents. These supply mechanisms have also been recognised in many siliciclastic-fed submarine canyons (Beer and Gorsline, 1971; Puig *et al.*, 2003; Baztan *et al.*, 2005; Antobreh and Krastel, 2006; Normark *et al.*, 2006). As a consequence, infilling geometries are similar: wedge-shaped and trough-shaped, concave-up sedimentary bodies (Galloway *et al.*, 1991; Popescu *et al.*, 2004; Baztan *et al.*, 2005).

6. Conclusions

During the Late Tortonian, the Granada Basin (S. Spain) was a marine embayment, open to the west and limited to the south by several small islands. At the eastern side of one of these islands, in the area of Alhama de Granada, shallow-water, temperate carbonates were deposited in a gentle ramp within a small bay. A beach system passed to a shoal system, with an inner belt of small dunes, moved by waves towards the coast, and an outer belt of large dunes and sandwaves, migrating SE to NW by longshore currents. Seawards of the shoals area was the "factory area", where coarse bivalve/bryozoan remains accumulated. Most of these bioclasts were remobilised by storms and deposited landward as tempestites. In the preserved ramp-sequences, (sub)horizontal, coarse-bioclastic tempestite-layers alternate with the cross-bedded shoal-layers.

At a given moment, the Alhama Submarine Canyon developed close to the shoreline, cross-cutting the temperate-carbonate ramp. Two large incision surfaces are recognized, linked to two major erosion events. The excavated relief in the lowermost surface was at least 50 m deep. Calcareous and terrigenous deposits with different geometries (large, wedge- and trough-shaped, concave-up sedimentary bodies) overlie these erosional surfaces. This canyon had an irregular profile and steep slopes (10-30º). A combination of processes linked to sea-level changes is proposed to explain the evolution of the Alhama Submarine Canyon. During sea-level fall, part of the carbonate ramp became exposed. Erosion significantly increased and a small river valley was excavated. As sea level rose, during sea-level lowstand, the distal reaches of the former river valley became inundated. River flows continued along the submerged former river-channel, eroding and deepening the valley. The canyon acted, at this stage, mainly as a by-pass area although some of the transported conglomerates were locally abandoned and accumulated inside the canyon. They appear now as discontinuous beds, hanging on the canyon walls, where they remained as a residual lag. As sea-level continued to rise, the river mouth became detached from the canyon head. Littoral sediments, moved by longshore and storm currents, were increasingly captured inside the canyon, generating erosive flows that contributed to its excavation as well. Most of the canyon sediment infilling was, however, supplied later, during sea-level highstand, once the profile along the canyon axis smoothed enough as to favour sediment deposition. In the Alhama Submarine Canyon, longshore-transported sediments are made up of well-sorted and ground bioclastic calcarenites/fine-grained calcirudites. They derived from longshore-drift sandwaves, collapsing into and feeding the canyon from the south. Storm-related sediments, which poured into the canyon from the north, are mostly made up of coarse-grained bioclastic calcirudites derived from the poorly-sorted, bioclastic factory facies.

Acknowledgements

This work was funded by the "Ministerio de Educación y Ciencia" (Spain), Proyect CGL 2004-04342/BTE and by a doctoral F.P.U. grant (MECD-UGR) awarded to A. Puga-Bernabéu (AP2003-3810). J.M. Martín and J.C. Braga were also supported by Topo-Iberia Consolider Ingenio 2006 (CSD 2006-00041). We are grateful to Christine Laurin for correcting the English text. Constructive reviews by Christian Betzler and John Reijmer are greatly appreciated.

7

MANGARARA FORMATION: REMNANTS OF A MIDDLE MIOCENE TEMPERATE CARBONATE SUBMARINE FAN SYSTEM ON EASTERN TARANAKI BASIN MARGIN, NEW ZEALAND

Ángel Puga-Bernabéu[1, 2*], Campbell S. Nelson[1], Adam J. Vonk[1] and Peter J.J. Kamp[1]

[1] *Department of Earth & Ocean Sciences, University of Waikato, Private Bag 3105, Hamilton (New Zealand)*

[2] *Departamento de Estratigrafía y Paleontología, Facultad de Ciencias, Campus de Fuentenueva s.n., Universidad de Granada, 18002 Granada (Spain)*

**corresponding author: Fax: +34-958-243203*

E-mail: angelpb@ugr.es

New Zealand Journal of Geology and Geophysics
Prepared for submission

Abstract

The Middle Miocene Mangarara Formation is a thin (1–60 m), laterally impersistent unit of characteristically moderately to highly calcareous (40–90%) facies involving conglomerate, bioclastic sandstone, and sandy to pure limestone that crops out only sporadically in central western North Island across the transition from King Country Basin into offshore Taranaki Basin. The unit is unconformably bounded in places by hemipelagic slope mudstone of Manganui Formation below and deep-water redeposited volcaniclastic sandstone of Mohakatino Formation above, but also interfingers and sits conformably within redeposited slope sandy mudstone of Moki Formation which itself is enclosed within Manganui slope mudstone. The calcareous facies of the Mangarara Formation are interpreted to be mainly deep-water mass emplaced deposits as indicated by a combination of channelized and sheet-like geometries, sedimentary structures supportive of redeposition, mixed environment fossil associations, and stratigraphic enclosure within slope-depth mudrocks and flysch. The carbonate component of the deposits consists mainly of bivalves, large benthic foraminifers (especially *Amphistegina*), coralline red algae including rhodoliths (*Lithothamnion* and *Mesophyllum*), and bryozoans, an otherwise warm temperate shallow marine skeletal association. While sediment derivation was partly from an eastern contemporary shelf, the bulk of the skeletal carbonate is inferred to have been sourced from shoal carbonate factories atop isolated upthrust basement highs (Patea-Tongaporutu High) to the south. The Mangarara facies identified are linked especially to redeposition within local platform margin submarine gullies and to broad open submarine channels and lobes in the vicinity of the channel-lobe transition zone of a submarine fan system. Different phases of sediment transport and deposition (lateral-accretion and aggradation stages) are recognised in the channel infilling. Dual fan systems likely co-existed, one dominating and predominantly siliciclastic in nature (Moki Formation), and the other infrequent and involving the temperate calcareous deposits of Mangarara Formation.

Keywords: submarine channel, temperate carbonates, sediment gravity flow, Mangarara Formation, Taranaki Basin, New Zealand

1. Introduction

Sediment gravity flow deposits are an integral part of submarine channel and fan systems on both passive and active continental margins worldwide (e.g. Normark *et al.*, 1998; Curray *et al.*, 2003; Pirmez and Imran, 2003; Posamentier and Kolla, 2003; Bonnel *et al.*, 2005; Ó Cofaigh *et al.*, 2006). In the main they are constructed of siliciclastic sediment sourced originally from erosion on the adjacent continental landmass and subsequently redeposited into slope and basin settings. Carbonate-dominated fan systems are numerically and volumetrically much less common (e.g. Ruíz-Ortíz, 1983; Wright and Wilson, 1984; Watts, 1988; Payros *et al.*, 2007), and especially those involving temperate-latitude or cool-water carbonate facies constructed of heterozoan skeletal material (James, 1997). Due to their general lack of early cementation, shallow-marine temperate skeletal sediments are readily prone to reworking and redeposition (Nelson *et al.*, 1982, 1988a), so that remobilized temperate carbonates behave similarly to their siliciclastic counterparts (e.g. Martín *et al.*, 1996, 2004; Anastas *et al.,* 1997; Betzler *et al.*, 1997a; Braga *et al.*, 2001; Puga-Bernabéu *et al.,* 2007b). A few ancient examples of deep-water mass-emplaced temperate carbonate systems have been described from eastern Mediterranean localities (Braga *et al.*, 2001; Vigorito *et al.*, 2005), where submarine channels have cut temperate carbonate platforms at shallow depths, funnelling bioclastic shelf carbonate basinwards onto submarine fans.

The Miocene sedimentary fill of Taranaki Basin (Fig. 69), presently New Zealand's only economically exploited hydrocarbon basin, involves an up to 3 km-thick succession of hemipelagic and mass-emplaced siliciclastic sediments deposited across a range of mainly bathyal depths (200–4000 m) in slope, submarine fan, and basin floor settings (Fig. 70) (Nodder, 1987; Nodder *et al.*, 1990; King *et al.*, 1993; King and Thrasher, 1996). A window into this succession is exposed through uplift in coastal onshore areas of easternmost Taranaki Basin and the adjoining King Country Basin (Fig. 69) (Kamp *et al.*, 2004). Within it is a Middle Miocene unit named the Mangarara Formation involving redeposited mixed siliciclastic and carbonate sediments that is unique compared to the bulk of the Miocene deposits because of its prominently calcareous nature, ranging from a few tens to near 100% $CaCO_3$. Moreover, the carbonate fraction comprises whole and fragmented skeletons typical of the shallow-water heterozoan skeletal association developed at temperate latitudes (James, 1997).

To date, no detailed sedimentary interpretation of the channelized and redeposited temperate carbonates of the Mangarara Formation has been reported. We do so here, expanding upon the sedimentary spectra of channelized and submarine fan deposits in temperate-latitude settings, as well as providing some additional insight into the palaeogeography of the eastern margin of Taranaki Basin in the western North Island of New Zealand during Middle Miocene time.

2. Geological setting

Taranaki Basin is a foreland basin developed off the west coast of the North Island of New Zealand in response to basement thrusting and loading inboard of the convergent Australian-Pacific plate boundary in the Southwest Pacific that was initiated in the earliest Miocene (Fig. 69). The basin occupies an area of about 100,000 km^2 and includes a Late Cretaceous to Recent fill up to 7 km thick (King and Thrasher, 1996). Most of this fill is offshore in the subsurface, but an uplifted window of the Neogene succession is well exposed onland in coastal Taranaki Peninsula and King Country Basin (Kamp *et al.*, 2004). Basement rocks are Palaeozoic and Mesozoic granite and schist west of Taranaki Fault and Triassic-Jurassic sandstone and mudstone, typically greywacke and argillite, east of it (Mortimer, 1995; Briggs *et al.*, 2004).

The sedimentary fill of western North Island sedimentary basins comprises five second-order sequences or groups of tectonic origin separated by unconformities (Fig. 70) (Kamp *et al.*, 2004): Te Kuiti Group (Late Eocene to Oligocene), Mahoenui Group (earliest Miocene), Mokau Group (late Early to Middle Miocene), Whangamomona Group (Middle Miocene to Early Pliocene), and Rangitikei Group (Pliocene to Pleistocene).

Formations deposited from late Early Miocene (New Zealand Altonian Stage; Pl) to Middle Miocene (New Zealand Waiauan Stage; Sw) are the key to understanding the depositional setting and sedimentary evolution of the Mangarara Formation under investigation here. In the late Early Miocene (Otaian–Altonian) westerly-directed overthrusting of basement rocks took place along the Taranaki Fault and other major faults (Fig. 69) (King *et al.*, 1993). As a consequence, topographic highs involving uplifted basement blocks (the Herangi High and Patea-Tongaporutu High) developed in eastern Taranaki Basin (Fig. 69, 70). In King Country Basin to the east, basin inversion occurred with reverse movement on the Ohura Fault segmenting the basin into the Whangamomona (western) and Taumarunui (eastern) blocks (Hunt, 1980; Vonk, 1999). The Mokau Group comprising fluviatile, coastal, and shallow-marine facies, and its basinal equivalents, the Manganui and Moki Formations, formed at this time (Fig. 70). Within a regime of regional transgression the Manganui Formation mudstones expanded to the east across the Patea-Tongaporutu High with Moki Formation

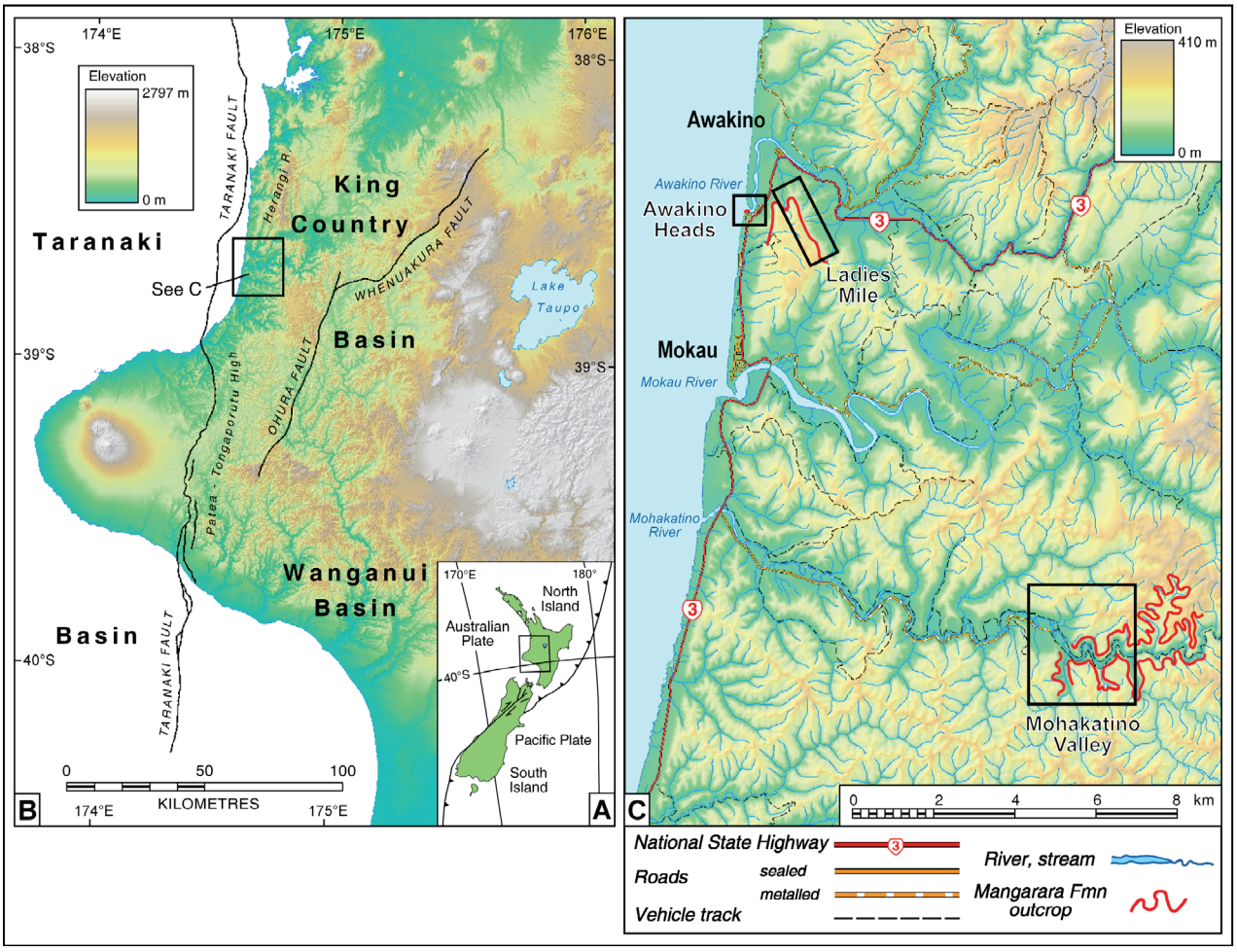

Fig. 69. Locality maps. A) Modern plate tectonic setting of New Zealand. B) Named Cenozoic sedimentary basins in western North Island, including some structural elements and faults. C) Enlargement of C in B showing the three main study sites (Ladies Mile, Awakino Heads, and Mohakatino Valley) and the outcrop distribution in red of Mangarara Formation.

submarine fan deposits accumulating on top of and adjacent to it. East of this high, the contemporary shelf was very narrow (~10 km), with a shoreline located on, or just to the east of the Ohura Fault.

In the Middle Miocene (upper Lillburnian) a regional tectonic downwarp event and associated marked transgression heralded initial deposition of shallow-marine *near-situ* sediments (bioclastic sandstones, bioclastic mudstone, and local limestone) of the Mangarara Formation inland and its redeposited counterparts basinward. Periodic redeposition of Mangarara facies continued through the Middle Miocene during regional subsidence that was accompanied by deposition of widespread siliciclastic shelf and slope deposits of the Otunui Formation, whose facies shallowed eastwards in King Country Basin, but passed westwards into deep-water Manganui Formation mudrocks in Taranaki Basin (Kamp *et al.*, 2004; Vonk and Kamp, 2006). The Mohakatino Formation, a lateral age equivalent of the upper part of the Otunui Formation in the vicinity of the transition between the King Country and Taranaki Basins, is composed of redeposited, deep-marine volcaniclastic mudstone and sandstone up to 80 m thick (Nodder *et al.*, 1990; King and Thraser, 1996); in several localities it lies directly above the Mangarara Formation. The volcaniclastic sediment was derived from a chain of now buried andesitic volcanoes (Mohakatino Volcanic Centre) located to the west of this region in offshore northern Taranaki Basin (Nodder *et al.*, 1990; Bergman *et al.*, 1990, 1992). The Mt Messenger Formation, comprising sandstone and mudstone deposited in basin floor fan and slope fan environments (King and Thrasher, 1996), caps the stratigraphy of the late-Early to Middle Miocene succession (Fig. 70).

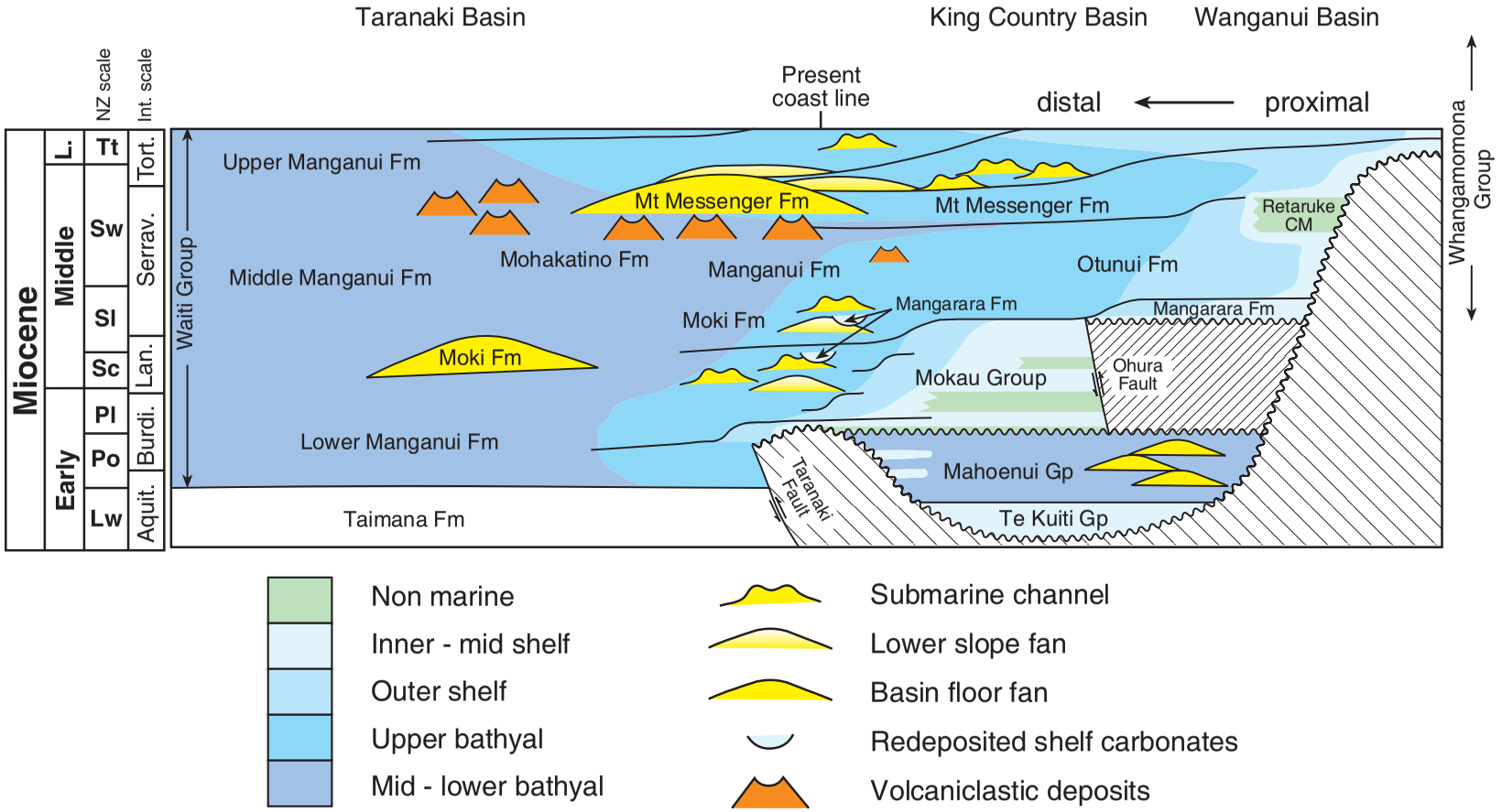

Fig. 70. Time-space stratigraphic panel for Early to Middle Miocene deposits and their inferred depositional settings in a roughly east (King Country Basin) to west (Taranaki Basin) section across the western North Island coastline (modified from Vonk and Kamp, 2006). Int. scale: International scale; NZ scale: New Zealand Stage; L.: Late; Tt: Tongaporutuan; Sw: Waiauan; Sl: Lillburnian; Sc: Clifdenian; Pl: Altonian; Po: Otaian, Lw: Waitakian; Tort.: Tortonian; Serrav. : Serravallian; Lan.: Langhian; Burdi.: Burdigalian; Aquit.: Aquitanian.

3. Mangarara Formation

3.1. Stratigraphic nomenclature, setting, and age

The Middle Miocene Mangarara Formation was defined originally during regional geological mapping in central western North Island, New Zealand by Hay (1967). Subsequently the formation has been mentioned in several MSc theses documenting the Tertiary sedimentary successions in this region (e.g. Happy, 1971; Wilson, 1994; Vonk, 1999; Ngatai, 2004). Of particular interest has been the interpretation of the stratigraphic position of the Mangarara Formation in relation to the surrounding Miocene units (e.g. King *et al.*, 1993). Vonk (1999) and Ngatai (2004) presented an historical review of the Mangarara Formation nomenclature. The Mangarara Formation has been previously called Mangarara Sandstone Formation (Hay, 1967), Mangarara Sandstone (Happy 1971), Mangarara (Sandstone) Member (King *et al.*, 1993), and Pongahuru Limestone Member (Gerritsen, 1994). The present name Mangarara Formation was proposed by Vonk (1999) so as to avoid the use of any lithological descriptor because the unit actually involves a wide variety of siliciclastic and carbonate lithologies. In general, the Mangarara Formation can be considered to comprise all deposits with a significant carbonate content of Middle Miocene age that occur in western North Island sedimentary basins (Vonk, *in prep*).

Outcrops of Mangarara Formation are sporadic and discontinuous, occurring mainly in the vicinity of the lower reaches of the Awakino, Mokau, and Mohakatino Rivers near the central western North Island coastline (Wilson, 1994; Ngatai, 2004). Specifically, the most significant and complete sections for the study of the Mangarara Formation beds occur at Ladies Mile, Awakino Heads, and Mohakatino River valley (Fig. 69). Here they consist mainly of redeposited carbonate and mixed siliciclastic-carbonate sediments intercalated within upper- to middle-slope muddy and sandy deposits of the Manganui and Moki Formations (Fig. 70). It is important to note, however, that a correlative *near situ* shallow-marine facies of the Mangarara Formation is identified locally further inland in the vicinity of Ohura and Taumarunui townships (Armstrong, 1987; Gerritsen, 1994; Vonk, 1999, *in prep*.).

While overall the Mangarara Formation is Middle Miocene in age (Fig. 70), in terms of the more refined New Zealand Stages based on foraminiferal biostratigraphy the ages vary between outcrop localities (King *et al.*, 1993; King and Thrasher, 1996; Ngatai, 2004). Thus a late Altonian (earliest Langhian) to Clifdenian (Langhian) age range is recorded at Ladies Mile and Awakino Heads (i.e. lower Middle Miocene), but from Clifdenian to Waiauan (Langhian to Serravallian) at Mohakatino Valley (upper Middle Miocene). Likely correlative beds assigned to the Tirua Formation by Nodder *et al.* (1990) on the coast north of Awakino Heads yield an exclusively Waiauan age (upper Serravallian).

3.2. Sedimentary facies

Five main facies are established in the Mangarara Formation (Facies A to E), as well as two subordinate ones (Facies F and G) which are, however, more common in the associated Moki Formation (Table 3). Due to their typical coarseness, the different facies types were visually characterised in the field, and supported by examination of 50 thin sections under a petrographic microscope to identify grain and matrix/cement types. Facies geometries are recorded as channelized, lenticular, wedge, tabular, or sheet-like at various scales (Table 3).

3.2.1. Facies A

Facies A consists of brownish medium-grained packstone/grainstone to fine-grained (granule-size) floatstone/rudstone rich in *Amphistegina* tests and fragmented coralline algae, which occur in variable proportions (Fig. 71A, B). Accessory skeletal remains include bryozoans, bivalves, gastropods, echinoderms (mainly spines), rhodoliths, solitary corals, and other foraminifers (e.g. *Lepidocyclina*). Dispersed mudstone and sandstone clasts occur in some beds. Fine-grained (mud) terrigenous material is negligible.

3.2.2. Facies B

Robust bivalve shells (*Cucullaea* sp., *Glycymeris* sp., *Glycymerita* sp., *Tucetona* sp., *Ostreinae* gen. sp. indet.) comprise more than 50% of this greyish rudstone and floatstone (Fig. 71C, D) with a fine to medium calcarenite matrix rich in *Amphistegina* and coralline algae. Valves are variably fragmented, disarticulated, 2–3 cm in average size (up to 7 cm for some oyster fragments), and densely packed (*sensu* Kidwell and Holland, 1991). Shells are stacked (concave-up and -down) and are oriented parallel to the base of beds. Other large bioclasts present are solitary corals (*Trunctoflabellum* sp.). Some pebbles of cemented mudstone are dispersed through the beds.

3.2.3. Facies C

This facies is mainly composed of rounded, well cemented, green to blue-green pebbles to boulders (Fig. 71E). Clasts are elongated ellipsoidal and spherical, and packing ranges from clast- to matrix-supported. Facies C can be divided into two subfacies according to the geometry, nature of the matrix, and bioclast content:

Table 3. Summary of facies attributes for the Mangarara Formation (A-E) and associated Moki Formation (F-G).

Facies	Site (ab)	Geometry and Thickness	Sedimentary structures	Lithology	Main components	Other components	Other characteristics
A	LM (a) AH (r) MV (a)	Channelized, tabular Up to 63 m Individual beds are decimetres in thickness	Massive, well- to rough-bedded, low-angle cross bedded, parallel lamination	*Amphistegina*-rich calcarenite and calcirudite (packstone, grainstone, floatstone, rudstone)	*Amphistegina*, coralline algae (variable proportions)	Bryozoans, bivalves, gastropods, echinoderms, rhodoliths, solitary corals, foraminifers	*Lepidocyclina* present Glauconitized bioclasts and matrix, minor glauconite grains Rhodoliths locally important/abundant in the bed bottoms Dispersed mud (loose and cemented) and sandstone clasts can be present
B	MV (p)	Sheet-like 8–50 cm	Crude parallel lamination, concave-up and-down bioclast stacking	Bivalve rudstone/floatstone with a calcarenite matrix rich in coralline algae and *Amphistegina*	Bivalves	*Amphistegina,* coralline algae, solitary corals.	Disarticulated shells Oysters up to 10 cm Dispersed cemented mudstone pebbles
C_1	LM (p) AH (r)	Channelized 0–60 cm	Massive, rare inverse grading	Conglomerate (pebble-to-boulder) in a bioclastic muddy packstone	Well-cemented mudstone concretions Rhodoliths 2–3 cm average size (up to 10 cm)	Bivalves, bryozoans	Some mudstone clasts bored by *Lithophaga* Some greywacke pebbles present
C_2	MV (c)	Sheet-like, channelized base locally 25–130 cm	Massive, rough bedded	Conglomerate pebble- to cobble-size (minor boulders) with large bioclasts in a calcarenite/calcirudite matrix rich in coralline algae and *Amphistegina*	Well-cemented mudstones Rhodoliths and bivalves in variable proportions	Mud and sandstone clasts Gastropods, solitary corals	Bivalves occur as shells and moulds Pebbles encrusted by thin rhodolith crusts
D	MV (c)	Sheet-like 15–65 cm	Massive	Rhodolith rudstone/floatstone with a calcarenite/calcirudite matrix rich in coralline algae and *Amphistegina*	Rhodoliths 3–5 cm on average (up to 10 cm), coralline algae, *Amphistegina*	Mud and sandstone clasts Bivalve shells, gastropods, bryozoans (matrix), echinoderms (matrix), benthic foraminifers (matrix)	Rhodoliths are spheroidal to ellipsoidal and composed of warty to laminar plants (mainly *Lithothamnion*) Intergrown with bryozoans and vermetids

Ab= Relative abundance (a=abundant; c=common; p=present; r=rare) at site specified: LM= Ladies Mile; AH= Awakino Heads; MV= Mohakatino Valley

Table 3. (continued)

Facies	Site (ab)	Geometry and Thickness	Sedimentary structures	Lithology	Main components	Other components	Other characteristics
E	LM (a) AH (p)	Channelized, tabular 220–600 cm (individual beds are decimetres in thickness)	Massive, well- to rough-bedded, parallel lamination, local normal grading, locally burrowed	Bioclastic sandstone with variable amounts of mud and bioclasts	Bivalves, bryozoans (branching and unilaminar), planktonic foraminifers	Dispersed cemented mudstone clasts (up to pebble-sized) Gastropods, solitary corals, echinoderms, *Amphistegina,* benthic forams	Glauconitized bioclasts and matrix Granule- to pebble-sized glauconite grains locally abundant Limonitized shell moulds common
F	AH (r) MV (a)	Channelized, sheet-like, lenticular 2–70 cm	Massive, locally burrowed	Mudstone with variable amounts of dispersed small bioclast fragments	Bivalves, bryozoans, planktonic foraminifers	Benthic forams, echinoderms, gastropods, coralline red algae, *Amphistegina*	Glauconitized bioclasts and rare glauconite grains Small bioclastic pockets occur in some beds
G	MV (a)	Wedge, sheet-like Up to 80 m Individual beds are centimetre to decimetre in thickness	Massive, horizontally bedded, parallel lamination, cross-lamination, bioturbation traces locally	Very fine to fine sandstone			Bed amalgamation occurs Some dispersed clasts and bioclastic pockets locally

Ab= Relative abundance (a=abundant; c=common; p=present; r=rare) at site specified: LM= Ladies Mile; AH= Awakino Heads; MV= Mohakatino Valley

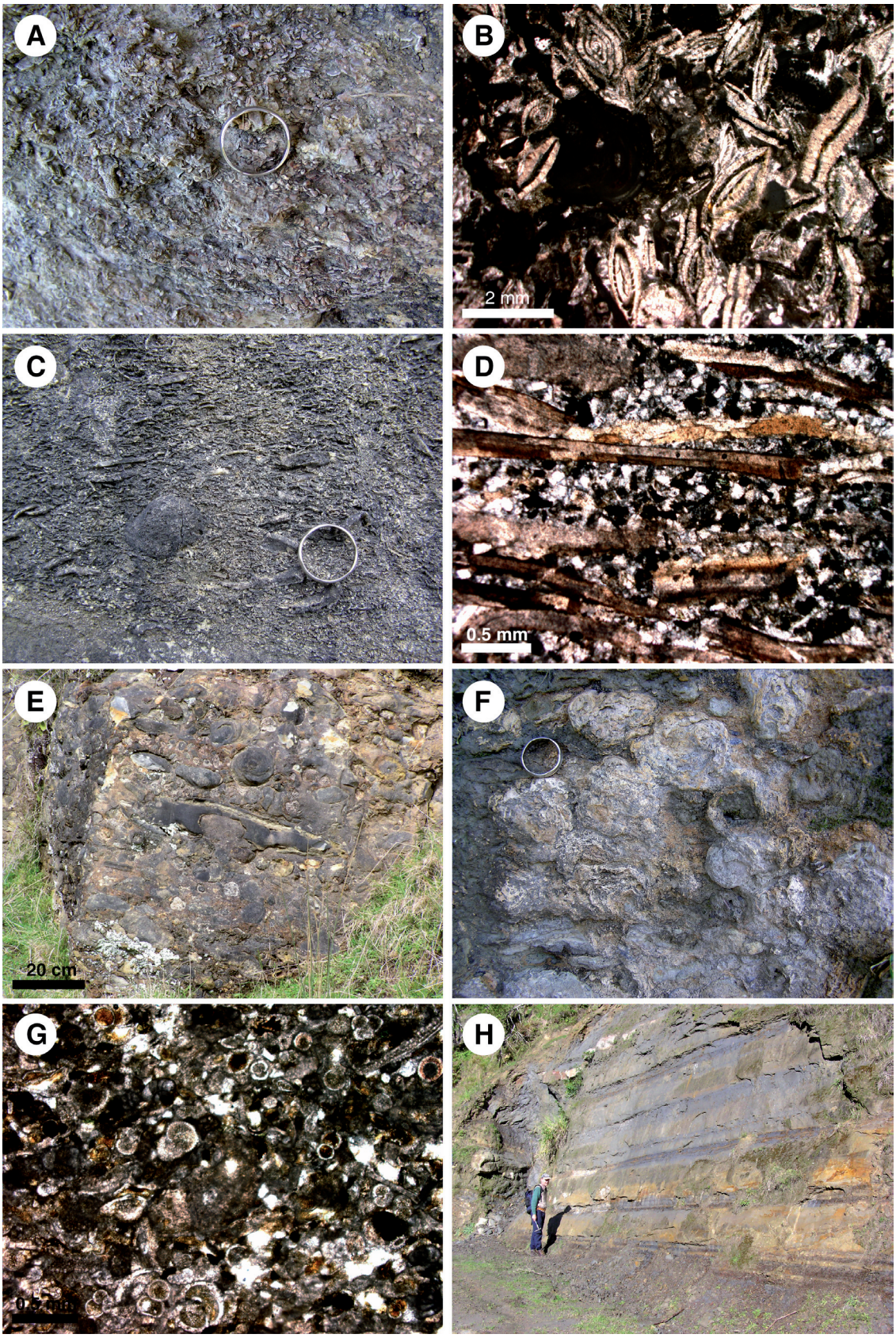
A
B
2 mm
C
D
0.5 mm
E
20 cm
F
G
H

◀ **Fig. 71.** Facies types in the Mangarara (A to E) and Moki (F and G) Formations. A) Close-up of Facies A showing well-preserved *Amphistegina* tests. Ring 2 cm in diameter. B) Photomicrograph showing the main components of Facies A: *Amphistegina* and coralline algae. C) Bivalve-dominated rudstone of Facies B. Ring 2 cm in diameter. D) Photomicrograph of Facies B showing bivalve shells within a silty matrix. E) Outcrop view of Facies C (subfacies C2). Most of the coarse-grained components are cemented mudstone clasts (dark) and rhodoliths (white). Sandstone clasts (yellow) are also present. F) Close-up of Facies D showing the spherical to ellipsoidal centimetre-sized rhodoliths. Ring 2 cm in diameter. G) Photomicrograph of Facies E showing the abundance of planktonic foraminifers (some glauconitized) in a packstone matrix. H) Outcrop view of the siliciclastic-dominated facies in the Moki Formation. In this view, Facies F is grey and Facies G is pale green to yellowish.

Facies C_1: occurs at the base of channelized bodies, has a muddy bioclastic matrix, and the main bioclasts are rhodoliths and minor bivalves. Some clasts are bioeroded by *gastrochaenolites* (*Lithophaga* borings).

Facies C_2: normally exhibits sheet-like geometry with planar limits, but locally has an irregular base. Matrix is bioclast-rich with abundant coralline algal and *Amphistegina* remains. Large bioclasts (rhodoliths and bivalves) are common. Solitary corals and gastropods are also present. Mudstone and sandstone clasts can be locally abundant.

3.2.4. Facies D

Spherical and ellipsoidal rhodoliths up to 10 cm in size (av. 3–5 cm) are the dominant component of this facies (Fig. 71F). Rhodoliths are formed mainly by warty and laminar thalli of *Lithothamnion* and occasional *Mesophyllum*. Matrix consists of a packstone-floatstone dominated by coralline algal fragments and subordinate *Amphistegina* tests. Bivalves (important locally), bryozoans, and gastropods are accessory components, and echinoderms and small benthic foraminifers also occur mainly within the matrix. Pebbles and cobbles of cemented mudstone and friable sandstone are also present.

3.2.5. Facies E

This facies consists of bioclastic sandstones (locally calcarenite and calcirudite) with variable amounts of mud (silt) and bioclasts. Granules and pebbles of cemented mudstone occur dispersed. Macrobioclasts (>0.5 cm) are mainly of bivalves and bryozoans (branching and unilaminar). Bivalve shells commonly occur as fragmented small remains, with minor disarticulated, pebble-sized valves. Some limonitized internal shell moulds are also present. Other skeletons are of gastropods, *Amphistegina*, solitary corals, and echinoderm spines. Planktic foraminifers are abundant in the matrix (Fig. 71G). Bioclasts (especially planktonic foraminifers) and matrix are commonly glauconitized.

3.2.6. Facies F

This facies comprises greenish grey mudstone (Fig. 71H) with bioclast content ranging from negligible to about 10–15%. Bivalves (especially *Lima colorata*), bryozoans, planktonic and benthic foraminifers, gastropods, coralline algae, *Amphistegina*, and echinoderms are present. Bioclasts occur mainly as fragmented remains, although some whole shells are also preserved. Burrowing is locally abundant, and small bioclastic pockets or nests (typically up to a few centimetres size) are scattered throughout Facies F. Bioclasts are partially glauconitized.

3.2.7. Facies G

Fine to very fine yellowish sandstones make up this facies (Fig. 71H). Several types of sedimentary structures occur (Table 3). Bioclasts are only present in small bioturbation pockets that occur locally. Dispersed granule- to pebble-size clasts are present in some beds.

3.3. Ladies Mile section

Ladies Mile section is a 1.7-km long cliff section, extending roughly NW-SE, located 2 km to the southeast of the coastal settlement of Awakino (from R17/522808-R18/528798 on NZMS 260 Series 1:50,000 topographic maps) (Fig. 69, 72). In the steep exposures of Ladies Mile, the mixed siliciclastic-carbonate sediments of the Mangarara Formation overlie the thick (up to 125 m) grey siliciclastic mudstones and intercalated sandstones of the Manganui Formation (King *et al.*, 1993). Volcaniclastic sediments of the Mohakatino Formation, overlying the Mangarara Formation, complete the stratigraphic succession at this locality.

3.3.1. Geometries

The panoramic view of the Ladies Mile outcrop highlights distinctive channel complexes in the Mangarara Formation at a large scale (Fig. 72). Channelized beds as a whole show an erosive and/or a sharp planar base on the underlying sediments (Manganui Formation). Individual channels within the channel complex have low- to very low-angle margins and a high width/height ratio. They range from 25 to 120 m across and up to 3 to 15 m thick at their axes. Nested small-scale channels are present at different positions cutting the underlying major channel (Fig. 73). Small-scale cut-and-fill structures are also recognized in some large channel-fills.

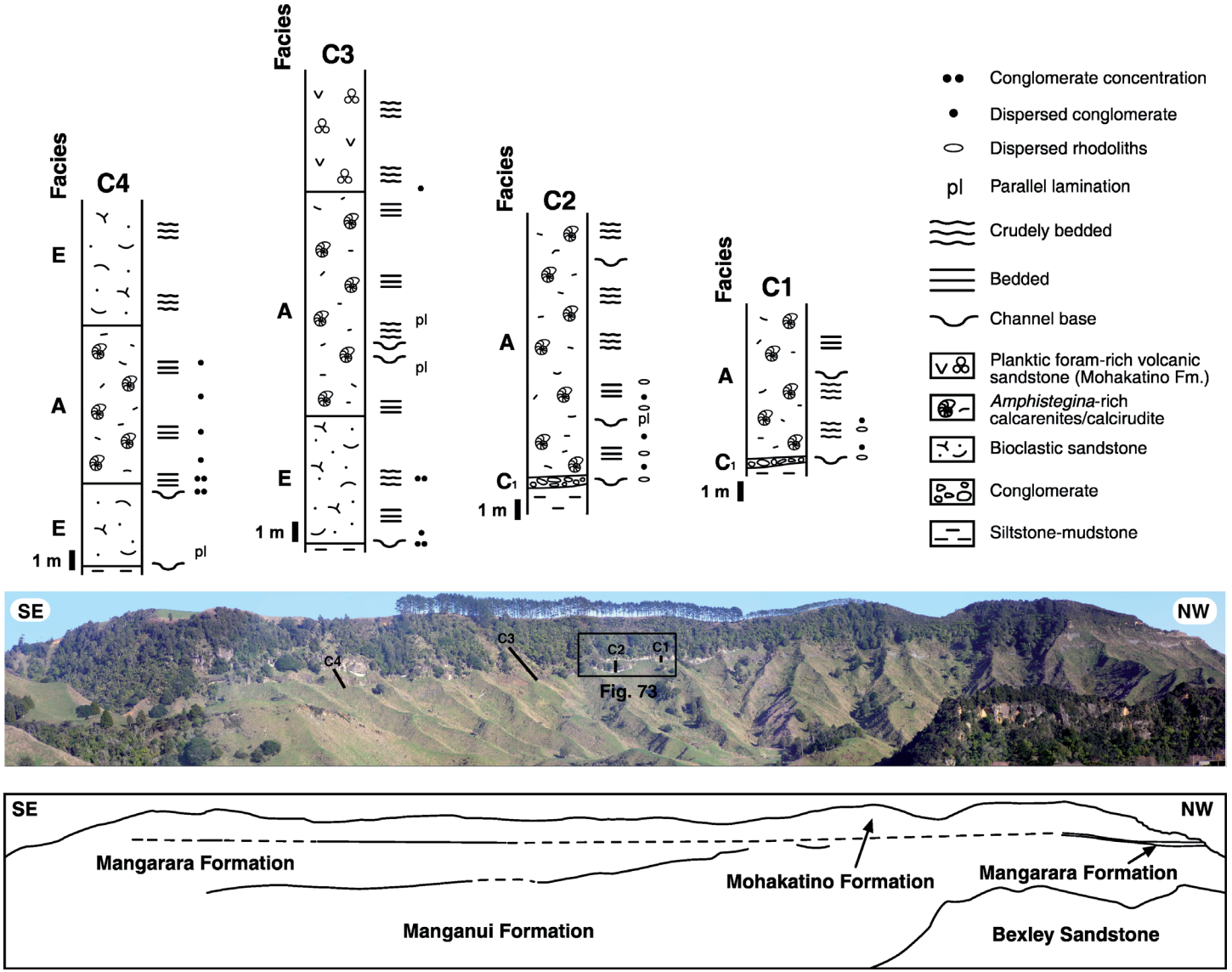

Fig. 72. Panoramic view of Ladies Mile section. Inset shows the location of Fig. 73 and black lines C1 to C4 mark the position of the logged columns with facies codes to their left. Interpreted geological boundaries among the different units are shown in the lower part of the figure.

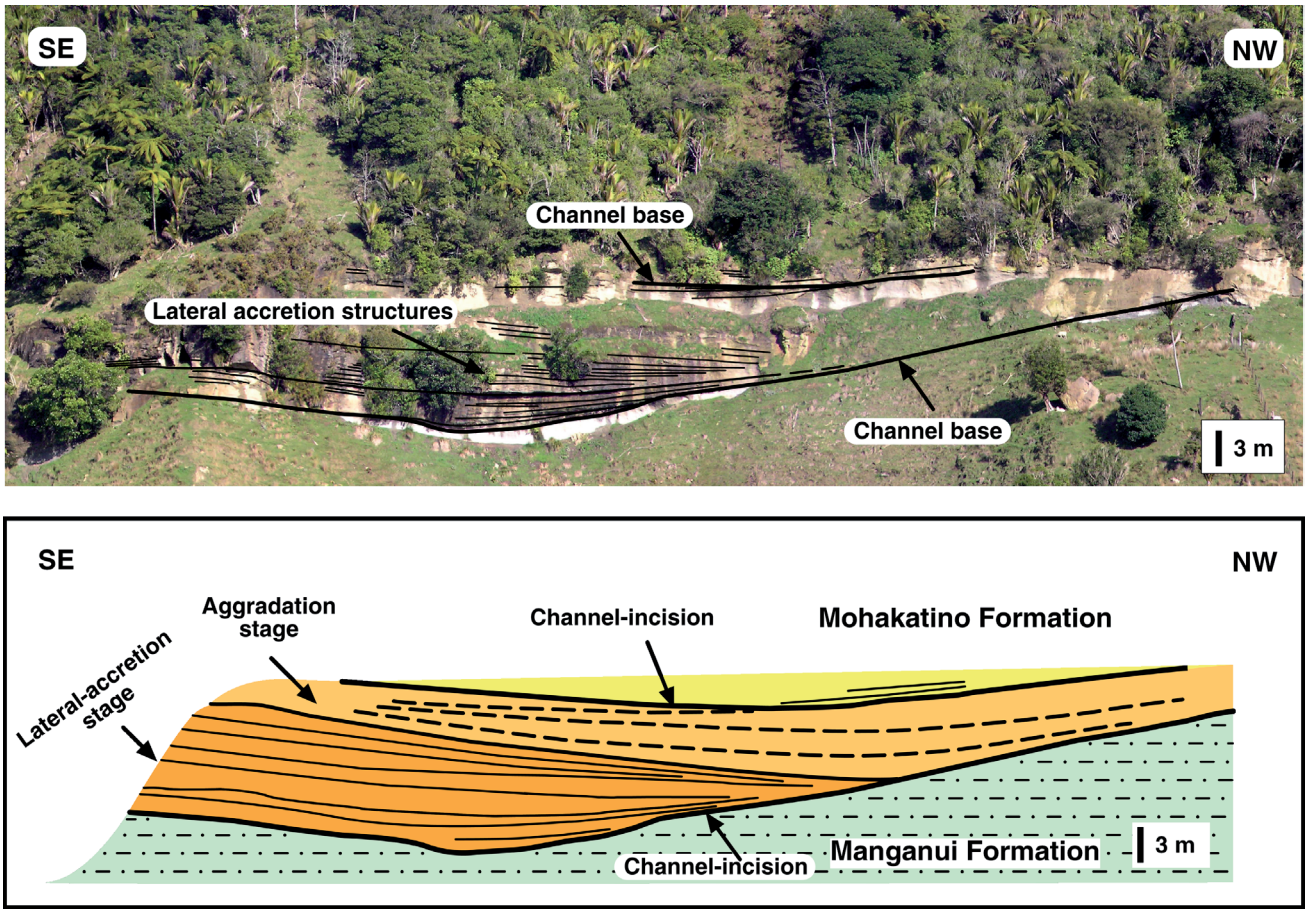

Fig. 73. Channels in Ladies Mile section (see Fig. 72). Outcrop view shows the channelized geometries of a large channel and a small nested channel on top. Low-angle cross-bedding is interpreted as lateral-accretion structures. Interpreted diagram below indicates the different stages of the channel fill. Lateral-accretion stage developed after channel incision. In this stage, lateral bars were deposited on the convex side during active sediment transport through the channel. Channel infilling occurred during the aggradation stage. The shift of the channel-lobe position after channel avulsion produced another channel incision.

Channel-fill normally consists of decimetre-thick beds conforming to the underlying surface. Asymmetric infilling is also present in some channels (Fig. 73). Beds are well to crudely stratified, have diffuse to planar limits, and are mostly massive and moderately to poorly sorted. Only a few beds show parallel lamination. Normal grading occurs locally. Average grain size ranges from medium sand to granule, with some coarser grains occurring dispersed at the base of beds.

Facies A, C_1, and E (Table 3) comprise the channel infilling at Ladies Mile. Facies A dominates the fill of the higher channels at the site. Beds of this facies are commonly well cemented and amalgamated with some intercalations of less cemented finer-grained intervals. Facies E occurs in the lower-channel fill and separates two superimposed facies A-filled channels. These two facies types contain dispersed pebbles at different positions of the infilling, usually in the basal beds. Facies C_1 is located at the base of some channels (Fig. 72).

3.3.2. Interpretation

Channelized bodies at the Ladies Mile section are mainly characterised by broad channel-geometries (i.e. high width/height ratios). Sediment fill conforms to the channel base and flattens up, building tabular beds that partially extend over the channel margins (Fig. 73). Within a submarine channel-fan system, channels at Ladies Mile are interpreted to lie in the proximity of the channel-lobe transition, where channels of the middle fan merge into outer-fan lobes (cf. Reading and Richards, 1994), or in the transition from the leveed channel to frontal splay according to Posamentier and Kolla (2003).

Low-angle structures that downlap the base of some channels (Fig. 73) are interpreted as lateral-accretion structures. This suggests a sinuous meandering morphology of the channel system and indicates that deposition was contemporaneous with channel lateral and downdip migration. Two different phases in the channel infilling

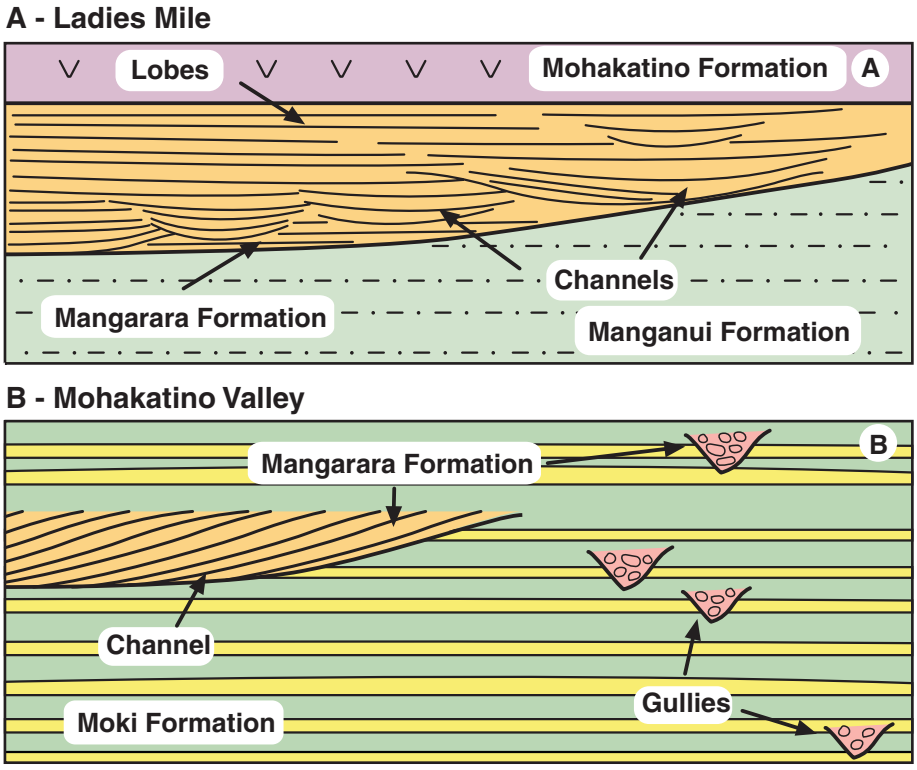

Fig. 74. Schematic diagrams illustrating the geometries and the main elements of the Mangarara Formation submarine-fan system in Ladies Mile section (A) and Mohakatino Valley section (B) (not to scale). The Mangarara Formation is composed of channel-fills and lobes at the Ladies Mile section. At the Mohakatino River section, the Mangarara Formation consists of channel-fills and gullies cutting the underlying sediments of the Moki Formation.

are recognized (Fig. 73): 1) lateral-accretion stage in which flows through the channel erode the concave-side and deposit sediment in lateral-accretion packages or lateral bars on the convex-side, and 2) aggradation-stage during which the channel-infilling accretes vertically. During the aggradation phase, channels begin to fill up and sediment backfill over the channel-margin may occur. After channel avulsion, channels are abandoned and the channel-lobe zone shifts position. In fact, the channelized and redeposited carbonates at Ladies Mile show a large-scale channelized geometry (channel complex) (Fig. 72) composed of channel-fills and backfilling deposits (Fig. 74A).

Cut-and-fill structures observed in the infilling of some large channels probably relate to small-scale channel development within major channels at certain times.

We consider that lateral accretion occurred during sustained-flow conditions. During such periods, concentrated density flows probably deposited structureless layers on the lateral bar. This steady flow was not prolonged for long periods but there was sufficient time to enable minor longitudinal flow transformation to occur. Subsequently, no differentiation of sedimentary structures occurred and the final result is a massive and poorly-sorted deposit. Flow partially decelerated when it climbed up the lateral bar (secondary helicoidal flow), and shear velocity decreased and coarser sediment was deposited. This explains the presence of dispersed clasts accumulated preferentially at the base of the beds conforming to the lateral-accretion structures. Parallel laminated beds that occur locally may also be related to flow deceleration.

Flow behaviour in the lower channel-lobe zone, where Facies E dominates, is poorly understood as sand, bioclasts, and mud occur in different proportions in massive or locally parallel laminated beds. Mud flows, concentrated debris flows (steady and waning flows,) and turbidity flows may produce these sorts of deposits (Ghibaudo, 1992; Clark and Pickering, 1996).

Coarse conglomerates at the base of some channels are interpreted as residual lag deposits left behind during sediment-bypass phases along the channel.

3.4. Awakino Heads section

Small outcrops of the channelized Mangarara Formation, accessible mainly during low tide, occur at the

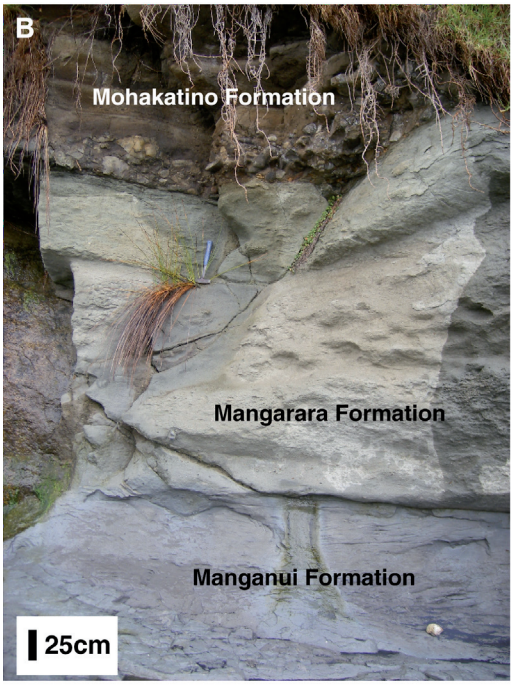

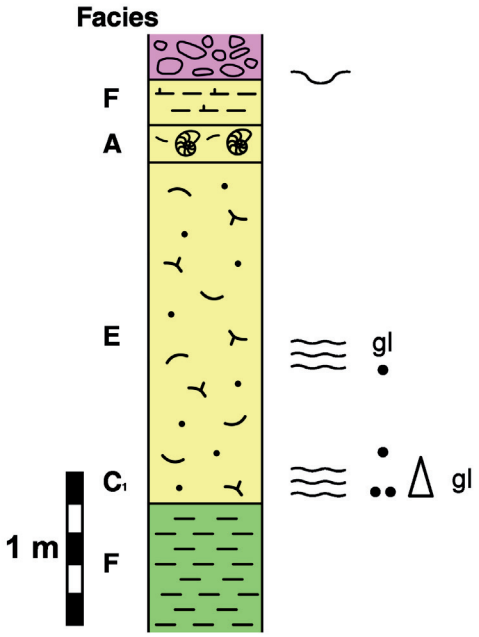

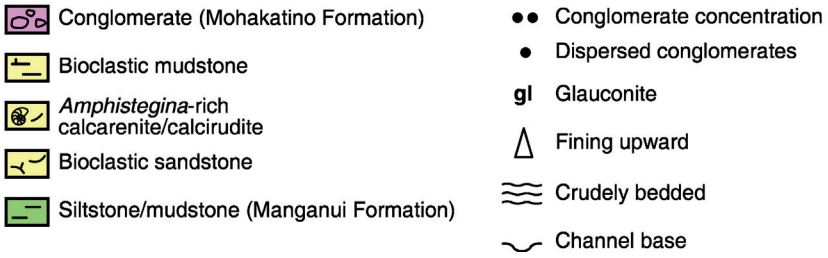

Fig. 75. A) Field view of the Awakino Heads section showing the geological boundaries among the different units. Note channel margin geometry in the Mangarara Formation. Channel axis is located to the northwest. Inset shows the position of B. B) Stratigraphic column of the Awakino Heads section with facies codes to its left. Burrowed and glauconite-rich sediment of Facies E comprises most of the channel infilling.

mouth of the Awakino River (R17/511808) (Fig. 69). Here the Mangarara Formation unconformably overlies the Manganui Formation, whose top is of Middle Miocene (Langhian or upper Altonian) age (King *et al.*, 1993), and is in turn unconformably overlain by the distinctly volcaniclastic sandstones of the Mohakatino Formation (Fig. 75).

3.4.1. Geometries

A channelized geometry (channel margin) is evident for the Mangarara Formation (Fig 75). However, the seaward dip of beds, the erosive contact with the overlying Mohakatino Formation and Quaternary terrace deposits, and modern coastal sand accumulations at the Awakino River mouth do not allow a precise determination of the whole channel geometry.

Channel-fill is almost 3 m thick, with sediment ranging from crudely bedded to mainly massive. At the base, a 10 cm-thick normally graded interval commonly occurs. Facies E, here thoroughly burrowed throughout, comprises most of the logged section with some decimetre-thick beds of Facies A and F in the upper part (Fig. 75). Exposed locally in channelled depressions at the seaward end of the section when modern sand has been scoured from the river mouth are pebbles and cobbles of concretionary mudstone at the very base of the section. Comparable smaller fragments are dispersed throughout the Facies E fill, along with common glauconitic and/or glauconitized grains, often concentrated in small, centimetre-sized pockets. A prominent conglomerate bed on top is similar to Facies C_1 but it does not contain bioclasts and its matrix is volcaniclastic sandstone (Fig. 75). Consequently it is assigned to the basal Mohakatino Formation and not the Mangarara Formation.

3.4.2. Interpretation

The sediments of the Mangarara Formation at Awakino Heads were deposited in a submarine channel. As noted above for Ladies Mile, different types of flows could generate the mixed sand-mud-bioclastic fill of the channel. The presence of highly burrowed intervals precludes flow interpretation as indicative sedimentary structures have been destroyed. Tentatively, we consider this channel to be located near to the channel-lobe transition zone. The localized conglomeratic deposits in basal depressions at the seaward end of the section are likely lag deposits, while the muddy interval of Facies F at the top of the channel infilling indicates channel abandonment and deposition of hemipelagic sediment instead.

The concretionary cobble conglomerate at the base of the Mohakatino Formation is interpreted to be residual lag from subsequent erosive channel cutting events or debris flows on the contemporary slope. The disconformity that spans this upper contact is approximately 4.5 m.y. duration based on the age assigned by King *et al.* (1993) to the Mangarara Formation of lower Clifdenian (c. 15.5–15.9 Ma) compared to that of the overlying Mohakatino Formation of latest Waiauan (c. 11 Ma). This disconformity suggests that continued erosive events occurred on the contemporary slope throughout this time period until the latest Waiauan when the Mohakatino volcaniclastic sediments were deposited over the partially eroded section from a combination of sediment gravity flows and submarine ash fallout (e.g. Nodder *et al.*, 1990).

Previously, the Mangarara-Mohakatino disconformity, in combination with the presence of shallow-water foraminifers (now appreciated as being redeposited) in the Mangarara Formation, led to a scenario invoking yoyo tectonics in which the unconformity was created by subaerial exposure and erosion of the Patea-Tongaporutu High, with carbonate-dominated sediments deposited *in situ* around the flanks of the high. With the recent discovery of the expanded stratigraphic section in the Mohakatino Valley (Fig. 69; see next section) and the revised submarine channel/fan interpretation for the Mangarara Formation presented here, our preferred interpretation is that this region of the eastern Taranaki Basin margin slowly tectonically subsided since the late Early Miocene (lower Altonian) and that the unconformity between the Mangarara and Mohakatino Formations at the Awakino Heads section was produced by submarine erosion during channel cutting or down-cutting by debris flows on the contemporary slope.

3.5. Mohakatino Valley section

The Moki Formation crops out widely along both sides of the Mohakatino River valley (Ngatai, 2004) (Fig. 69). About 10 km upstream from the river mouth (from R18/585704-R18/605698) this siliciclastic unit is cut and overlain at different positions by mixed siliciclastic-carbonate and carbonate deposits of the Mangarara Formation. Here, Moki Formation comprises decimetre-scale interbedded sandstone (Facies G) and mudstone (Facies F). The sandstone is typically fine- to very fine-grained, well sorted, locally bioturbated, and has sharp bases and sharp to abruptly gradational tops. Sandstone beds are interpreted to be sandy debris flow deposits (debrites). The mudstone is massive and locally thoroughly bioturbated. This mudstone contains common to rare well preserved bivalves, gastropods, scaphopods and solitary corals including *Lima colorata*, *Lentipecten hochstetteri*, *Limopsis lawsi*, *Amalda* sp., *Austrofusus* sp., *Penion crawfordi*, *Falsicolus* sp., *Alcithoe* aff. *bathgati*, *Austrotoma nevosa*,

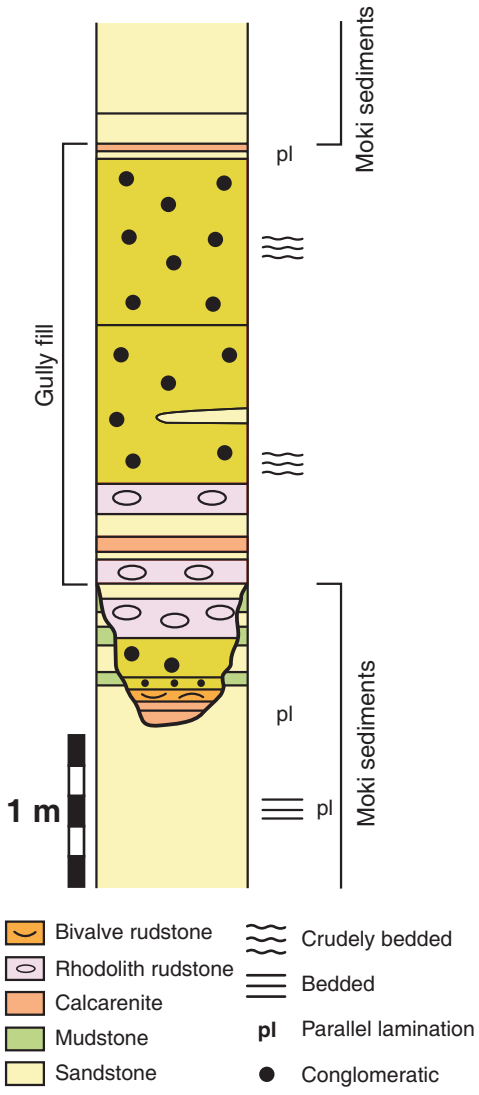

Fig. 76. Detailed log of a small Mangarara gully infill at the Mohakatino Valley section. Gully infilling is mostly coarse-grained sediments (bivalve and rhodolith rudstones and conglomerates) presumably deposited by debris flows.

Zemacies elatior, *Sigapatella* sp., *Dentalium otamaringaense*, and *Trunctoflabellum spenodeum* (Ngatai, 2004).

3.5.1. Geometries

Geometries of the mixed siliciclastic-carbonate bodies of the Mangarara Formation at this site can be assigned to poorly-defined channels, well-defined channels, or sheet-like beds.

Poorly-defined channels. These channels have subtle, poorly-defined channel geometries with steep margins, sometimes bounded by small faults. Where measurable, their orientation appears to be directed mainly towards the N to NW.

Channel widths range from 25 to 50 m and channel thickness from 2 to 5 m. Individual beds within channels are from a few centimetres to 1.5 m thick. Most bed bottoms are planar and sharp, but erosive bases are also present.

A coarse-grained fill, rich in carbonates with some intercalated siliciclastic beds, characterises these channels (Fig. 76). Coarse-grained beds (Facies B, C_2, and D) are crudely bedded, while parallel and cross lamination occur in some finer-grained beds (Facies A and E). Rip-up clasts of Facies F (mudstone) and G (sandstone) are common in the coarse-grained beds.

Well-defined channels. These are up to 200 m-wide channels with infillings up to 15 m thick, having width/height ratios of about 10:1. Channel-fill consists of amalgamated beds, mainly of Facies A and minor D, separated by thin mud layers (Facies F). Low-angle cross-bedded to sigmoidal beds occur locally (Fig. 77). Dip-angles of these beds range from 3 to 13°. Channel axes align NE-SW, but no other palaeocurrent indicators are observed. Steep walls of the outcrops and dense vegetation preclude thorough examination of these channels.

Sheet-like beds. These beds are up to 70 cm thick, have sheet-like geometry, and extend laterally more than 400 m. They are located beneath the main set of high aspect ratio (width: depth ratio) channelized deposits and intercalated between sandstones and mudstones of the Moki Formation. These latter deposits also exhibit sheet-like geometries. Tabular carbonate beds are made up of Facies A. A crude parallel lamination, associated with the alignment of *Amphistegina* tests, is evident in some beds.

3.5.2. Interpretation

Carbonate and mixed siliciclastic-carbonate bodies at the Mohakatino Valley site relate to different deep-water environments.

The poorly-developed channels are interpreted as the remnants of submarine gullies that cut the slope from the shelf-edge or an inner position in the platform, and served to funnel coarse sediment out onto the basin floor. Supporting evidence includes: 1) these channels are engulfed within the sheet-like sandstones and intercalated mudstones of Moki Formation, interpreted as submarine lobes deposited by a siliciclastic submarine-fan system or frontal-splay complex (*sensu* Posamentier and Kolla, 2003); 2) the channel-fills are cut into the underlying sediments and overlain by the same background sediment (Fig. 76); 3) no evidence exists

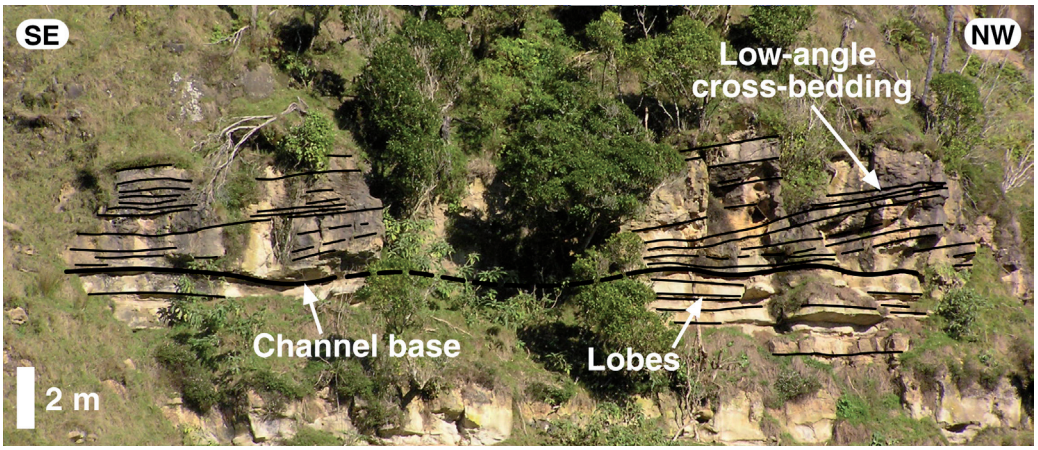

Fig. 77. Channel sedimentary structures at the Mohakatino Valley section. Low-angle cross-bedded calcirudites/calcarenites of Facies A (Amphistegina/coralline algal- dominated facies) interpreted as lateral bars.

for channel migration, avulsion, or appearance of related levees, overbank splays sediment waves, or frontal-splay complexes/lobes; 4) channel-size (smaller), margin-angles (steeper), and facies infilling (coarser) are different from those of the well-defined channels; and 5) the emplacement mechanism for these sediment bodies suggests erosion and simultaneous sediment deposition rather than sediment transport and redeposition along a channel (see below and previous section).

Although several facies types may infill the poorly-defined channels, they can be broadly grouped as coarse-grained (Facies B, C_2, and D) and fine-grained (Facies A, F, and G) varieties. Large clasts and bioclasts in the coarse-grained facies behaved similarly during transport in a density flow so that, for example, a rhodolith 5 cm in diameter had a comparable hydrodynamic behaviour to that of a cemented mudstone clast of similar size. These coarse beds were deposited in submarine gullies as debris flows. Rip-up clasts (of Facies F and G) were eroded from the underlying siliciclastic lobe sediments and incorporated into the flow when the debris flows reached the slope-basin transition. Fine-grained facies were funnelled through the gullies by turbidity currents and concentrated debris flows.

While previous gully morphology could have existed in the platform, affording a predestined sediment transport path downward along these gullies, we suspect that the debris flows were also responsible for the active erosion and maintenance of the gullies. Fine-grained sediment flows presumably contributed to the gully fill, but to a lesser extent.

The well-developed channels are similar to those described at the Ladies Mile section. Cross- to sigmoidal beds (Fig. 77) are interpreted to result from the migration of lateral bars in meandering submarine channels. However, in contrast to those at Ladies Mile, the lateral bars in these channels accreted over larger distances. Consequently the lateral-accretion stage and migration activity of the channels was more important at the Mohakatino Valley site than at Ladies Mile. This probably relates to an inner position in the submarine channel-fan system for the Mohakatino Valley section compared with the Ladies Mile position. Channels from the Mohakatino Valley are interpreted as lateral-accreting confined-channel system moving downslope into a channel-lobe transition zone at Ladies Mile. As noted above, outcrop quality precludes a more detailed interpretation and an aggradation infilling stage is not clearly recognized at Mohakatino Valley.

As interpreted for Ladies Mile, lateral bar migration was produced under steady flow conditions. Flow was partially decelerated during the helicoidal movement over the bar. Resulting deposits are massive and only locally did large rhodoliths accumulate as a lag deposit at the base of beds. Thin caps of mud were deposited during periods of quiescence.

Sheet-like beds are interpreted to represent submarine lobe deposits generated down-dip of channel-mouths when flows became unconfined. The flow deceleration produced by this unconfinement is reflected in the crude but common parallel lamination in these beds compared with those in the confined channel-fill (well-defined channels). Carbonate beds are intercalated within the sandstones and mudstones which indicate that the same channel was shared by both carbonate- and siliciclastic-dominant density flows. These lobe deposits are overlain by channel deposits, reflecting channel migration over the lobes, essentially a cross-cutting of two deep-water submarine sediment transport systems (Mangarara and Moki Formations systems).

The vertical stacking pattern at Mohakatino Valley (Fig. 74B) is characterised by the presence of carbonate and mixed siliciclastic-carbonate channelized bodies intercalated within the siliciclastic-dominated submarine-lobe deposits of the Moki Formation. In contrast to Ladies Mile architecture, channels prograded over the lobes (mainly those of the Moki Formation) and lateral changes in the position of the channel-lobe transition through time are not observed.

4. Discussion

4.1. Integrated submarine fan model

The channelized and redeposited carbonates and mixed siliciclastic-carbonate sediments comprising the Mangarara Formation in onshore eastern Taranaki Basin are here interpreted to be part of a submarine channel-fan system, linked more specifically to the channel-lobe transition zone (Fig. 78). Another element of deep-water settings, submarine gullies, is also recognized.

One of the platform-to-basin transport paths was via submarine gullies distributed along the contemporary palaeoslope. Such slope gullies are common morphological features of modern continental margins and are conduits for channelizing coarse-grained sediment into deep water from the shelf-break (e.g. Ricketts and Evenchick, 1999; Spinelli and Field, 2001). Spinelli and Field (2001) describe ancient submarine gullies up to 100 wide and 1-3 m deep that extended 10-15 km across the slope in the northern California Continental Borderland. These sizes are similar to those at the Mohakatino Valley site. We envisage for eastern Taranaki Basin that submarine gullies funnelled, via debris flows and other density flows, coarse sediment from shallow platforms out onto the basin floor where they cut into lobe and basinal sediments (Fig. 78). In some literature examples, gullies act as tributary channels that merge into large channels and submarine canyons (e.g. Vigorito *et al.*, 2005; García *et al.*, 2006). In our example, apparently no physical connection existed between the gullies and channels, although outcrop is limited.

The main paths of sediment remobilization to the basin floor were submarine channels. Lateral-accretion structures suggest a meandering geometry of the channels (Fig. 78). Active sediment transport and deposition occurred during the migration of these channels (lateral-accretion stage) that were later filled up (aggradation stage) and eventually smothered with overbank (backfill) deposits. Similar stages of channel drift have been recognized in other submarine meandering channel systems (Peakall *et al.*, 2000; Lien *et al.*, 2003). In the final stage, spillover deposits overtop the channel levees (Piper and Normark, 1983). In the Mangarara case, no evidence of levees has been observed in lateral-accreting confined channels (Mohakatino Valley). This is probably a consequence of the coarseness of the channel-fill sediment and the behaviour of the flow involved in its transport and deposition. The broad channel geometries (at Ladies Mile and Awakino Heads) relate to their proximity to the channel-lobe transition zone, where sediment flows become unconfined, decelerate and deposit the transported sediment.

The last elements recognized in the system are submarine lobes that spread over the basin floor from the channel-mouth. Channel migration over the lobes and change of the channel-lobe zone position due to the switch from a confined channel to an unconfined frontal splay (lobe), reflect the dynamic activity of these channels.

4.2. Depositional processes in mixed siliciclastic-carbonate fan systems

The architectural elements of the carbonate channelized system described above are present in many siliciclastic systems (e.g. Spinelli and Field, 2001; Gardner *et al.*, 2003b; Posamentier and Kolla, 2003; Klaucke *et al.*, 2004; Ó Cofaigh *et al.*, 2006), as well as in some carbonate deep-water systems (e.g. Braga *et al.*, 2001; Vigorito *et al.*, 2005, 2006; Payros *et al.*, 2007). Subaqueous sediment gravity flows are responsible for the transport and deposition into these deep-water settings. However, much controversy remains concerning the flow-type, flow-behaviour and the nature of the individual layers and bed sets that build the different architectural elements (e.g. Lowe, 1982; Shanmugam, 1996, 2000; Lowe and Guy, 2000; Mulder and Alexander, 2001; Keevil *et al.*, 2006). Complexity derives from the fact that density flows are vertically graded (Kneller and Buckee, 2000; Peakall *et al.*, 2000; Gladstone and Sparks, 2002) and experience flow transformation in time (surge, steady, waning, and waxing flows) and space (longitudinal) (Kneller and McCaffrey, 2003). Flow behaviour depends also on multiple physical factors, among which sediment concentration seems to be the most important one conditioning the final deposit (Mulder and Alexander, 2001; Gani, 2004).

For redeposited carbonates in submarine fans and channels the problem can be even more complicated. Carbonate particles have shapes, densities, and provenances different from siliciclastic particles, platform-produced in the case of coarse-grained carbonates versus continent-derived for most siliciclastics. Size, shape, and density first determine the hydrodynamic behaviour (sediment-support mechanism and rheology) of grain components, which can be highly variable amongst different skeletal particle types (Nelson and Hancock, 1984), and second the structure of the resulting deposit. Similar kinds of

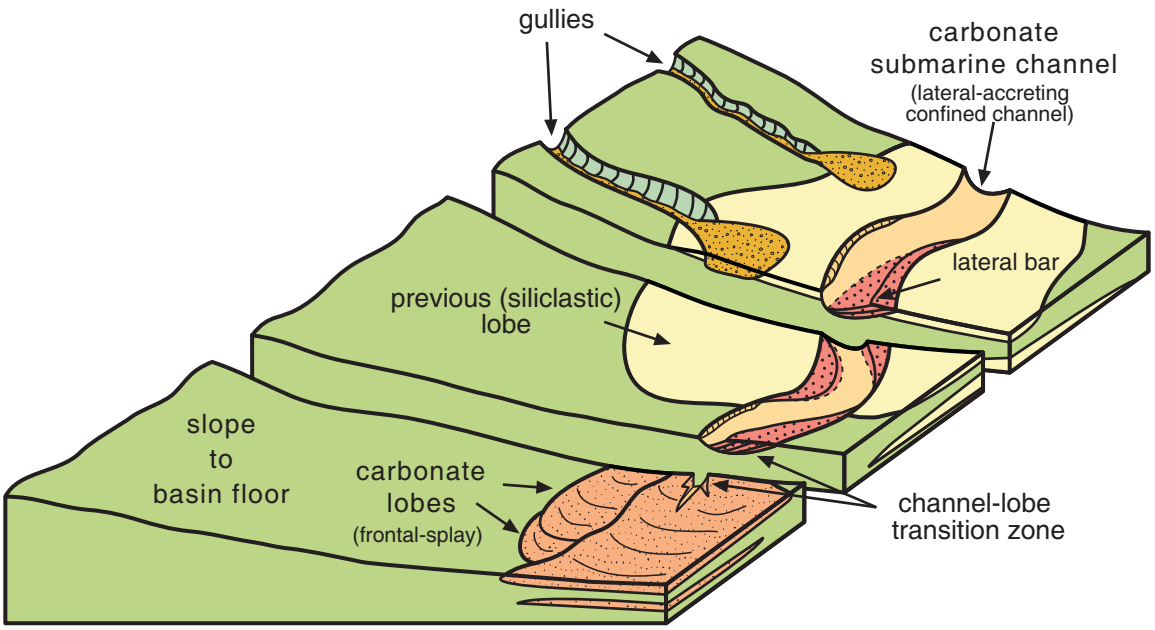

Fig. 78. Integrated depositional model for Middle Miocene redeposited carbonates on eastern Taranaki Basin (not to scale). Mangarara Formation comprises lateral-accreting confined channel (Mohakatino River section), moving downslope into a channel-lobe transition zone and lobes (Ladies Mile and Awakino Heads sections). This carbonate channel-fan system cut across the siliciclastic lobes (frontal-splay complex) of the Moki Formation. Slope gullies funnelled coarse-grained mixed carbonate-siliciclastic sediments into the basin floor that cut across the lobes of the Moki Formation.

hydrodynamic variability may characterise volcaniclastic submarine materials which, like redeposited deep-water carbonates, are usually poorly-sorted and mud-scarce (Gladstone and Sparks, 2002). Carbonates are commonly mixed with siliciclastic material, which further complicates the picture. In the case of carbonates, for example, a massive decimetre-thick bed of poorly-sorted, coarse carbonate sediment (coarse sand to granule) may be deposited by hyperconcentrated and concentrated density flows (*sensu* Mulder and Alexander, 2001), either as a surge-type or steady-type flow (Kneller and McCaffrey, 2003). Although some nexus between sediment concentration and longitudinal flow transformation can be proposed for explaining redeposition of these carbonates, further investigations are needed. Thus, in carbonate submarine channel-fan systems, to avoid misuse of otherwise widely used complex density-flow terminology (e.g. Lowe, 1982; Shanmugan, 1996; Mulder and Alexander, 2001) we recommend following Gani's (2004) simplified terminology. His classification divides gravites, a general term for deposits of any kind of sediment gravity flow, into turbidites (deposit from Newtonian fluid), densites (deposit from partly non-Newtonian fluid and partly Newtonian fluid), or debrites (deposit from non-Newtonian dilatant fluid and Bingham plastic). In this scheme, most of the Mangarara deposits would be densites (channel fill) and debrites (gully fill).

4.3. Benthic foraminiferal-red algal temperate carbonate facies

Temperate or cool-water limestones are widespread in the New Zealand Oligocene (Nelson, 1978). Tectonic upheavals associated with propagation of the Australian-Pacific convergent plate boundary through the New Zealand subcontinent at the start of the Miocene saw these temperate limestones largely replaced in the Early Miocene by siliciclastic, commonly redeposited, sedimentary facies (Kamp, 1986). Accompanying climatic amelioration involved increasingly warm subtropical conditions throughout the Early Miocene in New Zealand, indicated by widespread warm-water molluscs (Beu and Maxwell, 1990), a variety of larger foraminifers (Chaproniere, 1984), and even isolated heads of reef corals in northern New Zealand (Hayward, 1977). The climax of Neogene warmth occurred near the Early-Middle Miocene boundary (Hornibrook, 1992).

The ensuing Middle Miocene, when the Mangarara Formation was being deposited, saw the start of long-term climatic deterioration in New Zealand that was to continue throughout the remainder of the Cenozoic (Nelson and Cooke, 2001). Central western North Island lay at about 45°S latitude in the Middle Miocene, certainly well outside tropical latitudes, and was under the influence of warm

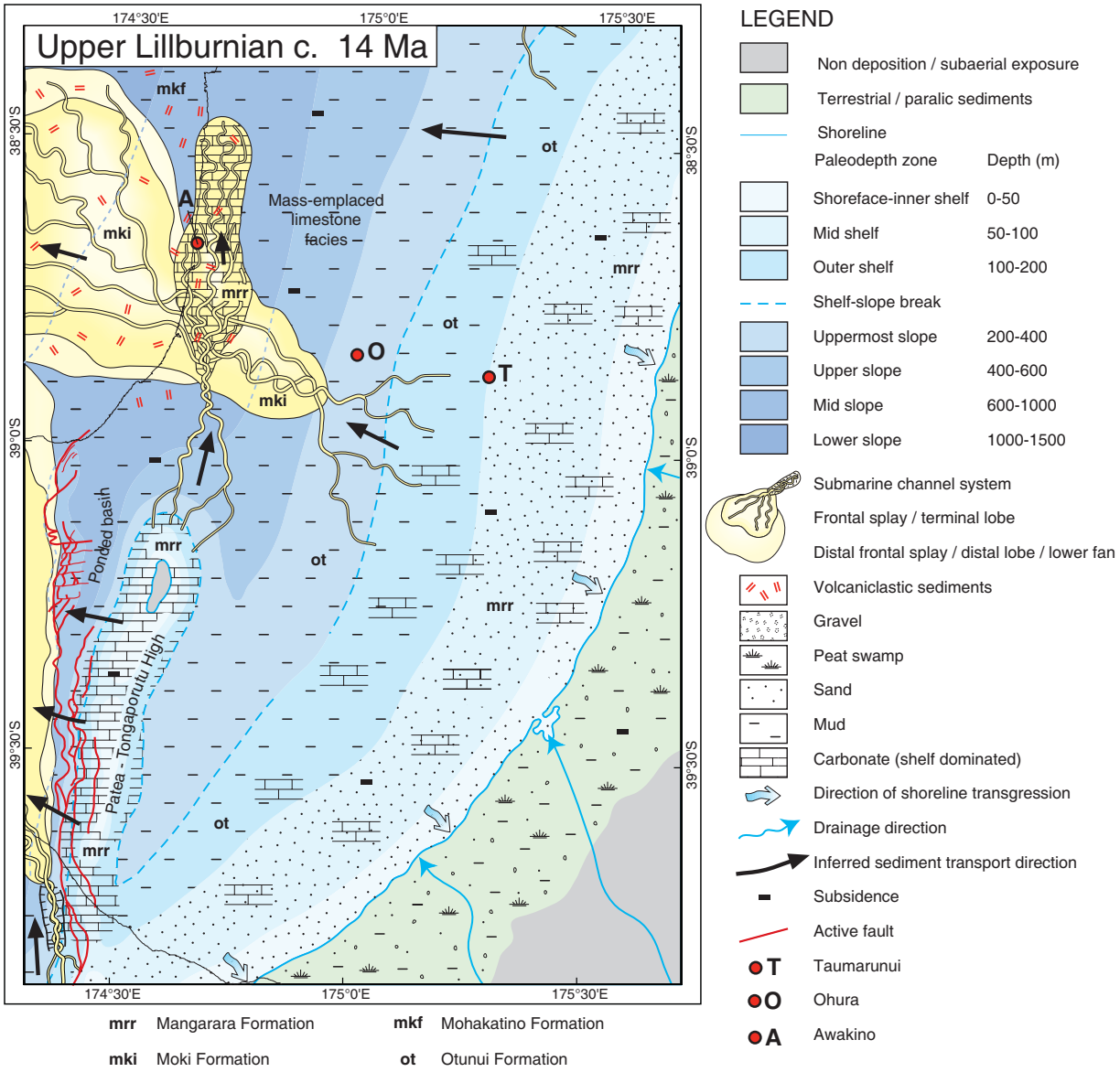

Fig. 79. Palaeogeographic reconstruction of central western North Island in the late Middle Miocene (upper Lillburnian), about 14 Ma. Adapted from Vonk, *in prep*.

temperate oceanic circulation patterns (Nelson and Cooke, 2001). The carbonates in the Mangarara Formation contain an exclusively heterozoan skeletal assemblage comprising the remains of bryozoans, echinoderms, bivalves, benthic foraminifers, and coralline algae (Hayton *et al.*, 1995; James, 1997). However, unlike most other New Zealand temperate limestone occurrences where bryozoans in particular, but also echinoderms, bivalves, and barnacles, are usually the major skeletal contributors (e.g. Nelson, 1978; Hayton *et al.*, 1995; Hood *et al.*, 2003; Nelson *et al.*, 2003), the Mangarara redeposited carbonates are dominated by robust large benthic foraminifers and coralline algae.

The benthic foraminifers include predominantly *Amphistegina* as well as less common larger foraminifers like *Lepidocyclina*, and possibly *Heterostegina* and *Cycloclypeus*. The coralline algae comprise both fragmented material and subspherical rhodoliths from a few up to 10 cm size. The algal genera involved in the rhodoliths include mainly *Lithothamnion* and some *Mesophyllum*. Today, the 20°C mean annual sea surface isotherm roughly corresponds to the southern limit of the distribution of *Amphistegina* in the Pacific (Hornibrook, 1968) which, together with the sporadic larger foraminifers and the coralline red algae, support the contention that the main carbonate factories for the Mangarara Formation were sited in warm, photic, very

shallow marine platform settings. Clearly these settings lay very much toward the warm end of the spectrum of cool-water or temperate shelf carbonate facies, closely analogous to the warm temperate carbonate realm discussed by Betzler *et al.* (1997b) and others (e.g. Halfar and Ingle, 2003). Incidentally, larger foraminifers became extinct in New Zealand by the end of the Middle Miocene, as did *Amphistegina* during the Pliocene (Hornibrook, 1992), despite the existence of appropriate facies for preservation, so that their ultimate disappearance reflects continued long-term cooling of marine temperatures through the late Tertiary (Nelson and Cooke, 2001).

4.4. Palaeogeography and skeletal carbonate sources

The heterozoan skeletal components in the channelized and redeposited carbonate sediments of the Mangarara Formation must have been sourced from nearby warm temperate shallow-marine shelves or platforms. A possible provenance is the coeval mixed carbonate-siliciclastic shelf deposits that accumulated to the east-southeast in the vicinity of Taumarunui and Ohura following transgressive flooding in the lower Middle Miocene (Altonian to Lillburnian) (Kamp *et al.*, 2004) (Fig. 79). At these sites, *near-situ* shelf sediments assigned to the Mangarara Formation occur at the base of the Otunui Formation (Kamp *et al.*, 2004). They consist mainly of bivalve-rich sandstones and mudstones, along with some local limestones (Armstrong, 1987; Gerritsen, 1994; Vonk, 1999). The bivalves are variably fragmented and often accumulated in shell-beds. Small amounts of *Amphistegina* and coralline algae may occur in the matrix sediment. Other bioclasts include solitary corals, gastropods, and echinoderms. Channels filled with conglomerates (cemented and bored mudstone and sandstone clasts) cut across these eastern shelf deposits and are exposed in stratigraphically higher positions of the Otunui Formation.

These sediments are very similar to those that constitute the infilling of the lower channels at Ladies Mile and the channel-fill at Awakino Heads. The conglomerate-filled channels cutting through the shelf seem to be related more to the gullies and their fills described at Mohakatino Valley. This comparison would imply an eastern provenance for the carbonates (Fig. 79), at least at certain times. However, the upper channels at Ladies Mile and Mohakatino Valley are completely dominated by coralline algae and *Amphistegina*, which are otherwise minor components in the eastern shelf sediments. Thus, some other carbonate source must be involved to explain the thick carbonates rich in coralline algae and *Amphistegina* redeposited in submarine channels at the Ladies Mile and Mohakatino Valley sites.

One strong possibility is located to the south, associated with the Patea-Tongaporutu High. Because the basin deepens to the north and west, provenance from a northerly or westerly direction is unlikely. Petroleum exploration wells drilled into this High indicate the presence within Manganui Formation or stratigraphically above basement rock of thick (up to 80 m) carbonate deposits rich in *Amphistegina* and coralline algae (Vonk, *in prep*). As previously emphasized, a close interaction existed between the carbonate submarine system and a siliciclastic submarine system. The main source area for the siliciclastic system (Moki Formation) was located to the east where shoreface sandstone deposits abound in the Mokau Group and Otunui Formation (Fig. 70). It can be inferred that there was a significant input of terrigenous sediment carried by rivers into the sea from the mainland located to the east. The terrigenous influence probably precluded the widespread development of carbonates in that area whereas to the south, upon the Patea-Tongaporutu High, terrigenous input was generally insignificant and an extensive carbonate platform, with prolific coralline algal fields and associated *Amphistegina*, developed (Fig. 79).

5. Conclusions

1) Mixed carbonate and siliciclastic sediments of the Mangarara Formation are interpreted to be mainly mass emplaced and deposited in deep-water settings, forming part of a submarine channel-fan system. The distal parts of lateral-accreting confined-channel complexes, channel-lobe transition zones, and lobes (frontal-splay) are the recognised parts of this system. Lateral-accretion structures interpreted as lateral bars are the best-represented architectural element in the channel-fan system. Phases of active sediment transport and deposition (lateral-accretion stage) and filling (aggradation stage) are recognised within channel infillings.

2) Submarine slope gullies, which are not connected with submarine channels or canyons, are also recognised. Gully fill is mainly composed of coarse-grained mixed carbonate-siliciclastic sediments that were emplaced within siliciclastic lobes of the Moki Formation.

3) Dual fan systems likely co-existed, one dominating and predominantly siliciclastic in nature (Moki Formation), and the other infrequent and involving the temperate calcareous deposits of the Mangarara Formation.

4) Sediment gravity flow deposits of the Mangarara Formation are classified as densites (channel fill) and debrites (gully fill) according to the simplified terminology of Gani (2004).

5) Carbonate components of the deposits consist mainly of coralline algae and large benthic foraminifers (especially *Amphistegina*), bivalves, and bryozoans. The high

abundance of large benthic foraminifers and coralline algae in this shallow-marine skeletal association is indicative of the warmest conditions of the temperate-carbonate realm. This situation was related to the influence of warm temperate currents along the western part of North Island of New Zealand during the Middle Miocene, a period of climatic deterioration in New Zealand.

6) The sediment source was partly from a contemporary eastern shelf, although the bulk of the skeletal carbonate is inferred to have been supplied from shoal carbonate factories atop isolated basement highs (Patea-Tongaporutu High) to the south.

Acknowledgements

Field work was carried out while the first author was on a short-stay leave at the University of Waikato. A. Puga-Bernabéu was funded by a doctoral contract (MECD-UGR) awarded by "Ministerio de Educación y Ciencia" (Spain). Many thanks to the Department of Earth Sciences for logistical support in Hamilton. We want to thank J.M. Martín and J.C. Braga for constructive comments on a previous version of this manuscript.

8

CYCLICITY IN PLEISTOCENE UPPER-SLOPE COOL-WATER CARBONATES: UNRAVELLING SEDIMENTARY DYNAMICS IN DEEP-WATER SEDIMENTS, GREAT AUSTRALIAN BIGHT, ODP LEG 182, SITE 1131A

Ángel Puga-Bernabéu[*1], Christian Betzler [2]

[1] *Departamento de Estratigrafía y Paleontología, Facultad de Ciencias,*

Campus de Fuentenueva s.n., Universidad de Granada,

18002 Granada, Spain

[2] *Geologisch-Paläontologisches Institut, Bundesstrasse 55,*

Universität Hamburg, 20146 Hamburg, Germany

**Corresponding author: Fax: +34 958 248528*

E-mail address: angelpb@ugr.es

Sedimentary Geology
Submitted 19 September 2007; under review 1 October 2007

Abstract

The integrated use of wireline logs, geochemical data, FMS images, and sedimentological analysis was used to test whether a seemingly monotonous upper slope succession of a distally-steepened carbonate ramp bears sea-level driven sedimentary cycles. Ocean Drilling Site 1131, located in the central Great Australian Bight, recovered an expanded series of Pleistocene temperate water carbonates.

Three distinct facies occur. The first facies consists of omission surfaces which form 20-50 cm thick firmground and hardground intervals, characterised by highly resistive FMS images, and elevated values in the other logs. The second facies forms 6–10 m thick intervals, and is typified by laminated FMS images and frequent high-Mg and Fe-stained bioclasts. Abrasion of bioclasts and lamination indicates that this facies formed under the action of bottom currents. The third facies, which occurs in up to 40 m-thick intervals, has a mottled appearance in the FMS log. The corresponding sediment is matrix-rich. It contains bryozoans, sponge spicules, mollusc shells, and foraminifers. It is also characterised by frequent calcareous nannoplankton and well-preserved planktonic foraminifers. The three facies are arranged in repeating

sedimentary cycles. Omission intervals form the base of the cycles and are overlain by the laminated deposits. The upper part of the cycles consists of bioturbated sediments. A correlation of the sedimentary cycles in the Pleistocene succession with MIS 11-19 shows that facies cyclicity parallels glacial–interglacial sea-level changes. Firmground/hardground surfaces formed during latest stages of sea-level falls. Laminated sediments were deposited during later sea-level fall and/or early phases of the sea-level lowstand, and the bioturbated intervals are related to interglacial sea-level highstands.

The study area lies too deep on the upper slope to be affected by a lowering of wave base abrasion during sea-level falls, and thus bottom current activity is interpreted to play an important secondary control on facies and cycle development. During the late stages of sea-level fall, before maximum sea-level lowering occurred, upwelling currents winnowed the slope sediments, leading to hardground formation. During latest sea-level falls and early sea-level lowstands, a relative increase in the ramp sediment supply to the slope leading to the formation of the laminated facies was also a response to the continued action of the near-bottom upwelling currents that reworked previously deposited sediments along the slope. During the early sea-level rises, laminated, upwelling-influenced facies were progressively covered by the bioturbated facies.

Our approach involving the integrated use of wireline logs, geochemical data, FMS images and sedimentological analysis of the lithofacies have allowed us to recognise subtle facies changes in upper-slope settings of a distally-steepened carbonate ramp and their relationship with the sea level as well as to unravel the importance of the oceanic-current regime in the deposition style on the ramp that otherwise would remain unsolved. This integrated method could be applied to study more precisely apparently homogeneous fine-grained calcareous sediment successions of distal-ramp outcrops.

Keywords: cyclicity, cool-water carbonates, upper slope, upwelling, southern Australia

1. Introduction

Carbonate ramps are thought to react to sea-level changes by shifting facies belts down- and up-ramp, without switching entire facies belts on and off during distinct sea-level stands (Burchette and Wright, 1992). Outer carbonate ramp environments and upper slopes of distally-steepened carbonate ramps are commonly too deep to be significantly affected by sea-level controlled hydrodynamic changes. Therefore, in order to delimit sea-level driven sequences and high-frequency sequences in deeper zones of carbonate ramps, subtle changes in the depositional modes during highstand and lowstand conditions have to be identified. Such changes are easily overlooked if, for example, outcrop conditions are not optimal, or no petrophysical data are available.

The integration of point-counting, geochemical, and stable isotope analyses can be a valuable approach to deciphering sea-level signals in apparently rather monotonous successions of outer-ramp carbonates. This was shown by Saxena and Betzler (2003) and Betzler *et al.* (2005) in Pleistocene carbonates of the Great Australian Bight (GAB). This approach, however, is time-consuming and increasingly inaccurate when primary carbonate geochemical signals are blurred by early diagenetic overprint. Moreover, it relies on sediment and rock sample availability that is not always given, for example in borings. Downhole logging data offer relatively poor resolution of carbonate facies and cyclicity (e.g. Rider, 2002). A number of studies, nonetheless, show that borehole images are a valuable tool to delineate facies and cycles in carbonate successions (e.g. Williams and Pirmez, 1999; Williams *et al.*, 2002; Betzler *et al.*, 2005).

In this study we use integrate borehole imaging, gamma ray, density, and sonic velocity data to test whether a rather monotonous Upper Pleistocene temperate water deeper carbonate ramp to upper slope succession deposited under a regime of major 100 ka sea-level cycles can be broken up into high frequency sequences. We show that the combination of distinct downhole logs with borehole imaging allows the differentiation of three distinct facies, and that facies stacking reflects a sea-level-driven cyclicity. In addition to sea-level fluctuations, other palaeoceanographic changes linked to sea level exerted a major effect on cyclicity.

2. Setting

2.1. Geology and geography

The Great Australian Bight (GAB) is a broad embayment with a continental shelf up to 260 km wide (James *et al.*, 2001). This shelf comprises the central and western part of the continental passive margin of southern Australia (Fig. 80A). This continental margin formed in the rifting process that separated the Antarctica and Australia plates which beginning in the late Mesozoic (Veevers *et al.*, 1991). It has remained relatively stable since the late Eocene, although slow seafloor spreading continues to the

present. The inner- to outer-carbonate shelf extends over 190 km with a gradient of less than 0.5º down to a water depth of ~200 m, where the shelf-edge is located. In the uppermost slope, in a water depth of 200–500 m below the sea surface, the gradient is 2º. Therefore, the Eucla Shelf is a distally-steepened ramp according to the shelf profile (*sensu* Burchette and Wright, 1992). This ramp geometry has also been described in the same way in other sectors of the GAB (e.g. Lincoln Shelf; James *et al.*, 1997).

Beginning in the Eocene, an 800 m-thick carbonate succession was deposited in the GAB (Eucla Basin). The basin fill is divided into seven uncomformity-bounded seismic sequences (Feary and James 1998) (Fig. 80B). Ocean Drilling Program (ODP) Leg 182 in the GAB drilled nine sites at different positions on the shelf, from outer-ramp and shelf-edge to lower-slope settings (Feary *et al.*, 2000a). Site 1131 is located on the uppermost slope of the Eucla Shelf at a water depth of 332.4 m and penetrated almost 617 m below the seafloor. Cores mainly recovered seismic sequence 2, which corresponds to Plio-Pleistocene cool-water carbonate prograding clinoforms (Fig. 80B). According to Feary *et al.* (2000b), this sedimentary succession can be divided into three lithostratigraphic units (Fig. 81): Unit I consists of unlithified intensely burrowed, bryozoan-rich carbonates with dominant packstone textures in the upper part, and floatstones to rudstones in the lower part. Silt- to fine sand-grained bioclastic packstones to grainstones and minor intercalated wackestones compose Unit II. These sediments are massive and burrowed throughout. Unit III is separated from Unit II by an unconformity that corresponds to the boundary between seismic sequences 2 and 3. It is made up of interbedded dark chert and lithified bioclastic grainstones. The upper two units are almost enterely Pleistocene in age, with only a late (?)-Pliocene basal part. The age of Unit III is probably early to middle Miocene.

2.2. Oceanography

Overall, he Great Australian Bight is a storm-dominated oceanographic setting where large swell waves (periods >12 s and up to 200 m in wavelength) from the southwest are common (James *et al.*, 1994, 2001). The complex interaction of water masses in the GAB produces seasonality in the current regime, which results in strong coastal downwelling most part of the year with local diffuse upwelling in summer (see James *et al.*, 2001 for further details). The Leeuwin Current and the South Australia Current, which are warm-water currents flowing east and south along the shelf-edge, are responsible for the sustained downwelling. The cold deep-water, westward flowing Flinders Current locally upwells when the warm currents weaken in summer (Kämpf *et al.*, 2004).

3. Methods and data

Site 1131A is located in the uppermost slope of the Plio-Pleistocene progradational outer-shelf to upper-slope sequence (Fig. 80C). This position is a key to understanding offshore transport from the outer-shelf to slope settings. Geophysical properties of the sediment drilled show enough variation to attempt to correlate electrical facies with lithological facies in order to study the presence of sedimentary cycles. The study interval ranges from 100 to 300 metres below the seafloor (mbsf).

Among the geophysical properties measured during the wireline logging, we have selected those properties that can provide information about lithological changes. The selected parameters are commonly measured in hydrocarbon exploration: natural radiation (gamma ray log), sediment resistivity (spherically focused log), calliper (calliper log), sediment density (bulk density), sediment porosity (neutron porosity log), and compressional velocity (sonic log). These data and geochemical data (Fe and Mn contents in the sediment) from Emmanuel *et al.* (2002) were put together in a composite log graphic (hereafter called composite log). FMS (Formation MicroScanner) images were used to study the presence of sedimentary structures, bedding planes and lithological changes. These FMS images were examined every 10 cm in intervals of 20 m. Large-scale bed geometries were studied from the seismic profile of the eastern transect (Fig. 80D).

The lithofacies study relies on 62 thin sections prepared from drilled core samples and analysed with the petrographic microscope. Lithological analysis was also supported with detailed core descriptions made onboard during the cruise (Feary *et al.*, 2000a). Age data (shipboard age model, see Appendix 1) used are the occurrence of *Pseudoemiliania lacunosa* (0.45 Ma) at 136.10 mbsf and the Brunhes/Matuyama boundary (0.78 Ma) at 295.15 mbsf. With the exception of the thin sections, all data used for this study are available online on the Ocean Drilling Programme website (http://www-odp.tamu.edu/; see also references and Appendix 1).

4. Results

4.1. Middle Pleistocene at Site 1131

4.1.1. Geometry

Pleistocene outer-shelf to uppermost-slope sediments show large-scale sigmoidal geometry in seismic sections resulting from the progradation of the shelf margin (Fig. 80D). In detail, this geometry consists of well-defined

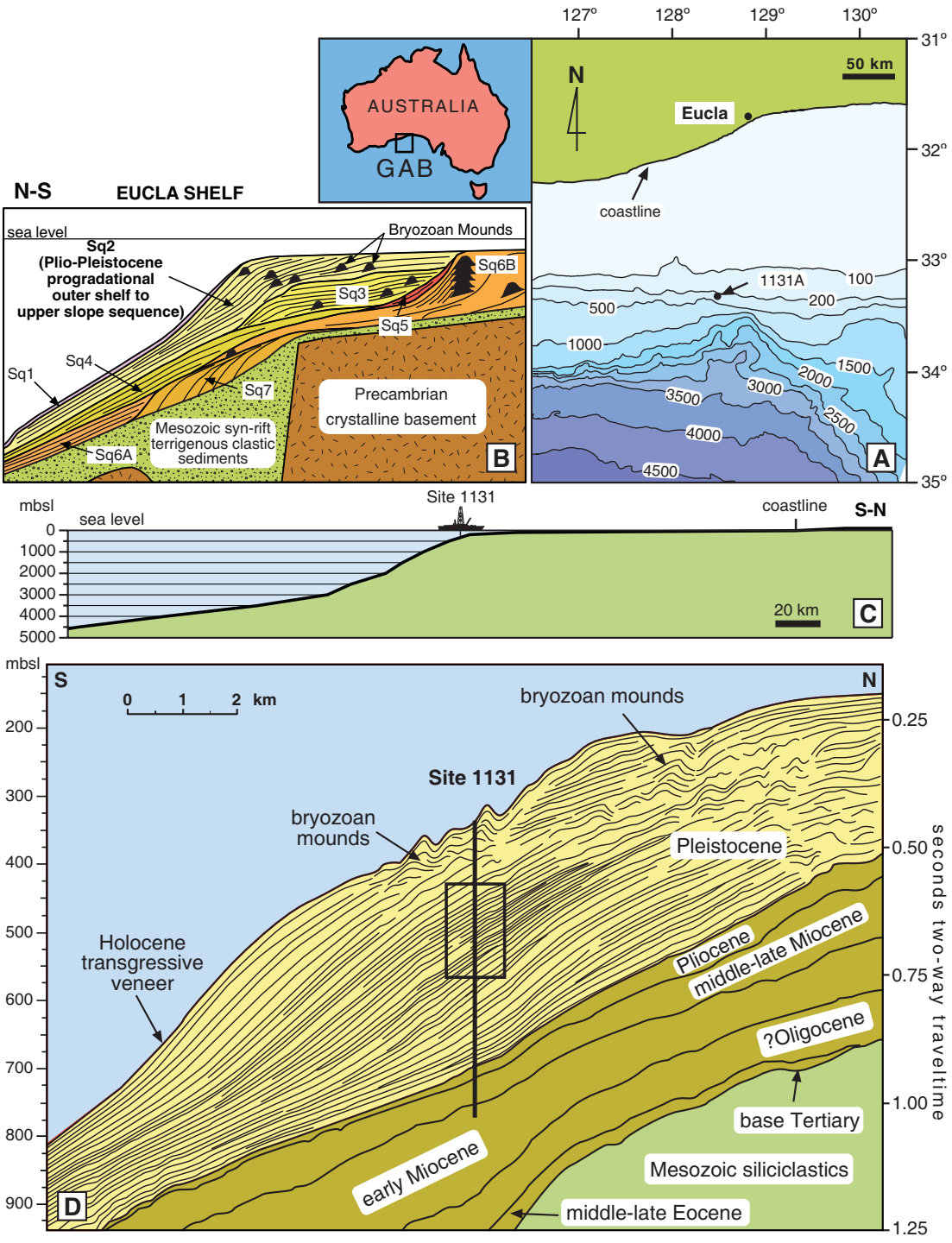

Fig. 80. A) Location of study area (small inset) and bathymetry of the Great Australian Bight (GAB) in the study region (depth contours in metres), and location of Ocean Drilling Program Leg 182 Site 1131A. B) Schematic south-north diagram along longitude 128° illustrating the distribution and relation of the seven seismic sequences interpreted from seismic profiles by Feary and James (1998). Note progradational geometries within seismic sequence 2. C) Bathymetric profile of the shelf and slope at Site 1131 (vertical exaggeration 10:1). D) Interpreted south-north seismic profile (seismic line AGSO-169/05a) through the eastern transect of ODP Leg 182 (Sites 1129, 1131 and 1127), illustrating the position of bryozoan mounds and sigmoidal progradational geometries. Inset indicates position of the study interval. Note presence of wedge-shaped packages pinching-out up- and down-slope, especially in the study interval.

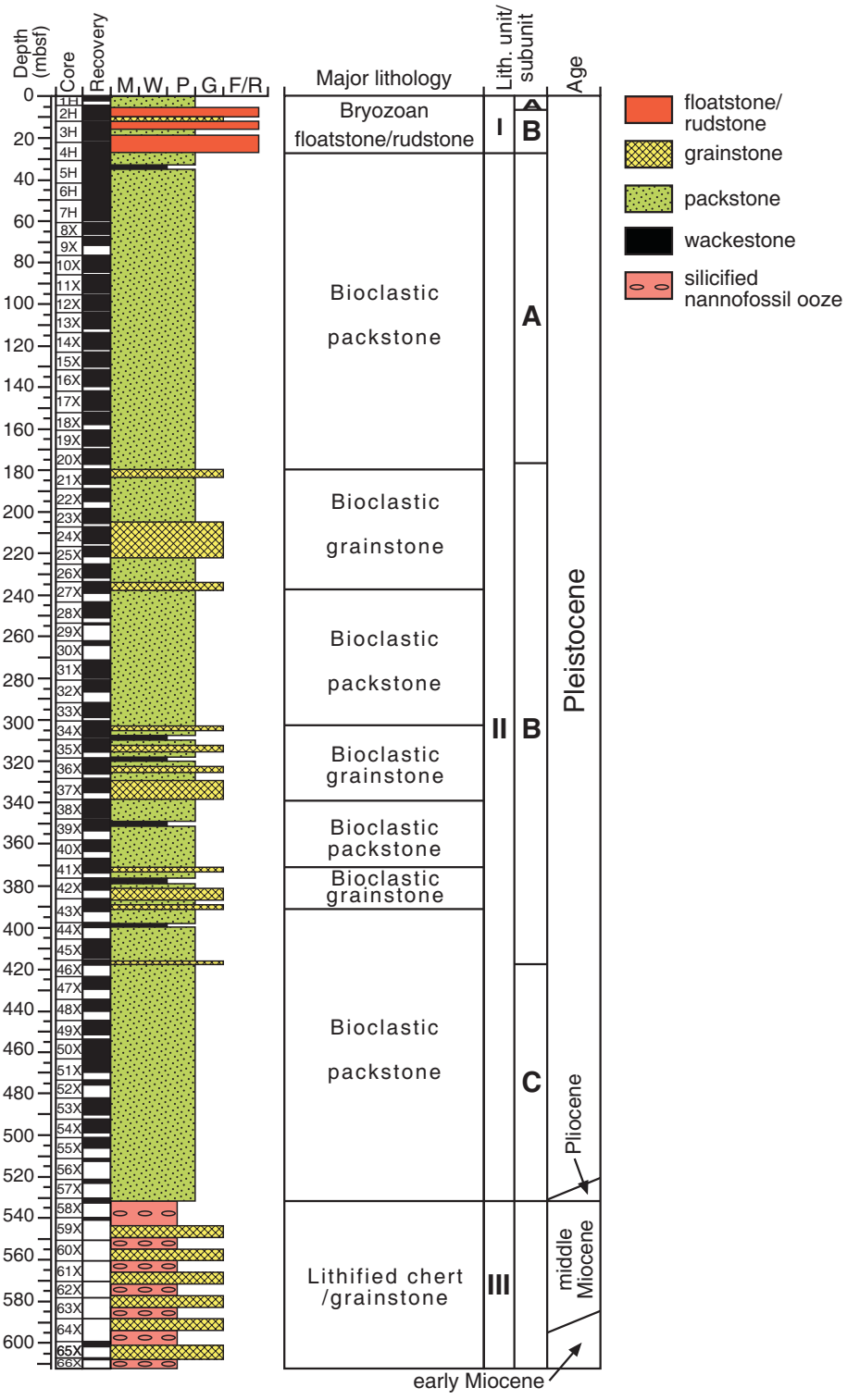

Fig. 81. Simplified lithostratigraphy at Site 1131 showing subdivision into lithostratigraphic units and subunits (after Feary *et al.*, 2000a). M: mudstone; W: wackestone; P: packstone; G: grainstone; F: floatstone; R: rudstone; Litho: lithostratigraphic.

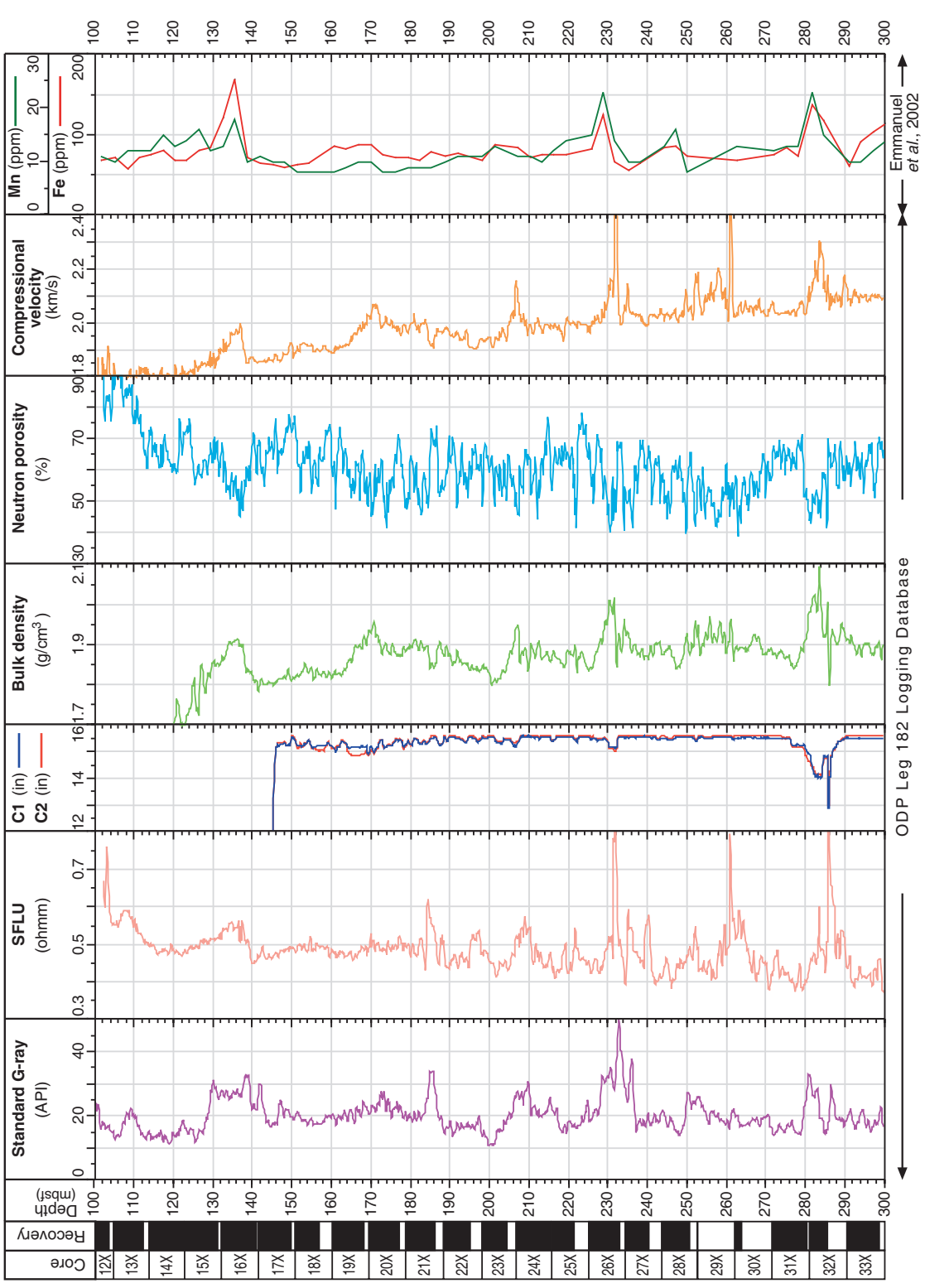

Fig. 82. Composite log of study interval (100–300 mbsf) at Site 1131A. From left to right, columns are core number, core recovery, depth (metres below seafloor), standard gamma ray log (API: American Petroleum Institute), resistivity log (SFLU: spherically focused log), calliper log (C1 and C2 are measurements in inches (in)), density log (bulk density in g/cm3), porosity log (neutron porosity in %), sonic log (compressional velocity in km/s), and downcore variation in Fe and Mn concentrations (ppm) from Emmanuel *et al.* (2002). See text for description of the log trends and variations in Fe-Mn contents.

sigmoidal sediment packages and wedge-shaped packages that pinch out up- and downslope (Fig. 80D). The interval studied (100–300 mbsf) contains at least 6 of these wedge bodies and part of the sediment is laterally equivalent (upslope) to the bryozoan mounds located at the shelf-break (James *et al.*, 2000, 2004).

4.1.2. Wireline geophysical well logs and geochemical (Fe-Mn) data

The composite log obtained from the downhole measurements of different physical properties and the geochemical data (Fe and Mn) of the sediments drilled in at Site 1131A are shown in Figure 82. The standard gamma ray log is characterised by the alternation of intervals with low-amplitude variation of the gamma-ray values, commonly 10–20 API (American Petroleum Institute) units, and peaks with values greater than 30 API units (Fig. 82). Slightly increasing upward trends, terminating in high gamma-ray values, commonly occur. Gamma radiation peaks are mostly due to high uranium concentration in the sediment (see link gamma ray in Appendix 1). Values of sediment resistivity in the spherically focused log show a low variation resistivity in the upper part (100–186 mbsf), and variable resistivity in the lower part (186–300 mbsf). Both intervals contain prominent resistivity peaks (Fig. 82). In the calliper log, the four-arm calliper shows similar and parallel values, with low variation in the borehole diameter. The normal trend is uniform and parallel between the measurements of the four arms, with values of 15–16 inches. A noteworthy break in calliper value (less than 13 inches) occurs at ~286 mbsf.

The bulk density of the sediments ranges from ~1.7 g/cm^3 to ~2.1 g/cm^3. Several decreasing-upward density trends occur at different depths (Fig. 82). Porosity values are highly variable throughout the study section. Increasing- and decreasing-upward trends in the porosity values are observed, with values commonly ranging from 30 to 75%. The sonic log (compressional velocity) shows a rise in compressional velocity with depth. Normal values range from ~1.8 km/s at ~100 mbsf to ~2.1 km/s at ~300 mbsf. This otherwise normal trend due to sediment compaction is interrupted by high velocity peaks at different depths. Geochemical data (Emmanuel *et al.*, 2002) indicate generally normal contents of Fe (60–90 ppm) and Mn (8–15 ppm) in the sediment, but with higher contents of both elements in several intervals Fe (>100 ppm) and Mn (>15ppm) (Fig. 82).

All the physical properties measured show anomalies (low and high values) that in most cases match anomalies in other parameters (Fig. 82). The Fe and Mn peaks in the sediment also coincide with these anomalous intervals, although usually sligthly upsection of them. Three intervals with an outstanding association of anomalies can be recognised in the study section at ~277–286 mbsf, ~224–234 mbsf, and ~128–138 mbsf (Fig. 82). Sediment in the interval ~178–186 mbsf shows peaks in gamma radiation, resistivity, and porosity, but lacks the decreasing-upward values in bulk density and compressional velocity, and the high values in the Fe and Mn concentrations that characterise the other anomalous intervals.

4.1.3. Lithology

According to Feary *et al.* (2000b), the study interval belongs to lithostratigraphic units IIA and IIB (Fig. 81). Silt- to fine-grained bioclastic packstones dominate this part of the section, with some intercalated grainstone intervals. Sediment is light olive grey to light grey, unlithified to partially lithified, and mostly burrowed throughout. Few sedimentary structures are recognised in the core samples due to intense bioturbation. Bioclastic components include planktonic and benthic foraminifers, sponge spicules, tunicate spicules, bivalves, bryozoans, gastropods, coralline algae, serpulids, ostracods, echinoderms, and coccoliths. Brown-stained bioclasts, organic filaments, blackened grains, and glauconite grains are abundant in some intervals, although these components are also scattered throughout the section.

Despite the overall uniformity and fine-grained texture of the sediment, the lack of sediment recovery in some cores, and the homogeneity of the biogenic components, two main lithofacies types can be distinguished based on bioclast preservation and the relative abundance of some components.

Facies A. This facies is the most common in the study interval. It consists of very fine- to fine-grained packstone/grainstone and minor wackestone. Bryozoans, sponge spicules, molluscs, and planktonic foraminifers are the most common bioclasts in this facies. Other bioclastic remains are minor benthic foraminifers, echinoids, rare tunicates, and radiolarians. Brown bioclasts are scattered throughout this facies. Matrix content ranges from 30–40% and mainly comprises micrite formed of calcareous nannoplankton and unidentified macerated bioclasts. Bioclasts are commonly but moderately fragmented (Fig. 83). Whole skeletons are less common and they comprise primarily planktonic and benthic foraminifers (Fig. 83), as well as bryozoan remains. This facies is intensely burrowed throughout.

Facies B. This silt- to very fine-grained packstone contains bioclastic particles similar to those in Facies A, with different relative abundances of bioclasts. Brownish bioclasts are common in the sediment (up to 20%).

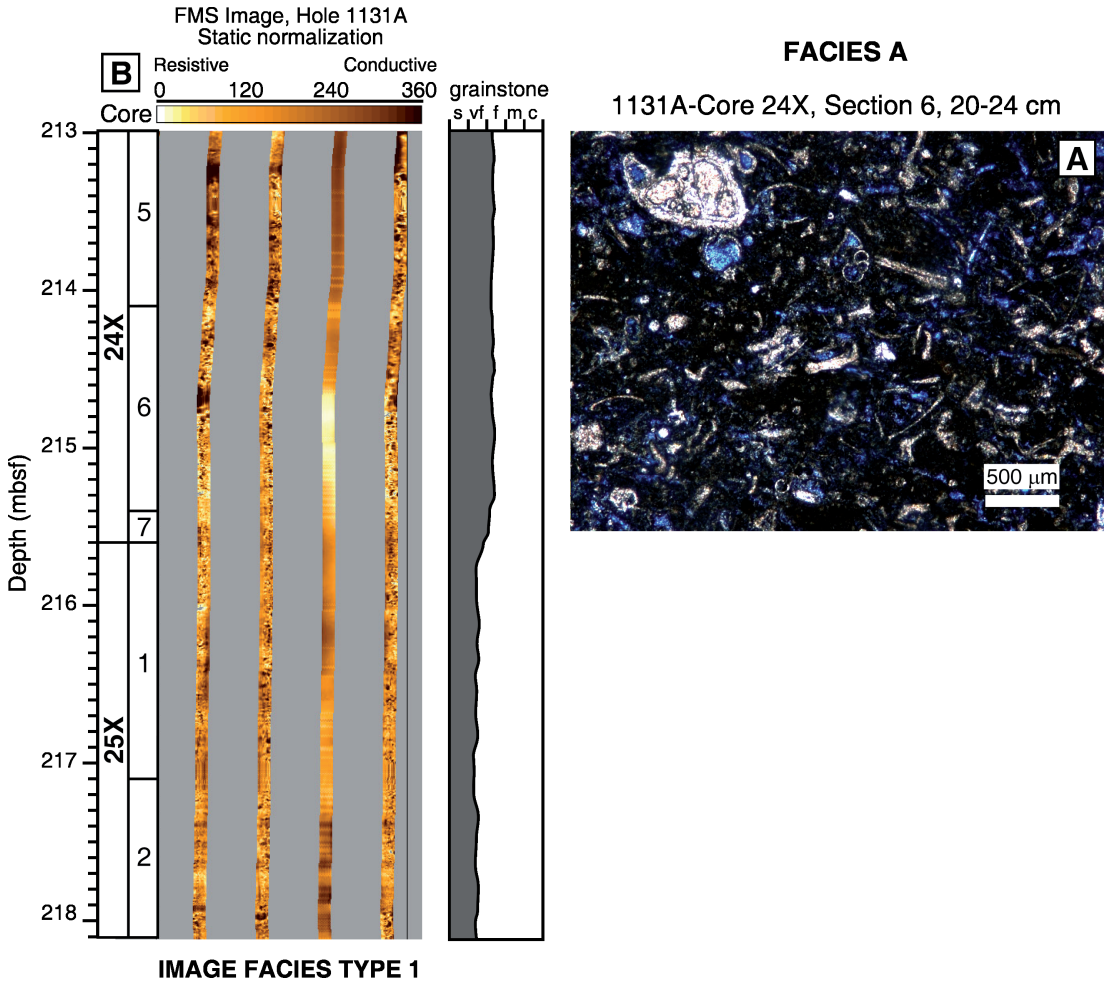

Fig. 83. A) Microfacies photograph of Facies A. This facies is matrix-rich, with relatively coarse-grained and moderately fragmented bioclastic remains, mainly benthic and planktic foraminifers, sponge spicules, and other unidentified bioclasts. Core 24X comprises a light grey, fine-grained partially lithified bioclastic grainstone. It is strongly bioturbated and some burrows are filled with pale green packstone to grainstone. Coarse fraction is dominated by bioclasts with sponge spicules, benthic foraminifers, echinoid spines, and ostracodes. Scattered blackened grains occur in section 6. Core 25 consists of a light olive grey to grey, fine-grained partially lithified bioclastic grainstone, homogeneous throghout. B) Formation MicroScanner (FMS) image of FMS-facies Type 1. Observe subtle mottling consisting of conductive and resistive speckles in tracks 1, 2, and 4. The track of the third pad has a poor data quality that leads to blurring of the resistivity image. Cores and core sections (left), and a grain-size column based on core description (right) are also illustrated. s: silt; vf: very fine; f: fine; m: medium; c: coarse.

Fe-rich blackened grains, conspicuous in core samples, are present in this facies, as well as reddish organic filaments. This facies is grainier than Facies A, although the matrix composition is similar. Bioclasts are fine-grained and are intensely fragmented and abraded, with only minor well-preserved skeletons (Fig. 84). Burrowing is less common in this facies. Fining-upward sequences and cross lamination are also recorded (e.g. 186 mbsf, 233 mbsf).

4.1.4. Formation MicroScanner (FMS) images

FMS images from Site 1131 can be classified into three image facies types. Overall quality of the FMS logs is good, although occasional image failures (no clear image) occur locally in some of the FMS tool pads, but do not influence the general characteristics of the FMS images.

Type 1. This image facies type is heterogeneous overall, displaying mottling that consists of resistive (orange to light yellow on the FMS images) and conductive (dark colours on the FMS images) speckles (Fig. 83). Subtle bedding comprising changes in sediment resistivity and a few laminated intervals are observed.

Type 2. The Type 2 image facies is generally more conductive (brown to dark orange colours on the FMS images) than Type 1. The main characteristic of this facies is the presence

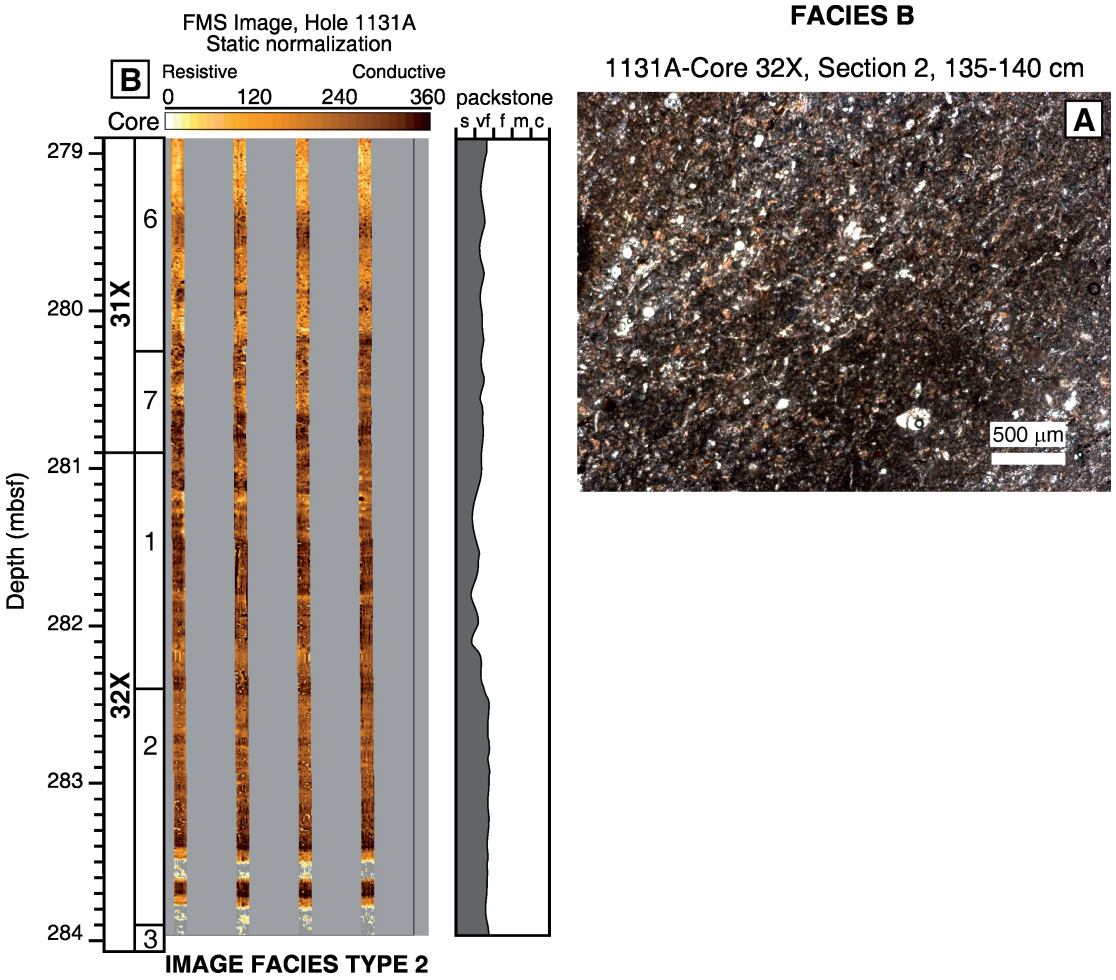

Fig. 84. A) Microfacies photograph of Facies B. This facies is very fine-grained, with highly fragmented and abraded bioclasts. Brown bioclasts are abundant in this facies. Core 31X is a lithified bioclastic packstone. Sediment is very fine-grained. Components consist mainly of lithoclasts, some sponge spicules, blackened grains, and brownish organic filaments. Core 32X consists of a light olive grey to light grey, very fine- to fine-grained partially lithified bioclastic packstone. Benthic foraminifers are scattered throughout the core. Section 1 is dominated by silty grains. The lowermost part of section 2 to the uppermost part of section 3 consists of a pale olive to reddish grey, very fine-grained bioclastic packstone, containing brown organic filaments. B) FMS image of Type 2. This image facies is characterised by well-defined lamination consisting of layers of different sediment resistivity, but overall conductive (dark colours in image). Cores and core sections (left) and a grain-size column based on core description (right) are also given.

of well-defined lamination of different sediment resistivity (Fig. 84). This lamination is usually horizontal, although cross-lamination is also observed. This facies is mottled (but laminated) at the transition to Type 1.

Type 3. This facies appears as striking highly resistive intervals (white to transparent on the FMS images). The base of these intervals is irregular and the top is flat to irregular (Fig. 85). The thickness of this facies ranges from 20–50 cm. In most cases, this image facies type is interbedded between Type 1 (below) and Type 2 image facies (above).

4.2. Facies interpretation

Donwhole measurements at Site 1131 have shown variability in physical properties of the drilled sediments such as natural gamma-ray radiation, resistivity, bulk density, porosity, compressional velocity, and also in geochemical values (Fe, Mn) (Fig. 82). Carbonate content of the sediments in the studied interval ranges between 85 and 96 % (Feary *et al.*, 2000a), producing an overall homogeneous signal in the physical data, only disturbed by a few peaks. Therefore, the attempt at correlating in full detail the physical signal of the sediment with lithological

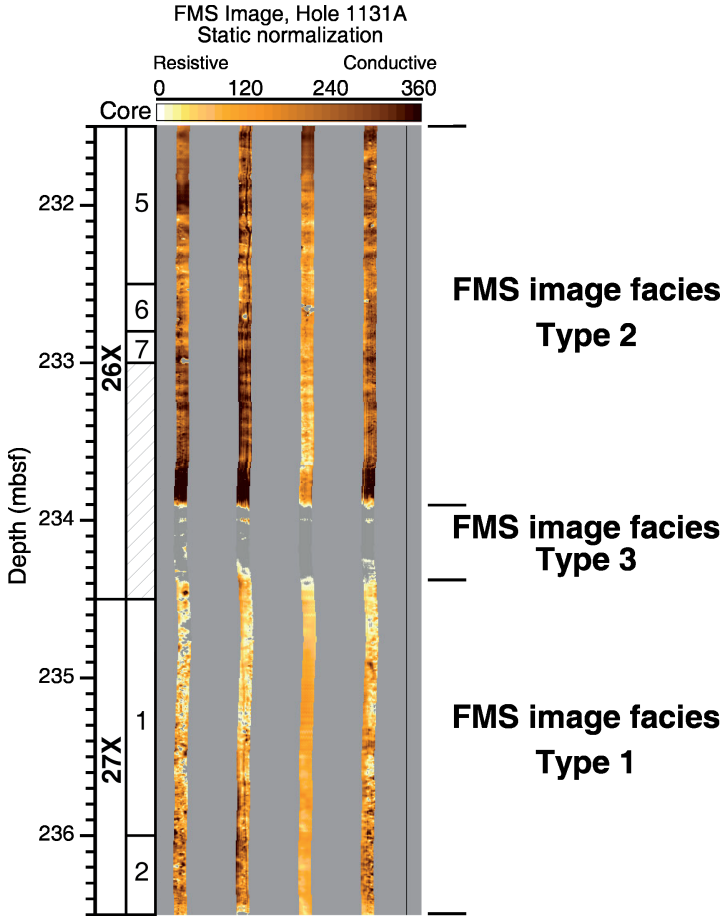

Fig. 85. FMS image facies relation among Type 1, Type 2 and Type 3 facies. Observe that Type 3 occurs as an approximately 30 cm-thick outstandingly high-resistivity level with irregular bottom and top. Cores and corresponding sections are also shown to the left. Note that 150 cm of Core 26X were not recovered.

facies data based on the core description and the study of thin sections did not produce unequivocal results. Changes in the wireline logs, however, can be used to recognise diagenetic changes, preservation differences, or subtle facies changes that otherwise remained macroscopically undetected.

The intervals with elevated log values at ~277–286 mbsf, ~224–234 mbsf, ~128–138 mbsf, and, to a lesser extent at ~178–186 mbsf) systematically indicate that the base of the corresponding sedimentary intervals are more lithified than over- and underlying deposits. In carbonate systems, peaks in gamma-ray logs are usually due to high uranium contents related to organic matter concentration, as it may occur in a firmground/hardground (Hassan, 1973; Rider, 2002). Peaks in the sonic log indicate the occurrence of well-cemented beds, which also produce associated high sediment resistivity. Further indicators of hardened or lithified intervals in the study interval are increases in bulk-density values and the related decrease in porosity (Fig. 82). Peaks of low-density values that coincide with gamma ray peaks indicate levels rich in organic matter.

These sediment properties contrast with the attributes of the most commonly unlithified to partially lithified sediments that have high water-saturation and high concentrations of H_2S and methane (Feary *et al.*, 2000a). This explains the overall high porosity and low density of the carbonate sediment compared with the opposite log values in the harder intervals. Elevated Fe and Mn concentrations are a further indicator for the presence of hardgrounds in the succession, because Fe/Mn stains are common characteristics of hardground surfaces in cool-water settings (Nelson and James, 2000; Noé *et al.*, 2006). "Tight spots" in the calliper log at the base of the intervals with elevated log values and generally no core recovery in the interpreted firmground/hardground intervals because hard sediments were just ground away also favour this interpretation (Fig. 82).

Lithological Facies A and B are similar in bioclast composition, but they differ in taphonomic properties of the skeletons, burrowing, and in presence of brown and black grains. Sedimentological differences are paralleled by variations in the FMS facies images. Uniformly bioturbated Type 1 image facies correspond to the intensely burrowed, matrix-rich Facies A (Fig. 83), whereas Type 2 shows images of laminated sediments that are compatible with the abraded grain-rich sediments of Facies B (Fig. 84). The transition from Facies A-Type 1 into Facies B-Type 2 is gradual. Type 3 image facies from FMS logs are interpreted as highly resistive beds (Fig. 85) that coincide with the omission surfaces interpreted from the wireline logs. Highly resistive beds (FMS Type 3 facies) that correspond to hardground surfaces separate Facies A/ Type 1 and Facies B/Type 2.

Based on the above-described wireline logs and geochemical data, on the lithofacies, and on FMS image facies, the facies are grouped into three facies associations.

(1) Firmground / hardground levels, characterised by highly resistive FMS images and prominent breaks in physical properties in the wireline logs. The intervals of these facies associations are 20–50 cm thick. It is proposed these omission surfaces developed during periods of low sedimentation rates, and sediment starvation on the upper slope.

(2) Laminated intervals 6–10 m thick with generally conductive and laminated FMS images. Wireline log response shows trends of increasing and decreasing values in the geophysical sediment properties. The grainier sediment of this facies association is fine-grained, with fragmented and abraded bioclasts, and high contents in brown and black grains, as well as organic filaments. High values in iron and manganese are common in the lower parts of these intervals. The presence of abraded bioclasts is interpreted as reflecting reworking of the components and lamination indicates the action of bottom currents. The most probable source of the bioclasts lies in shallower areas of the carbonate ramp profile. Brown grains are high-Mg bioclasts (Saxena and Betzler, 2003) altered during residence on the sea-floor before reworking. Black Fe-rich grains are associated to the underlying hardground surfaces that were also remobilized.

(3) Bioturbated intervals which are characterised by a mottling in the FMS images that correspond to the intense burrowing observed in core samples. The wireline log signal is variable, although the values of different geophysical properties commonly vary little. The sediment is matrix-rich, with bryozoan skeletons, sponge spicules, mollusc shells, and foraminifer tests as the main bioclastic remains. Although partially fragmented, the preservation grade of the bioclasts is different (generally large, better preserved and with subangular edges) from that in facies association 2, pointing to a fragmentation due to biogenic reworking (i.e. burrowing) rather than physical reworking. The presence of well-preserved planktonic foraminifers and nannofossils indicates an important contribution of pelagic rain. Overall, this facies is interpreted as periplatform ooze, although some remobilized layers can also occur within this association.

All these facies associations, although similar in composition and deposited in the same depositional environment (upper slope), show recognizable variations that correspond to subtle changes in sedimentation conditions.

5. Discussion

5.1. Sequence stratigraphy

Three facies associations have been identified based on the detailed analysis of the the wireline log, lithofacies, and FMS images from the study interval at Site 1131A (100–300 mbsf) taking into account the iron and manganese data from Emmanuel *et al.* (2002): firmground/hardground level, laminated facies interval, and bioturbated facies interval. These facies associations comprise a sedimentary sequence (Sq) (Fig. 86) that is repeated at least four times (sequences 1–4 from bottom to top) in the study interval. The lower 20–50 cm of the sequence comprises a hardground facies, which is overlain by the laminated facies interval. Up-sequence there follows a 38–42 m thick bioturbated interval that composes most of the sedimentary sequence. On top of this burrowed facies, the next hardground surface developed.

5.2. Changes in sea level and palaeoceanography

Sea-level changes and related changes in oceanic circulation are interpreted to be the major factors controlling sequence formation. Two available age data at 295.15 mbsf (780 ky) and at 136.10 mbsf (450 ky) respectively (age model for Site 1131A, see Appendix 1) were used to correlate the study interval with the oxygen isotope curve of Lisiecki and Raimo (2005) (Fig. 87). Firmground/hardground levels and laminated facies associated to anomalous values in the composite wireline log at ~277–286 mbsf (Sq-1), ~224–234 mbsf (Sq-2), ~178–186 mbsf (Sq-3) and ~128–138 mbsf (Sq-4) closely match with excursions of the oxygen isotope values corresponding to marine isotopic stages (MIS) 18 (Sq-1), 16 (Sq-2), 14 (Sq-3) and 12 (Sq-4) (Fig. 87). More precisely, hardgrounds/firmgrounds developed in late stages of falling sea-level, and deposition

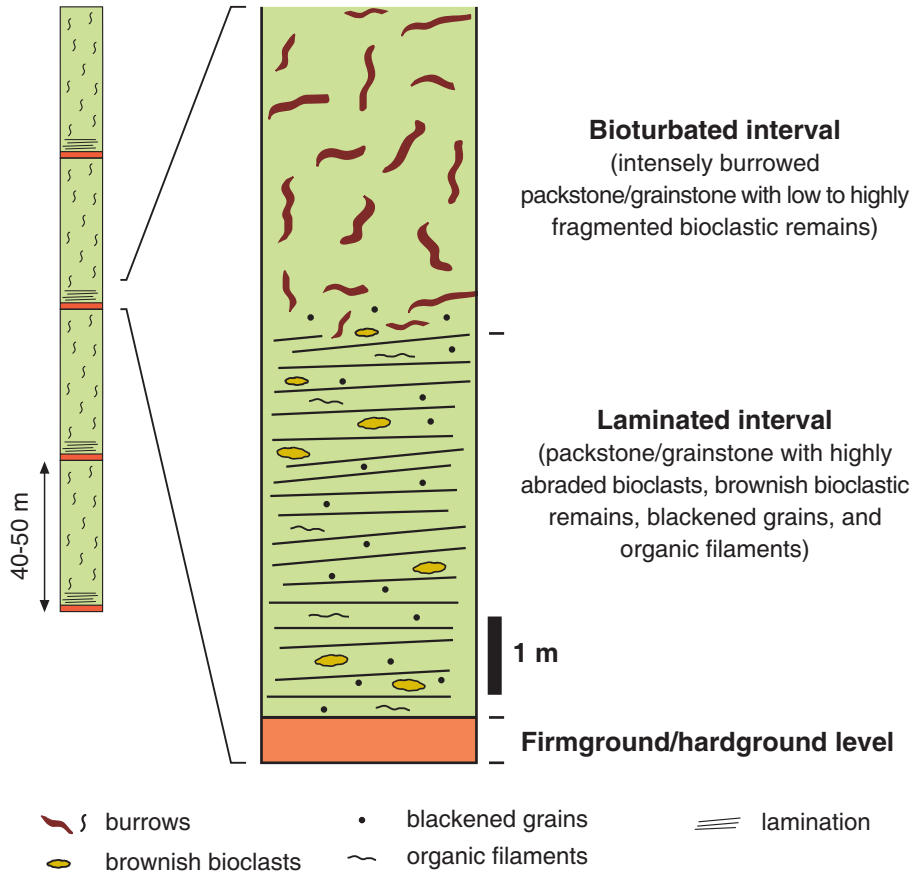

Fig. 86. Conceptual model of sedimentary cyclicity in study interval. Individual cycles are 40–50 cm thick and dominated by bioturbated sediments. Each cycle is delimited by a firmground/hardground level, which is overlain by a laminated interval rich in brown high-Mg calcite and Fe-stained bioclasts. The remaining cycles consist of rather monotonous intensely bioturbated packstone.

of the laminated facies extended until times of the lowest sea level or until the early sea-level lowstand stage. The rest of the sequence (bioturbated interval) is related to the interglacial sea-level highstands of MIS 17, 15, 13 and 11. Therefore, it is proposed that sedimentary sequences in the upper slope sediments are related to eccentricity-driven sea-level cycles (~100 ky).

The lower part of sequence 3 has no significant breaks in the wireline log signal as it occurs in the rest of the sequences. However, the presence of a fining-upward interval observable in core samples, the presence of blackened grains in the sediment, and peaks in the gamma-ray and resistivity curve can be interpreted in a similar way as for sedimentary sequences 1, 2 and 4. Correlation with the isotopic curve also shows that sedimentary sequence 3 was deposited during the same relative position in the isotopic curve as sedimentary sequences 1, 2 and 4 (late falling sea level to early lowstand sea level).

We are aware that the accumulation rate is not constant during the deposition of sedimentary sequences, as omission surfaces occur and the sedimentary dynamics of the laminated and bioturbated intervals seem to be different. Correlation of the sedimentary sequence with the stable isotope curve has been done, considering a constant accumulation rate just for graph purposes, to avoid isotopic and wireline log curve distortion, which would have to remain arbitrary with the available data. If an external controlling factor, however, is accepted, individual sedimentary cycles would have formed during equal time intervals.

Several researchers have postulated that increased production in the Antarctic Bottom Water and associated increased wind force, together with northward movement of the Subtropical Convergence Zone, took place during Pleistocene glacial times (Nelson *et al.*, 1993; Nees, 1997; Hall *et al.*, 2001; Nürnberg and Groeneveld, 2006). Along the carbonate ramp of the Great Australian Bight, this

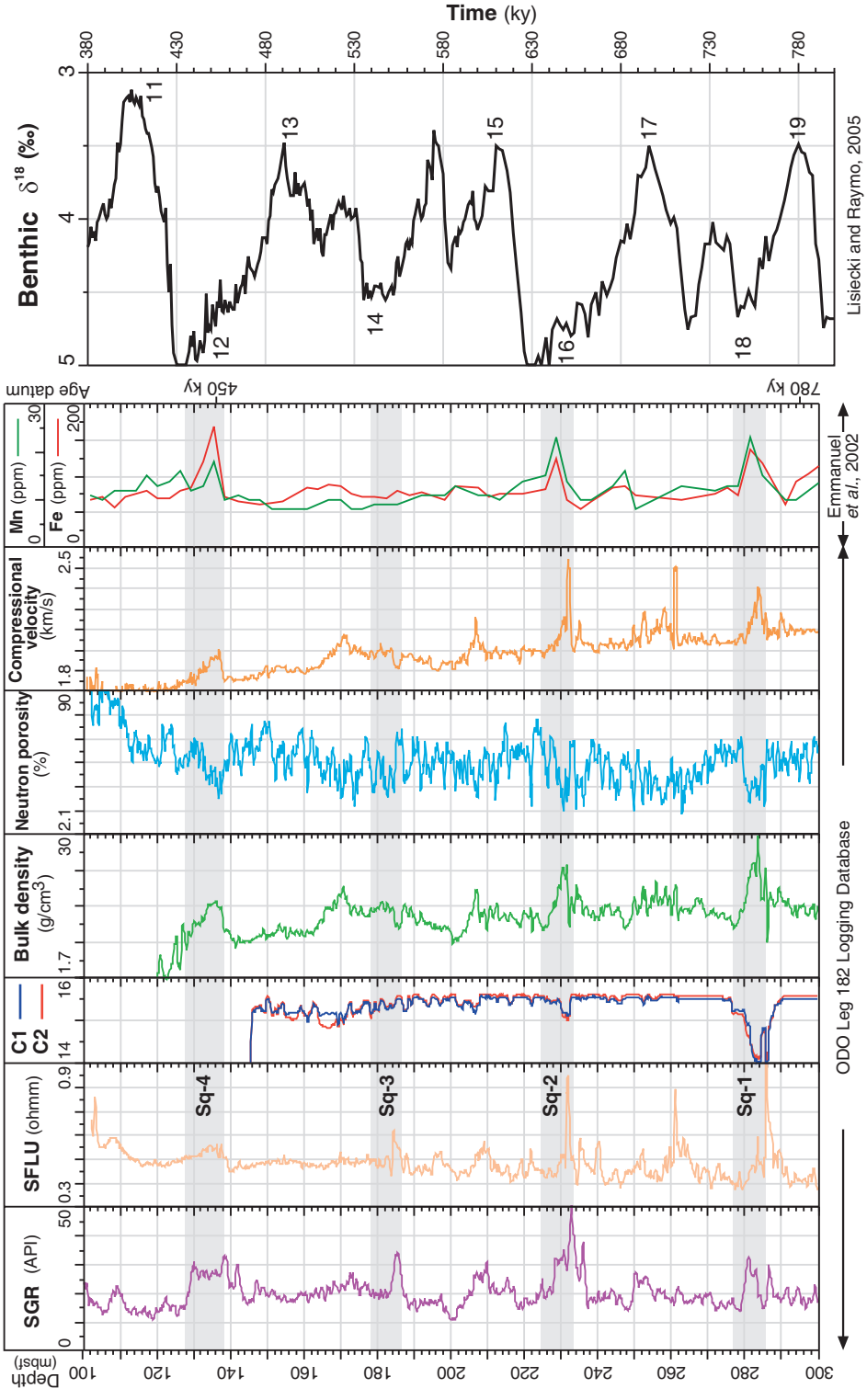

Fig. 87. Interpretation of the composite log of the study interval (100–300 mbsf) at Site 1131A. From left to right, columns are the same to those shown in Figure 3. Basal position of the sedimentary sequences (Sq-) is indicated. Shadowed zones mark intervals with anomalous values in the composite log associated to the firmground/hardground levels and laminated facies (see text). White zones are bioturbated intervals. on the right side of the composite log, age data are indicated. Benthic oxygen isotope global curve after Lisiecki and Raimo (2005) is illustrated on the left. Numbers indicate marine isotopic stages (MIS). Observe the close match of the position of anomalous intervals with late stages of sea-level falls and sea-level lowstand stages (see text for further explanation). Areas sandwiched between shadowed intervals correspond to the bioturbated facies deposited during phases of rising and high sea-level.

event caused an increase in nutrient supply on a regional scale and local upwelling during Pleistocene glacial periods, triggering the growth of bryozoan mounds (James *et al.*, 2000, 2004). Some of these biogenic mounds are laterally coeval to the sediment interval studied here (Fig. 80D). We consider that cyclicity observed in the upper-slope sediments at Site 1131A was also the result of hydrodynamic readjustments in the oceanic conditions affecting the continental margin during glacial and interglacial periods.

5.3. Integrated cyclostratigraphic model

The Pleistocene and Holocene south Australian carbonate shelf is a distally steepened ramp (sensu Burchette and Wright, 1992) and is the type location for the shaved-shelf depositional model of James *et al.* (1994) (Fig. 88). The wave- and swell-dominated hydrodynamic regime of this ramp determines that there is no significant deposition above the deep-lying fair-weather wave base (~70 mbsl; James *et al.*, 1994). Sediment accumulates on the outer ramp and upper slope as prograding wedges and in bryozoan mounds (James *et al.*, 1994, 2000, 2004).

During sea level highstands (Fig. 88), the GAB is affected by an oceanic current regime characterised by year-round strong downwelling linked to the eastward flow of the warm, shallow-water (<200 m) Leeuwin Current (James *et al.*, 2001, 2004). The Recent deep ocean circulation involves the Flinders Current which flows anticlockwise, and the Intermediate Antarctic Water mass. During interglacials, sedimentation on the upper slope is dominated by pelagic rain and *in situ* carbonate production, mainly by bryozoans (James *et al.*, 2001). The highstand sediment is fine grained and matrix rich. Calm conditions on the seafloor allowed pervasive bioturbation, deposition of glauconite grains, and iron staining of bioclasts. We propose that part of this fine-grained sediment was transported downslope from shallower zones of the ramp as a result of the downwelling conditions.

Early stages of the sea-level falls seem not to have affected the sedimentation mode at the slope. Facies changes apparently occurred during the latest stages of sea-level fall with the development of firmground/hardground surfaces (Figs. 87 and 88), followed by laminated sediments deposited during later sea-level fall and/or the early phases of sea-level lowstand. Contemporaneously to sea-level fall, the disappearance of the Leeuwin Current and readjustment of oceanic circulation due to the northward movement of the Subtropical Convergence Zone (Nelson *et al.*, 1993; Nees, 1997; James *et al.*, 2004) enhanced primary productivity near the shelf-edge, enhancing mound growth (James *et al.* 2004), and producing local upwelling currents, probably related to the palaeo-Flinders Current. This redistribution of the oceanic currents most likely did not occur suddenly, but rather evolved progressively during the sea-level fall. The upwelling current systems had a significant influence on the seafloor sediments only during the late stages of sea-level fall, before the maximum sea-level lowstand occurred. In this stage, upwelling currents were strong enough to sweep the slope sediments, thus preventing significant sediment deposition and leading to hardground formation (Fig. 88).

Although the influence of upwelling currents on slope and shelf sediments are commonly considered with regard to nutrient flux, their hydrodynamic impact as bottom currents able to mobilize sediment cannot be dismissed. Bottom currents or bottom nepheloid layers associated to upwelling currents are observed to actively mobilize particles at the upper continental slope off Namibia (Inthorn *et al.*, 2006), and can also produce seafloor erosion and sedimentary structures (e.g. Séranne and Nzé Abeigne, 1999). According to Nelson and James (2000), cemented horizons in cool-water carbonates may develop where sedimentation is arrested due to current-driven turbulence.

During late sea-level fall and early sea-level lowstand, a relative increase in the ramp sediment supply to the slope as a response to the basinward shift of the shoreline and to the continued action of the near-bottom upwelling currents which reworked previously deposited sediments along the slope occurred. These reworked material forms the laminated facies. Erosion possibly also affected to part of the hardground levels), and of the outer ramp sediments. Inthorn *et al.* (2006) describe the Benguela upwelling separated in two cells, the main upwelling close to the coast and another component below the shelf-edge where an offshore-directed flow occurs as a bottom layer. The abraded nature of the bioclasts in the laminated facies is interpreted as the result of the sediment reworking under the action of bottom currents, and favoured by the fragmented state of the bioclastic remains in the burrowed facies. Brown grains in the Pleistocene cool-water carbonates consist of high-Mg calcite (Saxena and Betzler, 2003), and indicate that the sediment remained on the seafloor long enough for early seafloor processes to act on the skeletal particles (Smith and Nelson, 2003), as commonly described in the cool-water depositional realm (Nelson *et al.*, 1988a; James, 1997).

During the early sea-level rises, laminated, upwelling-influenced facies were progressively covered by the bioturbated facies. In contrast to sea-level falls, sea-level rises took place over a shorter time (see gradient in the isotopic curve, Fig. 87). This may condition rapid reorganization of the ocean current system from upwelling-dominated

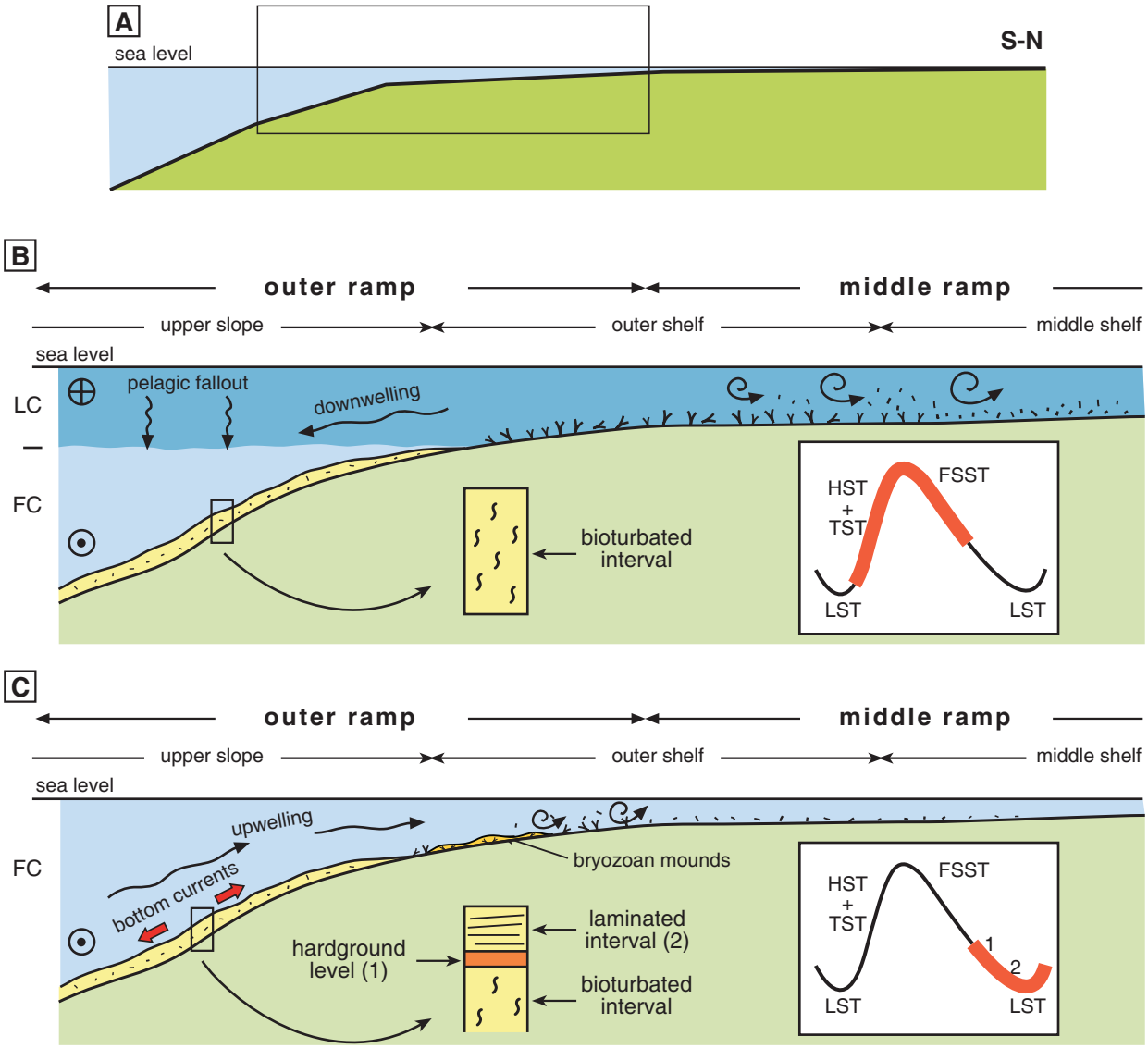

Fig. 88. A) Simplified diagram showing topographic profile of distally-steepened ramp in Great Australian Bight. Inset marks position of B and C. B) Depositional model of distally-steepened ramp for most of the time throughout the sea-level curve (late-lowstand system tract, transgressive system tract, highstand system tract and early-falling sea-level system tract). During these periods, the dominant currents affecting the ramp are the warm-water Leeuwin Current (LC) in the first 200 m of the water column (light-grey shadowed zone) flowing eastwards (arrow tail circle) and the cool-water Flinders Current (FC) underneath that flows westwards (arrowhead circle). This mass-water distribution leads to overall downwelling situation in the ramp. Middle-ramp setting is characterised by swell and storm current action (spiral arrows) that remobilize the sediment on the seafloor and precludes net sediment accumulation, especially in the innermost mid-ramp. *In-situ* carbonate production is in the outer ramp (outer shelf and uppermost slope) where sedimentation from pelagic rain is also important. During these stages, the upper slope is unaffected by current action and hence sediment is matrix rich and intensely bioturbated (bioturbated interval in Fig. 87). Offshore transport from shelf to slope can also take place in this phase. C) Depositional model that characterises the distally steepened ramp during the late falling sea-level stage and early sea-level lowstand. Due to sea-level fall, middle-ramp and proximal outer-ramp settings are affected at lower depths but with similar sedimentary patterns as shown in A). Reorganization of ocean currents as a consequence of northward movement of the Subtropical Convergence Zone (see text) began in early falling sea level stage. This change in current patterns, which progressively weaken the Leeuwing Current and favour upwelling of the Flinders Current, did not occur instantaneously but rather took place progressively during falling sea level. Only during the late stages of the falling sea-level were the effects of the upwelling significant enough to affect sediment on the slope. Bottom currents associated to the upwelling currents swept the sediment on the sea floor, generating firmground/hardground levels (1) and later remobilized and redeposited sediments forming laminated intervals (2) during the early sea-level lowstand. LST: lowstand system tract; TST: transgressive system tract; HST: highstand system tract; FSST: falling sea-level system tract.

to downwelling-dominated, and consequently a short-term turnover from the laminated back to the bioturbated facies.

5.4. Implications for the sedimentary record of sea-level cycles in slope sediments

Outer-carbonate ramp environments and upper slopes of distally-steepened carbonate ramps such as the case studied herein are commonly too deep to be affected by sea-level changes. The integrated use of wireline logs, geochemical data, FMS images, and the sedimentological analysis of the lithofacies, however, allowed us to recognise such subtle facies changes in the upper-slope setting of a distally steepened temperate-water carbonate ramp and to depict their relationship with sea-level. It remains to be tested, whether the Pleistocene study interval is a peculiar case, due to the importance of the oceanic current regime in the deposition style on the ramp. In any event, the integrated method presented herein could be applied to study more precisely apparently homogeneous fine-grained calcareous sediment successions of distal-ramp outcrops. It also shows that seemingly small variations in the downhole logs of carbonates bear relevant informations for the reconstruction of facies and cyclicity.

5.5. Other remarks

Pushing the interpretation further, we propose that, apart from the major 100 ka sea-level fluctuations (heavier oxygen isotopes values), some correlation of the sedimentary sequence can also be made with higher-frequency lower-magnitude sea-level fluctuations (Fig. 87). These fluctuations are marked in the composite log by peaks in compressional velocity, resistivity, and, to a lesser extent by gamma ray peaks. However, FMS images and lithofacies do not show significant variations and the corresponding intervals can broadly be assigned to facies of the bioturbated interval. Anomalously high values of Fe and Mn are also absent. Only some resistive beds indicate the occurrence of hardground levels. Laminated intervals were not identified. However, the position of the wireline log peaks does not match the isotopic curve as it does in the sedimentary sequences1 to 4, since these peaks seem to be related only to falling sea level (~210 mbsf) or to rising sea level (~259 mbsf). These secondary peaks therefore may not be fully explained by the proposed ocean circulation pattern and the inferred depositional model. With the data available, we cannot state whether they truly form sedimentary sequences related to minor sea-level falls, or if there are other factors involved such as lowered sediment supply, low sedimentation rates, different behaviour of ocean currents, or other local conditions.

6. Conclusions

1) The integrated use of wireline logs, geochemical data, FMS images, and sedimentological analysis of the lithofacies has revealed three distinct facies in the upper slope of the Pleistocene distally steepened carbonate ramp of the GAB. The first facies consists of 20–50 cm firmground and hardground intervals, characterised by highly resistive FMS images and elevated values in the other logs. This facies is assumed to represent omission surfaces. The second facies, which forms 6–10 m-thick intervals, is typified by laminated FMS images and common high-Mg calcite bioclasts as well as Fe-stained bioclasts. Abrasion of bioclasts and lamination indicates that this facies formed under the action of bottom currents. The third facies, which occurs in up to 40 m-thick intervals, stands out due to its mottled appearance in the FMS log. The corresponding sediment is matrix-rich and contains bryozoa, sponge spicules, mollusc shells, and foraminifers. It also has frequent calcareous nannoplankton and well-preserved planktonic foraminifers.

2) The three outer-ramp facies association form sedimentary cycles. Cycles start with hardgrounds at the base. Hardgrounds are overlain by the laminated deposits. The upper part of the cycles consists of bioturbated sediments.

3) A correlation of the log patterns and the sedimentary cycles in the Pleistocene succession with MIS 11–19 shows that facies stacking in the cycles is linked to distinct sea-level stands. Firmground/hardground surfaces formed during the latest stages of sea-level falls. Laminated sediments were deposited during later sea-level fall and/or early phases of sea-level lowstand, bioturbated intervals are related to the interglacial sea-level highstands of MIS 17, 15, 13 and 11.

4) As the analysed area lies too deep on the outer slope to be affected by lowering of wave base abrasion during sea-level falls, the activity of bottom currents is thought to be an important control on facies and cycle development. During the late stages of sea-level fall, before maximum lowstand, upwelling currents winnowed the slope sediments, leading to hardground formation. During latest sea-level falls and early sea-level lowstands, a relative increase in ramp sediment supply to the slope leading tot formation of the laminated facies was also a response to the continued action of the near-bottom upwelling currents that reworked previously deposited sediments along the slope. During the early sea-level rises, laminated, upwelling-influenced facies were progressively covered by bioturbated facies.

5) Our results show that seemingly monotonous upper-slope successions of distally-steepened ramps bear a subtle

but diagnostic record of sea-level changes. It remains to be tested, however, whether the case presented here is a result of peculiar conditions at the GAB margin, or whether it is a more widely applicable model.

Acknowledgements

We would like to thank the Schlumberger officers, crew, and drillers and the Ocean Drilling Program laboratory personnel on Leg 182 for their assistance on board the Joides Resolution. A. Puga-Bernabéu was funded by "Ministerio de Educación y Ciencia" (Spain), Proyect CGL 2004-04342/BTE and by a doctoral F.P.U. grant (MECD-UGR, AP2003-3810). C. Betzler was supported by the Deutsche Forschungsgemeinschaft (Be 1272/6). This research used samples and data provided by the Ocean Drilling Program (ODP). The ODP is sponsored by the US National Science Foundation (NSF) and participating countries under the management of Joint Oceanographic Institutions (JOI), Inc. We want to thank J.M. Martín and J.C. Braga for constructive comments on a previous version of this manuscript. We are indebted to Christine Laurin for improving the English text.

Appendix 1

General information, geophysical and image data, core descriptions and age data from the ODP Leg 182, Site 1131A (Available from the World Wide Web)

A. General information

Initial Reports: http://www-odp.tamu.edu/publications/182_IR/182TOC.HTM

Scientific Results: http://www-odp.tamu.edu/publications/182_SR/182TOC.HTM

B. Wireline log data

Resistivity (SFLU):

http://www.ldeo.columbia.edu/BRG/online2/Leg182/1131A/standard/1131A-dit.dat

Gamma ray (SGR):

http://www.ldeo.columbia.edu/BRG/online2/Leg182/1131A/standard/1131A-ngt-fms.dat

Calliper-Formation MicroScanner Tool:

http://www.ldeo.columbia.edu/BRG/online2/Leg182/1131A/standard/1131A-cali-fms.dat

Bulk density (RHOM):

http://www.ldeo.columbia.edu/BRG/online2/Leg182/1131A/standard/1131A-hlds.dat

Neutron porosity (APCL):

http://www.ldeo.columbia.edu/BRG/online2/Leg182/1131A/standard/1131A-aps.dat

Compressional velocity:

http://www.ldeo.columbia.edu/BRG/online2/Leg182/1131A/standard/1131A-sdt-lin.dat

C. Formation MicroScanner (FMS) images

FMS images 20 meters interval:

http://www.ldeo.columbia.edu/BRG/online2/Leg182/1131A/fms/20m/index_fms20.html

Formation MicroScanner (FMS) images 100 meters interval:

http://www.ldeo.columbia.edu/BRG/online2/Leg182/1131A/fms/100m/index_fms100.html

D. Age Data

Age model: http://iodp.tamu.edu/janusweb/paleo/agemodel.shtml

E. Core descriptions

General visual core description

http://www-odp.tamu.edu/publications/182_IR/VOLUME/CORES/COR_1131.PDF

Detailed visual core description

http://iodp.tamu.edu/janusweb/imaging/primedataimages.shtml?dataType=VCD

F. Acronyms
http://www.ldeo.columbia.edu/BRG/online2/Database_Documents/acronyms.html

PART THREE

9

DEPOSITIONAL MODELS CONTRASTED

9.1. Shared and distinctive features

The depositional models for temperate-carbonate deposition in the study areas have certain characteristics in common or are comparable to classic sedimentary models of non-tropical carbonates. In this section, shared features concerning ramp geometry, biogenic composition of the sediment, facies belt distribution, sediment transport and deposition mechanisms, and cyclicity are summarized.

9.1.1. Ramp geometry

According to the ramp profile, two types of temperate carbonate ramps (*sensu* Burchette and Wright, 1992) are recognised in this study: homoclinal ramp (southern margin of the Sorbas Basin and Granada Basin) and distally-steepened ramp (northern margin of the Sorbas Basin and Great Australian Bight). These two ramp profiles are recognised in many other sites with temperate carbonate sedimentation worldwide. Examples include homoclinal ramps in the Agua Amarga Basin (Martín *et al.*, 1996), Carboneras Basin (Braga *et al.*, 2003a; Martín *et al.*, 2004), Sicily (Pedley and Grasso, 2002), and the Three Kings Platform (Nelson *et al.*, 1988a), and distally-steepened ramps in the Carboneras Basin (Martín *et al.*, 2004), Sicily (Massari and Chiocci, 2006), and Lincoln Shelf (James *et al.*, 1997). The presence of both types of carbonate ramps in large open-ocean platforms such as southern Australia and New Zealand, and in relatively low-energy seas such as the Mediterranean, indicates that the ramp profile in the temperate-carbonate depositional realm is not conditioned by the general oceanographic setting.

Carbonate banks related to submarine highs is another type of temperate-carbonate ramp depositional environment exemplified in this study, as inferred from sedimentological data in the case of the limestones of the Mangarara Formation in the Taranaki Basin (see Chapter 7). This type of carbonate accumulation is common in the Cenozoic temperate carbonates of New Zealand (Kamp *et al.*, 1998; Hayton *et al.*, 1995; Caron *et al.*, 2004b), and its development is associated to the tectonic faulting and thrusting that characterise this region.

9.1.2. Biogenic composition

In a broad sense and in terms of overall composition, the bioclastic limestones (with varying proportions of terrigenous grains) found in all the studied examples are similar. The biogenic components of the limestones belong to the heterozoan skeletal association. However, the relative proportions of these components vary significantly from one study site to another. Bivalves, coralline algae, and bryozoans are the main constituents of the carbonate factories; benthic foraminifers, echinoderms and brachiopods are the most important accessory components, although they are also locally abundant.

Although bivalves and bryozoans are important components of the carbonate factories in the Taranaki Basin, the most abundant elements are coralline algae and large benthic foraminifers, mainly *Amphistegina* and subordinate *Lepidocyclina*. As discussed in Chapter 7, in the Middle Miocene (when the Mangarara Formation was deposited), following the Neogene climate optimum of the Early–Middle Miocene (~16 Ma), there was a long-term climatic deterioration throughout the remainder of the Cenozoic, although the western North Island of New Zealand was still under the influence of a warm-temperate current from the north. In this case, the presence of the coralline algal

and large benthic foraminifer (*Amphistegina*) association is interpreted to be indicative of the warmest conditions within the temperate-carbonate realm spectrum.

In the Sorbas Basin, the factory areas mainly comprise bivalves (oyster and pectinid-dominated), bryozoans and brachiopods (in the inner factory, see Chapters 4 and 5) and coralline algae (in the outer factory, see Chapters 4 and 5). In the other example in southern Spain, the Granada Basin, the carbonate factory is made up almost exclusively of bryozoans and bivalves (mostly pectinids). Brachiopods are absent and coralline algae are uncommon. The water temperature is interpreted to have been cooler in the Granada Basin than in the Sorbas Basin (as inferred from the absence of large benthic foraminifers, see Chapter 6), probably due to a nearby Atlantic connexion of the Granada Basin. This means that relatively warmer Mediterranean waters supported coralline algal fields and associated benthic foraminifers in the Sorbas Basin in contrast with the relatively cooler waters in the Granada Basin, where those components appear to be insignificant. However, a similar bioclast segregation is found if the Sorbas Basin is compared with nearby basins such as the Agua Amarga Basin, where bryozoans and bivalves are abundant and coralline algae are minor components (Martín *et al.*, 1996; Brachert *et al.*, 1998). This indicates that other factors besides water temperature (such as terrigenous input and hydrodynamic patterns) must be invoked to explain, at least locally, the difference in the biogenic components of the factory areas in the examples from southern Spain.

In the Great Australian Bight, segregation in the composition of the carbonate factories is conditioned by water depth. Below the photic zone (~110 m; James *et al.*, 2001), where the sediment studied was deposited (see Chapter 8), the main components are bryozoans, sponge spicules, and molluscs. In shallower waters, especially in the inner shelf, rhodolith and other algal fields developed in association with large photosymbiont-bearing foraminifers (*Marginopora*; James *et al.*, 2001).

9.1.3. Facies belt distribution

The southern margin of the Sorbas Basin and Granada Basin share a common pattern of factory areas and coastal facies belt distribution. In both locations, the inferred depositional models (Fig. 34, 38 and 61) show the development of a coastal belt comprising a shoal system changing landwards to a beach system, and the occurrence of carbonate factories seawards of the shoals, presumably below the fair-weather wave base. This facies distribution is similar to that proposed in other examples from southern Spain Miocene basins such as the Agua Amarga and Carboneras basins (Martín *et al.*, 1996, 2004). In addition, the temperate ramp at the southern margin of the Sorbas Basin exhibits a double factory zone, an inner factory, located in the middle-ramp, extensively colonized by bivalves (oysters-pectinids), brachiopods and bryozoans, and an outer factory on the outer ramp, formed by coralline algal remains. The presence of shallow and deep carbonate factories of similar biogenic composition is also recorded in Upper Miocene sediments around Monte Ricardillo in the Cabo de Gata region (Betzler *et al.*, 2000) and in the Pliocene Carboneras Basin (Martín *et al.*, 2004). In the Sorbas Basin, at the outer ramp, there is a gradual transition from coralline algal-dominated sediments to intensely burrowed and planktonic foraminifer-rich fine-grained sediments.

In the Great Australian Bight, only outer-shelf to upper-slope environments have been studied in this work, but taking into account numerous data from research papers dealing with shallower settings (e.g. James *et al.*, 1994, 2001; James and Bone, 2007), facies belt distribution can be compared with southern Spain examples. Extensive carbonate production (bryozoan- and sponge-rich factories) is located in the outer ramp and upper slope. The middle shelf is a zone of active and continuous sediment remobilization by swells ("shaved" shelf *sensu* James *et al.*, 1994), commonly forming sand ripples in the seafloor sediment. Broadly speaking, the facies belt distribution is similar in Australian and Spanish examples as the fair-weather wave base determines the position of the main carbonate factories, that is, below the fair-weather wave base. However, due to the deeper position of the fair-weather wave base and higher energy of the swells in the Great Australian Bight in comparison with the small intermontane basins in southern Spain such as the Sorbas and Granada basins, carbonate production and accumulation take place in water depths of more than 70 m (that of the distalmost part of the carbonate ramp in the Sorbas and Granada basins). The shaved mid-ramp in southern Australia is comparable to the shoals system in the southern Spain basins in terms of facies belt distribution and wave action.

9.1.4. Sediment transport and deposition mechanisms

Due to their general lack of early cementation, shallow-marine temperate skeletal sediments are readily prone to reworking and redeposition (Nelson *et al.*, 1982, 1988a). Remobilized temperate-carbonate particles on the seafloor, behave similarly to siliciclastic clasts. As a result, equivalent deposits are generated either by traction currents (waves and longshore currents), traction-like currents (storm currents), or by subaqueous sediment gravity flows (turbidite flows, mud flows, debris-flows, and so on) (Martín *et al.*, 1996, 2004; Anastas *et al.*, 1997; Betzler *et al.*, 1997a; Braga *et al.*, 2001, 2003a).

Waves and longshore currents mobilized sediment and built sedimentary bodies of different scale (sandwaves and megaripples) on the sea bottom of the carbonate ramps in the south Sorbas and Granada basins. These bodies are characteristic of the shoal system that extends over nearshore settings of the temperate-carbonate ramps in Neogene basins in southern Spain such as the Agua Amarga Basin (Martín et al., 1996; Betzler *et al.*, 1997a), Carboneras Basin (Braga *et al.*, 2003a; Martín *et al.*, 2004), and Vera Basin (Braga *et al.*, 2001). Large swells in the Great Australian Bight also mobilize the sediment, generating calcareous sand-ripples on the seafloor in middle- and outer-ramp settings (James *et al.*, 1992, 2001). Sandwaves are also found in the sedimentary infill of the Alhama Submarine Canyon in the Granada Basin (southern Spain).

Tempestite (bivalve-dominated) deposits associated to storm currents are also recognised in the Sorbas and Granada basins. In the Sorbas Basin, storm backflow currents affected bivalve biostromes from the inner factory (mid-ramp), removing shells and transporting them seawards to the outer ramp, where they finally accumulated as lag deposits. Storm layers in the Granada Basin are composed of bioclasts from the factory area that were remobilized during storms and redeposited landwards as horizontally-bedded to gently-dipping tempestites cross-cutting and alternating with shoal deposits. Storm action is also recorded in other intermontane basins of southern Spain, generating similar storm deposits, for instance, in the Carboneras Basin (Martín *et al.*, 2004) and the Agua Amarga Basin (Martín *et al.*, 1996). Furthermore, in the Granada Basin, storm currents also played an important role of the sedimentary infilling of the Alhama Submarine Canyon, as they supplied sediment from the carbonate factory into the canyon which in turn evolved downward into turbidite flows. Storm-linked deposits from the Great Australian Bight are poorly studied deposits, despite being a high-energy oceanographic setting where storms constitute an important process of sediment remobilization and transportation (James and Bone, 1991; James et al., 1994, 2001).

Deposits produced by sediment gravity flow are commonly found in outer-ramp and offshore settings, as well as inside submarine channels and forming submarine lobes. In the Mangarara Formation, densites (*sensu* Gani, 2004) mostly comprise channel infills, turbidites make up the submarine lobes, and debrites (*sensu* Gani, 2004) mostly form the gully infills. Similar deposits are recognised in the submarine lobes and feeder channels of the Azagador carbonates of the Vera Basin (Braga *et al.*, 2001).

9.1.5. Cyclicity

Eccentricity-driven (~100 ky) and higher-frequency sedimentary cycles were recognised in ramp sediments of the Sorbas Basin and Great Australian Bight. These cycles are recorded in different positions along the ramp and slope, displayed by different structures and/or facies changes.

In the Sorbas Basin (southern margin), the sedimentary cycles are interpreted to be forced by orbital precession or higher-frequency processes (see Chapter 5). These high-frequency cycles are recorded by the alternation of distinctive facies from outer- and middle-ramp environments (coralline algal fields and bivalve biostromes). Outer-ramp cycles recorded in the Sorbas Basin are of similar frequency to those recognised in middle-ramp settings in the Agua Amarga Basin (Martín *et al.*, 1996).

Cycles in upper-slope environments were recognised in Pleistocene offshore sediments of the Great Australian Bight. These eccentricity-driven cycles, which were identified using integrated geophysical and lithological methods, are recorded as subtle facies changes from hardgrounds to laminated and burrowed levels (see Chapter 8).

Although age constraint is not well established in the Alhama de Granada example, eccentricity-driven sea-level cycles might have controlled the sedimentary infill of the Alhama Submarine Canyon in the Granada Basin, as occurred in submarine canyons with similar incision–infilling–re-excavation patterns (Batzan *et al.*, 2005). In the Alhama Submarine Canyon, cycles comprise large erosional surfaces and distinctive overlying deposits generated in connection with the different phases of incision and infilling of the submarine canyon in response to sea-level fluctuations.

9.2. New aspects

Although detailed results on the work done in the different study areas are given above, an integrated view of all the new aspects concerning temperate-carbonate depositional models are highlighted here. The new features refer to platform and offshore settings.

9.2.1. Platform

New considerations concerning platform setting relate to event deposits, sedimentary cyclicity, and submarine canyon occurrence.

Event deposits

Event deposits (*sensu* Einsele *et al.*, 1996) such as storm beds and tempestites are recognised in some of the study areas (Sorbas Basin and Granada Basin), but the original aspect of this work is the identification, characterisation, and interpretation of tsunami-related deposits in the Sorbas Basin. These types of deposits had not previously been described in temperate-carbonate ramps. Tsunamites were preserved in outer-ramp settings and were therefore unaffected by wave and storm-current reworking. The distinctive sedimentary features of these tsunamites (megahummockites and a thick shell-debris bed) and the inferred inflow and backflow effects were controlled by the different palaeotopographic profiles of the carbonate ramps. These tsunami-related deposits also contribute to our information on the poorly-known sedimentary record of tsunamites in outer-ramp settings (Dawson and Stewart, 2007). In addition, tsunamites in the Sorbas Basin provide a linkage between well-known shallow-water marine and continental tsunamites with tsunami-associated deposits (seismites and megaturbidites) in deep-water offshore settings.

Cyclicity

The identification of sedimentary cycles, especially high-frequency cycles, in mid- and outer-ramp environments provides new data for understanding the response of temperate-carbonate ramps to sea-level fluctuations. These middle- and outer-ramp settings are relatively unaffected by sea-level changes, and facies belt movements produced by sea-level fluctuations do not essentially modify facies distribution in the outer ramp. In the Sorbas Basin, high-frequency cycles of two alternating facies (bivalve concentrations and coralline algal beds) are recorded in outer-ramp settings due to the taphonomic response of these facies. These high-frequency cycles contribute to completing the sedimentary record of sea-level-driven cycles along temperate carbonate ramps. In the Sorbas Basin, cyclicity on the outer ramp is time equivalent to that identified in lateral basinal sediments (see Chapter 5), and also similar to time-equivalent inner-ramp sediments in nearby basins (see Chapter 5; Martín *et al.*, 1996).

Submarine canyon

Submarine canyons, incised valleys, and submarine channels that cross-cut the ramp sediments are poorly known in the sedimentary record of carbonate sediments in general and within the temperate-carbonate realm in particular. The study of the Alhama Submarine Canyon in the Granada Basin represents a further step in this topic. The full description of the facies types, bed geometries, infilling patterns, and origin of this canyon has provided new data for completing the characterisation of these submarine erosional incisions. Although different phases of erosion and infilling have been recognised in other submarine channels and canyon-like channels excavated on temperate ramps (e.g. Braga *et al.*, 2001; Vigorito *et al.*, 2005), the cyclicity observed in the sedimentary infill of the Alhama Submarine Canyon can no doubt be linked to and reflect the response of the submarine canyon to sea-level fluctuations. It also contributes to the overall knowledge of submarine canyons because it represents the innermost part of submarine canyons (near the coastline), an area relatively poorly known in the sedimentary record. As it is a subaerially exposed example, it also allows a better comparison with submerged and subsurface examples.

9.2.2. Offshore settings: ramp-to-slope transition, slope, and slope-to-basin transition

In offshore settings, the new aspects revealed in this study relate to sea-level driven cyclicity and the occurrence of the submarine channel-fan system and submarine gullies.

Cyclicity

Cyclicity is a relatively poorly-known phenomenon in the literature dealing with temperate carbonates deposited in upper-slope settings. Outermost-ramp and upper-slope settings are commonly too deep to be significantly affected by sea-level controlled hydrodynamic changes and therefore high-frequency, sea-level-driven cycles may remain obscure. Sedimentary cycles were recorded in upper-slope sediments of the Great Australian Bight due to a distinctive hydrodynamic model changing with sea-level oscillations. The recognition of these cycles helps to complete the sedimentary record spectrum of sea-level-driven cycles in the high-energy, open-ocean, temperate-carbonate ramps. In the Great Australian Bight, cycles of similar frequency to those recognised in this study are found in deeper-water settings (Betzler *et al.*, 2005), as well as in shallower settings, along the Eucla Shelf and other nearby shelves in southern Australia at different periods (James and Bone, 1994; Boreen and James, 1995).

Submarine channel-fan system and submarine gullies

The identification and description of these submarine elements provide additional data to characterise deep-water carbonate environments. The study of the Mangarara Formation in the Taranaki Basin has shown that meandering channels, with lateral-accretion structures, are common features in temperate-carbonate, submarine channel-fan systems (Braga *et al.*, 2001; Vigorito *et al.*, 2005). Several phases of lateral accretion and aggradation are recognised in the channel infill. Facies studied in submarine channels and gullies from the Taranaki Basin

show the high number of sediment types that can be found in these deep-water settings. Suabqueous sediment gravity flows responsible for the transportation and deposition of calcareous sediment in these deep-water settings can yield deposits quite different to those resulting from siliciclastic gravity flows. This is an important fact to be taken into account when interpreting carbonate channel-fan systems as they are not entirely comparable to siliciclastic systems in terms of sediment transport and deposition.

9.3. Controlling factors at the regional scale

Apart from water temperature and nutrients contents, the other most important controlling factors on temperate-carbonate ramp deposition have been repeatedly shown to be local hydrodynamic conditions and type and geometry of the underlying substrate, regardless of the oceanographic setting (i.e. open ocean or moderate- to low-energy ramps) (Scoffin, 1988; James *et al.*, 1994, 2001; Gillespie and Nelson, 1996; Freiwald, 1998; Betzler *et al.*, 2000; Hageman *et al.*, 2000; Braga *et al.*, 2003a; Caron *et al.*, 2004b; Martín *et al.*, 2004, Johnson *et al.*, 2005; Titschack *et al.*, 2005 among others). For example, the substrate topography conditioned the development of different ramp profiles within a single basin such as the Sorbas Basin. Similarly, the position of the fair-weather wave base in shallow water depths in southern Spain basins allowed the development of relatively shallow-water factories, in contrast to southern Australia. Special hydrodynamic conditions can also modify the facies types even in deep-water settings as shown in the upper slope of the Great Australian Bight.

However, the work carried out in this thesis has shown that there are additional factors that influence and condition the type of temperate-carbonate depositional model, whether in the platform or in offshore settings.

9.3.1. Platform

It is unquestionable that high-energy events can affect the ramp and significantly modify sediment distribution on the ramp after the event as they remove, remobilize, and redeposit large amounts of sediments. This study has been shown the effects of tsunami wave(s) on temperate-carbonate ramps and the type of tsunamites generated (megahummocks and a thick shell-debris bed depending on ramp topography). These tsunamites, which were preserved in outer-ramp settings, produced short-lived variations in the prevailing depositional model that left significant marks in the sedimentary record.

The presence of large-scale geomorphic elements such as submarine canyons excavated into ramps also impinges on the typical sedimentary model of temperate-carbonate ramps as they funnel coarse-grained sediments from the ramp to deep-water settings. The Alhama Submarine Canyon (shallower part), which was incised into the ramp, modified sediment distribution and the subsequent depositional model, by altering the sedimentary dynamics in the ramp. Although it has not been preserved, the offshore continuation of this submarine canyon could also have modified the sedimentary pattern in the slope.

Depositional models should also be interpreted taking into account sea-level driven modulations as they can have an important effect. High-frequency sea-level oscillations affect deposition on the ramp and usually result in landward/seaward displacement of the facies belts, especially in nearshore settings.

9.3.2. Offshore settings: ramp-to-slope transition, slope, and slope-to-basin transition

Background facies in basinal, deep-water offshore environments commonly remain unmodified as they are not generally affected by sea-level oscillations. Mass-transport deposits such as turbidites, and mud-flow deposits, and slumps can, however, disturb normal sedimentation in deep-water settings. The work carried out in the Great Australian Bight has shown that sea-level fluctuations can also repeatedly affect sedimentation in shelf-to-slope and upper-slope environments when these oscillations imply modifications in the ocean-current circulation regime. The reorganization of the current systems, from downwelling-dominated conditions during interglacial periods to upwelling-dominated conditions during part of the glacial periods, favoured facies changes in slope settings that otherwise would have remained unaltered (as shown in the Australian example). Similarly to ramp settings, high-frequency sea-level cycles can also modify the depositional model in upper-slope settings, leaving a significant imprint in the sedimentary record of temperate carbonates.

In the same way as the Alhama Submarine Canyon locally controlled and modified sedimentation on the carbonate ramp, the offshore continuation of submarine canyons cross-cutting the shelf-edge and slope may also modify sedimentation patterns in deep-water settings. Geomorphic, submarine canyon-associated elements such as the submarine channel- and fan-systems and the submarine gullies described in the Taranaki Basin margin are examples of local variations to normal sedimentation conditions. In the studied example, the important fact is that a temperate-carbonate system expands its presence beyond the ramp realm into slope and basin-floor settings, within an area largely influenced by a siliciclastic-dominated channel-fan system.

10

CONCLUSIONS

This chapter presents the main results obtained in this PhD thesis. It highlights the factors that control the development of temperate carbonates on platform and offshore environments. This study has shown the main characteristics of temperate carbonates in the study areas, shedding light on the less-known outer-ramp and offshore settings, and revealing new aspects of temperate-carbonate deposition. These results are given below.

- Temperate carbonates in southern Spain, North Island of New Zealand, and southern Australia were deposited on homoclinal ramps, distally-steepened ramps and isolated banks. Ramp profile seems to be controlled by the topography of the underlying substrate (e.g. Sorbas Basin, Taranaki Basin) and the local hydrodynamic regime (Great Australian Bight).

- The biogenic components of the temperate carbonates studied in the different basins belong to the heterozoan skeletal assemblage. Bivalves, bryozoans, coralline algae and benthic foraminifers are the main bioclastic components of the carbonate sediments, although the relative proportion of these bioclasts in the sediment can vary locally. The warmest facies found is from the Middle Miocene temperate carbonates of New Zealand, and it is represented by the coralline algal-large benthic foraminifer (*Amphistegina*) association.

- Observations on the temperate ramps of the Sorbas and Granada basins and the depositional models for these basins indicate that the Agua Amarga depositional model of Martín *et al.* (1996), characterised by the presence of a carbonate-production zone below the fair-weather wave base (factory area) that changes landwards to a shoal-and-beach system, can be considered as representative of the sedimentary models of temperate-carbonate deposition in southern Spain, and can probably be extended to the entire Mediterranean region.

- Temperate-carbonate particles can be transported throughout the ramp by different sediment-transport mechanisms, from traction currents to subaqueous sediment gravity flows. The resultant sedimentary structures and deposits are similar to those observed in the siliciclastic realm, such as ripples, sandwaves, tempestites, tsunamites, turbidites, densites, and debrites. Especially noteworthy is the similarity of temperate-carbonate architectural elements (e.g. lateral-accretion structures and lobes) in submarine canyons and submarine channel-fan systems to their siliciclastic counterparts even though sediment transport and deposition mechanisms may be slightly different due to the unique features (i.e. larger size, irregular shape, and lesser density) of the carbonate particles.

- Different order cyclicity of (eccentricity/precession-linked and/or higher frequency), recorded in the sediment by different structures and facies changes, are recognised in outer-ramp and upper-slope settings, either in small microtidal basins (Sorbas Basin) or open-ocean basins (Great Australian Bight). Sedimentary cycles were controlled by sea-level oscillations, in some cases (Australian examples) inducing oceanographic changes without any signs of being driven by climatic (humid/dry) changes. Cyclicity is an important factor to be taken into account in order to precisely identify the sedimentary models as the deposition style on the ramp may vary over short intervals.

▪ Event-deposits linked to tsunami(s) have been recognised intercalated within outer-ramp deposits in the Sorbas Basin. Distinctive tsunamites (megahummockites and a thick shell-debris bed), developed at the northern and southern margin of the basin respectively in accordance with the inferred inflow and backflow effects. These effects were in turn conditioned by the different palaeotopographic profiles at both sides of the basin.

▪ Submarine canyons close to the shoreline such as the Alhama Submarine Canyon in the Granada Basin, can be significant geomorphological features in temperate-carbonate ramps. The periodically repeated sequence of incision and infilling events of this submarine canyon was controlled by sea-level fluctuations. The presence of submarine canyons can condition sediment distribution on the ramp and locally modify the general depositional model, as shown in the Alhama de Granada example.

▪ Carbonate submarine channel-fan systems (Mangarara Formation), which are the basinward continuation of submarine canyons, are other geomorphic elements that expand the deposition settings of the temperate-carbonate realm beyond the ramp context. Architectural elements recognised in these deep-water systems are similar to their siliciclastic counterparts.

CONCLUSIONES

En este capítulo se destacan los principales resultados obtenidos en esta tesis, resaltando los factores que controlan el desarrollo de carbonatos templados en ambientes de plataforma y marino abierto profundos. En este estudio se han expuesto las principales características de los carbonatos templados en las áreas estudiadas, prestando especial atención a los ambientes menos estudiados de rampa externa y marino abierto profundos, y revelando nuevos aspectos relacionados con la sedimentación carbonatada templada. Los principales resultados son:

- Los carbonatos templados en el sur de España, Isla Norte de Nueva Zelanda y sur de Australia se depositaron en rampas homoclinales, en rampas con pendiente distal y bancos aislados. El perfil de la rampa parece estar controlado por la topografía del sustrato infradyacente (ej. Cuenca de Sorbas, Cuenca de Taranaki) y las condiciones hidrodinámicas locales (*Great Australian Bight*).

- Los componentes biogénicos de los carbonatos templados estudiados en las distintas cuencas pertenecen a la asociación esqueletal de tipo heterozoan. Bivalvos, briozoos, algas coralinas y foraminíferos bentónicos son los principales componentes bioclásticos de los sedimentos carbonatados aunque la proporción relativa de estos bioclastos en el sedimento puede variar de forma local. Las facies más cálidas encontradas proceden de los carbonatos templados del Mioceno Medio de Nueva Zelanda, y están representadas por la asociación algas coralinas-macro foraminíferos bentónicos (*Amphistegina*).

- Las observaciones realizadas en las rampas templadas de las Cuencas de Sorbas y Granada y los modelos deposicionales interpretados para dichas cuencas indican que el modelo sedimentario de Agua Amarga de Martín *et al.* (1996), caracterizado por la presencia de una zona de producción de carbonato (zona de factoría) situada por debajo del nivel de base de oleaje de buen tiempo y que cambia hacia tierra a un sistema de bajíos (barras) y playas, puede considerarse como el modelo deposicional representativo de la sedimentación de carbonatos templados en el sur de España, y probablemente puede ser aplicable a la región Mediterránea en conjunto.

- Las partículas de carbonatos templados pueden ser retrabajadas en la rampa por diferentes mecanismos de transporte y depósito, desde corrientes tractivas a flujos de sedimentos por gravedad. Las estructuras sedimentarias y depósitos resultantes son similares a aquellos observados en sistemas siliciclásticos, tales como rizaduras, dunas submarinas, tempestitas, tsunamitas, turbiditas, densitas o debritas. Especialmente notable es la similitud de los elementos arquitecturales de carbonatos los templados en cañones submarinos y sistemas de canal-abanico submarinos (ej. estructuras de acreción lateral y lóbulos) con sus homólogos siliciclásticos, incluso aunque los mecanismos de transporte y depósito puedan ser ligeramente diferentes debido a ciertas características peculiares de las partículas carbonatadas (ej. mayor tamaño, forma irregular, menor densidad).

- Ciclicidades de diferente orden (excentricidad/precesión y/o mayor frecuencia), registradas en el sedimento mediante cambios de facies y en las estructuras sedimentarias, han sido reconocidas en ambientes de rampa externa y talud superior, tanto en pequeñas cuencas micromareales (Cuenca de Sorbas) como en cuencas abiertas (G*reat Australian Bight*). Los ciclos sedimentarios estuvieron controlados por oscilaciones en el nivel de mar, en algunos casos (sur de Australia), induciendo cambios oceanográficos sin indicios claros de conexión a cambios climáticos (húmedo/seco). La ciclicidad es un factor importante a tener en cuenta para precisar los modelos sedimentarios ya que el estilo de depósito en la rampa puede variar a lo largo de cortos periodos de tiempo.

▪ Depósitos de eventos ligados a tsunami(s), intercalados en depósitos de rampa externa, han sido reconocidos en la Cuenca de Sorbas. Las características sedimentarias distintivas de estas tsunamitas ("megahummockites" y "thick shell-debris bed") son consecuencia de los efectos inferidos del flujo y reflujo en los márgenes de la cuenca, y estuvieron condicionados por los diferentes perfiles paleotopográficos de las rampas carbonatadas en dichos márgenes.

▪ Los cañones submarinos cercanos a la costa como el Cañón Submarino de Alhama en la Cuenca de Granada pueden ser importantes elementos fisiográficos excavados en rampas de carbonatos templados. La secuencia de incisión y los eventos de relleno de este cañón submarino, repetidos periódicamente, estuvieron controlados por fluctuaciones del nivel de mar. La presencia de cañones submarinos puede condicionar la distribución de sedimento en la rampa y modificar localmente el modelo sedimentario general como ocurre en el ejemplo de Alhama de Granada.

▪ Los sistemas carbonatados de canal-abanico submarino (Formación Mangarara), continuación hacia cuenca de cañones submarinos, son otros elementos geomórficos que expanden los ambientes deposicionales de los carbonatos templados fuera del contexto de la rampa. Los elementos arquitecturales identificados en estos sistemas de aguas profundas son similares a sus homólogos siliciclásticos.

11

FUTURE PERSPECTIVES

Research carried out in this PhD thesis has brought to light aspects that have remained relatively poorly known in the temperate-carbonate depositional realm, such as cyclicity in outer-ramp and offshore settings, high-energy events, and submarine canyons and related channel-fan systems. Studies concerning these topics should continue, and others, as indicated below, be undertaken to reach a fuller knowledge of these carbonates.

Temperate carbonates have been shown to record sedimentary cycles along ramp- and slope-settings. Careful and detailed observations and the use of integrated methods can help to discern among different processes that drive cyclicity, such as sea level, tectonics, climate, and changes in ocean circulation. Further studies on the ocean current regime will probably show the importance of local changes in controlling cyclicity in depositional sequences.

Although tsunami deposits have been well described in the literature (see Chapter 4 for references), many more studies concerning tsunamis have been published since the Indonesian tsunami of December 26th, 2004 (see, for example, special volumes by Tappin, 2007 and Gehrels and Long, 2007). Recently, Dawson and Stewart (2007) have pointed out that patterns of sediment transport and deposition in offshore zones have not been properly described in modern tsunami deposits. Offshore transects along the Indonesian platforms and slopes could be useful to clarify this issue and characterise the behaviour and effects of tsunami waves from offshore to continental settings. Upper Miocene tsunamites in the Sorbas Basin provide ancient examples to compare with those results if they are eventually carried out. Fossil tsunami deposits in the Sorbas Basin could also help to provide more precise numerical models that predict the behaviour of the tsunami waves (e.g. Heinrich *et al.*, 2001; Piatanesi and Tinti, 2002; Bondevik *et al.*, 2005; Cherniawsky *et al.*, 2007) since these waves behave differently depending on the coast and ramp morphology.

Overall, research on carbonate submarine canyons, channels and fans is relatively poorly developed if compared with their siliciclastic counterparts. However, the study of these systems, especially the temperate-type, may be expanded in the near future as they can act as potential hydrocarbon reservoirs (see below) and can record sea-level fluctuations that could help to a better understanding of carbonate sequence stratigraphy. Moreover, similarities between these two types of systems (such as infilling geometries or sediment-supply mechanisms) and dissimilarities (such as the sediment source area and probably their response to sea-level oscillations) indicate that further research is needed to verify whether there is a single sedimentary model for submarine canyon-channel-fan systems or, on the contrary, whether carbonate systems need a new depositional model.

An important issue concerning temperate-carbonate deposits is to characterise the type of sediment transport and deposition mechanisms. If they are simply compared with siliciclastic deposits without taking into account the differences between carbonate and siliciclastic particles, deposits will be misinterpreted and therefore also the depositional models inferred from their study. This work should be carried out comparing results obtained from laboratory experiments (using carbonate particles alone and mixed with siliciclastics) with fossil deposits (which are fully represented in the different examples studied in this thesis).

Apart from their use as building materials (Grossi and Murray, 1999), carbonate rocks can host ore deposits (e.g. Martín *et al.*, 1984; Kuznetsov *et al.*, 2005; Kamona and Friedrich, 2007), and are also potential hydrocarbon reservoirs (Burchette and Wright, 1992;

Neilson *et al.*, 1998; Ehrenberg and Nadeau, 2005; Schröder *et al.*, 2005). Most carbonate hydrocarbon reservoirs are tropical (mainly reefal) carbonates (e.g. Alsharhan and Magara, 1995; Cerepi *et al.*, 2003; Wilson and Evans, 2002; Huvaz *et al.*, 2007). However, studies carried out in temperate carbonates have shown that these sediments can also be potential reservoirs (Harmsen, 1990; Martindale and Boreen, 1997; Anastas *et al.*, 1998; Nelson *et al.*, 2003). In this regard, submarine canyon-channel-fan systems are probably the better reservoirs, as it occurs with siliciclastic counterparts. Examples studied in this thesis (see Chapters 6 and 7) have shown the wide variability of carbonate facies (generally coarse-grained) possible in these systems. Furthermore, carbonate and siliciclastic submarine channel-fan systems can co-exist within the same basin as in the case of the hydrocarbon-exploited Taranaki Basin (see Chapter 7). The interaction of the two systems implies a more detailed study of the geometric relationships and porosity/permeability distribution during exploration campaigns.

Although not dealt with in this thesis, the diagenesis of temperate carbonates is a field of investigation that needs further research. Studies in this area have a clear link to hydrocarbon exploration. Although generally porous (Nelson *et al.*, 2003), temperate-carbonate sediments can almost completely lose their porosity during burial diagenesis (e.g. Hood *et al.*, 2004b). Nelson and James (2000) have shown that early cementation in these carbonates helps to preserve the original porosity during deep burial. Therefore, a more detailed study on the diagenesis of these carbonates is needed.

PART FOUR

12

ACKNOWLEDGEMENTS

Since I was a child, it has always been clear to me that I wanted to be a researcher, to explain why things are one way and not another, to know the why when others do not. I have been doing this for the last four years in order to present this PhD thesis. In this time, many things have happened in my life, both professionally and personally, which would not have occurred if I had not become involved in this thesis. Along the way, I have met many people; with them and with the people already by my side I have lived these thesis years intensely. Therefore, I would like to dedicate these lines to express my gratitude to all the persons that have supported me and trusted in me.

First of all, I want to express my most sincere gratitude to the two persons that have made this PhD thesis possible: my supervisors, José Manuel Martín and Juan Carlos Braga. Thanks to them, I was able to enter the research realm some years ago and, with their help and support, I have been able to continue in it. To expound more on their qualities as human beings would need an additional chapter to recount all kinds of experiences, struggles and stories, recounted in their own characteristic way. This chapter is being written day by day, and I invite the reader to confirm that I am not wrong when I describe my supervisors as excellent people. From the scientific point of view, I will state the opinion of my friend Christian, which I share, that Pepe and Juan Carlos are great scientists. From the first, I was impressed by their critical capacity and their approach to understanding geology. These qualities, noteworthy when at the foot of an outcrop or when writing a manuscript, continuously remind me of all the things that I still have to learn. Once again, thanks Pepe, thanks Juan Carlos.

Thanks also to all my partners of the Departamento de Estratigrafía y Paleontología. To Soco for all her assistance since the first day—everything is easier with her help. To Alberto and Pepe for making the thin sections I have studied. To Julio, whom I could call my "third supervisor" as he has always been there to lend me a hand with geology subjects or share a few laughs in the cafeteria. To Isa, for her help with the "bugs," although this help could not be incorporated to this thesis due to time constraints, it will be written up in the near future—thanks Isa. To all my doctoral partners in the department, because we are all in the same tight spot. To those that were here when I entered the department (Matías, Raef, Gonzalo, Nono, Fernando, Jose María, Alicia, and Esteban) and to those that joined us later or are about to do so (Sila, Pili, Rute, and Jose Noel). To Francis, Agustín, and everyone that has shown an interest when asking about the progress of my studies over the last few years.

Of course, thanks to all my undergraduate classmates with whom I have shared so much; unfortunately, distance makes it difficult to do so more often. Although many of them considered (and probably still do) that I have wasted my time when I could have done most anything else,

I have always had their support. To Vicente (he knows what follows his name), a companion in times of uncertainty, thanks for sharing your experiences with me. To Alberto, the petroleum geologist, who insists I should work in the same field—maybe in other circumstances, but for the moment, you know I am happy where I am. To Nera, for whom, quite simply, no words are needed. To Esther, Captain C, thanks for all the fun moments we have spent since we met nine years ago. To Pedrochero, Quillo, Mimosín, Higi, Jose Mari, Bea, Pera, Chinchi...; thanks to all for one reason or another.

To Carol, Irene and Ale, I'd like to take this opportunity to thank you for everything, not only for these four years, but also for these last two decades of friendship.

In my experience in Germany, I sincerely want to thank Christian Betzler, a special German. First a teacher, now a friend. Thanks for allowing me to work with you on these slope carbonates, for being so generous with your attention and effort to keep this project on track. To Juan Manuel Cuevas, an essential helping hand while I was there. To Björn, Sebastian, Merle and David. To Marcus and Ronald, other "curious" Germans with whom I had heaps of laughs in the "Europa Haus."

In Kiwiland, first, I would like to thank Professor Campbell S. Nelson for allowing me to spend four months collaborating with him and his department. Thanks to him and Margaret for all the logistical support in and outside of the university. Although circumstances did not allow closer collaboration, our talks on temperate carbonates and other issues were always very fruitful. Time permitting, I hope we'll be able to chat about many other things. Thanks to all the staff of the Department of Earth and Ocean Sciences of Waikato University for their support. My gratitude to Peter Kamp for receiving me and helping me to settle in Hamilton. Thank you for all the assistance over those four months and for always being ready to lend me a hand from the very beginning. Thanks also for all the talks about the complex regional geology in the field. To the rest of the Kamp family, to Betty-Anne for everything, to Josef and Stephanie, for making me laugh. To Adam Vonk and Kyle Bland—thanks for all the talks and for inviting me to play soccer. The soccer matches were, without doubt, one of my best experiences there—thanks to all the players for those special moments. To Sydney for her willingness to help me anytime. To Steve, a good person, to Xu for teaching and helping me to make thin sections, to Anand, Mathias, Susan, Debra, and Christian. To Orla and Rachel for their hospitality and for awarding me the honorific of "best flatmate ever."

The work carried out in this thesis has been primarily funded by the projects BTE2001-3023 of the "Ministerio de Ciencia y Tecnología" (Spain) and CGL2004-04342 of the "Ministerio de Educación y Ciencia" (Spain), and by a F.P.U. grant-contract (MECD-UGR) awarded to the author, supporting the short stay leaves as well.

Many thanks to Christine Laurin, because her corrections and improvements of the texts are always very productive, and because she has put considerable effort into having the corrections ready in record time, making it possible for me to present this thesis today.

Thanks to my club, C.N. Granada, to Victor, Juan Antonio, Javi, Alicia, Belén, Roberto, and all my "children", because they are my escape hatch in moments of sadness, uncertainty, frustration and stress.

To my family, for all their support and love. To my father, the first person that should be here today to see this work come true, to see me start a new period in my life and share it with me, to be here with me today, tomorrow and forever. Because I could not tell it to you then, thanks dad. To my mother—I lack the words to thank her for all she has done for me. To my brother, Ale, who has helped me with the computer subjects. To my uncles, my grandpa, thanks.

And especially to you, my darling, because you are my moral support for everything. Thanks for putting up with me and encouraging me to keep on when things were difficult. Because you trusted in me and encouraged me to begin this thesis even when there were other better things for us; because my joy is your joy, because your sorrows are my sorrows, because everything we achieve we do together, because our future is one. Thanks Ana.

AGRADECIMIENTOS

Desde pequeñito siempre he tenido claro que lo que me gustaría hacer es investigar, explicar porque las cosas son de una forma y no de otra, el saber el por qué cuando otros lo desconocen. Hace ya casi 4 años que me llevo dedicando a eso para poder hoy presentar esta memoria de tesis. En este tiempo, han ocurrido muchas cosas en mi vida, tanto en lo profesional como en lo personal, que no hubiesen ocurrido si no me hubiese embarcado a realizar esta tesis. Por el camino he conocido a mucha gente, con ellas y con las que ya tenía a mi lado he vivido intensamente estos años de tesis. Por ello, quiero dedicar estas líneas a transmitir mi gratitud a todos aquellas personas que me han apoyado y confiado en mí.

En primer lugar, quiero mostrar mi más sincero agradecimiento a las dos personas que han hecho posible la realización de esta tesis doctoral: a mis directores, José Manuel Martín y Juan Carlos Braga. Gracias a ellos, me pude iniciar en el mundo de la investigación hace ya algunos años y, también con su ayuda y apoyo, he podido continuarla hasta hoy. Entrar a valorar las cualidades humanas de ambos necesitaría de un capítulo adicional donde incluir todo tipo de vivencias, batallitas y anécdotas narradas de la forma tan particular que tienen Pepe y Juan Carlos. Este capítulo se escribe día a día e invito al lector a comprobar que no me equivoco en calificar a mis directores como "buenas personas". Desde el punto de vista de la investigación, me quedo con la definición de mi amigo Christian, Pepe y Juan Carlos son unos "estupendos científicos". Desde el principio me impresionaron la capacidad crítica y la forma de entender la geología que tienen estos geólogos. Estas cualidades, visibles notablemente a pie de afloramiento y a la hora de escribir un artículo, son las que recuerdan a uno todo lo que le queda por aprender. Una vez más, gracias Pepe, gracias Juan Carlos.

A todos los compañeros del Departamento de Estratigrafía y Paleontología. A Soco por toda la ayuda desde el primer día, todo resulta más fácil gracias a ella. A Alberto y Pepe por la elaboración de las láminas delgadas. A Julio, que podría llamar el "tercer director" porque la verdad es que siempre ha estado allí para todo, ya sea ayudándome en cualquier cosa relacionada con la geología o para echar unas risas en la cafetería. A Isa, por toda su ayuda con los "bichos", que aunque al final no ha podido verse plasmada en un capítulo de estas tesis por motivos de tiempo, lo será en un futuro cercano, y por ello gracias. A todos los compañeros "precarios" del departamento, porque todos estamos metidos en el mismo embolao, a los que estaban por aquí cuando me incorporé (Matías, Raef, Gonzalo, Nono, Fernando, Jose María, Alicia, Esteban) y a los que han ido llegando o están casi por llegar (Sila, Pili, Rute, Jose Noel). A Francis, Agustín, y todos aquellos que han mostrado su interés al preguntarme sobre el desarrollo de esta tesis en estos últimos años.

Por supuesto, a mis compañeros de promoción con quienes tantas cosas he pasado y que la distancia nos impide repetir más a menudo. Y aunque muchos consideraban (y puede que nunca dejen de hacerlo) que perdía el tiempo pudiendo hacer cualquier otra cosa, siempre he tenido su apoyo. A Vicente (el ya sabe lo que sigue a su nombre), compañero de incertidumbre, gracias por compartir tus experiencias conmigo. A Alberto, el petrolero, que insiste en que me dedique a lo mismo que él, quizá en otras circunstancias, pero de momento, sabes que estoy bien donde estoy. A Nera, simplemente, sobran las palabras para ella. A Esther, la capitán C, por todos los buenos momentos que hemos pasado desde que nos conocimos hace ya 9 años. A Pedrochero, a Quillo, a Mimosín, Higi, Jose Mari, Bea, Pera, Chinchi...; gracias a todos de una u otra forma.

A Carol, Irene, y Ale, aprovecho estas líneas y os doy las gracias por todo en general, no sólo por estos últimos 4 años, sino por estas dos últimas décadas de amistad.

En mi experiencia germánica, mi más sincera gratitud a Christian Beztler, un alemán "especial", primero "profesor", ahora un amigo. Gracias por permitirme trabajar contigo en estos "slope carbonates" poniendo todo tu esfuerzo y atención en que esto vaya para delante. A Juan Manuel Cuevas, una ayuda fundamental mientras estuve allí. A Björn, Sebastian, Merle y David, "precarios" europeos. A Marcus y Ronald, otros alemanes "curiosos" con quienes compartí muchas risas en la "Europa Haus".

En kiwilandia, en primer lugar agradecer al Profesor Campbell S. Nelson, el padre de los carbonatos templados, por permitirme pasar 4 meses colaborando con él y su departamento. Gracias a él y Margaret por toda la ayuda logística dentro y fuera de la Universidad. Y aunque las circunstancias no permitieron una colaboración más estrecha, las charlas sobre carbonatos templados y temas diversos han resultado fructíferas. Si el tiempo lo permite, Cam, todavía podemos comentar muchas más cosas. Gracias a todo el "Department of Earth and Ocean Sciences" de la Universidad de Waikato por todo el apoyo que me prestaron. A Peter Kamp, por acogerme los primeros días y ayudarme a establecerme en Hamilton. Por toda la ayuda en esos 4 meses, del primer al último día, siempre dispuesto a echar una mano. Por las charlas sobre geología regional en el campo, muy útiles a la hora de entender la complicada geología de la zona. Al resto de la familia Kamp, a Betty-Anne, por todo, a Josef y Stephanie, por hacerme reír. A Adam Vonk y Kyle Bland por todas las charlas sobre cualquier cosa, y por invitarme a jugar al fútbol con su equipo. Sin duda una de mis mejores experiencias, fueron los estos partidos, gracias a todos jugadores por esos buenos momentos. A Sydney por su disposición a prestarme ayuda con todo el papeleo. A Steeve, una buena persona, Xu por enseñarme y ayudarme a preparar láminas delgadas, Anand, Mathias, Susan, Debra, Christian. A Orla y Rachel por su hospitalidad y la concesión del título honorífico de "best flatmate ever".

El trabajo realizado en esta tesis ha sido financiado fundamentalmente por los proyectos BTE2001-3023 del Ministerio de Ciencia y Tecnología de España y CGL2004-04342 del Ministerio de Educación y Ciencia de España, y por una beca-contrato F.P.U. (MECD-UGR) concedida al autor de la tesis, al amparo del cual, se realizaron las estancias en el extranjero.

Muchas gracias a Christine Laurin, porque sus correcciones y mejoras de los textos son siempre productivas y porque ha hecho todo lo posible para tener las correcciones en un tiempo record, para que hoy pudiese presentar esta memoria.

A mi club, al C.N. Granada, a Victor, Juan Antonio, Javi, Alicia, Belén, Roberto, y a todos mis niñ@s porque me sirven de vía de escape en los momentos de tristeza, incertidumbre, frustración y estrés.

A mi familia, por todo su apoyo y cariño. A mi padre, el primero que debería estar hoy aquí para ver realizado este trabajo, para verme empezar una nueva etapa en mi vida y compartirla conmigo, para estar aquí hoy, mañana y siempre, porque no te lo pude decir, gracias papá. A mi madre, para la que no tengo suficientes palabras para agradecerle todo lo que ha hecho por mí. A mi hermano Ale, que me ha ayudado con las cuestiones informáticas. A mis tíos, a mi abuelo, gracias.

Y especialmente a ti, nena, porque eres mi apoyo moral para todo. Por soportarme y animarme a seguir cuando las puertas se cerraban. Porque confiaste en mí y me animaste a empezar esta tesis aún cuando puede que tuviese otra cosa mejor para los dos, porque mis alegrías son tus alegrías, porque tus penas son mis penas, porque las todas cosas las logramos juntos, porque nuestro futuro es uno. Gracias Ana.

13

REFERENCES

Aguirre, J., Braga, J.C. and Martín, J.M., 1993. Algal nodules in the upper Pliocene deposits at the coast of Cádiz (S Spain). In: F. Barattolo, P. de Castro and M. Parente (Eds.), Studies on fossil benthic algae. Bolletino della Societá Paleontologica Italiana, Special Volume 1, 1–7.

Aguirre, J., 1998. El Plioceno de SE de la Península Ibérica (provincia de Almería). Síntesis estratigráfica, sedimentaria, bioestratigráfica y paleogeográfica. Revista de la Sociedad Geológica de España 11, 297-315.

Aguirre, J., 2000. Evolución paleoambiental y análisis secuencial de los depósitos pliocenos de Almayate (Málaga, sur de España). Revista de la Sociedad Geológica de España 13, 431–443.

Alexandersson, E.T., 1978. Destructive diagenesis of carbonate sediments in the eastern Skagerrak, North Sea. Geology 6, 324–327.

Alexandersson, E.T., 1979. Marine maceration of skeletal carbonates in the Skagerrak, North Sea. Sedimentology 26, 845–852.

Alonso, B. and Ercilla, G., 2003. Small turbidite systems in a complex tectonic setting (SW Mediterranean Sea): morphology and growth patterns. Marine and Petroleum Geology 19, 1256-1240.

Alsharhan, A.S. and Magara, K., 1995. Nature and distribution of porosity and permeability in Jurassic carbonate reservoirs of the Arabian Gulf Basin. Facies 32, 237–254.

Anastas, A.S., Dalrymple, R.W., James, N.P. and Nelson, C.S., 1997. Cross-stratified calcarenites from New Zealand: subaqueous dunes in a cool-water, Oligo-Miocene seaway. Sedimentology 44, 869–891.

Anastas, A.S., James, N.P., Nelson, C.S. and Dalrymple, R.W., 1998. Deposition and textural evolution of cool-water limestones: outcrop analog for reservoir potential in cross-bedded calcitic reservoirs. American Association of Petroleum Geologists Bulletin 82, 160-180.

Andrade, C., 1992. Tsunami generated forms in the Algarve barrier islands (South Portugal). Science of Tsunami Hazards 10, 21–34.

Anderson, K.S., Graham, S.A. and Hubbard, S.M., 2006. Facies, architecture, and origin of a reservoir-scale sand-rich succession within submarine canyon fill: insights from Wagon Caves Rock (Paleocene), Santa Lucía Range, California, U.S.A. Journal of Sedimentary Research 76, 819–838.

Andrews, J.E. and Hurley, R.J., 1978. Sedimentary processes in the formation of a submarine canyon. Marine Geology 26, 47–50.

Andruleit, H., Freiwald, A. and Schäfer, P., 1996. Bioclastic carbonate sediments on the southwestern Sualbard shelf. Marine Geology 134, 163–182.

Antobreh, A.A. and Krastel, S., 2006. Morphology, seismic characteristics and development of Cap Timiris Canyon, offshore Mauritania: a newly discovered canyon preserved-off a major arid climatic region. Marine and Petroleum Geology 23, 37–59.

Armstrong, B.D., 1987. Tertiary geology of Mangapehi Coalfied, King Country. BSc Hons Thesis, Victoria University, Wellington, New Zealand.

Aurell, M.,Bosence, D. and Waltham, D., 1995. Carbonate ramp depositional systems from a late Jurassic epeiric plarform (Iberian Basin, Spain): a combined computer modelling and outcrop analysis. Sedimentology 42,75–94.

Babonneau, N., Savoye, B., Cremer, M. and Klein, B., 2002. Morphology and architecture of the present canyon and channel system of the Zaire deep-sea fan. Marine and Petroleum Geology 19, 445–467.

Badenas, B., Aurell, M., Rodríguez-Tovar, F.J. and Pardo-Igúzquiza, E., 2003. Sequence stratigraphy and bedding rhythms of an outer ramp limestone succession (Late Kimmeridgian, Northeast Spain). Sedimentary Geology 161, 156–174.

Ballance, P.F., 1993. The New Zealand Neogene forearc basins. In P.F. Ballance (Ed.), Sedimentary basins of the world, 2. South Pacific sedimentary basins. Amsterdam, Elsevier, p. 177-193.

Bassi, D., Carannante, G., Murru, M., Simone, L. and Toscazo, F., 2006. Rhodalgal/bryomol assemblages in temperate-type carbonate channelized depositional systems: the Early Miocene of the Sarcidano area (Sardinia, Italy). In: H.M. Pedley and G. Carannante (Eds.), Cool-Water Carbonates: Depositional Systems and Palaeonvironmental Controls. Geological Society, London, Special Publication 255, 35–52.

Bathurst, R.G.C., 1975. Carbonate sediments and their diagenesis. Amsterdam, Elsevier, pp. 658.

Baztan, J., Berné, S., Olivet, J.L., Rabineau, M., Gaudin, D.M., Réhault, J.P. and Canals, M., 2005. Axial incision: the key to understand submarine canyon evolution (in the western Gulf of Lion). Marine and Petroleum Geology 22, 805–526.

Beer, R.M. and Gorsline, D.S., 1971. Distribution, composition and transport of suspended sediment in Redondo submarine canyon and vicinity (California). Marine Geology 10, 153–175.

Bergman, S.C. Atkinson C.D., Talbot, J. and Thompson, P.R. / ARCO Petroleum NZ Inc., 1990. Nature and reservoir potential of Miocene sedimentary and volcanic rocks, Western North Island, New Zealand. A reconnaissance field and laboratory study. PPL38449. Ministry of Economic Development New Zealand. Unpublished Petroleum Report PR1581, pp. 343.

Bergman, S.C., Talbot, J. and Thompson, P.R., 1992. The Kora Miocene submarine andesite stratovolcano hydrocarbon reservoir, Northern Taranaki Basin, New Zealand. 1991 New Zealand Oil Exploration Conference Proceedings. Wellington. Ministry of Commerce, p. 178–206.

Bertoni, C. and Cartwright, J., 2005. 3D seismic analysis of slope-confined canyons from the Plio-Pleistocene of the Ebro continental margin (western Mediterranean). Basin Research 17, 43–62.

Betzler, C., Brachert, T.C., Braga, J.C. and Martín, J.M., 1997a. Nearshore, temperate, carbonate depositional systems (lower Tortonian, Agua Amarga Basin, southern Spain): implications for carbonate sequence stratigraphy. Sedimentary Geology 113, 27–53.

Betzler, C., Brachert, T.C. and Nebelsick, J., 1997b. The warm temperate carbonate province–a review of facies, zonations, and delimitations. Courier Forschsungsinstitute Senckendberg 201, 83–99.

Betzler, C., Martín, J.M. and Braga, J.C., 2000. Non-tropical carbonates related to rocky submarine cliffs (Miocene, Almería, southern Spain). Sedimentary Geology 131, 51–65.

Betzler, C., Saxena, S., Swart, P.K., Isern, A. and James, N.P., 2005. Cool-water carbonate sedimentology and eustasy; Pleistocene upper slope environments, Great Australian Bight. Sedimentary Geology 175, 169–188.

Betzler, C., Braga, J.C., Martín, J.M., Sánchez-Almazo, I.M. and Lindhorst, S., 2006. Closure of a seaway: stratigraphic record and facies (Guadix Basin, southern Spain). International Journal of Earth Sciences (Geologische Rundschau) 95, 903–910.

Beu, A.G., 1995. Pliocene limestones and their scallops. Institute of Geological and Nuclear Sciences Monograph 10. Lower Hutt, New Zealand, Institute of Geological and Nuclear Sciences Ltd., pp. 243.

Beu, A.G. and Maxwell, P.A., 1990. Cenozoic Mollusca of New Zealand. New Zealand. Geological Survey Paleontological Bulletin 58, pp. 518.

Beuchamp, B. and Desrochers, A., 1997. Permian warm- to very cold-water carbonates and cherts in northwest Pangea. In: N.P. James and A.D. Clarke (Eds.), Cool-Water Carbonates. SEPM Special Publication 56, 327–347.

Bjørlykke, K., Bue, B. and Elverhøl, A., 1978. Quaternary sediments in the northwestern part of the Barents Sea and their relation to the underlying Mesozoic bedrock. Sedimentology 25, 227–246.

Blom, W.M. and Alsop, D.B., 1988. Carbonate mud sedimentation on a temperate shelf, Bass Basin, southeastern Australia. Sedimentary Geology 60, 269–280.

Bondevik, S., Svendsen, J.I. and Mangerud, J., 1997. Tsunami sedimentary facies deposited by the Storegga tsunami in shallow marine basins and coastal lakes, western Norway. Sedimentology 44, 1115–1131.

Bondevik, S., Løvholt, F., Harbitz, C., Mangerud, J., Dawson, A. and Svendsen J.I., 2005. The Storegga Slide tsunami–comparing field observations with numerical simulations. Marine and Petroleum Geology 22, 195–208.

Bonnel, C., Dennielou, B., Droz, L., Mulder, T. and Berné, S., 2005. Architecture and depositional pattern of the Rhône Neofan and recent gravity activity in the Gulf of Lions (western Mediterranean). Marine and Petroleum Geology 22, 827–843.

Boreen, T.D. and James, N.P., 1993. Holocene sediments dynamics on a cool-water carbonate shelf: Otway, southern Australia. Journal of Sedimentary Petrology 63, 574–588.

Boreen, T.D. and James, N.P., 1995. Stratigraphic sedimentology of Tertiary cool-water limestones, SE Australia. Journal of Sedimentary Research 65B, 142–159.

Bosence, D.W.J., 1983. The occurrence and ecology of recent rhodoliths. In: T.M. Peryt (Ed.), Coated Grains. Springer-Verlag, Berlin Heidelberg, p. 225–242.

Brachert, T.C., Betzler, C., Braga, J.C. and Martín, J.M., 1996. Record of climatic change in neritic carbonates: turnover in biogenic associations and depositional modes (Late Miocene, southern Spain). International Journal of Earth Sciences (Geologische Rundschau) 85, 327–337.

Brachert, T.C., Betzler, C., Braga, J.C. and Martín, J.M., 1998. Microtaphofacies of a warm-temperate carbonate ramp (Uppermost Tortonian/Lowermost Messinian, southern Spain). Palaios 13, 459–475.

Brachert, T.C., Hultzsch, N., Knoerich, A.C., Krautworst, U.M.R. and Stückrad, O.M., 2001. Climatic signatures in shallow-water carbonates: high-resolution stratigraphic markers in structurally controlled carbonate buildups (Late Miocene, southern Spain). Palaeogeography, Palaeoclimatology, Palaeoecology 175, 211–237.

Braga, J.C. and Aguirre, J., 2001. Coralline algal assemblages in upper Neogene reef and temperate carbonates in southern Spain. Palaeogeography Palaeoclimatology Palaeoecology 175, 27–41.

Braga, J.C. and Martín, J.M., 1988. Neogene coralline-algal growths-forms and their palaeoenvironments in the Almanzora river valley (Almería, SE Spain). Palaeogeography, Palaeoclimatology, Palaeoecology 67, 285–303.

Braga, J.C. and Martín, J.M., 1996. Geometries of reef advance in response to relative sea-level changes in a Messinian (uppermost Miocene) fringing reef (Cariatiz reef, Sorbas Basin, SE Spain). Sedimentary Geology 107, 61–81.

Braga, J.C., Martín, J.M. and Alcalá, B., 1990. Coral reefs in coarse-terrigenous sedimentary environments (Upper Tortonian, Granada Basin, southern Spain). Sedimentary Geology 66, 135–150.

Braga, J.C., Martín, J.M. and Riding, R. 1995. Controls on microbial dome fabric development along a carbonate-siliciclastic shelf-basin transect, Miocene, SE Spain. Palaios 10, 347–361.

Braga, J.C., Martín, J.M., Betzler, C. and Brachert, T.C., 1996a. Miocene temperate carbonates in Agua Amarga Basin (Almería, SE Spain). Revista de la Sociedad Geológica de España 9, 285–296.

Braga, J.C., Martín, J.M. and Riding, R. 1996b. Internal structure of segment reefs: *Halimeda* algal mounds in the Mediterranean Miocene. Geology 24, 35–38.

Braga, J.C., Martín, J.M. and Wood, J.L., 2001. Submarine lobes and feeder channels of redeposited, temperate carbonate and mixed siliciclastic-carbonate platform deposits (Vera Basin, Almería, southern Spain). Sedimentology 48, 99–116.

Braga J.C., Betzler, C., Martín J.M. and Aguirre, J., 2003a. Spit-platform temperate carbonates: the origin of landward-downlapping beds along a basin margin (Lower Pliocene, Carboneras Basin, SE Spain). Sedimentology 50, 553–563.

Braga, J.C., Martín, J.M. and Quesada, C., 2003b. Patterns and average rates of late Neogene-Recent uplift of the Betic Cordillera, SE Spain. Geomorphology 50, 3–26.

Braga, J.C., Martín, J.M., Betzler, C. and Aguirre, J., 2006a. Models of temperate carbonate deposition in Neogene basins in SE Spain: a synthesis. In: H.M. Pedley and G. Carannante (Eds.), Cool-Water Carbonates: Depositional Systems and Palaeonvironmental Controls. Geological Society, London, Special Publication 255, 121–135.

Braga, J.C., Martín, J.M., Riding, R., Aguirre, J., Sánchez-Almazo, I.M. and Dinarés-Turrel, J., 2006b. Testing models for the Messinian Salinity Crisis: the Messinian record in Almería, SE Spain. Sedimentary Geology 188–189, 131–154.

Brandley, R.T. and Krause, F.F., 1997. Upwelling, thermoclines and wave-sweeping on an equatorial carbonate ramp: Lower Carboniferous strata of western Canada. In: N.P. James and A.D. Clarke (Eds.), Cool-Water Carbonates. SEPM Special Publication 56, 365–390.

Bressan, G. and Babbini, L., 2003. Corallinales del Mar Mediterraneo: guida alla determinazione. Biología Marina Mediterranea 10, 1–237.

Briggs, R.M., Middleton, M.P. and Nelson, C.S., 2004. Provenance history of a Late Triassic-Jurassic Gondwana margin forearc basin, Murihiku Terrane, North Island, New Zealand: petrographic and geochemical constraints. New Zealand Journal of Geology and Geophysics 47, 589–602.

Brookfield, M.E., 1988. A mid-Ordovician temperate carbonate shelf-the Black River and Trenton Limestone Groups of southern Ontario, Canada. Sedimentary Geology 60, 137–153.

Bryant, E.A. and Nott, J., 2001. Geological indicators of large tsunami in Australia. Natural Hazards 24, 231–249.

Bryant, E.A., Young, R.W. and Price, D.M., 1992. Evidence of tsunami sedimentation on the southeastern coast of Australia. The Journal of Geology 100, 753–765.

Burchette, T.P. and Wright, V.P., 1992. Carbonate ramp depositional systems. Sedimentary Geology 79, 3–57.

Burne, R.V. and Colwell, J.B., 1982. Temperate carbonate sediments of northern Spencer Gulf, South Australia: a high salinity "foramol" province. Sedimentology 29, 223–238.

Bussert, R. and Aberhan, M., 2004. Storms and tsunamis: evidences of event sedimentation in the Late Jurassic Tendaguru beds of southeastern Tanzania. Journal of African Earth Sciences 39, 549–555.

Cantalamessa, G. and Di Celma, C., 2005. Sedimentary features of tsunami backwash deposits in a shallow marine Miocene setting, Mejillones Peninsula, northern Chile. Sedimentary Geology 178, 259–273.

Carannante, G., Esteban, M., Milliman, J.D. and Simone, L., 1988. Carbonate lithofacies as paleolatitude indicators: problems and limitations. Sedimentary Geology 60, 333–346.

Carey, J.S., Moslow, T.F. and Varrie, J.V., 1995. Origin and distribution of Holocene temperate carbonates, Hecate Strait, western Canada continental shelf. Journal of Sedimentary Research 65, 185–194.

Carey, S., Morell, D., Sigurdsson, H. and Bronto, S., 2001. Tsunami deposits from major explosive eruptions: an example from the 1883 eruption of Krakatau. Geology 29, 347–350.

Caron, V., Nelson, C.S. and Kamp, P.J.J., 2004a. Transgressive surfaces of erosion as sequence boundary markers in cool-water shelf carbonates. Sedimentary Geology 164, 179–189.

Caron, V., Nelson, C.S. and Kamp, P.J.J., 2004b. Contrasting carbonate depositional systems for Pliocene cool-water limestones cropping out in central Hawke's Bay, New Zealand. New Zealand Journal of Geology and Geophysics 47, 697–717.

Caron, V., Nelson, C.S. and Kamp, P.J.J., 2005. Sequence stratigraphic context of syndepositional diagenesis in cool-water shelf carbonates: Pliocene limestones, New Zealand. Journal of Sedimentary Research 75, 231-250.

Cerepi, A., Barde, J.P. and Labat, N., 2003. High-resolution characterization and integrated study of a reservoir formation: the danian carbonate platform in the Aquitane Basin (France). Marine and Petroleum Geology 20, 1161–1183.

Chaproniere, G.C.H., 1984. Oligocene and Miocene larger Foraminiferida from Australia and New Zealand. Bureau of Mineral Resources Bulletin 188.

Chave, K.E., 1967. Recent carbonate sediments: an unconventional view. Journal of Geological Education 19, 200–204.

Cherniawsky, J.Y., Titov, V.V., Wang, K.L. and Jing-Yang, L., 2007. Numerical simulations of tsunami waves and currents for souther Vancouver Island from a Cascadia megathrust earthquake. Pure and Applied Geophysics 164, 465–492.

Cita, M.B., Camerlenghi, A. and Rimoldi, B., 1996. Deep-sea tsunami deposits in the eastern Mediterranean: new evidence and depositional models. Sedimentary Geology 104, 155–173.

Clague, J.J. and Bobrowsky, P.T., 1994. Evidence for a large earthquake and tsunami 100-400 years ago on western Vancouver Island, British Columbia. Quaternary Research 41, 176–184.

Clague, J.J., Bobrowsky, P.T. and Hutchinson, I., 2000. A review of geological records of large tsunamis at Vancouver Island, British Columbia, and implications for hazards. Quaternary Science Reviews 19, 849–863.

Clark, J.D. and Pickering, K.T., 1996. Submarine channels: Processes and architecture. Vallis Press, London, pp. 229.

Clarke, J.D.A., Bone, Y. and James, N.P., 1996. Cool-water carbonates in an Eocene palaeoestuary, Norseman Formation, Western Australia. Sedimentary Geology 101, 213–226.

Conolly, R., 1968. Submarine canyons of the continental margin, East Bass Strait (Australia). Marine and Petroleum Geology 6, 449-461.

Cronin, B.T., Akhmetzhanov, A.M., Mazzini, A., Akhmanov, G., Ivanoc, M. and Kenyon, N.H., 2005. Morphology, evolution and fill: implications for sand and mud distribution in filling deep-water canyons and slope channel complexes. Sedimentary Geology 179, 71–97.

Cuffey, R.J., 1977. Bryozoan contribution to reefs and bioherms through geologic time. In: S.H. Frost, M.P. Weiss and J.B. Saunders (Eds.), Reefs and Related Carbonates Ecology and Sedimentology. American Association of Petroleum Geologists, Studies in Geology 4, 181–194.

Curray, J.R., Emmel, F.J. and Moore, D.G., 2003. The Bengal Fan: morphology, geometry and processes. Maringe and Petroleum Geology 19, 1191–1223.

Davies, G.R., 1970. Carbonate-bank sedimentation, eastern Shark-Bay, Western Australia. American Association of Petroleum Geologists, Memoir 13, 85–168.

Dabrio, C.J., Fernández, J., Peña, J.A., Ruíz-Bustos, A. and Sanz de Galedeano, C.M., 1978. Rasgos sedimentarios de los conglomerados Miocénicos del borde NE de la Depresión de Granada. Estudios Geológicos 34, 89–97.

Dabrio, C.J., Martín, J.M. and Megías, A.G., 1982. Signification sédimentaire des évaporites de la depresión de Grenade (Espagne).Bulletin de la Société Géologique de France 4, 705–710.

Davies, P. and Hasslet, S.K., 2000. Identifying storm or tsunami events in coastal basin sediments. Area 32.3, 1–2.

Dawson, A.G. and Shi, S., 2000. Tsunami deposits. Pure and Applied geophysics 157, 875–897.

Dawson, A.G. and Stewart, I., 2007. Tsunami deposits in the geological record. Sedimentary Geology 200, 166–183.

Dawson, A.G., Shi, S., Dawson, S., Takahashi, T. and Shuto, N., 1996. Coastal sedimentation associated with the June 2nd and 3rd, 1994 tsunami in Rajegwesi, Java. Quaternary Science Reviews 15, 901–912.

Dix, G.R. and Nelson, C.S., 2004. The role of tectonism in sequence development and facies distribution of Upper Oligocene cool-water carbonates: Coromandel Peninsula, New Zealand. Sedimentology 51, 231–251.

Dix, G.R. and Nelson, C.S., 2006. Diagenetic potential for lithification of cool-water carbonate shelf mud. Sedimentary Geology 185, 41–58.

Domack, E.W., 1988. Biogenic facies in the Antarctic glacimarine environment: basis for a polar glacimarine summary. Palaeogeography, Palaeoclimatology, Palaeoecology 63, 357–372.

Drexler, T.M., Nittrouer, C.A. and Mullenbach, B.L., 2006. Impact of local morphology on sedimentation in a submarine canyon, ROV studies Eel Canyon, northern California, U.S.A. Journal of Sedimentary Research 76, 839–853.

Druckman, Y., Buchbinder, B., Martinotti, G.M., Siman Tov, R. and Aharon, P., 1995. The buried Afiq Canyon (eastern Mediterranean, Israel): a case study of a Tertiary submarine canyon exposed in Late Messinian times. Marine Geology 123, 167–185.

Dunham, R.J., 1962. Classification of carbonate rocks according to depositional texture. In: W.E. Ham (Ed.), Classification of carbonate rocks. American Association of Petroleum Geologists Memoir 1, 108–121.

Ehrenberg, S.N. and Nadeau, P.H., 2005. Sandstone vs. Carbonate petroleum reservoirs: A global perspective on porosity-depth and porosity-permeability relationships. American Association of Petroleum Geologists 89, 435–445.

Einsele, G., Chough, S.K. and Shiki, T., 1996. Depositional events and their records–an introduction. Sedimentary Geology 104, 1–9.

Elliott, G.M., Shannon, P.M, Haughton, P.D.W., Praeg. D. and O'Reilly, B., 2006. Mid- to Late Cenozoic canyon development on the eastern margin of the Rockall Trough, offshore Ireland. Marine Geology 229, 113–132.

Elrick, M., 1995. Cyclostratigraphy of Middle Devonian carbonates of the eastern Great Basin. Journal of Sedimentary Research 65, 61–79.

Elrick, M. and Hinnov, L.A., 2007. Millennial-scale paleoclimate cycles recorded in widespread Palaeozoic deeper water rhythmites of North America. Palaeogeography, Palaeoclimatology, Palaecology 243, 348–372.

Embry, A.F. and Klovan, J.F., 1971. A late Devonian reef tract on northeastern Banks Island, Northwest Territories. Bulletin of Canadian Petroleum Geology 19, 730–781.

Emmanuel, L., Robin, C. and Renard, M., 2002. Data report: Trace element geochemistry of Cenozoic cool-water carbonates, Sites 1126–1132, Great Australian Bight. In: A.C. Hine, D.A. Feary and M.J. Malone (Eds.), Proceedings of the Ocean Drilling Program, Scientific Results, 182, 1–24. Available online from http://www-odp.tamu.edu/publications/182_SR/VOLUME/CHAPTERS/008.PDF.

Farrow, G.E. and Fyfe, J.A., 1988. Bioerosion and carbonate mud production on high-latitude shelves. Sedimentary Geology 60, 281–297.

Farrow, G.E., Allen, N.H. and Akpan, E.B., 1984. Bioclastic carbonate sedimentation on a high-latitude tide-dominated shelf: northeast Orkney Islands, Scotland. Journal of Sedimentary Petrology 54, 373–393.

Feary, D.A. and James, N.P., 1998. Seismic stratigraphy and geological evolution of the Cenozoic, cool-water Eucla Platform, Great Australia Bight. American Association of Petroleum Geologists Bulletin 82, 792–816.

Feary, D.A., Hine, A.C., Malone, M.J., *et al.*, 2000a. Leg 182 Summary: Great Australian Bight–Cenozoic cool-water carbonates. Proceedings of the Ocean Drilling Program, Initial Reports, Volume 182, pp. 58. Available online from http://www-odp.tamu.edu/publications/182_IR/VOLUME/CHAPTERS/IR182_01.PDF. doi:10.2973/odp.proc.ir.182.101.2000

Feary, D.A., Hine, A.C., Malone, M.J., *et al.*, 2000b. Site 1131. Proceedings of the Ocean Drilling Program, Initial Reports Volume 182, pp. 82. Available online from http://www-odp.tamu.edu/publications/182_IR/VOLUME/CHAPTERS/IR182_09.PDF. doi:10.2973/odp.proc.ir.182.109.2000

Fernández, J. and Rodríguez-Fernández, J., 1991. Facies evolution of nearshore marine clastic deposits during the Tortonian transgression–Granada Basin, Betic Cordilleras, Spain. Sedimentary Geology 71, 5–21.

Fernández, J., Soria, J. and Viseras, C., 1996. Stratigraphic architecture of the Neogene basins in the central sector of the Betic Cordillera (Spain); Tectonic control and base level changes. In: P.F. Friend and C.J. Dabrio (Eds.), Tertiary basins of Spain: The stratigraphic record of crustal kinematics, Cambridge University Press, Cambridge, p. 353–365.

Fildani, A. and Normark, W.R., 2004. Late Quaternary evolution of channel and lobe of Monterey Fan. Marine Geology 206, 199–223.

Fisher, A.G., 1964. The Lofer cyclothems of the Alpine Triassic. Kansas Geological Survey Bulletin 169, 107–149.

Fornos, J.J. and Ahr, W.M., 1997. Temperate carbonates on a modern, low-energy, isolated ramp: the Balearic platform, Spain. Journal of Sedimentary Research 67, 364–373.

Franseen, E.K., Goldstein, R.H. and Farr, M.R., 1997. Substrate-slope and temperature controls on carbonate ramps: revelations from upper Miocene outcrops, SE Spain. In: N.P. James and A.D. Clarke (Eds.), Cool-Water Carbonates. SEPM Special Publication 56, 271–290.

Freiwald, A., 1998. Modern nearshore cold-temperate calcareous sediments in the Troms District, nothern Norway. Journal of Sedimentary Research 68, 763–776.

Fujiwara, O., Masuda, F., Sakai, T., Irizuki, T. and Fuse, K., 2000. Tsunami deposits in Holocene bay mud in southern Kanto region, Pacific coast of central Japan. Sedimentary Geology 135, 219–230.

Fukushima, Y, Parker, G. and Pantin, H.M., 1985. Prediction of ignitive turbidity currents in Scripps Submarine Canyon. Marine Geology 67, 55–81.

Galloway, W.E., Dingus, W.F. and Paige, R.E., 1991. Seismic and depositional facies of Paleocene-Eocene Wilcox Group Submarine canyon fills, Northwest Gulf Coast, USA. In: M.H. Link and P. Weimer (Eds), Seismic Facies and Sedimentary Processes of Submarine Fans and Turbidite Systems. Springer-Verlag, New York, p. 247–271.

Gani, M.R., 2004. From turbid to lucid: a straightforward approach to sediment gravity flows and their deposits. The Sedimentary Record 2, 4–8.

García, M., Alonso, B, Ercilla, G. and Gracia, E., 2006. The tributary valley systems of the Almeria Canyon (Alboran Sea, SW Mediterranean): sedimentary architecture. Marine Geology 226, 207–223.

Gardner, J.V., Dartnell, P., Mayer, L.A. and Clarke, J.E.H., 2003a. Geomorphology, acoustic backscatter, and processes in Santa Monica Bay from multibeam mapping. Marine Environmental Research 56, 15–46.

Gardner, M.H., Borer, J.M., Melick, J.J., Mavilla, N., Dechesne, M. and Wagerle, R.N., 2003b. Stratigraphic process-response model for submarine channels and related features from studies of Permian Brushy Canyon outcrops, West Texas. Marine and Petroleum Geology 20, 757–787.

Gaudin, M., Mulder, T., Cirac, P., Berné, S. and Imbert, P., 2006. Past and present sedimentary activity in the Capbreton Canyon, southern Bay of Biscay. Geo-Marine Letters 26, 331–345.

Gautier, F., Clauzon, G., Suc, J.P., Cravatte, J. and Violanti, D., 1994. Age et durée de la crise de la salinité messinienne. Comptes Rendus de l'Académie de Sciences de Paris 318, 1103–1109.

Gehrels, W.R. and Long, A.J., (Eds.) 2007. Quaternary land–ocean interactions: sea-level change, sediments and tsunami. Marine Geology 242, 1–220.

Gerritsen, S.W., 1994. The regional stratigraphy and sedimentology of the Miocene sequence in the Ohura-Taumarunui region. Unpublished MSc. Thesis, University of Waikato, Hamilton, New Zealand, pp. 208.

Ghibaudo, G., 1992. Subaqueous sediment gravity flow deposits: Practical criteria for their field description and classification. Sedimentology 39, 423–454.

Gillespie, J.L., 1992. Late Quaternary carbonate clastic sedimentation on a temperate shelf, offshore Wanganui, New Zealand. Unpublished MSc. Thesis, University of Waikato, Hamilton, New Zealand, pp. 303.

Gillespie, J. L. and Nelson, C.S., 1996. Distribution and control of mixed terrigenous-carbonate surficial sediment facies, Wanganui shelf, New Zealand. New Zealand Journal of Geology and Geophysics 39, 533–549.

Gillespie, J. L. and Nelson, C.S., 1997. Mixed siliciclastic-skeletal carbonate facies on Wanganui Shelf, New Zealand: a contribution to the temperate carbonate model. In: N.P. James and A.D. Clarke (Eds.), Cool-Water Carbonates. SEPM Special Publication 56, 127–140.

Gillespie, J.L., Nelson, C.S. and Nodder, S.D., 1998. Post-glacial sea-level control and sequence stratigraphy of carbonate-terrigenous sediments, Wanganui shelf, New Zealand. Sedimentary Geology 122, 245–266.

Ginsburg, R.N., 1956. Environmental relationships of grain size and constituent particles in some south Florida carbonate sediments. American Association of Petroleum Geologists Bulletin 40, 2384–2427.

Gladstone, C. and Sparks, R.S.J., 2002. The significance of grain-size breaks in turbidites and pyroclastic density current deposits. Journal of Sedimentary Research 72, 182–191.

Gläser, I. and Betzler, C., 2002. Facies partirioning and sequence stratigraphy of cool-water, mixed carbonate-siliciclastic sediments (Upper Miocene Guadalquivir Domain, southern Spain). International Journal of Earth Sciences (Geologische Rundschau) 91, 1041–1053.

Goff, J., Chagué-Goff, C. and Nichol, S., 2001. Palaeotsunami deposits: a New Zealand perspective. Sedimentary Geology 143, 1–6.

Goff, J., McFadgen, B.G. and Chagué-Goff. C., 2004. Sedimentary differences between the 2002 Easter storm and the 15 th-century Okoropunga tsunami, southeastern North Island, New Zealand. Marine Geology 204, 235–250.

Goff, J., Dudley, W.C., deMaintenon, M.J., Cain, G. and Coney, J.P., 2006. The largest local tsunami in 20th century Hawaii. Marine Geology 226, 65–79.

Gong, Y.M., Li, B.H., Wang, C.Y. and Wu, Y., 2001. Orbital cyclostratigraphy of the Devonian Frasnian–Famennian transition in South China. Palaeogeography, Palaeoclimatology, Palaecology 168, 237–248.

Goodwin, R.H. and Prior, D.B., 1989. Geometry and depositional sequences of the Mississippi Canyon, Gulf of Mexico. Journal of Sedimentary Petrology 56, 318–329.

Gorsline, D.S., 1970. Submarine canyons: an introduction. Marine Geology 8, 183–186.

Grossi, C.M. and Murray, M., 1999. Characteristics of carbonate building stones that influence the dry deposition of acidic gases. Construction and Building Materials 13, 101–108.

Hageman, S.J., James, N.P. and Bone, Y., 2000. Cool-water carbonate production from epizoic bryozoans on ephemeral substrates. Palaios 15, 33–48.

Halfar, J. and Ingle, J.C., 2003. Modern warm-temperate and subtropical shallow-water benthic foraminifera of the southern Gulf of California, Mexico. Journal of Foraminiferal Research 33, 309–329.

Halfar, J., Godinez-Orta, L. and Ingle, J.C., 2000. Microfacies analysis of recent carbonate environments in the southern Gulf of California, Mexico–a model for warm-temperate to subtropical carbonate formation. Palaios 15, 323–342.

Halfar, J., Ingle, J.C. and Godinez-Orta, L., 2004. Modern non-tropical mixed carbonate-siliciclastic sediments and environments of the southwestern Gulf of California, Mexico. Sedimentary Geology 165, 93-115.

Halfar, J., Godinez-Orta, L., Mutti, M., Valdez-Holguin., J.E. and Borges, J.M., 2006. Carbonates calibrated against oceanographic parameters along a latitudinal transect in the Gulf of California, Mexico. Sedimentology 53, 297–320.

Hall, I.R., McCave, I.N., Shackleton, N.J., Weedon, G.P. and Harris, S.E., 2001. Intensified deep Pacific inflow and ventilation in Pleistocene glacial times. Nature 412, 809–812.

Happy, A.J., 1971. Tertiary geology of the Awakino Area, North Taranaki. Unpublished MSc. Thesis, University of Auckland, New Zealand, 136 pp.

Haq, B.U., Hardenbol, J. and Vail, P.R., 1987. Chronology of fluctuating sea levels since the Triassic. Science 235, 1156–1167.

Harmsen, F.J., 1990. Te Aute Group limestones: a potential reservoir rock in the East Coast Basin, New Zealand. In: 1989 New Zealand Oil Exploration Conference Proceedings. Wellington, Petroleum and Geothermal Unit, Ministry of Commerce, p. 181–190.

Hassan, M., 1973. Radioelements and diagenesis in shale and carbonate sediments. SAID 2nd Annual Symposium Trans., paper 8, 1–7.

Hay, R.F., 1967. Sheet 7-Taranaki. Geological Map of New Zealand 1:250,000. Wellington, New Zealand. Department of Science and Industrial Research.

Hayton, S., Nelson. C.S. and Hood, S.D., 1995. A skeletal assemblage classification system for non-tropical deposits based on New Zealand Cenozoic limestones. Sedimentary Geology 100, 123–141.

Hayward, B.W., 1977. Lower Miocene corals from the Waitakere Ranges, North Auckland, New Zealand. Journal of the Royal Society of New Zealand 7, 99–111.

Heinrich, P., Piatanesi, A. and Hebert, H., 2001. Numerical modelling of tsunami generation and propagation from submarine slumps: the 1998 Papua New Guinea event. Geophysical Journal International 145, 97–111.

Henrich, R., Freiwald, A., Bickert, T. and Schäfer, P., 1997. Evolution of an Arctic open-shelf carbonate platform, Spitsbergen Bank (Barents Sea). In: N.P. James and A.D. Clarke (Eds.), Cool-Water Carbonates. SEPM Special Publication 56, 163–181.

Herb, R., 1984. Récifs à Huitres actuels et miocènes. In : J. Geister and R. Herb (Eds), Géologie et Paléoécologie des Récifs. Institut de Géologie de l'Université de Berne, Berne, p. 6.1–6.22.

Herzer, R.H. and Lewis, D.W., 1979. Growth and burial of a submarine canyon off Motunau, north Canterbury, New Zealand. Sedimentary Geology 24, 69–83.

Hetzinger, S., Halfar, J., Riegl, B. and Godinez-Orta, L., 2006. Sedimentology and acoustic mapping of modern rhodolith facies on a non-tropical carbonate shelf (Gulf of California, México). Journal of Sedimentary Research 76, 670–682.

Hilgen, F.J., Krijgsman, W., Langereis, C.G., Lourens, L.J., Santarelli, A. and Zachariasse, W.J., 1995. Extending the astronomical (polarity) time scale into the Miocene. Earth and Planetary Science Letters 136, 495–510.

Hindson, R.A. and Andrade, C., 1999. Sedimentation and hydrodynamic processes associated with the tsunami generated by the 1755 Lisbon earthquake. Quaternary International 56, 27–38.

Holdgate, G. and Gallagher, S., 1997. Microfossil paleoenvironments and sequence stratrigraphy of Tertiary cool-water carbonates, onshore Gippsland Basin, southeastern Australia. In: N.P. James and A.D. Clarke (Eds.), Cool-Water Carbonates. SEPM Special Publication 56, 205–220.

Hood, S.D. and Nelson, C.S., 1996. Cementation scenarios for New Zealand Cenozoic nontropical limestones. New Zealand Journal of Geology and Geophysics 39, 109–122.

Hood, S.D., Nelson, C.S. and Kamp, P.J.J., 2003. Petrogenesis of diachronous mixed siliciclastic-carbonate megafacies in the cool-water Oligocene Tikorangi Formation, Taranaki Basin, New Zealand. New Zealand Journal of Geology and Geophysics 46, 387–405.

Hood, S.D., Nelson, C.S. and Kamp, P.J.J., 2004a. Discriminating cool-water from warm-water carbonates and their diagenetic environments using element geochemistry: the Oligocene Tikorangi Formation (Taranaki Basin) and the dolomite effect. New Zealand Journal of Geology and Geophysics 47, 857–869.

Hood, S.D., Nelson, C.S. and Kamp, P.J.J., 2004b. Burial dolomitisation in a non-tropical carbonate petroleum reservoir: the Oligocene Tirorangi Formation, Taranaki Basin, New Zealand. Sedimentary Geology 172, 117–138.

Hornibrook, N.deB., 1968. Distribution of some warm water benthic foraminifera in the N.Z. Tertiary. Tuatara 16, 11–15.

Hornibrook, N.deB., 1992. New Zealand Cenozoic marine paleoclimates: a review based on the distribution of some shallow water and terrestrial biota. In: T. Tsuchi and J. Ingle (Eds.), Pacific Neogene environment, evolution, and events, Tokyo. University of Tokyo Press, p. 83–106.

Hosking, C.M. and Nelson, Jr, R.V., 1969. Modern marine carbonate sediments, Alexander Archipelago, Alaska. Journal of Sedimentary Petrology 39, 581–590.

Hunt, T.M., 1980. Basement structure of the Wanganui Basin, onshore, interpreted from gravity data. New Zealand Journal of Geology and Geophysics 23, 1–16.

Huvaz, O., Sarikaya, H. and Isik, T., 2007. Petroleum systems and hydrocarbon potential analysis of the northwestern Uralsk basin, NW Kazakhastan, by utilizing 3D basin modelling methods. Marine and Petroleum Geology 24, 247–275.

Inman, D.L., Nordstrom, C.E. and Flick, R.E., 1976. Currents in submarine canyons: an air-sea-land interaction. Annual Reviews of Fluid Mechanics 8, 275–210.

Inthorn, M., Mohrholz, V. and Zabel, M., 2006. Nepheloid layer distribution in the Benguela upwelling area offshore Namibia. Deep-Sea Research I 53, 1423–1438.

James, N.P., 1997. The cool-water carbonate depositional realm. In: N.P. James and A.D. Clarke (Eds.), Cool-Water Carbonates. SEPM Special Publication 56, 1–20.

James, N.P. and Bone, Y., 1991. Origin of a cool-water Oligo-Miocene deep-shelf limestone, Eucla Platform, southern Australia. Sedimentology 60, 323–341.

James, N.P. and Bone, Y., 1994. Palaeoecology of cool-water, subtidal cycles in Mid-Cenozoic limestones, Eucla Platform, southern Australia. Palaios 9, 457–476.

James, N.P. and Bone, Y., 2007. A late Pliocene-Early Pleistocene,inner-shelf, subtropical, seagrass-dominated carbonate: Roe Calcarenite, Great Australian Bight, Western Australia. Palaios 22, 343–359.

James, N.P. and Bourque, P.A., 1992. Reefs and mounds. In: R.G. Walker and N.P. James (Eds.), Facies models: Response to sea level. St. John's Newfoundland, Geological Association of Canada, p. 323–347.

James, N.P. and Clarke, A.D., (Eds.) 1997. Cool-Water Carbonates. SEPM Special Publication 56, pp. 440.

James, N.P., Bone, Y., Von der Borch, C.C. and Gostin, V.A., 1992. Modern carbonate and terrigenous clastic sediments on a cool-water, high energy, mid-latitude shelf, Lacepede Shelf, southern Australia. Sedimentology 34, 877–904.

James, N.P., Boreen, T.D., Bone, Y. and Feary, D.A., 1994. Holocene carbonate sedimentation on the west Eucla Shelf, Great Australian Bight: a shaved shelf. Sedimentary Geology 90, 161–177.

James, N.P., Bone, Y., Hageman, S.J., Feary, D.A. and Gostin, V.A., 1997. Cool-water carbonate sedimentation during the terminal Quaternary sea-level cycle: Lincoln Shelf, southern Australia. In: N.P. James and A.D. Clarke (Eds.), Cool-Water Carbonates. SEPM Special Publication 56, 53–75.

James, N.P., Collins, L.B., Bone, Y. and Hallock, P., 1999. Subtropical carbonates in a temperate realm: modern sediments on the southwest Australian shelf. Journal of Sedimentary Research 69, 1297–1321.

James, N.P., Feary, D.A., Surlyk, F., Simo, J.A.T., Betzler, C., Holbourn, A.E., Li, Q., Matsuda, H., Machiyama, H., Brooks, G.R., Andres, M.S., Hine, A.C. and Malone, M.J., 2000. Holocene bryozoan reef mounds in cool-water, upper slope environments: Great Australian Bight. Geology 28, 647–650.

James, N.P., Bone, Y., Collins, L.B. and Kyser, T.K., 2001. Surficial sediments of the Great Australian Bight: facies dynamics and oceanography on a vast cool-water carbonate shelf. Journal of Sedimentary Research 71, 549–568.

James, N.P., Feary, D.A., Betzler, C., Bone, Y., Holbourn, A.E., Li, Q., Machiyama, H., Simo, T.J.A. and Surlyk, F., 2004. Origin of late Pleistocene bryozoan reef mounds: Great Australian Bight. Journal of Sedimentary Research 74, 20–48.

James, N.P., Bone, Y. and Kyser, T.K., 2005. Where has all the aragonite gone? Mineralogy of Holocene neritic cool-water carbonates, southern Australia. Journal of Sedimentary Research 75, 454–463.

Jenkyns, H.C., 1986. Pelagic environments. In: H.G. Reading (Ed.), Sedimentary Environments and Facies. Blackwell Scientific Publication, Oxford, p. 343–397.

Jiménez de Cisneros, C. and Vera, J.A., 1993. Milankovitch cyclicity in Purbeck peritidal limestones of the Prebetic (Berriasian, southern Spain). Sedimentology 40, 513–537.

Johnson, C.L., Franseen, E.K. and Goldstein, R.H., 2005. The effects of sea level and paleotopography on lithofacies distribution and geometries in heterozoan carbonates, south-eastern Spain. Sedimentology 52, 513–536.

Kamen-Kaye, M., 1970. Geology and productivity of Persian Gulf synclinorium. American Association of Petroleum Geologists Bulletin 54, 2371– 2394.

Kamona, A.F. and Friedrich, G.H., 2007. Geology, mineralogy and stable isotope geochemistry of the Kabwe carbonate-hosted Pb-Zn deposits, Central Zambia. Ore Geology Reviews 30, 217–243.

Kamp, P.J.J., 1986. The mid-Cenozoic Challenger Rift System of western New Zealand and its implications for the age of the Alpine Fault inception. Geological Society of America Bulletin 97, 255–281.

Kamp, P.J.J. and Nelson, C.S., 1988. Nature and occurrence of modern and Neogene active margin limestones in New Zealand. New Zealand Journal of Geology and Geophysics 31, 1–20.

Kamp, P.J.J., Harmsen, F.J., Nelson, C.S. and Boyle, S.F., 1988. Barnacle-dominated limestone with giant cross-beds in a non-tropical, tide-swept, Pliocene forearc seaway, Hawke's Bay, New Zealand. Sedimentary Geology 60, 173–195.

Kamp, P.J.J., Vonk, A.J., Bland, K.J., Hansen, R.J., Hendy, A.J.W., McIntyre, A.P., Ngatai, M., Cartwrigth, S.J., Hayton, S. and Nelson, C.S., 2004. Neogene stratigraphic architecture and tectonic evolution of Wanganui, King Country, and eastern Taranaki Basins, New Zealand. New Zealand Journal of Geology and Geophysics 47, 625–644.

Kämpf, J., Doubell, M., Griffin, D., Matthews, R.L. and Ward, T.M., 2004. Evidence of a large seasonal coastal upwelling system along the southern shelf of Australia. Geophysical Research Letters 31, LO9310.

Keevil, G.M., Peakall, J., Best, J.L. and Amos, K.J., 2006. Flow structure in sinuous submarine channels: velocity and turbulence structure of an experimental submarine channel. Marine Geology 229, 241–257.

Kelsey, H.M., Nelson, A.R., Hemphill-Haley, E. and Witter, R.C., 2005. Tsunami history of an Oregon coastal lake reveals a 4600 yr record of great earthquakes on the Cascadia subduction zone. Geological Society of America Bulletin 117, 1009–1032.

Kenyon, N.H., Klaucke, I., Millington, J. and Ivanov, M., 2002. Sandy submarine canyon-mouth lobes on the western margin of Corsica and Sardinia, Mediterranean Sea. Marine Geology 184, 69–84.

Kidwell, S.M. and Holland, S.M., 1991. Field description of coarse bioclastic fabrics. Palaios 6, 426–434.

Kidwell, S.M., Fürsich, F.T. and Aigner, T., 1986. Conceptual framework for the analysis and classification of fossil concentrations. Palaios 1, 228–238.

King, P.R. and Thraser, G.P., 1996. Cretaceous-Cenozoic geology and petroleum systems of the Taranaki Basin, New Zealand. Institute of Geological and Nuclear Sciences Monogragh 13, Lower Hutt, IGNS Ltd., New Zealand, pp. 243.

King, P.R., Scott, G.H. and Robinson, P.H., 1993. Description, correlation and depositional history of Miocene sediments outcropping along the North Taranaki coast. Institute of Geological and Nuclear Sciences Monograph 5, Lower Hutt, IGNS Ltd., New Zealand, pp. 199.

Kinsman, D.J.J., 1968. Reef coral tolerance of high temperature and salinities. Nature 202, 1280–1282.

Klaucke, I., Masson, D.G., Kenyon, N.H. and Gardner, J.V., 2004. Sedimentary processes of the lower Monterey Fan channel and channel-mouth lobe. Marine Geology 206, 181–198.

Kleverlaan, K., 1987. Gordo megabed: a possible seismite in a Tortonian submarine fan, Tabernas Basin, province Almería, southeast Spain. Sedimentary Geology 51, 165–180.

Kleverlaan, K., 1989. Three distinctive feeder-lobe systems within one time slice of the Tortonian Tabernas fan, SE Spain. Sedimentology 36, 25–45.

Kneller, B. and Buckee, C., 2000. The structure and fluid mechanics of turbidity currents: a review of some recent studies and their geological implications. Sedimentology 47 (supplement 1), 62–94.

Kneller, B.C. and McCaffrey, W.D., 2003. The interpretation of vertical sequences in turbidite beds: the influence of longitudinal flow structure. Journal of Sedimentary Research 73, 706–713.

Krijgsman, W., Hilgen, F.J., Raffi, I., Sierro, F.J. and Wilson, D.S., 1999. Chronology, causes and progression of the Messinian salinity crisis. Nature 400, 652–655.

Kroon, D., Williams, T., Pirmez, C., Spezzaferri, S., Sato, T. and Wright, J.D., 2000. Coupled early Pliocene-middle Miocene bio-cyclostratigraphy of Site 1006 reveals orbitally induced cyclicity patterns of Great Bahama Bank carbonate production. Proceedings of the Ocean Drilling Program, Scientific Results, Volume 166, 155-166.

Kuznetsov, A.B., Krupenin, M.T., Ovchinnikova, G.V., Gorokhov, I.M., Maslov, A.V., Kaurova, O.K. and Ellmies, R., 2005. Diagenesis of carbonate and siderite deposits of the Lower Riphean Bakal Formation, the southern Urals: Sr Isotopic characteristics and Pb-Pb age. Lithology and Mineral Resources 40, 195–215.

Kyser, T.K., James, N.P. and Bone, Y., 1998. Alteration of Cenozoic cool-water carbonates to low-Mg calcite in marine waters, Gambier Embayment, south Australia. Journal of Sedimentary Research 68, 947–955.

Langer, M. and Hottinger, L., 2000. Biogeography of selected "larger" foraminifera. Micropaleontology 46, 277–301.

Lawton T.F., Shipley, K.W., Aschoff, J.L., Giles, K.A. and Vega, F.J., 2005. Basinward transport of Chicxulub ejecta by tsunami-induced backflow, La Popa Basin, notheastern Mexico, and its implications for distribution of impact-related deposits flanking the Gulf of Mexico. Geology 33, 81–84.

Leach, A.S. and Wallace, M.W., 2001. Cenozoic submarine canyon systems in cool water carbonates from the Otway Basin, Victoria, Australia. In: K.C. Hill and T. Bernecker (Eds), PESA-Eastern Australasian Basins Symposium, A Refocused Energy Perspective for the Future. PESA, Melbourne, Victoria, p. 465–473.

Lees, A., 1975. Possible influences of salinity and temperature on modern shelf carbonate sedimentation. Marine Geology 19, 159–198.

Lees, A. and Buller, A.T., 1972. Modern temperate-water and warm-water shelf carbonate sediments contrasted. Marine Geology 13, 1767–1773.

Leonard, J.E., Cameron, B., Pilkey, O.H. and Friedman, G.M., 1981. Evaluation of cold-water carbonates as a possible paleoclimatic indicator. Sedimentary Geology 28, 1–28.

Lewis, K.B. and Barnes, P.M., 1999. Kaikoura Canyon, New Zealand: active conduit from near-shore sediment zones to trench-axis channel. Marine Geology 162, 39–69.

Lewis, K.B. and Pantin, H.M., 2002. Channel-axis, overbank and drift sediment waves in the southern Hikurangi Trough, New Zealand. Marine Geology 192, 123–151.

Li, M.Z. and Amos, C.L., 1999. Sheet flow and large wave ripples under combined waves and currents: field observations, model predictions and effects on boundary layer dynamics. Continental Shelf Research 19, 637–663.

Lien, T., Walker, R.G. and Martinsen, O.J., 2003. Turbidites in the Upper Carboniferous Ross Formation, western Ireland: reconstruction of a channel and spillover system. Sedimentology 50, 113–148.

Lisiecki, L.E. and Raimo, M.E., 2005. A Pliocene-Pleistocene stack of 57 globally distributed benthic $\delta^{18}O$ records. Paleoceanography 20, PA1003.

Liu, J.T. and Lin, H., 2004. Sediment dynamics in a submarine canyon: a case of river-sea interaction. Marine Geology 207, 55–81.

Lowe, D.R., 1982. Sediment gravity flows: II. Depositional models with special reference to the deposits of high-density turbidity currents. Journal of Sedimentary Petrology 52, 279–297.

Lowe, D.R., and Guy, M., 2000. Slurry-flow deposits in the Britannia Formation (Lower Cretaceous), North Sea: a new perspective on the turbidity current and debris flow problem. Sedimentology 47, 31–70.

Lukasik, J.L., James, N.P., McGowran, B. and Bone, Y., 2000. An epeiric ramp: low-energy, cool-water carbonate facies in a Tertiary inland sea, Murray Basin, South Australia. Sedimentology 47, 851–881.

Luque, L., Lario, J., Civis, J., Silva, P.G., Zazo, C., Goy, J.L. and Dabrio, C.J., 2002. Sedimentary record of a tsunami during Roman times, Bay of Cadiz, Spain. Journal of Quaternary Science 17, 623–631.

Maiklem, W.R., 1970. Carbonate sediments in the Capricorn Reef Complex, Great Barrier Reef, Australia. Journal of Sedimentary Petrology 40, 55–80.

Martín, J.M. and Braga, J.C., 1994. Messinian events in the Sorbas Basin in southeastern Spain and their implications in the recent history of the Mediterranean. Sedimentary Geology 90, 254–268.

Martín, J.M. and Braga, J.C., 1996. Tectonic signals in the Messinian stratigraphy of the Sorbas Basin (Almería, SE Spain). In: F. Friend and C.J. Dabrio (Eds.), Tertiary basins of Spain. Tectonics, climate and sea-level change. Cambridge University Press, Cambridge, p. 387–391.

Martín, J.M., Ortega-Huertas, M. and Torres-Ruíz, J., 1984. Genesis and evolution of strontium deposits of the Granada Basin (southeastern Spain): evidence of diagenetic replacement of a stromatolite belt. Sedimentary Geology 39, 281–298.

Martín, J.M., Braga, J.C. and Rivas, P., 1989. Coral successions in Upper Tortonian reefs in SE Spain. Lethaia 22, 271–286.

Martín, J.M., Braga, J.C., Riding, R., 1993. Siliciclastic stromatolites and thrombolites, late Miocene, SE Spain. Journal of Sedimentary Petrology 63, 131–139.

Martín, J.M., Braga, J.C., Betzler, C. and Brachert, T., 1996. Sedimentary model and high-frequency cyclicity in a Mediterranean, shallow-shelf, temperate-carbonate environment (uppermost Miocene, Agua Amarga Basin, southern Spain). Sedimentology 43, 263–277.

Martín, J.M., Braga, J.C. and Riding, R. 1997. Late Miocene *Halimeda* alga-microbial segment reefs in the marginal Mediterranean Sorbas Basin, Spain. Sedimentology 44, 441–456.

Martín, J.M., Braga, J.C. and Sánchez-Almazo, I.M., 1999. The Messinian record of the outcropping marginal Alboran Basin deposits: significance and implications. Proceedings of the Ocean Drilling Program, Scientific Results, Volumen 161, 543–551.

Martín, J.M., Braga, J.C. and Betzler, C., 2001. The Messinian Guadalhorce corridor: the last northern Atlantic-Mediterranean gateway. Terra Nova 13, 418–424.

Martín, J.M., Braga, J.C., Aguirre, J. and Betzler, C., 2004. Contrasting models of temperate carbonate sedimentation in a small Mediterranean embayment: the Pliocene Carboneras Basin, SE Spain. Journal of the Geological Society, London 161, 387–399.

Martín, J.M., Braga, J.C., Sánchez-Almazo, I.M. and Aguirre, J., (*in press*). Temperate and tropical carbonate-sedimentation episodes in the Neogene Betic basins (S Spain) linked to climatic oscillations and changes in the Atlantic-Mediterranean connections. Constraints with isotopic data. In: C. Betzler, M. Mutti and W. Piller (Eds.), Oligocene-Miocene carbonate systems. IAS Special Publication.

Martín-Suárez, E., Freudenthal, M. and Agusti, J., 1993. Micromammals from the Middle Miocene of the Granada Basin (Spain). Geobios 26, 377–387.

Martín-Suárez, E., Freudenthal, M., Krijgsman, W., Fortuin, A.R., 2000. On the age of the continental deposits of the Zorreras Member (Sorbas Basin, SE Spain). Geobios 33, 505–512.

Martindale, W. and Boreen, T.D., 1997. Temperature-stratified Mississipian carbonates as hydrocarbon reservoirs–examples from the foothills of the Canadian Rockies. In: N.P. James and A.D. Clarke (Eds.), Cool-Water Carbonates. SEPM Special Publication 56, 391–409.

Massari, F. and D'Alessandro, A., 2000. Tsunami-related scour-and-drape undulations in Middle Pliocene restricted-bay carbonate deposits (Salento, south Italy). Sedimentary Geology 135, 265–281.

Massari, F. and Chiocci, F., 2006. Biocalcarenite and mixed cool-water prograding bodies of the Mediterranean Pliocene and Pleistocene: architecture, depositional setting and forcing factors. In: H.M. Pedley and G. Carannante (Eds.), Cool-Water Carbonates: Depositional Systems and Palaeonvironmental Controls. Geological Society, London, Special Publication 255, 95–120.

Mastronuzzi, G. and Sansò, P., 2000. Boulders transport by catastrophic waves along the Ionian coast of Apulia (southern Italy). Marine Geology 170, 93–103.

Mastronuzzi, G. and Sansò, P., 2004. Large boulders accumulations by extreme waves along the Adriatic coast of southern Apulia (Italy). Quaternary International 120, 173–184.

Mather, A.E., 1993. Basin inversion: some consequences for drainage evolution and alluvial architecture. Sedimentology 40, 1069–1089.

Mather, A.E., 2000. Impact of headwater river capture on alluvial system development: an example for SE Spain. Journal of the Geological Society, London 157, 957–966.

Mather, A.E. and Stokes, M., 2001. Marine to continental transition. In: A.E. Mather, J.M. Martin, A.M. Harvey and J.C. Braga (Eds.), A Field Guide to the Neogene Sedimentary Basins of the Almería Province, South-East Spain. Blackwell Science, Oxford, p. 186–189.

McAdoo, B.G., Orange, D.L., Screaton, E., Lee, H. and Kayen, R., 1997. Slope basins, headless canyons, and submarine palaeoseismology of the Cascadia accretionary complex. Basin Research 9, 313–324.

McHugh, C.M.G. and Olson, H.C., 2002. Pleistocene chronology of continental margin sedimentation: new insights into traditional models, New Jersey. Marine Geology 186, 389–411.

McHugh, C.M.G., Damuth, J.E. and Mountain, G.S. 2002. Cenozoic mass-transport facies and their correlation with relative sea-level change, New Jersey continental margin. Marine Geology 184, 295–334.

McKinney, F. and Jackson, J., 1989. Bryozoan Evolution. Unwin Hyman, London, pp. 238.

Merefield, J.R., 1984. Modern cool-water beach sands of southwest England. Journal of Sedimentary Petrology 54, 413–424.

Minoura, K., Nakaya, S. and Uchida, M., 1994. Tsunami deposits in a lacustrine sequence of the Sanriku coast, northeast Japan. Sedimentary Geology 89, 25–31.

Minoura, K., Gusiakovb, V.G., Kurbatovc, A., Takeutid, S., Svendsene, J.I., Bondevike, S. and Odaa, T., 1996. Tsunami sedimentation associated with the 1923 Kamchatka earthquake. Sedimentary Geology 106, 145–154.

Mitchell, J.K., Holdgate, G.R., Wallace, N.W. and Gallagher, S.J., 2007a. Marine geology of the Quaternary Bass Canyon system, southeast Australia: a cool-water carbonate system. Marine Geology 237, 71–96.

Mitchell, J.K., Holdgate, G.R. and Gallagher, S.J., 2007b. Pliocene-Pleistocene history of the Gippsland Basin outer shelf and canyon heads, southeast Australia. Australian Journal of Earth Sciences 54, 49–64.

Montenat, C., 1990. Les Bassins Neógènes du domaine Bétique Oriental (Espagne). Documents et Travaux, IGAL, Paris.

Mortimer, N., 1995. Origin of the Torlesse Terrane and coeval rocks, North Island, New Zealand. International Geology Review 36, 891–910.

Mulder, T. and Alexander, J., 2001. The physical character of subaqueous sedimentary density flows and their deposits. Sedimentology 48, 269–299.

Mutti, M. and Bernoulli, D., 2003. Early marine lithification and hardground development on a Miocene ramp (Maiella, Italy): Key surfaces to track changes in trophic resources in nontropical carbonate settings. Journal of Sedimentary Research 73, 296–308.

Nanayama, F., Shigeno, K., Satake, K., Shimokawa, K., Koitabashi, S. Miyasaka, S. and Ishii, M., 2000. Sedimentary differences between the 1993 Hokkaido-nansei-oki tsunami and the 1959 Miyakojima typhoon at Taisei, southwestern Hokkaido, northern Japan. Sedimentary Geology 135, 255–264.

Nees, S., 1997. Late Quaternary palaeoceanography of the Tasman Sea: the benthic foraminiferal view. Palaeogeography, Palaeoclimatology, Palaeoecology 131, 365–389.

Neilson, J.E., Oxtoby, N.H., Simmons, M.D., Simpson, I.R. and Fortunatova, N.K., 1998. The relationship between petroleum emplacement and carbonate reservoir quality: examples from Abu Dhabi and the Amu Darya Basin. Marine and Petroleum Geology 15, 57–72.

Nelson, C.S., 1978. Temperate shelf carbonate sediments in the Cenozoic of New Zealand. Sedimentology 25, 737–771.

Nelson, C.S., 1988a. An introductory perspective on non-tropical shelf carbonates. Sedimentary Geology 60, 3–12.

Nelson, C.S., (Ed.) 1988b. Non-tropical shelf carbonates–Modern and ancient. Special Issue, Sedimentary Geology 60.

Nelson, C.S. and Bornhold, B.D., 1983. Temperate skeletal carbonate sediments on Scott shelf, north-western Vancouver Island, Canada. Marine Geology 52, 241–266.

Nelson, C.S. and Hancock, 1984. Composition and origin of temperate skeletal carbonate sediments on South Maria Ridge, northern New Zealand. New Zealand Journal of Geology and Geophysics 18, 221–239.

Nelson, C.S. and Smith, A.M., 1996. Stable oxygen and carbon isotope compositional fields for skeletal and diagenetic components in New Zealand Cenozoic nontropical carbonate sediments and limestones: a synthesis and review. New Zealand Journal of Geology and Geophysics 39, 93–107.

Nelson, C.S. and James, N.P., 2000. Marine cements in mid-Tertiary cool-water shelf limestones of New Zealand and southern Australia. Sedimentology 47, 609–629.

Nelson, C.S. and Cooke, P.J., 2001. History of oceanic front development in the New Zealand sector of the Southern Ocean during the Cenozoic–a synthesis. New Zealand Journal of Geology and Geophysics 44, 535–553.

Nelson, C.H., Carlson, P.R., Byrne, J.V. and Alpha, T.R., 1970. Development of the Astoria canyon-fan physiography and comparison with similar systems. Marine Geology 8, 259–291.

Nelson, C.S., Hancock, G.E. and Kamp, P.J.J., 1982. Shelf to basin temperate skeletal carbonates sediments, Three Kings Plateau, New Zealand. Journal of Sedimentary Petrology 52, 717–732.

Nelson, C.S., Harris, G.J. and Young, H.R., 1988b. Burial-dominated cementation in non-tropical carbonates of the Oligocene Te Kuiti Group, New Zealand. Sedimentary Geology 60, 233–250.

Nelson, C.S., Keane, S.L. and Head, S., 1988a. Non-tropical carbonate deposits on the modern New Zealand shelf. Sedimentary Geology 60, 71–94.

Nelson, C.S., Cooke, P.J., Hendy, C.H. and Cuthbertson, A.M., 1993. Oceanographic and climatic changes over the past 160,000 years at Deep Sea Drilling Project Site 594 off southeastern New Zealand, southwest Pacific Ocean. Paleoceanography 8, 435–458.

Nelson, C.S., Kamp, P.J.J. and Young, H.R., 1994. Sedimentology and petrography of mass-emplaced limestone (Orahiri Limestone) on a late Oligocene shelf, western North Island, and tectonic implications for eastern margin development of Taranaki Basin. New Zealand Journal of Geology and Geophysics 37, 269–285.

Nelson, C.S., Winefield, P.R., Hood, S.D., Caron, V., Pallentin, A. and Kamp, P.J.J., 2003. Pliocene Te Aute limestones, New Zealand: expanding notions for models of cool-water shelf carbonates. New Zealand Journal of Geology and Geophysics 46, 407–424.

Ngatai, M., 2004. Miocene sedimentary geology of the Awakino/Mohakatino region, King Country Basin, with special mention of the carbonate/dominated Middle Miocene Mangarara Formation. PhD Thesis, University of Waikato, Hamilton, New Zealand, pp. 207.

Nodder, S.D., 1987. The mid-Miocene geology of the Waikawau region, North Taranaki, New Zealand: catastrophic sedimentation in a restricted slope basin. Unpublished MSc Thesis, University of Waikato, Hamilton, New Zealand, pp. 306.

Nodder, S.D., Nelson, C.S. and Kamp, P.J.J., 1990. Mass-emplaced siliciclastic/volcanoclastic/carbonate sediments in Middle Miocene shelf-to-slope environments at Waikawau, northern Taranaki, and some implications for Taranaki Basin development. New Zealand Journal of Geology and Geophysics 33, 599–615.

Noé, S., Titschack, J., Freiwald, A. and Dullo, W.C., 2006. From sediment to rock: diagenetic processes of hardground formation in deep-water carbonate mounds of the NE Atlantic. Facies 52, 183–208.

Normark, W.R., Piper, D.J.W. and Hess, G.R., 1979. Distributary channels, sand lobes, and mesotropography of Navy Submarine Fan, California Borderland, with applications to ancient fan sediments. Sedimentology 26, 749–774.

Normark, W.R., Mutti, E. and Bouma, A.H., 1983/84. Problems in turbidite research: a need for COMFAN. Geo-Marine Letters 3, 53–56.

Normark, W.R., Piper, D.J.W. and Hiscott, R.N., 1998. Sea level controls on the textural characteristics and depositional architecture of the Hueneme and associated submarine fan systems, Santa Monica Basin, California. Sedimentology 45, 53–70.

Normark, W.R., Piper, D.J.W. and Sliter, R., 2006. Sea-level and tectonic control of middle to late Pleistocene turbidite systems in Santa Monica Basin, offshore California. Sedimentology, 53, 867–897.

Norris, R.M., 1953. Buried oyster reefs in some Texas bays. Journal of Paleontology 27, 569–576.

Nott, J., 1997. Extremely high-energy wave deposits inside the Great Barrier Reef, Australia: determining the cause-tsunami or tropical cyclone. Marine Geology 141, 193–207.

Nott, J., 2004. The tsunami hypothesis–comparisons of the field evidence against the effects, on the Western Australian coast, of some of the most powerful storms on Earth. Marine Geology 208, 1–12.

Nürnberg, D. and Groeneveld, J., 2006. Pleistocene variability of the Subtropical Convergence at East Tasman Plateau: Evidence from planktonic foraminiferal Mg/Ca (ODP Site 1172A). Geochemistry Geophysics Geosystems 7, QO4P11.

Ó Cofaigh, C., Dowdeswell, J.A. and Kenyon, N.H., 2006. Geophysical investigations of a high-latitude submarine channel system and associated channel-mouth lobe in the Lofoten Basin, Polar North Atlantic. Marine Geology 226, 41–50.

Ott d'Estevou, P. and Montenat, C., 1990. Le Basin de Sorbas-Tabernas. In: C. Montenat (Ed.), Les bassins néogènes du domaine bétique oriental (Espagne). Documents et Travaux IGAL Paris 12–13, 101–128.

Payros, A., Pujalte, V. and Orue-Etxebarria, X., 2007. A point-sourced calciclastic submarine fan complex (Eocene Anotz Formation, western Pyrenees): facies architecture, evolution and controlling factors. Sedimentology 54, 137–168.

Peakall, J., McCaffrey, B. and Kneller, B., 2000. A process model for the evolution, morphology, and architecture of sinuous submarine channels. Journal of Sedimentary Research 70, 434–448.

Pedley, H.M. and Grasso, M., 2002. Lithofacies modelling and sequence stratigraphy in microtidal cool-water carbonates: a case study from the Pleistocene of Sicily, Italy. Sedimentology 49, 533–553.

Pedley, H.M. and Carannante, G., (Eds.) 2006. Cool-water carbonates: depositional systems and palaeoenvironmental controls. Geological Society, London, Special Publication 255, pp. 373.

Pedley, H.M. and Grasso, M., 2006. The response of cool-water carbonates to eustatic change in microtidal, Mediterranean Quaternary settings of Sicily. In: H.M. Pedley and G. Carannante (Eds.), Cool-Water Carbonates: Depositional Systems and Palaeonvironmental Controls. Geological Society, London, Special Publication 255, 137–156.

Pérès, J.M. and Picard, J., 1964. Nouveau Manuel de bionomie benthique de la Mer Meditérrannée. Reuncil des Travaux de la Station Marine d'Endoume 31, 1–137.

Piatanesi, A. and Tinti, S., 2002. Numerical modelling of the September 8, 1905 Calabrian (southern Italy) tsunami. Geophysical Journal International 150, 271–284.

Pickering, K.T., Soh, W. and Taira, A., 1991. Scale of tsunami-generated sedimentary structures in deep water. Journal of the Geological Society, London 148, 211–214.

Piper, D.J.W., 1970. Transport and deposition of Holocene sediment on La Jolla deep sea fan, California. Marine Geology 8, 211–227.

Piper, D.J.W. and Normark, W.R., 1983. Turbidite depositional patterns and flow characteristics, Navy submarine fan, California Borderland. Sedimentology 30, 681–694.

Piper, D.J.W., Hiscott, R.N. and Normark, W.R., 1999. Outcrop-scale acoustic facies analysis and latest Quaternary development of Hueneme and Dume fans, offshore California. Sedimentology 46, 47–78.

Pirmez, C. and Imran, J., 2003. Reconstruction of turbidity currents in Amazon Channel. Marine and Petroleum Geology 20, 823–849.

Popescu, I., Lericolais, G., Panin, N., Normand, A., Dinu, C. and Le Drezen, E., 2004. The Danube submarine canyon (Black Sea): morphology and sedimentary processes. Marine Geology 206, 249–265.

Posamentier, H.W. and Vail, P.R., 1988. Eustatic controls on clastic deposition II-Sequence and systems tract models. In: C.K.Wilgus, B.S. Hastings, C.G. St. C. Kendall, H.W. Posamentier, C.A. Ross and J.C. Van Wagoner (Eds), Sea-level changes: an integrated approach, SEPM Special Publication 42, 125–154.

Posamentier, H.W. and Kolla, W., 2003. Seismic geomorphology and stratigraphy of depositional elements in deep-water settings. Journal of Sedimentary Research 73, 367–388.

Pratson, L.F., Ryan, W.B.F., Mountain, G.S. and Twichell, D.C., 1994. Submarine canyon initiation by downslope-eroding sediment flows: evidence in late Cenozoic strata on the New Jersey continental slope. Geological Society of America Bulletin 106, 395–412.

Prokoph, A. and Thurow, J., 2000. Diachronous pattern of Milankovitch cyclicity in late Albian pelagic marlstones of the North German Basin. Sedimentary Geology 134, 287–303.

Pufahl, P.K., James, N.P., Bone, Y. and Lukasik, J.J., 2004. Pliocene sedimentation in a shallow, cool-water, estuarine gulf, Murray Basin, South Australia. Sedimentology 51, 997–1027.

Puga-Bernabéu, A., Braga, J.C. and Martín, J.M., 2007a (Chapter 5). High-frequency cycles in upper Miocene, ramp temperate carbonates (Sorbas Basin, SE Spain). Facies 53, 329–345.

Puga-Bernabéu, A., Martín, J.M. and Braga, J.C., 2007b (Chapter 4). Tsunami-related deposits in temperate carbonate ramps, Sorbas Basin, southern Spain. Sedimentary Geology 199, 107–127.

Puig, P., Ogston, A.S., Mullenbach, B.L., Nittrouer, C.A. and Sternberg, R.W., 2003. Shelf-to-canyon sediment-transport processes on the Eel continental margin (northern California). Marine Geology 193, 129–149.

Purdy, E.G., 1963. Recent carbonate facies of the Great Bahama Bank, II. Sedimentary facies. Journal of Geology 71, 472–497.

Radke, B.M., 1987. Sedimentology and diagenesis of sediments encountered by Vic. D.M. Piangil West-1, Murray Basin, southeastern Australia. Division of Continental Geology, Groundwater Series 3, Bureau of Mineral Resources. Australia Record 1987/25.

Rao, C.P., 1981. Criteria for recognition of cold-water carbonate sedimentation: Berriedale Limestone (Lower Permian), Tasmania, Australia. Journal of Sedimentary Petrology 51, 491–506.

Rao, C.P., Goodwin, I.D. and Gibson, J.A.E., 1998. Shelf coastal and subglacial polar carbonates, East Antarctica. Carbonates and Evaporites 13, 174–188.

Reading, H.G. and Richards, M., 1994. Turbidite systems in deep-water basin margins classified by grain size and feeder system. American Association of Petroleum Geology Bulletin 78, 792–822.

Reeckmann, S.A., 1988. Diagenetic alterations in temperate shelf carbonates from southeastern Australia. Sedimentary Geology 60, 209–219.

Ricketts, B.D. and Evenchick, C.A., 1999. Shelfbreak gullies; products of sea-level lowstand and sediment failure: examples from Bowser Basin, northern British Columbia. Journal of Sedimentary Research 69, 1232–1240.

Rider, M., 2002. The gamma ray and spectral gamma ray logs. In: M. Rider (Ed.), The Geological Interpretation of Well Logs. Rider-French Consulting Ltd, Scotland, pp. 280.

Riding, R., Martín, J.M. and Braga, J.C., 1991. Coral-stromatolite reef framework, upper Miocene, Almería, Spain. Sedimentology 38, 187–217.

Riding, R., Braga, J.C., Martín, J.M. and Sánchez-Almazo, I., 1998. Mediterranean Messinian Salinity Crisis: constraints from a coeval marginal basin, Sorbas, southeastern Spain. Marine Geology 146, 1–20.

Riding, R., Braga, J.C. and Martín, J.M., 2000. Late Miocene Mediterranean desiccation: topography and significance of the "Salinity Crisis" erosion surface on-land in southeast Spain: Reply. Sedimentary Geology 33, 175–184.

Rivas, P., Braga, J.C. and Sánchez-Almazo, I.M., 1999. Arrecifes del Tortoniense inferior en la Cuenca de Granada, Cordillera Bética, España. Trabajos Geológicos 21, 309–320.

Rodgers, J., 1957. The distribution of marine carbonate sediments: a review. In: R.J. Le Blanc and J.G. Breeding (Eds.), Regional aspects of carbonate deposition. SEPM Special Publication 5, 2–13.

Rodríguez-Fernández, J., 1982. El Mioceno del sector central de las Cordilleras Béticas. PhD Thesis, Universidad de Granada, Spain, pp. 224.

Rodríguez-Fernández, J. and Sanz de Galdeano, C., 2006. Late orogenic intramontane basin development: the Granada basin, Betics (southern Spain). Basin Research 18, 85–102.

Rogala, B., James, N.P. and Reid, C.M., 2007. Deposition of polar carbonates during interglacial highstands on an early Permian shelf, Tasmania. Journal of Sedimentary Research 77, 587–606.

Rossetti, F., Góes, A.M., Truckenbrodt, W. and Anaisse, J., 2000. Tsunami-induced large-scale scour-and-fill structures in Late Albian to Cenomanian deposits of the Grajaú Basin, northern Brazil. Sedimentology 47, 309–323.

Ruegg, G.J.H., 1964. Geologische onderzoekingen in het bekken van Sorbas, S Spanje. Geological Institute, University of Amsterdam, p. 1–64.

Ruíz, F., Rodríguez-Ramírez, A., Cáceres, L.M., Rodríguez, J., Carretero, M.I., Abad, M., Olías, M. and Pozo, M., 2005. Evidence of high-energy events in the geological record: Mid-holocene evolution of the southwestern Doñana National Park (SW Spain). Palaeogeography Palaeoclimatology Palaeoecology 229, 212–229.

Ruíz-Ortíz, P.A., 1983. A carbonate submarine fan in a fault-controlled basin of the Upper Jurassic, Betic Cordillera, southern Spain. Sedimentology 30, 33–48.

Ruíz-Ortíz, P.A., de Gea, G.A. and Castro, J.M., 2006. Timing of canyon-fed turbidite deposition in a rifted basin: The Early Cretaceous turbidite complex of the Cerrajón Formation (Subbetic, Southern Spain). Sedimentary Geology 192, 141–166.

Sami, T.T. and James, N.P., 1994. Peritidal carbonate platform growth and cyclicity in an early Proterozoic foreland basin, upper Pethei Group, Northwest Canada. Journal of Sedimentary Research 64, 111–131.

Sánchez-Almazo, I.M., Spiro, B., Braga, J.C. and Martín, J.M., 2001. Constraints of stable isotope signatures on the depositional palaeoenvironments of upper Miocene reef and temperate carbonates in the Sorbas Basin, SE Spain. Palaeogeography, Palaeoclimatology, Palaeoecology 175, 153–172.

Satur, N., Kelling, G., Cronin, B.T., Hurst, A. and Gürbüz, K., 2005. Sedimentary architecture of a canyon-style fairway feeding a deep-water clastic system, the Miocene Cingöz Formation, southern Turkey: significance for reservoir characterisation and modelling. Sedimentary Geology 173, 91–119.

Savazzi, E., 1995. Parasite-induced teratologies in the Pliocene bivalve *Isognomon maxilatus*. Palaeogeography, Palaeoclimatology, Palaeoecology 116, 131–139.

Saxena, S. and Betzler, C., 2003. Genetic sequence stratigraphy of cool water slope carbonates (Pleistocene Eucla Shelf, southern Australia). International Journal of Earth Sciences (Geologische Rundschau) 92, 482–493.

Scheffers, A. and Kelletat, D., 2004. Bimodal tsunami deposits–a neglected feature in paleo-tsunami research. Coastal Reports 1, 67–75.

Scheffers, A. and Kelletat, D., 2005. Tsunami relics on the coastal landscape west of Lisbon, Portugal. Science of Tsunami Hazards 23, 3–16.

Schnyder, J., Baudin, F. and Deconinck, J.F., 2005. A possible tsunami deposit around the Jurassic-Cretaceous boundary in the Boulonnais area (northern France). Sedimentary Geology 177, 209–227.

Schröder, S., Grotzinger, J.P., Amthor, J. and Matter, A., 2005. Carbonate deposition and hydrocarbon reservoir development at the Precambrian–Cambrian boundary: The Ara Group in South Oman. Sedimentary Geology 180, 1–28.

Schwalbach, J.R., Edwards, B.D. and Gorsline, D.S., 1996. Contemporary channel-levee systems in active borderland basin plains, California Continental Borderland. Sedimentary Geology 104, 53–72.

Scoffin, T.P., 1988. The environments of production and deposition of calcareous sediments on the shelf west of Scotland. Sedimentary Geology 60, 107–124.

Scoffin, T.P., Alexyersson, E.T., Bowes, E.T., Clokie, J.J., Farrow, G.E. and Milliman, J.D., 1980. Recent, temperate, subphotic, carbonate sedimentation: Rockall Bank, northeast Atlantic. Journal of Sedimentary Petrology 50, 331–356.

Selg, M., 1988. Origin of peritidal carbonate cycles: Early Cambrian, Sardinia. Sedimentary Geology 59, 115–124.

Séranne, M. and Nzé Abeigne, C.R., 1999. Oligocene to Holocene sediment drifts and bottom currents on the slope of Gabon continental margin (west Africa): Consequences for sedimentation and southeast Atlantic upwelling. Sedimentary Geology 128, 179–199.

Shanmugam, G., 1996. High-density turbidity currents: are they sandy debris flows? Journal of Sedimentary Research 66, 2–10.

Shanmugam, G., 2000. 50 years of turbidite paradigm (1950s-1990s): deep-water processes and facies models–a critical perspective. Marine and Petroleum Geology 17, 285–342.

Shepard, F.P., 1972. Submarine canyons. Earth-Science Reviews 8, 1–12.

Shepard, F.P. and Marshall, N.F., 1973. Storm-generated current in La Jolla Submarine Canyon, California. Marine Geology 15, 19–24.

Shepard, F.P., Marshall, N.F. and McLoughlin, P.A. 1974. Currents in submarine canyons. Deep-Sea Research I 21, 691–706.

Shinn, E.A., Lloyd R.M. and Ginsburg, R.N., 1969. Anatomy of a modern carbonate tidal flat, Andros Island, Bahamas. Journal of Sedimentary Petrology 39, 1202–1228.

Sierro, F.J., Flores, J.A., Civis, J., González-Delgado, J.A. and Francés, G., 1993. Late Miocene globorotaliid event-stratigraphy and biogeography in the NE-Atlantic and Mediterranean. Marine Micropaleontology 21, 143–168.

Sierro, F.J., Hilgen, F.J., Krijgsman, W., and Flores, J.A., 2001. The Abad composite (SE Spain): a Messinian reference section for the Mediterranean and the APTS. Palaeogeography, Palaeoclimatology, Palaeoecology 168,141–169.

Sierro, F.J., Flores, J.A., Frances, G., Vazquez, A., Utrilla, R., Zamarreño, I., Erlenkeuser, H. and Barcena, M.A., 2003. Orbitally-controlled oscillations in planktic communities and cyclic changes in western Mediterranean hydrography during the Messinian. Palaeogeography, Palaeoclimatology, Palaeoecology 190, 289–316.

Smith, A.M., 1988. Preliminary steps toward formation of a generalized budget from cold-water carbonates. Sedimentary Geology 60, 323–331.

Smith, A.M. and Nelson, C.S., 2003. Effects of early sea-floor processes on the taphonomy of temperate shelf skeletal carbonate deposits. Earth-Science Reviews 63, 1–31.

Smith, D.P., Kvitek, R., Iampietro, P.J. and Wong, K., 2007. Twenty-nine months of geomorphic change in upper Monterey Canyon (2002-2005). Marine Geology 226, 79–94.

Smoot, J.P., Litwin, R.J., Bischoff, J. and Lund, S.J., 2000. Sedimentary record of the 1872 earthquake and "Tsunami" at Owens Lake, southeast California. Sedimentary Geology 135, 241–254.

Spinelli, G.A. and Field, M.E., 2001. Evolution of continental slope gullies on the northern California Margin. Journal of Sedimentary Research 71, 237–245.

Stanley, D.J., 1967. Comparing patterns of sedimentation in some modern and ancient submarine canyons. Earth and Planetary Science Letters 3, 371–380.

Stemmerik, L., 1997. Permian (Artinskian-Kazanian) cool-water carbonates in North Greenland, Svalbard and the Western Barent Sea. In: N.P. James and A.D. Clarke (Eds.), Cool-Water Carbonates. SEPM Special Publication 56, 349–364.

Stenzel, H.B., 1971. Oysters. In: R.C. Moore (Ed.), Treatise on invertebrate paleontology. Geological Society of America and University of Kansas, Lawrence, KA, USA, vol 3, p. 952–1224.

Stoffers, P. and Ross, D.A., 1979. Late Pleistocene and Holocene sedimentation in the Persian Gulf-Gulf of Oman. Sedimentary Geology 23, 181–208.

Surlyk, F. and Noe-Nygaard, N., 1986. Hummocky cross-stratification from the Lower Jurassic Hasle Formation of Bornholm, Denmark. Sedimentary Geology 46, 259–273.

Switzer, A.D., Bristow, C.S. and Jones, B.G., 2006. Investigation of large-scale washover of a small barrier system on the southern Australian coast using ground penetrating radar. Sedimentary Geology 183, 145–156.

Taft, W.H., 1967. Modern carbonate sediments. In: G. Chilingarm H.J. Bissell and R.W. Fairbridge (Eds), Carbonate rocks: origin, occurrence, and classification. Developments in Sedimentology 9A, 29–50. Elsevier, Amsterdam.

Takashimizu, Y. and Masuda, F., 2000. Depositional facies and sedimentary successions of earthquake-induced tsunami deposits in Upper Pleistocene incised valley fills, central Japan. Sedimentary Geology 135, 231–239.

Tappin, D. R., (Ed.) 2007. Sedimentary features of tsunami deposits–Their origin, recognition and discrimination: An introduction. Sedimentary Geology 200, 151–388.

Titschack, J., Bromley, R.G. and Freiwald, A., 2005. Plio-Pleistocene cliff-bound, wedge-shaped, warm-temperate carbonate deposits from Rhodes (Greece): Sedimentology and facies. Sedimentary Geology 180, 29–56.

Tucker, M.E., 1981. Sedimentary petrology. An introduction. Geoscience Texts 3. Blackwell Scientific Publications, Oxford, pp. 252.

Tucker M.E. and Wright, V.P., 1992. Carbonate sedimentology. Blackwell Scientific Publication, Oxford, pp. 482.

Vail, P.R., Audemard, F., Bowman, S.A., Eisner, P.N. and Pérez-Cruz, C., 1991. The stratigraphic signatures of tectonics, eustacy and sedimentology–an overview. In: G. Einsele, W. Ricken and A. Seilacher (Eds), Cycles and Events in Stratigraphy. Springer-Verlag, Berlin, p. 618–659.

van den Bergh, G.D., Boer, W. de Haas, H., van Weering, Tj. C. E. and van Wijhe, R., 2003. Shallow marine tsunami deposits in Teluk Banten (NW Java, Indonesia), generated by the 1883 Krakatau eruption. Marine Geology 197, 13–34.

Veevers, J.J., Powell, McA. and Roots, S.R., 1991. Review of seafloor spreading around Australia, 1. Synthesis of patterns of spreading, Australian Journal of Earth Sciences 38, 373–390.

Vigorito, M., Murru, M. and Simone, L., 2005. Anatomy of a submarine channel system and related fan in a foramol/rhodalgal carbonate sedimentary setting: a case history from the Miocene syn-rift Sardinia Basin, Italy. Sedimentary Geology 174, 1–30.

Vigorito, M., Murru, M. and Simone, L., 2006. Architectural patterns in a multistorey mixed carbonate-siliciclastic submarine channel, Porto Torres Basin, Miocene, Sardinia, Italy. Sedimentary Geology 186, 213–236.

Vonk, A.J., 1999. Stratigraphic architecture and sedimentology of the early Miocene Mokau Group, North Wanganui Basin, western North Island, New Zealand. Unpublished MSc. Thesis, University of Waikato, Hamilton, New Zealand, pp. 320.

Vonk, A.J., (*in prep*). Stratigraphy of a paleo-continental margin in western North Island: Implications for prospectivity, PhD Thesis, University of Waikato, Hamilton, New Zealand.

Vonk, A.J. and Kamp, P.J.J., 2006. Cross-sections through the Miocene continental margin of Onshore Taranaki Basin. In: 2006 New Zealand Petroleum Conference Proceedings, 6-8 March, Auckland. Crown Minerals, Ministry of Economic Development, Wellington New Zealand.

Wahlman, G.P., 2002. Upper Carboniferous-Lower Permian (Bashkirian-Kungurian) mounds and reefs. In: W. Kiessling, E. Flügel and J. Golanka (Eds.), Phanerozoic Reef Patterns. SEPM Special Publication 72, 271–338.

Watts, K.F., 1988. Triassic carbonate submarine fans along the Arabian platform margin, Sumeini Group, Oman. Sedimentology 35, 43–71.

Webby, B.D., 2002. Patterns of Ordovician Reef Development. In: W. Kiessling, E. Flügel and J. Golanka (Eds.), Phanerozoic Reef Patterns. SEPM Special Publication 72, 129–179.

Weber, M.E., Wiedicke, M.H., Kudrass, H.R., Hübscher, C. and Erlenkeuser, H., 1997. Active growth of the Bengal Fan during sea-level rise and highstand. Geology 25, 315–318.

Wentworth, C.K. 1922. A scale of grade and class terms for clastic sediments. Journal of Geology 30, 377–392.

Williams, T. and Pirmez, C., 1999. FMS images from carbonates of the Bahamas Bank Slope, ODP Leg 166: Lithological identification and cyclo-stratigraphy. In: M.A. Lovell, G. Williamson, P.K. Harvey (Eds.), Borehole Imaging: applications and case histories, Geological Society, London, Special Publication 159, 227–238.

Williams, T., Kroon, D. and Spezzaferri, S., 2002. Middle and Upper Miocene cyclostratigraphy of downhole logs and short- to long-term astronomical cycles in carbonate production of the Great Bahamas Bank. Marine Geology 185, 75–93.

Wilson, J.L., 1975. Carbonate facies in geologic time. Springer-Verlag, New York, pp. 471.

Wilson, B., 1994. Sedimentology of the Miocene succession (coastal section), eastern Taranaki Basin margin: a sequence stratigraphic interpretation. Unpublished MSc Thesis, University of Waikato, Hamilton, New Zealand, pp, 184.

Wilson, E.J. and Evans, M.J., 2002. Sedimentology and diagenesis of Tertiary carbonates on the Mangkalihat Peninsula, Borneo: implications for subsurface reservoir quality. Marine and Petroleum Geology 19, 873–900.

Winslow, J.H., 1966. Raised submarine canyons: and explanatory hypothesis, 1966. Annals of the Association of American Geographers 56, 634–672.

Wood, R., 1993. Nutrients, predation and the history of reef-building. Palaios 8, 526–543.

Wood, J., 1996. An introduction to the lower Messinian temperate water facies of the Sorbas Basin (Abad and Azagador Members). In A.E. Mather and M. Stokes (Eds.), Cortijo Urra field meeting, Southeast Spain: Field Guide. University of Plymouth, England, p. 14–23.

Wood, R., 1999. Reef evolution. Oxford University Press, Oxford, pp. 414.

Wright, V.P. and Wilson, C.L., 1984. A carbonate submarine-fan sequence from the Jurassic of Portugal. Journal of Sedimentary Petrology 54, 394–412.

Xu, J.P., Noble, M.A. and Rosenfeld, L.K., 2004. In-situ measurements of velocity structure within turbidity currents. Geophysical Research Letters 31, L09311.

Yagishita, K., Arakaw, S. and Taira, A., 1992. Grain fabric of hummocky and swaley cross-stratification. Sedimentary Geology 78, 181–189.

Yesares, J. and Aguirre, J., 2004. Quantitative taphonomic analysis and taphofacies in lower Pliocene temperate carbonate–siliciclastic mixed platform deposits (Almería-Níjar Basin, SE Spain). Palaeogeography, Palaeoclimatology, Palaeoecology 207, 83–103.

Young, H.R. and Nelson, C.S., 1988. Endolithic biodegradation of cool-water skeletal carbonates on Scott shelf, northwestern Vancouver Island, Canada. Sedimentary Geology 60, 251–267.

14

SUBJECT INDEX

C

D

E

F

G

H

I

K

L

M

N

O

P

Q

R

S

T

U

V

W

Y

Z

DEPOSITIONAL MODELS OF TEMPERATE CARBONATES:

Insights into *in situ* and redeposited sediments from Southern Spain, South Australia and North New Zealand

In the last two decades, research on the temperate-carbonate depositional realm has significantly increased knowledge on these, up to then, poorly known carbonates, achieving a degree of comprehension comparable to that of tropical carbonates. However, some aspects need further research, especially those concerning depositional models due to the high variability and number of controlling factors.

The Mediterranean Sea, New Zealand, and southern Australia are the most important temperate-carbonate sedimentary provinces in the world. This thesis deals with the study of temperate-carbonate deposits in these regions. It attempts to expand upon the spectrum of the temperate-carbonate depositional models, clarifying sediment transport mechanisms, describing their resulting deposits, and identifying and analysing some aspects related to cyclicity and sequence stratigraphy in temperate carbonates.

Interpreted depositional models in the study areas share certain characteristics in common or with comparable classic sedimentary models of temperate carbonates. These features mainly concern the ramp geometry, biogenic composition of the sediment, facies belt distribution, sediment transport and deposition mechanisms, and cyclicity.

New aspects concerning temperate-carbonate deposition were found in platform and offshore environments. In platform settings, the main innovations involve event deposits (tsunamites), sedimentary cyclicity, and submarine canyon occurrence and development. Sea-level driven cyclicity, deep-water submarine channel-fan systems and submarine gullies are the main features found in offshore settings.

Although the most important controlling factors on temperate-carbonate ramp deposition (apart from water temperature and nutrient contents) have been repeatedly shown to be local hydrodynamic conditions and type and geometry of the underlying substrate, there are additional factors to be taken into account. This thesis work has demonstrated that high-energy events (tsunamis), large-scale geomorphic elements (submarine canyons and submarine channel-fan system), and sea-level driven modulations condition the type of temperate-carbonate depositional model that develops, whether in the platform or in offshore settings.

Departamento
de
Estratigrafía y Paleontología
UNIVERSIDAD DE GRANADA